Kinase Activities of RIPK1 and RIPK3 Direct Host Immune Cytokine Production that Manifests Independent of Cell Death

A thesis submitted by

Danish Saleh

In partial fulfillment of the requirements for the degree of

PhD

In

Neuroscience

Tufts University

May 2017

Advisor: Alexei Degterev, PhD

Abstract

Macrophages function as a crucial component of the innate immune system in sensing bacterial pathogens and promoting local and systemic inflammation. RIPK1 and RIPK3 are serine/threonine kinases that have been well-characterized as key regulators of programmed necrotic cell death or necroptosis that is dependent on downstream pseudokinase MLKL. The work presented in the ensuing chapters describes a new function of these kinases as master regulators of cytokine gene expression and the synthesis of inflammatory mediators in primary macrophages activated by LPS, in the absence of caspase-8 activation. RIPK1 and RIPK3 kinase-dependent cytokine production requires the Toll-like receptor 4 (TLR4) adaptor molecule, TRIF, and proceeds independently of MLKL and the well-documented death functions of these kinases. Mechanistically, RIPK1 and RIPK3 kinases promote sustained activation of at least two canonical cytokine response axes: the acute inflammatory response mediated by downstream factors, Erk1/2, c-Fos, and NFκB; and the Type-I interferon (IFN-I) response pathway mediated by TBK1/IKKε and IRF3/7. The evidence summarized here suggests that detergent-insoluble complexes of RIPK1 and RIPK3 (necrosomes) serve as a signaling platform to engage downstream signaling molecules. Using genetic and pharmacologic tools, the data reveal that RIPK1 and RIPK3 kinase functions account for a major fraction cytokine elicited by LPS challenge *in vivo*. Notably, in contrast to the circumstance observed *in vitro*, the regulation *in vivo* did not require exogenous manipulation of caspase-8 activity, suggesting that RIPK1 and RIPK3 kinase-dependent cytokine responses may serve as a feature of the host-inflammatory response in gram-negative bacterial (GNB) infection.

Intriguingly, in primary macrophages, RIPK1 and RIPK3 kinase-dependent synthesis of IFNβ can be markedly induced by a variety of gram-negative bacterial species (*Yersinia* and *Klebsiella*). Furthermore, data show that RIPK1 and RIPK3 kinase-dependent IFNβ synthesis is strongly induced by avirulent strains of gram-negative bacteria, *Yersinia* and *Klebsiella*, and less-so by their wild-type counterparts.

Similarly, RIPK1 kinase-dependent TNFα synthesis is more pronounced following *in vivo* infection with an avirulent strain of *Klebsiella* compared to the wild type.

These data suggest that TRIF-RIPK1-RIPK3 kinase-dependent signaling may be a mechanism of immune-surveillance employed against non-pathogens or commensal bacteria. Conversely, TRIF-RIPK1-RIPK3 signaling may be selectively suppressed by invading microbes to facilitate bacterial pathogenesis. Consistent with this hypothesis, GNB species are armed with specific mechanisms to attenuate RIPK1 and RIPK3 kinase-dependent signaling. As a result, exogenous activation of TRIF-RIPK-RIPK3 kinase-dependent signaling may aid in the clearance of GNB infection. Importantly, the findings reported here identify new drug-targetable activities that may be relevant to infection and/or inflammatory pathologies associated with inappropriate RIPK1 and RIPK3 kinase activation.

Acknowledgements

Human beings are a product of their biology and their environment. As this is a fundamental belief of mine, I have grown to appreciate that my life and, in particular, my successes have been shaped and made possible by the enrichment provided by the people around me. To my good fortune, I have had many excellent people commit themselves to my development. Here, I recognize and express gratitude to the people who have been most influential during my PhD training.

Alexei Degterev

I begin by recognizing Alexei (Dr. Alexei Degterev), my closest scientific mentor and advisor, during my PhD training. In an early conversation, I told Alexei that it was important to me that I manage multiple scientific projects as I was intent on maximizing the likelihood of authoring numerous works. In response, Alexei offered me chances to contribute scientifically to multiple projects within his lab as well as projects being developed by his colleagues and collaborators. Additionally, he provided me the important and early opportunity to author an invited Review/Book Chapter which also served me during the writing of my thesis. And finally, Alexei granted me the responsibility of driving the two major projects examining roles for RIPK1 and RIPK3 in directing cytokine responses to LPS, resulting in two high-quality first author publications. Indeed, Alexei took my early request sincerely and provided more-than-adequate opportunities to synthesize a PhD that I can regard as successful.

Apart from facilitating opportunity, Alexei was an outstanding scientific mentor. With some shame, I recognize that Alexei has probably performed as many experiments (if not more) than I have during the past 3-4 years. His dedication and commitment to the investigative process taught me the importance of perseverance in basic scientific discovery. His informal style and his sincere interest in discussing research at all times of day (and night) complimented my approach and inspired me to a level of productivity in the laboratory that was instrumental to my training and achievements. His commitment to scientific integrity and responsible research are admirable. And lastly, the responsibility he assumed for

my well-being and training furnished an outstanding and memorable experience over the course of my graduate years. For the reasons above, I am grateful for my training experience.

Joan Mecsas

Another mentor who provided important guidance, resources, and support during my training was Joan (Dr. Joan Mecsas). In contrast to Alexei's style, she provided me with traditional/formal mentorship, including, regularly scheduled lab meetings, recurrent opportunities to present my research, and dedicated journal clubs to keep up with relevant literature. This structured training was important in building discipline as a collaborative academic investigator within me. Moreover, Joan provided me the freedom to advance my research project using the tools, reagents, and resources available in her laboratory. Indeed, her personal and academic investment in my work was important to the evolution of my research over the years and contributed to a publication as well. Finally, Joan's compassionate persona, scientific interests and approach, and commitment to high quality work are a combination that I admire and hope to carry-forward in my career.

Ferial and Salim Saleh

Just as my achievements in the laboratory would not have been possible without the investments of my scientific mentors, these achievements would also not have been possible without the resources and love provided by my parents (Ferial and Salim Saleh). For illustrative purposes: The only food I prepared during my graduate training was cereal at the end of the day and on Saturday mornings. Apart from these meals, my day-to-day expenses exceeded my stipend and were supported by my parents' generosity – I ate out for almost every lunch and dinner during my training. Additionally, I also made numerous impulsive and extravagant purchases, including, many *Cole Haan's* – which satisfied my materialistic desires. My peace of mind and day-to-day happiness/contentment were made possible by the resources made available by my parents. As a direct consequence of their support, I was able to commit 10-12 hours to my research daily without competing responsibilities.

Fahad Saleh

Fahad (Saleh), my younger brother (~1.5 years junior to me), possesses an exceptional intellect and it was his influence that prompted my interest in academic research. I recall, many years ago, as he and I we were sitting and deliberating examples of 'right' and 'wrong' behavior (I cannot remember the exact time and place; however, I believe it was before I matriculated to college), he challenged me to ask why and how I defined/reconciled my valuations. He also persistently demanded that I critically evaluate how one might reason valid from invalid approaches/responses in addressing a variety of academic and philosophic questions. His partnership instilled within me a fondness for academic rigor – he has been crucially responsible for the emergence of my (scientific) curiosity.

Ekaterina Pak

Finally, Kat (Ekaterina Pak), my girlfriend during my PhD training, my fiancée today, and my soon-to-be-wife, has been the strongest emotional resource available to me since I've known her. Having completed her PhD in Biological and Biomedical Sciences, she is one of the few people in my personal life with the ability to provide constructive insights and directive in managing the (varying) circumstances familiar only to a scientist. She and I have produced a close partnership and understanding that was founded on a mutual passion for science, a commitment to personal enrichment, and an unyielding love for our roles in society. Her unique companionship has been important to my peace of mind and has facilitated my personal achievements.

Other important people during my training

Apart from the people mentioned above, there have been many others who have been crucially important in my development. Although I can write lengthy prose about each of these individuals, I will refrain from doing so for because the focus of this document is the research and not the people. Below, I briefly mention some these people and the capacity in which they have contributed to my growth.

Morrie (Dr. Morris J. Birnbaum, M.D. Ph.D.), was my research advisor as an undergraduate at the University of Pennsylvania (Penn). He would readily apply his medical training to inform his research in hypothesis generation and experimental interpretation. Admiration of his approach to research inspired me to pursue MD/PhD training.

Karla (now, Dr. Karla Leavens) was an MD/PhD student at Penn and Russell (Dr. Russell Miller) was a post-doctoral fellow in Morrie's lab during my undergraduate years. Both of these people taught me the fundamentals of basic research and were particularly encouraging mentors to me. Others in Morrie's lab who contributed to my training include Min (Post-doctoral scholar; Dr. Min Wan), Bob Monks (Mouse geneticist), Helen (graduate student; now, Dr. Helen Chen), and Ming-jian (Post-doctoral scholar; Dr. Ming-jian Lu).

The MD/PhD leadership at Tufts University, comprised of Dr. Jim Schwob (Jim), Dr. Naomi Rosenberg (Naomi), and Dr. Gordon Huggins (Gordon), provided me with an extraordinary opportunity by accepting me into the MD/PhD program at Tufts. They have been a constant supportive influence overseeing my training. While Jim and Naomi were important in helping me identify a suitable laboratory to initiate my thesis work, Gordon has been made time to mentor me in clinical medicine beyond what is designated in the curriculum for MD/PhD students. The influence of these three mentors will be fingerprinted in my final achievements at Tufts.

My thesis committee, comprised of Dr. Rob Jackson (Committee chair), Dr. Larry Feig, Dr. Jim Schwob, and Dr. Joan Mecsas have all provided constructive criticisms to facilitate my growth as a scientist. I thank them for their investment in my training. Here, I would also like to express gratitude to Dr. Francis Chan (University of Massachusetts Medical School) who has agreed to serve as the outside examiner on my committee for my formal defense.

I would also like to recognize the people in the (Sackler) Dean's office who invested themselves in my training. Associate Dean Kathryn Lange has been exceptionally generous with her time in providing

instruction and guidance in preparation of my thesis. Dean Rosenberg's staff who manage the administrative side of the MD/PhD program have been useful resources. They have always been there to answer questions pertaining to matters ranging from grant writing and enrolling in coursework to government documentation/filing taxes. Additionally, they have been particularly valuable in reminding me of important upcoming deadlines. Among the staff, I would like to specifically recognize the effort of Sara Abbott who has been a helpful since my first days at Tufts. I've also enjoyed and appreciated email correspondences and the concern shown by Jeffrey Miller.

Within the Neuroscience Program administrative staff, I would like to recognize the efforts of Shelley Antonio who has helped me with managing administrative and logistical tasks associated with my graduate training. These include tasks such as booking rooms for committee meetings and my defense as well as ordering food for graduate research seminar.

Collaborators

The work I present in this thesis would not have been possible without many excellent collaborators and companions. Many of these individuals are recognized below.

Degterev Lab

A previous graduate student, Malek (Dr. Malek Najjar), generated much of the initial data making the observations elaborated in this thesis. He was a hardworking labmate and friend to me during our time in lab together. Saumil Shah was an outstanding Research Tech who managed the laboratory during my first year and a half as a graduate student. He and I became good friends working together. The work presented in this thesis is a direct result, in part, of the dedication of these two individuals.

Mecsas Lab (Tufts University)

All the members of Joan's lab were a pleasure to work with; they were fun to converse with and extremely helpful to me in getting my work done. Because the people in her lab, I looked forward to days

when I had to perform experiments in her lab, in spite of the difficulties associated with carrying out experiments in a foreign space. These people include, Michelle (now, Dr. Michelle Paczosa), Erin (now, Dr. Erin Green), Giang (Giang Nguyen), Lamyaa (Lamyaa Shaban), Becca (Rebecca Silver), Alyssa (Alyssa Fasciano), and Ben (Benjamin Mecsas-Faxon). Michelle also contributed directly to the work presented in Chapter 3 by providing a useful reagent for the studies. Dr. Kim Davis, a post-doctoral fellow in Dr. Ralph Isberg's lab, and Stacie Clark, a graduate student in Dr. Ralph Isberg's lab, regularly attended Mecsas lab meeting and provided useful thoughts, suggestions, and discussion for my work.

Poltorak Lab (Tufts University)

The Poltorak lab (Lab of Dr. Alexander (Sasha) Poltorak) was an early collaborator of ours during my graduate training. He provided reagents and discussion that contributed to the work presented in Chapter 2 of this thesis. I developed a close relationship with Stephen Schworer (now, Dr. Stephen Schworer), an MD/PhD student in Sasha's lab, as Stephen was also interested in RIPK1 biology pertinent to cell death and inflammation (a subject-matter closely related to the content of this thesis). Stephen validated many of the foundational observations reported in this thesis. Other students, Guy (now, Dr. Guy Surpris), Dan (now, Dr. Daniel Ram) and Caitlin Liu, also provided reagents and useful discussion.

Joseph Sarhan, another MD/PhD student who matriculated to Tufts with me, is currently completing his thesis work under the advisorship of Dr. Alexander Poltorak. At various points during our training together he has been a friend to me and been helpful in discussion and sharing reagents.

Slavov Lab (Northeastern University)

Dr. Nikolai Slavov and his graduate student, Harrison Specht, were crucial to developing the approach using sucrose-gradients and velocity sedimentation to separate and isolate necrosomes in macrophages. Dr. Slavov was instrumental to generating much of the early data and getting the system working. Some of this work is featured in Chapter 3 of this thesis.

Michael Whalen

Mike Whalen (Dr. Michael Whalen M.D.; Massachusetts General Hospital) is a Pediatrician and Physician-Scientist who has been a longstanding collaborator of the Degterev Lab. Mike and I have worked on experiments together and Mike has also served as a mentor to me as an example of a successful Physician-Scientist.

Friends

I have been fortunate to have many close friends who have served in a variety of roles throughout my PhD training years. These people have provided comradery and companionship, advice, emotional support, entertainment – and dependable friendship during my training. They include:

MD/PhD classmates: Wenhui Zhou, Sanna Herwald, Thomas Dixon, and Joseph Sarhan. Notably, Wenhui and I were roommates during our first year of medical school. This crew has been fantastic.

Some MD/PhD program-mates: Jacob Ludington (now, Dr. Jacob Ludington), Daniel Herrick (now, Dr. Daniel Herrick), Averi Leahy Gibson (now, Dr. Averi Gibson), Eniola Yeates (now, Dr. Eniola Yeates), Benjamin Moss (now, Dr. Benjamin Moss), Patrick Davis, Alexander (Alex) Neil, Frank Scangarello, and David Dickson. Notably, Jacob has served as an exceptional friend at many times and I've thoroughly enjoyed engaging/being engaged by Patrick and Alex in scientific discussion/inquiry.

Soshian Sarrafpour (now, Dr. Soshian Sarrafpour), Andrew Petrone, Jennifer (Jenn) Cheung (now, Dr. Jennifer Cheung), Philip (Phil) Chan (now, Dr. Philip Chan), Matthew (Matt) Kwong (now, Dr. Matthew Kwong), and Omid Moghimi (now, Dr. Omid Moghimi): Soshian, Jenn, Phil, Matt, and Omid were classmates of mine in medical school – they have since graduated with their Medical Degrees and are now completing their residencies. Andrew was Soshian's (college) roommate and is a healthcare statistician (or, at least, that's how I introduce him because I've never bothered to really learn what exactly he does) who is exceptionally skilled at picking the most entertaining Cocktail bars/Restaurants in Boston and New York. These people have been great friends to me.

Nicole Castagnozzi and Stephen Downey: I met Nicole while she was a graduate student in Immunology at Tufts. Stephen is her husband – he reintroduced me to the sport of basketball, a love of mine that I had neglected since matriculating to Tufts. Both of them are outstanding company and great friends.

Table of Contents

List of Tables

List of Figures

Chapter 1

Chapter 2

Chapter 3

Chapter 4

List of Copyrighted Materials

Najjar, M., **Saleh, D.**, Zelic, M., Nogusa, S., Shah, S., Tai, A., … **Degterev, A.** (2016). RIPK1 and RIPK3 Kinases Promote Cell-Death-Independent Inflammation by Toll-like Receptor 4. Immunity, 45(1), 46–59.
**Permission was granted to reprint this publication in Chapter 2 of this thesis.*

Ofengeim, D., & Yuan, J. (2013). Regulation of RIP1 kinase signalling at the crossroads of inflammation and cell death. *Nature Reviews. Molecular Cell Biology*, *14*(11), 727–36.
**Permission was granted to reprint Figure 2 of this publication for Figure 1 in Chapter 1 of this thesis.*

Saleh, D., & Degterev, A. (2015). Emerging Roles for RIPK1 and RIPK3 in Pathogen-Induced Cell Death and Host Immunity. In *Current topics in microbiology and immunology*.
**Permission was granted to reprint text from this publication in Chapters 1 and 4.*
**Permission was granted to reprint Table 1 from this publication for Table 1 in Chapter 1 of this thesis.*

Saleh, D., Najjar, M., Zelic, M., Shah, S., Nogusa, S., Polykartis, A., … Degterev, A. (2017). Kinase Activities of RIPK1 and RIPK3 Can Direct IFN-β Synthesis Induced by Lipopolysaccharide. *The Journal of Immunology.*198(10).
**Permission was granted to reprint this publication in Chapter 3 of this thesis.*

Wegner, K. W., **Saleh, D., & Degterev, A.** (2016). Complex Pathologic Roles of RIPK1 and RIPK3: Moving Beyond Necroptosis. *Trends in Pharmacological Sciences*, *38*(3), 202–225.
**Permission was granted to reprint Figure 1 of this publication for Figure 2 in Chapter 1 of this thesis.*

Permission letters for all copyrighted material are included in supplement to this work.

List of Abbreviations

ΔcpsB – Capsule-deficient *Klebsiella pneumonia (Kp)*

ΔyscF – Pin mutant of *Yersinia pseudotuberculosis (Yptb)*

DNA – Deoxyribonucleic Acid

ELISA – Enzyme-linked immunosorbent assay

Erk1/2 – Extracellular-signal regulated kinases 1/2 (MAP kinases)

GNB – Gram-negative bacteria

GSK – GlaxoSmithKline

IκB – Inhibitor of NFκB

IFN-I – Type I interferon

IFNβ – Interferon-beta

IKKε – IκB kinase subunit epsilon

IRF3/7 – Interferon regulatory factor 3/7

Kp – Klebsiella pneumonia

LPS – Lipopolysaccharide

MLKL – Mixed lineage kinase-like

mRNA – messenger RNA

MyD88 – Myeloid differentiation primary response gene 88

Nec-1 or Nec-1s – Necrostatin-1 or Necrostatin-1s

NFκB – Nuclear factor kappa B

PCR – Polymerase chain reaction

PIC – Poly(I:C)

qPCR/qRT-PCR – Quantitative PCR/ Quantitative Real-Time PCR

RIPK1 – Receptor interacting protein kinase 1

RIPK3 – Receptor interacting protein kinase 3

RNA – Ribonucleic acid

siRNA – Small interfering RNA

shRNA – Short hairpin RNA

STING – Stimulator of interferon genes

TBK1 – TANK-binding kinase 1

TRIF – TIR-domain-containing adapter-inducing interferon-beta

TLR3 – Toll-like receptor 3

TLR4 – Toll-like receptor 4

Yptb – Yersinia pseudotuberculosis

zVAD – zVAD.fmk (Valine-Alanine-Aspartate fluoromethyl ketone)

Chapter 1

Introduction

1.1 Clinical perspective

Hospital-acquired infections impose significant social and financial costs that impact ~4% of all hospitalized patients and amount to over 100 billion dollars in excess healthcare expenditures annually. Gram-negative bacterial (GNB) infections are particularly problematic as these species account for ~70% of all infections in critical care settings and are highly efficient at acquiring and expressing antibiotic-resistance genes (Peleg & Hooper 2010). Upon GNB infection, host immune cells sense bacterial cell membrane glycolipid, lipopolysaccharide (LPS), and initiate localized anti-microbial cellular reprogramming while sequentially inducing production of pro-inflammatory molecules, which act systemically (Tan & Kagan 2014; Kawai & Akira 2010). Together, these changes serve to promote microbial clearance in the infected host. Advancing understanding of mechanisms underlying bacterial pathogenesis and host-defense will uncover new medicinal targets to manage and prevent bacterial infections in times of growing antibiotic resistance in our healthcare settings.

1.2 RIPK1 and RIPK3[1]

Receptor interacting protein kinase 1 and 3 (RIPK1 and RIPK3) are homologous serine-threonine kinases belonging to the RIPK family of proteins. These kinases have attracted interest as key regulators of death-receptor induced programmed necrosis pathway, termed "necroptosis" (Vanden Berghe et al. 2014; Christofferson & Yuan 2010). Given the pro-inflammatory nature of necrotic cell death, pathologic contributions of RIPK1 and RIPK3 in human disease have garnered significant interest. Experimental approaches utilizing genetic deletion of RIPK3, expression of kinase dead RIPK1, or use of small molecule RIPK1 inhibitors, necrostatins, in

[1] Reprinted from *(Saleh and Degterev 2015, pages 1-3)* with permission from publisher.

models of human disease, indeed suggested important contributions of these kinases in many pathologic states associated with inflammation, including ischemia-reperfusion injuries, atherosclerosis, pancreatitis, multiple sclerosis, Amylotropic Lateral Sclerosis (ALS), inflammatory bowel diseases and others (Linkermann & Green 2014; You et al. 2008; Degterev et al. 2005; Ofengeim et al. 2015; Ito et al. 2016). While physiologic roles of RIPK1 and RIPK3 are poorly defined, a growing body of evidence, much of which is a central focus for this thesis, suggests that these molecules may emerge as important players in host-immune regulation.

RIPK1 is comprised of three functionally distinct domains, namely, an N-terminal kinase domain, an intermediate domain, and a C-terminal death domain. Kinase function of RIPK1 is important for Tumor Necrosis Factor Receptor (TNFR)-dependent necroptosis as well as apoptosis (Christofferson et al. 2014; Ofengeim & Yuan 2013) (Figure 1). The Serine/Threonine kinase domain includes an aspartate-leucine-glycine (DLG) motif-containing binding pocket for the allosteric RIPK1 kinase inhibitor, Necrostatin-1 (Nec-1) (Degterev et al. 2008; Xie, Peng, Liu, et al. 2013). Although highly-specific, the first-generation of Nec-1 was found to have some inhibitory activity against Indoleamine-2,3-dioxygenase (IDO). Optimization of this compound yielded 7-Cl-O-Nec-1 (Nec-1 or Nec-1s) with exclusive specificity against RIPK1 kinase (Degterev et al. 2013). Nec-1 and Nec-1s have been widely used to define kinase-dependent

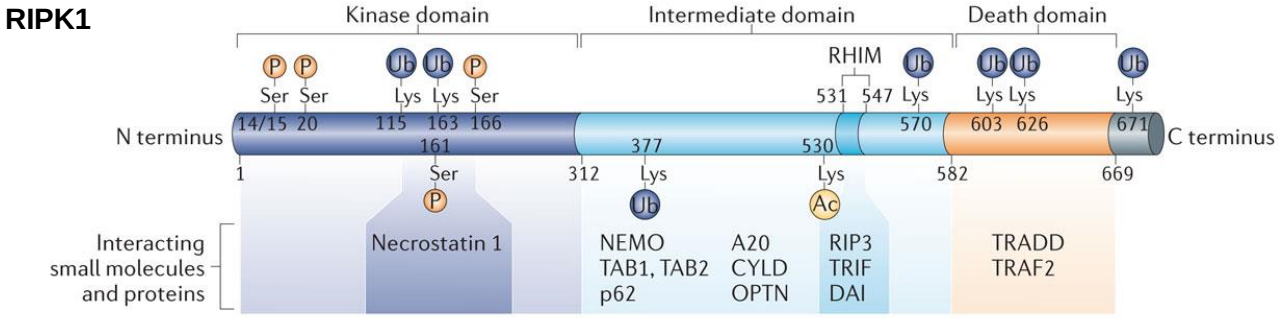

Figure 1. RIPK1. Ofengeim and Yuan, 'Regulation of RIP1 kinase signalling at the crossroads of inflammation and cell death.' *Nature Reviews: Molecular Cell Biology.*

functions of RIPK1; however, the recent generation of RIPK1 kinase-inactive mouse models has expanded the repertoire of tools available to distinguish kinase-dependent from kinase-independent functions of this protein (Polykratis et al. 2014; Berger et al. 2014). The intermediate domain of RIPK1 contains a RIP-Homotypic Interacting Motif (RHIM), which facilitates RIPK1 interaction with other RHIM-domain containing proteins, including DAI, TRIF and RIPK3. RHIM-domain interactions are required for "amyloid-like" RIPK1/RIPK3 "necrosome complex" formation and RIPK-dependent death signaling (Kaiser et al. 2013; Li et al. 2012; Wu et al. 2014; Upton et al. 2012). Lastly, the C-terminal death domain mediates interaction of RIPK1 with death-domain containing receptors such as FasR and TNFR1 (Christofferson et al. 2014; Ofengeim & Yuan 2013). Distinct properties associated with the various domains of RIPK1 enable the enzyme to act as a dynamic regulator of cell death signaling.

RIPK3 shares many similarities to RIPK1, including highly homologous kinase and RHIM domains. Early work suggested that kinase activities of both proteins are required to initiate necroptosis by means of phosphorylation-driven assembly of a necrosome complex (Xie, Peng, Yan, et al. 2013; Cho et al. 2010). Nevertheless, available and emergent evidence highlights distinct regulation for RIPK3, setting it apart from RIPK1 functionally. For example, RIPK3 lacks the death domain present in RIPK1, leaving it unable to engage death-domain containing receptors independent of RIPK1. Additionally, execution of TNFα-induced necroptosis requires RIPK3 kinase-dependent phosphorylation of Mixed-Lineage Kinase-domain Like (MLKL), a downstream effector of necroptosis (Xie, Peng, Yan, et al. 2013; Wu et al. 2013). MLKL is a requisite executioner of necroptosis: phosphorylation-dependent oligomerization and translocation of MLKL to the plasma membrane is directly linked to increases in plasma

membrane permeability, and reactive-oxygen species generation (Hildebrand et al. 2014; Li et al. 2014; Murphy et al. 2013; Cai et al. 2014; Zhao et al. 2012). Notably, RIPK3 can also activate necroptosis independent of RIPK1 (Kaiser et al. 2013; Upton et al. 2012; Wu et al. 2014). Conversely, kinase activity of RIPK3 is not required for RIPK1 kinase-dependent apoptosis (Dondelinger et al. 2013).

1.3 A brief history of Necroptosis

In living organisms, the loss of cellular and/or tissue homeostasis results in pathology and disease. Similarly, disruption in the regulation of cell death regulation has been intimately linked to a variety of disease phenotypes (Linkermann & Green 2014; You et al. 2008; Degterev et al. 2005; Ofengeim et al. 2015; Ito et al. 2016; Thompson 1995). Apoptosis, a form of cell death characterized morphologically by cellular blebbing and the appearance of apoptotic bodies, has been long viewed as an exclusive form of regulated cell death; however, it is clear today this this form of death is not solely responsible for the complexity of disease pathology. Early observations suggesting existence of the non-apoptotic, yet regulated, forms of cell death emerged from *in vitro* studies using tumor necrosis factor alpha (TNFα). In one example, Laster, Wood, and Gooding observed that TNFα could induce cell death with morphology common to either apoptosis or necrosis, the latter being reported as cellular 'boiling' or swelling and loss of plasma membrane integrity (Galluzzi & Kroemer 2008; Laster et al. 1988). Further experiments uncovered that apoptotic versus necrotic cell-death decision making was dictated in a cell-type-specific manner and was influenced by the activation status of caspases (Laster et al. 1988; Vercammen et al. 1998). In time, it became evident that necrosis can be executed in a regulated manner by the same pro-death signals that are associated with regulated apoptotic cell death. Additional works reported that a known component of TNFα-induced signaling complexes, the

kinase RIPK1, and inhibition of the activity of the specific initiator caspase, caspase-8, provides conditions for selective initiation of TNF-induced necrosis (Matsumura et al. 2000; Holler et al. 2000). These seminal studies provided first insights into the specific factors negotiating this newly defined, non-apoptotic, and regulated form of cell death that manifested with necrotic morphology (Vanden Berghe et al. 2014; Vanden Berghe et al. 2010). A small molecule screen identifying Necrostatin-1 (Nec-1) as a selective inhibitor of TNFα-induced necrosis initially qualified the term 'necroptosis' as cell death that could be blocked by Nec-1. Ensuing work reported RIPK1 kinase as the specific target of Nec-1, thereby allowing for the evaluation of RIPK1 kinase-dependent necroptosis pharmacologically in clinically relevant disease models (Degterev et al. 2008; Degterev et al. 2005).

Necroptosis signaling is initiated by numerous triggers, including, TNFα, FasL, and TRAIL, IFNs, TLRs, and virus-mediated pathways (Matsumura et al. 2000; Holler et al. 2000; Dillon et al. 2014; He et al. 2011; Thapa et al. 2013; Upton et al. 2012; Kearney et al. 2014). TNFα induced RIPK1 kinase activation and necroptosis are best understood mechanistically (Figure 2). Receptor engagement of TNFR1 by TNFα promotes formation of a membrane bound complex (Complex I), which includes RIPK1, TNF receptor-associated protein with death domain (TRADD), and TNFR-associated factors (TRAF2/TRAF5) (Micheau & Tschopp 2003). At this point, cellular inhibitors of apoptosis (cIAP1/2) and linear ubiquitin chain assembly complex (LUBAC) are recruited to the complex and ubiquitinate RIPK1; this regulation has been associated with NFκB activation that is independent of the catalytic function of RIPK1 (Figure 2).

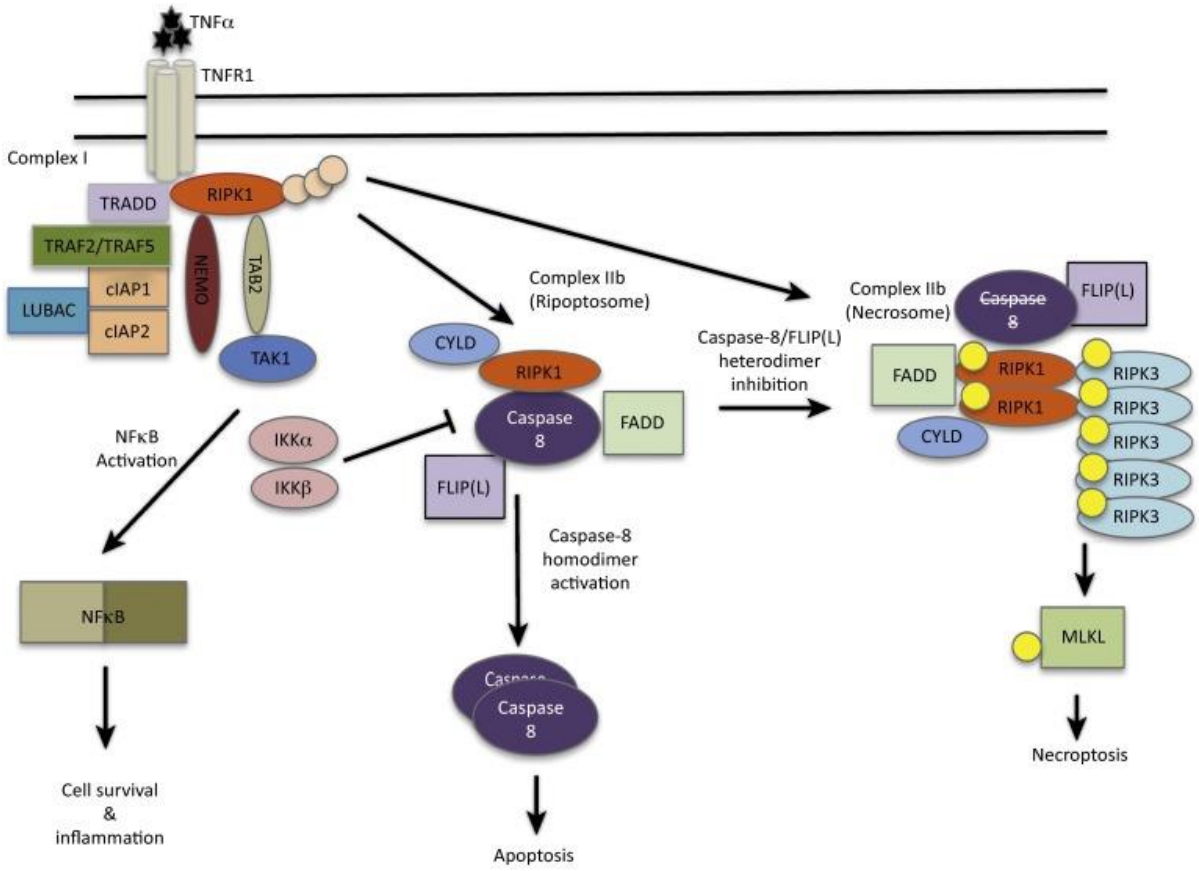

Figure 2. TNFα-induced RIPK1 kinase signaling. Wegner et al., 'Complex Pathologic Roles of RIPK1 and RIPK3: Moving Beyond Necroptosis.' *Trends in Pharmacological Sciences*. 2016. (Wegner et al. 2016).

Deubiquitination of Complex I and its association with Fas-associated protein with death domain (FADD) and caspase-8 facilitates the transition of Complex I into Complex II, a death inducing complex that may function in a RIPK1 kinase dependent or independent manner (Micheau & Tschopp 2003). 'Complex IIb' serves to signify the pro-death version of Complex II that is dependent on RIPK1 kinase, distinguishing it from 'Complex IIa' that functions independent of RIPK1 kinase (Dickens et al. 2012). Formation of Complex IIb requires deubiquitination catalyzed by CYLD (Moquin et al. 2013; Wang et al. 2008). When Complex IIb catalyzes RIPK1 kinase-dependent apoptosis that also requires caspase-8, the complex is termed the 'Ripoptosome'. In contrast, when caspases are inhibited, Complex IIb engages RIPK3, by way of homologous RHIM domains shared by RIPK1 and RIPK3. This interaction promotes formation

of a larger detergent-insoluble amyloid-like complex, also familiarly known as a 'Necrosome' (Li et al. 2012; Najjar et al. 2016) (Figure 2). Notably, the main function of necrosome nucleation in necroptosis may be to promote formation of RIPK3 homodimers, as enforced homodimerization of just RIPK3 is sufficient for necroptosis even in the absence of interaction with RIPK1 (Cook et al. 2014; Orozco et al. 2014; Wu et al. 2014). As discussed above, some studies have also demonstrated that RIPK1 kinase may be dispensable for RIPK3 kinase-dependent necroptosis (Kaiser et al. 2013; Upton et al. 2012; Dillon et al. 2014; Kaiser et al. 2014). Within necrosomes, RIPK3 undergoes phosphorylation on Ser232, which is essential for recruitment of downstream necroptosis effector, MLKL (Mandal et al. 2014; Chen et al. 2013). MLKL is unconditionally required for necroptosis as *Mlkl*$^{-/-}$ cells are resistant to this form of cell death (Wu et al. 2013; Sun et al. 2012; H. Wang et al. 2014). MLKL is directly phosphorylated by RIPK3 on Thr357/Ser358 sites within its activation loop, inducing oligomerization and a conformational change that releases the pro-necrotic plasma membrane-disrupting N-terminal four-helix bundle (Hildebrand et al. 2014; Sun et al. 2012; Chen et al. 2013; Murphy et al. 2013; Cai et al. 2014). Plasma membrane translocation of MLKL has been linked to perturbation of calcium and sodium fluxes, which are associated with increased osmotic pressure and membrane rupture (Chen et al. 2014). MLKL-dependent membrane permeabilization can be induced by enforced dimerization of just the N-terminal bundle and brace domains, and involves interactions with phospholipids, including, phosphatidyl-inositides (especially PI(4,5)P2) and cardiolipin (Quarato et al. 2016; Dondelinger et al. 2014; H. Wang et al. 2014). However, the precise mechanism of how this ultimate step in necroptosis execution occurs is still a matter of discussion.

Today we understand necroptosis as cell death that morphologically resembles classical or unregulated necrosis, displaying enlarged and swollen organelles, early plasma membrane damage with eventual rupture. Similar to un-regulated or accidental necrosis, rapid loss of plasma membrane integrity during necroptosis leads to the release of multiple damage (or danger) associated molecular pattern molecules (DAMPs), such as, IL-1α, HMGB1, ATP, uric acid, and HSPs, leading to pro-inflammatory changes (Kaczmarek et al. 2013). Importantly, specific activation of MLKL by RIPK3 kinase that may or may not also require RIPK1 kinase, defines the necroptosis pathway and distinguishes it from other forms of regulated and unregulated necrosis.

1.4 Pathogen-induced cell death[2]

1.4.1 Viral-induced cell death

The pathogenesis of viral species is uniquely dependent on their ability to replicate within host cells. Accordingly, viruses have evolved mechanisms inhibiting cell death and prolonging survival of host cells to ensure reliable replication (Galluzzi et al. 2010; Roy & Mocarski 2007; Lamkanfi & Dixit 2010). Viruses equipped to inhibit apoptosis are commonplace and are described extensively in the literature (Mocarski et al. 2012; Lamkanfi & Dixit 2010). Among known examples, Kaposi's sarcoma herpesvirus (HSV-8) and human poxvirus molluscum contagiosum encode viral-FLICE inhibitory protein (v-FLIP) family members; these molecules act in a dominant-negative fashion to inhibit caspase-8 and caspase-10 recruitment to the death-inducing signaling complex (DISC) (Bertin et al. 1997; Hu et al. 1997; Thome et al. 1997; Shisler & Moss 2001; Thurau et al. 2006). Orthopoxviruses, including cowpox, vaccinia,

[2] Reprinted from *(Saleh and Degterev 2015, pages 4-17)* with permission from publisher.

ectromelia, and rabbitpox viruses bear homologous serine-protease (serpin) inhibitors of caspases (Dobbelstein et al. 1996; Macen et al. 1996; Turner et al. 2000; Best 2008). These peptides are among a broad class of serpin protease inhibitors that bind within the active sites of target enzymes rendering them inactive. Herpesvirus family members, HSV-1 and HSV-2, encode a caspase-8 inhibitor gene, UL-39, which generates ribonucleotide reductase subunit protein, R1, also known as ICP6 or ICP10 for HSV-1 an HSV-2, respectively (Dufour et al. 2011; Mocarski et al. 2012). A third herpesviridae, cytomegalovirus (CMV), encodes a distinct inhibitor of caspase-8 function, viral-inhibitor of caspase-8 activation (vICA) (Skaletskaya et al. 2001). Caspase-8 inhibitors are also present in adenoviruses and human papilloma virus-16 (HPV-16), a strain commonly associated with cervical cancer (Kabsch & Alonso 2002). Baculoviruses express inhibitors of apoptosis, including a homologue of human X-linked inhibitor of apoptosis (XIAP) and a pan-caspase inhibitor, p35 (Birnbaum et al. 1994; Deveraux & Reed 1999; Crook et al. 1993). Apoptosis inhibitors have also been identified in the Influenza virus (Yatim & Albert 2011). Although this list is not exhaustive, it serves to illustrate that apoptosis inhibitors are common in viral species.

Emerging evidence suggests that caspase-independent death may become paramount for host-defense in the presence of anti-apoptotic signals or caspase-inhibitors. For example, fibroblasts infected with vaccinia virus underwent necrotic cell death that was reduced in cells infected with a mutant lacking caspase inhibitor B13R (Li & Beg 2000). In vaccinia infection, RIPK1- and RIPK3-dependent cell death is required to contain viral dissemination; RIPK1 kinase-inactive mice of the D138N flavor ($RIPK1^{D138N}$) and RIPK3 knockout ($Ripk3^{-/-}$) mice displayed a 10 to 100-fold increase in viral titers compared to wild-type (WT) counterparts (Cho et al. 2010; Polykratis et al. 2014). $Ripk3^{-/-}$ mice were also observed to have diminished survival and

increased viral dissemination compared to that observed in RIPK1^{D138N} mice suggesting that RIPK3 may play a more prominent role in virus-induced necroptosis. For example, cell death induced by MCMV virus, lacking RIPK inhibitor M45, has been found to involve direct activation of RIPK3 by viral DNA sensor DAI (Upton et al. 2012). These data suggest that RIPK1 and RIPK3 may play significant roles in anti-viral responses, but their activities may not be linearly connected as has been proposed in TNFα-induced cell death (Vandenabeele, Declercq, et al. 2010).

1.4.1.2 Herpes Simplex Virus 1 and 2

Herpes simplex viruses, HSV-1 and HSV-2, are viral pathogens commonly recognized for causing tissue ulceration around the oral cavity and genitals, respectively (Klein 2015a; Albrecht 2014). More severely, HSV-1 can also manifest as a life-threatening encephalitis following inoculation of the oral-pharyngeal cavity. HSV-1 encephalitis is regarded as the most common cause of sporadic encephalitis in the world (Klein 2015b).

Molecular studies have demonstrated that in murine cells HSV-1 induces programmed necrosis which limits viral replication (Xing Wang et al. 2014; Huang et al. 2015). RIPK3 deletion completely protected mouse embryonic fibroblasts (MEFs) and L929 cells from HSV-1-induced cell death. This function of RIPK3 is attributed to its kinase activity as cells expressing a kinase-dead mutant were just as viable as *Ripk3*$^{-/-}$ counterparts. L929 cells lacking RIPK1 were partially protected from cell death indicating that RIPK1 is also important for HSV-1 induced cell death. Not surprisingly, HSV-1-induced cell death also required canonical effector of necroptosis, MLKL. Knock-down of MLKL in WT MEFs or L929 cells protected against HSV-1 induced cell death. Importantly, HSV-1-induced cell death effectively limited viral propagation as *Ripk3*$^{-}$

$^{-/-}$ L929 cells generated larger viral titers than WT counterparts post-infection (Huang et al. 2015; Xing Wang et al. 2014).

Mechanistic analyses revealed that HSV-1 induced cell death was dependent on RHIM domain interactions. MEFs expressing RHIM-domain mutant of RIPK3 were protected from HSV-1 induced cell death. Authors identified that the viral RHIM-domain containing protein, ribonucleotide reductase subunit 1 (R1), also known as ICP6, induced necrosis in target cells (Xing Wang et al. 2014; Huang et al. 2015). Conversely, HSV-1 carrying a RHIM-domain mutant of ICP6 (ICP6mutRHIM) did not cause cell death. Specifically, RIPK1 and RIPK3 could be co-immunopreciptated with ICP6 in HSV-1 infected MEFs; however, no interaction was detected upon infection with virus carrying ICP6mutRHIM (Huang et al. 2015). Huang and colleagues further demonstrated that ICP6 can induce RIPK1-RIPK3 hetero interactions and RIPK3-RIPK3 homo interactions in HEK293T cells. These findings suggest that HSV-1 induced programmed necrosis requires RHIM-domain interactions of ICP6 with RIPK1 and RIPK3, which leads to induction of necroptosis in infected cells and limits viral infections (Table 1). This presents an interesting mechanism linked to the life-cycle of HSVs as expression of ICP6 has been found to be essential for the reactivation of the virus in quiescent cells and has also been reported to inhibit caspase-8 activation (DJ & Weller 1988; Langelier et al. 2002; Dufour et al. 2011).

Necroptosis improved host health and survival while limiting viral titers and propagation *in vivo* (Huang et al. 2015; Xing Wang et al. 2014). *Ripk3*$^{-/-}$ mice lost more bodyweight following infection compared to WT counterparts. Moreover, HSV-1 viral DNA was detected in greater abundance in serum, liver, and nervous tissue in *Ripk3*$^{-/-}$ animals suggesting increased viral propagation. Greater viral dissemination corresponded to worse outcomes as *Ripk3*$^{-/-}$ mice had

diminished survival compared to controls. Concordantly, viral dissemination was increased and animal survival decreased in WT mice infected with ICP6mutRHIM HSV-1 compared to WT HSV-1.

Interestingly, while two groups reported that HSV-1 is able to effectively induce cell death in murine cells, HSV-1 induced cell death was not similarly observed in human cells (Guo et al. 2015; Huang et al. 2015). Data showed that RHIM-domains of ICP6 in HSV-1 and ICP10 in HSV-2 inhibited TNFα-induced RIPK3-dependent necroptosis in human HT29 cells by competing for RHIM-domain interactions of RIPK1 and RIPK3 (Guo et al. 2011). Accordingly, ICP6mutRHIM HSV-1 did not impair TNFα-induced RIPK3 kinase dependent cell death and limited viral titers (Table 1) (Guo et al. 2015).

In sum, ICP6 induced necroptosis in a RHIM-dependent manner in murine cells while serving the opposite function, by blocking necroptosis, in human cells. These seemingly contradictory observations stress the versatility of the RHIM-domain in necroptosis signaling. It also suggests that important, yet currently unknown, mechanistic differences must exist in how human and mouse RHIM-domains interact. Irrespective of further mechanistic clarification, these findings may be reconciled by the fact that HSV-1 is a natural human pathogen and thus, may have evolved to evade human and not mouse RIPK1 and RIPK3 kinase-dependent necroptosis. Alternatively, HSV-1 may have emerged as a human pathogen because of its ability to block necroptosis specifically in human cells. Although differences between the abilities of host-pathogen interactions in humans and mice to induce necroptosis are not yet well-established, these differences may materialize as important clues in defining innate immune roles for RIPK1 and RIPK3.

1.4.1.3 Cytomegalovirus

Cytomegalovirus (CMV) is highly prevalent in the general population. Although it is benign in healthy individuals, the virus can be lethal in the immunocompromised population, including AIDS patients and transplant recipients (Friel 2014). Due to its prevalence, CMV is the most common cause of congenital infection in newborns. Mothers experiencing primary CMV infection or viral reactivation are at increased risk for vertical transmission to their unborn children. Congenital infection can lead to permanent damage, marked by hearing loss, vision impairment, and or cognitive retardation (Demmler-Harrison 2015).

In 2010, Kaiser and colleagues reported that murine CMV (MCMV) M45 protein, a RHIM-domain containing viral inhibitor of RIP activation (vIRA), was required for viral dissemination and decreased host survival (Upton et al. 2010). Further investigation resolved that the RHIM domain of vIRA inhibited RHIM domain interactions between DNA-dependent activator of interferon regulatory factors (DAI), an intracellular sensor of viral DNA, and RIPK3 that were required for RIPK3-dependent cell death. In accord, mice infected with MCMV carrying a mutation in the RHIM domain of M45 protein (M45mutRHIM) had improved survival and lower viral titers in lymphoid organs compared to mice infected with WT MCMV. Similarly, deletion of DAI or RIPK3 rescued the pathogenicity of the M45mutRHIM virus, suggesting that RIPK3-dependent necrosis mitigated viral-induced health decline of the organism and minimized viral dissemination (Upton et al. 2010; Upton et al. 2012). These findings are consistent with a model in which RIPK3-dependent necrotic cell death limits viral replication by triggering necroptosis in the infected cells to protect the host against a pathogen fortified to suppress pro-apoptotic signals (Table 1).

Analogous to MCMV, human CMV (hCMV) is able to block necrotic death in target cells. In 2015, Mocarski's group reported that low passage, newborn human foreskin fibroblasts

transduced with hRIPK3 and infected with hCMV were protected from necrotic cell death induced by either a combination of TNFα, smac mimetics (SM), and zVAD.fmk (zVAD) or M45mutRHIM MCMV infection. Importantly, in the absence of hCMV, both conditions induced death dependent on the kinase-activity of hRIPK3 as death was not observed in cells transduced with a kinase-dead mutant of RIPK3 (hRIPK3 K50A). Remarkably, phosphorylated forms of hRIPK3 and MLKL were still observed in hCMV infected cells, suggesting that hCMV differs from MCMV in that it blocks programmed necrosis downstream of RIPK3 and MLKL activation through a yet to be defined mechanism. An approach utilizing UV-light induced viral mutagenesis revealed that viral regulatory protein, IE1, known to modulate host gene expression and innate immune signaling, was required by hCMV to block programmed necrosis. Expectedly, deletion of IE1 increased sensitivity to hRIPK3-induced cell death and resulted in decreased viral titers *in vitro* (Omoto et al. 2015).

Human and murine CMVs apply different strategies in blocking RIPK3-dependent cell death. This may reflect evolutionary variations in viral species to accommodate specificities of host cell biology. For example, although RHIM-domain interactions may be sufficient to block RIPK3-dependent cell death in murine cells, this may not be true for human hosts. The current evidence indicates that hCMV is armed with mechanisms independent of RHIM-domain interactions to block necroptosis. This hypothesis is further supported by the previous observation that the RHIM-domain containing protein that blocks HSV-induced cell death in mouse cells fails to do so in human hosts. Altogether, these dichotomous observations suggest that fundamental differences between RIPK3-dependent cell death pathways in human and mouse systems are not fully understood.

1.4.1.4 Reoviruses

Mammalian orthoreoviruses (Reoviruses) comprise a family of double-stranded RNA viruses known to cause respiratory and enteric infections. Although most reoviruses are not associated with clinical disease, the rotavirus, a species of reovirus, is the most common cause of gastroenteritis, resulting in diarrhea and fever in children (O'Ryan & Matson 2015).

Reoviruses are known to induce caspase-dependent apoptosis in target cells (Clarke et al. 2003; Richardson-burns et al. 2002; Danthi et al. 2013). However, recent studies also suggested activation of viral-induced necroptosis. The Type-3 Dearing (T3D) strain induced cell-death in murine L929 fibrosarcoma cells that could not be blocked by inhibition of caspases, but was blocked by Nec-1, suggesting that cell death was RIPK1 kinase dependent (Berger & Danthi 2013) (Table 1).

Mechanisms responsible for the activation of necroptosis by reoviruses are currently unknown. Additionally, the functional value of RIPK1 kinase-dependent mechanisms in reoviral disease, including control of viral counts *in vivo*, duration of infection, tissue histopathology, and health outcomes, remains to be established.

1.4.5 Influenza A

Influenza viruses, part of the broader orthomyxoviridae family, are enveloped negative-strand RNA viruses that include strains A and B. The virus is readily aerosolized and communicable in the human population, causing a self-limited, acute, seasonal respiratory tract infection, identified as *Influenza* or *Flu*. Patients manifest with upper and or lower-respiratory tract illness in conjunction with signs of systemic illness including, fever, headache, muscle pain, and weakness. Certain high-risk patient populations, such as the elderly, pregnant, and

immunosuppressed may develop a more complicated illness, marked by pneumonia or infection of the nervous system (Dolin 2015; Yatim & Albert 2011).

Three studies have closely examined roles for RIPK3 in driving cell death signaling following Influenza A viral (IAV) infection. Experiments revealed that IAV infection of MEFs and alveolar epithelial cells drives cell death that is dependent on RIPK3 and is associated with (necrosome) complex formation of RIPK3 with RIPK1, FADD, and MLKL (Nogusa, Thapa, et al. 2016; Kuriakose 2016). RIPK3 activates pro-apoptotic signaling by way in coordination with RIPK1, FADD, and caspases as well as necroptotic signaling, which requires MLKL, to drive cell death. Notably, this signaling is induced by the intracellular nucleotide sensor DAI/ZBP1/DLM-1 which also nucleates necrosome complexes (Thapa et al. 2016). *In vivo*, *Ripk3*$^{-/-}$ mice had diminished survival, increased viral titers, and decreased lung inflammatory cell infiltrates, compared to WT counterparts following IAV infection. Similarly, in the absence of FADD and MLKL, mice had diminished survival and increased viral titers compared to in the absence of MLKL alone, suggesting that RIPK3 dependent apoptosis and necroptosis are required for protection against IAV (Nogusa, Thapa, et al. 2016).

In another study, deletion of RIPK1 ubiquitin-ligase, cellular-inhibitor of apoptosis 2 (cIAP2), promoted Influenza A-induced respiratory tissue necrosis that was dependent on RIPK1 kinase-activity and RIPK3. This study also reported that cIAP2 deficient mice had diminished survival without alterations in viral load (Rodrigue-Gervais et al. 2014). Moreover, cIAP2 knockout mice treated with Nec-1 or also carrying a deletion of RIPK3 were protected from pathologic features of tissue necrosis and displayed improved survival. Nevertheless, loss of RIPK3 on a cIAP2 knockout background did not alter viral titers, indicating that early death in cIAP2 knockout mice was likely a consequence of respiratory-failure as opposed to unbridled viral burden. These

data provide evidence that in the absence of cIAP2, RIPK1 and RIPK3-dependent cell death are not required to limit viral propagation, but rather to promote lethal tissue injury as a feature of the viral pathogenesis (Rodrigue-Gervais et al. 2014) (Table 1).

It is well-established that cIAPs are important physiologic inhibitors of RIPK-dependent necroptosis (McComb et al. 2012). Accordingly, RIPK1 and/or RIPK3 may be inappropriately activated in the absence of cIAP2. Acute activation of RIPK1 and RIPK3-dependent cell death following viral infection suggests that RIPK1 and RIPK3 function is specifically modified following infection, either as a consequence of direct viral regulation or secondary to local tissue inflammation and death receptor ligation. Indeed, deletion of death-receptor ligand, FasL, normalized animal survival, suggesting that RIPK1 and RIPK3 are inappropriately activated downstream of FasL in cIAP2 knockout mice (Rodrigue-Gervais et al. 2014). Furthermore, fluorescence activated cell-sorting (FACS) analysis demonstrated that both uninfected and infected respiratory epithelia of cIAP2 knockout mice were more likely than their WT counterparts to undergo necrotic cell death, suggesting that cell death is induced by an exogenously released factor(s) rather than the virus itself (Rodrigue-Gervais et al. 2014). Finally, authors found that *Ripk3*$^{-/-}$ mice did not have surplus viral burden, deficits in viral clearance, or excess tissue-injury compared to WT counterparts (Rodrigue-Gervais et al. 2014). Notably, this was in marked contrast to more recent studies summarized above in spite of the fact that both groups reported studies using the PR8 strain. Altogether, these works point to an important role for cell death pathways mediated by RIPK1 and RIPK3 kinases in controlling host-responses in the context of Influenza pathogenesis.

1.4.2 Bacterial-induced cell death

Bacteria are able to replicate independently of the host-cell and thus bacterial pathogenesis is oftentimes not strictly dependent on host-cell survival. Nevertheless, certain bacterial species survive and proliferate intracellularly. For these species, host-cell integrity and longevity may be paramount (Pujol & Bliska 2005). Recent studies have underscored the roles of RIPK1 and RIPK3 dependent cell death as important features of bacterial infection. However, it remains to be fully determined whether infection-associated activation of RIPK1 and RIPK3 signaling serves as a feature of the host-response or an exploitable weakness in host-defense. Examples of RIPK1 and RIPK3 dependent regulation of the host-response against specific bacterial pathogens are examined below.

1.4.2.1 Yersinia

Yersinia species are gram-negative enteric pathogens that include the human pathogenic forms *Yersinia Pestis*, *Yersinia Pseudotuberculosis*, and *Yersinia Entercolitica*. *Pestis* is notorious for its ferocity and was the root of the black plague in medieval Europe (Sexton 2014). Unlike *Pestis*, *Pseudotuberculosis* and *Entercolitica* are generally not lethal and produce similar symptoms with fever, abdominal pain, and diarrhea (Tauxe 2013). However, *Pseudotuberculosis* can also manifest with tuberculosis-like symptoms, including tissue necrosis and granulomas in the spleen, liver, and lymph nodes (Viboud & Bliska 2005). Virulence of these bacteria is dependent on the translocation of a series of pathogenicity factors, called, Yersinia outer proteins (Yops), which are exported from the bacteria into host cells by a bacterial encoded protein translocation system, the type-III secretion system (TTSS) (Viboud & Bliska 2005; Zhang et al. 2011; LaRock & Cookson 2012).

Phagocytic cells, in particular macrophages and dendritic cells, play important roles in the pathogenesis of *Yersinia* species. During infection, these host immune cells engulf bacteria and

facilitate their systemic spread, specifically to mesenteric lymph nodes, spleen, and liver (Viboud & Bliska 2005). Significantly, all three human pathogenic *Yersinia* species have also been shown to survive and possibly replicate within macrophages and dendritic cells (Pujol & Bliska 2005; Bliska 2003; Pujol et al. 2009). Accordingly, programmed cell death of phagocytic cells in *Yersinia* infection may be an important feature of the host-response.

Recent studies have uncovered important roles for RIPK1 in *Yersinia*-induced macrophage cell death. Pharmacologic inhibition of RIPK1 prevented *Yersinia* induced cell death in macrophages (Weng et al. 2014; Philip et al. 2014). RIPK1 deficient fetal-liver derived macrophages were also resistant to *Yersinia Pestis* induced cell death. Notably, *Yersinia*-induced cell death was also shown to require caspase-8 and kinase activity of RIPK3 (Weng et al. 2014). Although macrophages lacking caspase-8 or RIPK3 or treated with RIPK3 inhibitor, GSK'872, were not protected from *Pestis*-induced death, combined loss of caspase-8 and deletion or inhibition of RIPK3 resulted in complete protection (Weng et al. 2014). The sufficiency of RIPK1 kinase and either caspase-8 or RIPK3 for cell death, suggests that RIPK1 may function to activate either caspase-8-dependent apoptosis or RIPK3-dependent cell death in response to *Yersinia* infection.

Caspase-8 and RIPK3 double-knockout animals had increased susceptibility to infection by *Yersinia* (Weng et al. 2014; Philip et al. 2014). These mice had increased bacterial colony-forming units in spleens, increased inflammatory infiltrates in hepatic tissue sections, and diminished survival. As noted during viral infection, inhibition of cell death during *Yersinia* infection was detrimental to organism survival. Resultantly, elimination of infected host-cells is likely important for the control of *Yersinia* as it is for viruses because both pathogens can survive and replicate intracellularly. Altogether, these observations suggest that engaging RIPK1 kinase

dependent apoptosis requiring caspase-8 or RIPK1 kinase-dependent necroptosis requiring RIPK3 may be utilized by the host to combat *Yersinia* infection. (Table 1).

In parallel, caspase-1-dependent pro-inflammatory cell death, pyroptosis, may also be engaged in *Yersinia*-induced, RIPK1 dependent, cell death of phagocytic cells. This hypothesis is supported by an experiment showing that *Yersinia*-infection resulted in reduced production of the cleaved or active form of caspase-1 in the absence of RIPK1 (Weng et al. 2014). This regulation is likely driven by cell extrinsic TNFα (Peterson et al. 2016)

Yersinia-induced RIPK1 kinase dependent cell death has been attributed to YopJ, one of the Yop pathogenicity factors that is well known for inhibiting pro-inflammatory and pro-survival NFκB and MAPK signaling in target cells. Interestingly, macrophages infected with *Yersinia* mutants lacking functional YopJ (Δ*YopJ*) were protected from RIPK1 kinase dependent cell death. YopJ induced cell death was prompted by two independent signaling axes, one which required the Toll-like receptor 4 adaptor protein, TRIF, and the other which was dependent on cell extrinsic TNFα released from poorly infected cells in culture (Peterson et al. 2016). These data support a model in which host immune cells may have evolved new modalities of YopJ-induced cell death to mitigate bacterial pathogenicity in the face of a bacterial agent, YopJ, which limits protective inflammatory responses (Table 1).

Observations reported here cement a role for RIPK1 (kinase)-dependent cell death in *Yersinia*-infection. Although it is unclear whether RIPK1 induces primarily an apoptosis, necroptosis, or pyroptosis, or perhaps some combination of the three, the *Yersinia*-infection model uncovers novel infection-associated cell death regulation by RIPK1. Moreover, recognizing that *Yersinia* species have the capacity to survive and possibly replicate within phagocytic cells, it is not

surprising that programmed elimination of infected immune cells protects against dissemination of *Yersinia* in the host.

1.4.2.2. *Salmonella*

Salmonella Enterica species *(Salmonella)* are gram-negative facultative intracellular bacilli which cause gastroenteritis in humans with symptoms including fever, diarrhea, and abdominal pains (Kotton & Hohmann 2013). Similar to other bacteria which can survive and replicate in host immune cells, *Salmonella* is able to commandeer anti-inflammatory M2 macrophages, spread systemically, and seed lymphoid tissue (Behnsen et al. 2015; Alpuche-aranda et al. 1994; Nix et al. 2007; Kotton & Hohmann 2013; McCoy et al. 2012). Dissemination of *Salmonella* can promote tissue specific damage including abscess formation and osteomyelitis as well as systemic infection or sepsis (Hohmann 2014).

A recent study demonstrated that *Salmonella* induced type-I interferon (IFN-I) signaling resulted in macrophage necroptosis (Robinson et al. 2012). Macrophages deficient in the interferon-alpha receptor *(Ifnar$^{-/-}$)*, which is required for sensing IFN-Is (Inteferon α and/or Interferon β), or cultured with anti-IFN-I antibodies, were resistant to *Salmonella* induced death. Inhibition of RIPK1 blocked over 60% of cell death induced by S*almonella* in WT macrophages which was similar to the extent of death observed in IFNaR knockout macrophages. Moreover, deletion or knockdown of RIPK3 in macrophages abrogated *Salmonella*-induced cell death (Robinson et al. 2012).

Both *Ifnar$^{-/-}$* and *Ripk3$^{-/-}$* mice had decreased bacterial load and increased numbers of circulating macrophages compared to WT counterparts. This protective phenotype was likely conferred by the hematopoietic compartment as *Ifnar$^{-/-}$* bone-marrow transplanted into WT mice limited

bacterial titers. Curiously, *Ripk3*$^{-/-}$ mice did not have improved survival indicating that bacterial titers do not necessarily correlate with organism survival in the case of *Salmonella* infection (Robinson et al. 2012).

These paradoxical observations merit investigation into the relationship between *Salmonella* titers and manifestation of disease. One may inquire whether increased macrophage survival in the absence RIPK3 is underestimating total bacterial loads by excluding intracellular bacteria. In this case, necroptosis of anti-inflammatory M2 macrophages may serve to limit intracellular proliferation of *Salmonella* and contain infection. Nevertheless, these data suggest that *Salmonella* infection presents another model of RIPK1 and RIPK3-dependent innate immune regulation. Interestingly, this regulation manifests by a mechanism that is distinct, and perhaps functionally opposite, from cell death induced by *Yersinia* (Table 1).

1.4.2.3. *Escherichia coli*

Escherichia coli (E.coli) is a gram-negative bacterial species that includes a diversity of strains or serotypes. Although the majority of these serotypes are benign, some have procured the capacity to cause serious infection and tissue damage. One such pathogenic strain, *Enteropathogenic E.coli (EPEC)*, is associated with sporadic diarrheal illness, particularly in young children. The pathogenesis of virulent strains of *E.coli* are attributed to the acquisition of toxic effectors that are injected into target or host cells (Wanke 2013).

Nleb1 is a pathogenicity effector protein found among species of *E.coli* and *Salmonella*. Mechanistic analyses revealed Nleb1 possesses N-acetylglucosamine transferase activity that modifies a conserved arginine residue in death-domain containing proteins, including TNFα Receptor (TNFR), TNF receptor-associated death domain (TRADD), FAS receptor (FasR), and

RIPK1 (Li et al. 2013; Pearson et al. 2013). Nleb1 enzymatic activity blocked TRADD oligomerization and death receptor induced signaling complex (DISC) formation (Li et al. 2013; Pearson et al. 2013). Pearson and colleagues found that Nleb1 co-immunoprecipitated with death domain proteins, TRADD, FADD, and RIPK1 in 293T cells. In addition, Nleb1 abolished death-receptor induced apoptosis in HeLa-cells and TNFα/zVAD/SMAC mimetic-induced necroptosis in RIPK3-expressing HeLa cells (Li et al. 2013). In murine infection models, *EPEC* either lacking Nleb1 or carrying enzymatically inactive Nleb1 mutants were unable to effectively colonize host gastrointestinal tracts (Li et al. 2013). These findings suggest that multiple cell death pathways, including RIPK3-dependent cell death, may be manipulated by Nleb1 expressing *E.coli* to establish infection, potentiate survival of infected cells, and minimize associated tissue destruction. Specific roles for RIPKs in Nleb1-associated infection remain to be elucidated (Table 1).

1.4.2.4 Pore-forming toxin producing bacteria

Pore-forming proteins (PFPs) are bacterial toxins that increase host-cell membrane permeability and thereby contribute to bacterial virulence. Some commonly recognizable virulent bacterial species and their significant clinical presentations include: *E.coli* (urinary tract infections and gastroenteritis), *C. diphtheria* (diphtheria; upper respiratory infections), *C. perferinges* (tissue necrosis and gas gangrene), *C. septicum* (tissue necrosis and gas gangrene), *B. anthracis* (anthrax; pneuomonia, gastroenteritis, and or cutaneous ulcers), *L. monocytogenes* (gastroenteritis and meningitis), *S. aureus* (cellulitis, impetigo, abscess, and respiratory tract infections), *V. cholera* (diarrhea and dehydration), and *Y. pseudotuberculosis* (gastroenteritis) (Bischofberger et al. 2012).

PFP associated changes in membrane permeability may serve in any of a variety of functions in bacterial pathogenesis. The literature includes precedents of PFPs that direct translocation of effector proteins or other toxins into host-cells; facilitate microbial invasion of the intracellular space; disrupt host-cell ion-homeostasis and energy balance; alter membrane compartment dynamics; and/or promote direct host-cell destruction. For example, type-III secretion systems (TTSS) of gram-negative bacteria, like *Yersinia* and *Salmonella* species, use PFPs to translocate effector proteins into target cells (Zhang et al. 2011). Alternatively, *Listeria monocytogenes'* PFP, listeriolysin O (LLO) blocks acquisition of anti-bacterial proteins by *Listeria* containing host-cell vacuoles (Bischofberger et al. 2012).

At high PFP concentrations, host-cell death occurs by necrosis; however, at low PFP concentrations, cell death has been linked to apoptosis, necroptosis, as well as pyroptosis (Knapp et al. 2010; Kennedy et al. 2009; Lin et al. 2010; Boyden & Dietrich 2006; Craven et al. 2009). In the latter instance, the lack of uniformity in cell-death suggests that host-cell demise may be part of a regulated host-response as opposed to a generalized manifestation of death secondary to overly cumbersome cell stress or membrane perforation. Notably, Nec-1 inhibited necrosis induced by *clostridium perferingees*' PFP, *clostridium perferingees* β-toxin (CPB), specifying RIPK1 kinase-dependent regulation of CPB-induced necrosis (Autheman et al. 2013).

A study published by Kitur and colleagues suggested that RIPK1 and RIPK3-dependent necrosis may not be beneficial to the host. Kitur observed that toxin-induced programmed necrosis is a major mechanism of lung damage by methicillin-resistant *Staphylococcus Aureus (MRSA or SA)*, strain USA300. Authors reported that *SA* infection induced programmed necrosis in THP-1 human monocytes that was inhibited by Nec-1 or the MLKL inhibitor necrosulfonamide (NSA). Cytotoxicity was attributed to pore-forming toxin, α-hemolysin (Hla), and other leukotoxins as

macrophage cell death could be induced by bacterial conditioned media alone, but was abrogated by conditioned media from selective toxin-null mutant strains. Remarkably, murine lung infection models uncovered that deletion of RIPK3 or blockade of necrosis by Nec-1 enhanced bacterial clearance and limited tissue injury. Furthermore, WT mice had diminished macrophage populations in lung tissue compared to *Ripk3*$^{-/-}$ counterparts following infection (Kitur et al. 2015). These findings suggest that toxin-producing bacterial species such as SA, may aggravate tissue damage and cause localized immunodeficiency to enhance bacterial infection and thereby compromise host-survival (Table 1).

Although the collected data indicates that RIPK1 and RIPK3 may be important in models of PFP-bacterial infection models, it is unclear as to whether RIPK1 or RIPK3 dependent cell death generally serves as an advantageous or injurious feature of the host-response. The majority of reports available do not explore the contribution of RIPK1 or RIPK3 dependent cell death in PFP-associated bacterial dissemination and organism survival. Accordingly, the role of RIPK1 and RIPK3 dependent cell death in PFP-associated bacterial pathogenesis remains unclear.

1.4.2.5. *Mycobacterium tuberculosis*

Mycobacterium tuberculosis (M.tb) is the causative agent of *Tuberculosis (Tb)*, an infectious disease that is communicable by respiratory secretions in humans. Although Tb commonly manifests in the lungs because aerosolized particles descend into pulmonary recesses, the infection can disseminate systemically if poorly contained. *Tb* is established in one of three forms: primary, latent, and reactivation. Primary *tb* is active or fulminant *tb* that occurs following a new or initial exposure. Latent *tb* is established when a new infection enters a state of dormancy and is thought to occur when invading M.tb are confronted by a robust immune response. In this case, the host is neither contagious nor exhibits the symptoms of *tb*, and is

labeled a carrier. The third form, reactivation *tb*, is defined as the emergence of active or symptomatic *tb* in a carrier (Pozniak 2015; Schluger & Rom 1998).

The genesis of *tb* is a complex process that is poorly understood; however, it is accepted that macrophages are required to contain infection (Ulrichs & Kaufmann 2006). Additionally, TNFα is recognized as a critical cytokine in the development of *tb*; for example, patients with Rheumatoid Arthritis on an anti-TNFα regimen are more likely to develop reactivation of *tb* (Miller & Ernst 2009). Patients with compromised immunity, who are immunodeficient or immunosuppressed, are also at increased risk of developing primary or reactivation *tb* (Pozniak 2015). Models of tuberculosis in zebrafish have demonstrated that exogenous TNFα can limit mycobacterial titers in animals with deficiencies in TNFα synthesis (Tobin et al. 2012; Tobin et al. 2010; Roca & Ramakrishnan 2013). Roca and Ramakrishnan have specifically reported that high TNFα induces production of reactive oxygen species (ROS) and thereby augments macrophage bacteriocidal activity while promoting RIPK1 kinase and RIPK3 dependent necroptosis. As TNFα is the best known inducer of necroptosis *in vitro* and *in vivo*, these data may suggest involvement of RIPK1 and RIPK3, but this has not yet been established directly in a physiologic M.tb infection model. Additionally, the associations noted above prompt questions examining the roles of RIPK1 and RIPK3 on organism health and survival in M.tb infection (Table 1).

1.4.2.6. Summary of pathogen-induced cell death

Multiple lines of evidence suggest that activation of RIPK1 and RIPK3 dependent cell death is an important consequence of host-pathogen interactions. In cases of viral infections, the available data indicate that engagement of RIPK1 and RIPK3 signaling limits viral pathogenesis. By comparison, in cases of bacterial infection, the available data reveal that the competitive

advantage conferred by initiating RIPK1 and/or RIPK3 dependent cell death may lie with the host or the bacteria, depending on the identity of the bacteria. For example, cell death may function as part of the productive innate immune responses to mitigate infection; alternatively, cell death may be induced by bacteria to eliminate immune cells and trigger massive tissue damage and thus, may be targeted for therapeutic intervention. A broader understanding of the bacterial contexts regulating RIPK1 and RIPK3 dependent cell death and their underlying mechanisms remain to be clarified.

Table 1. Roles of RIPK1 and RIPK3 in Pathogen-induced cell death.

**Reprinted from (Saleh and Degterev 2015, Table 1) with permission from publisher.*

Microbe	Host-Species	Caspase-inhibitor	Mechanism of RIPK inhibition	Mechanism of RIPK activation	RIPKs	Function of RIPK-dependent signaling in host cell	Impact of RIPK-dependent signaling on organism
Vaccinia Virus	Murine	SPI-2 or B13R (Serpin)		Undefined	RIPK3	Induces host-cell death	Reduced viral titers and improved host-survival
Reoviruses (T3D strain)	Murine (L929 cells)	Undetermined		Undefined	RIPK1	Induces host-cell death	Undefined
Influenza-A	Human	NS1		Death-receptor ligation/FasL-Fas	RIPK1 and RIPK3	Induces tissue injury/death (in the absence of cIAP2)	Diminished survival (in the absence of cIAP2)
				DAI-dependent	RIPK3	Induces host-cell death	Limits viral propagation
HSV-1	Murine	UL-39/ICP6		RHIM-domain interaction of ICP6	RIPK1 and RIPK3	Induces host-cell death	Reduced viral titers and improved survival
HSV-1	Human	UL-39/ICP6	ICP6 competing for RHIM-domain interactions between RIPKs		RIPK1 and RIPK3	Inhibits host-cell death	Enhanced viral propagation
HSV-2	Human	UL-39/ICP10	ICP10 competing for RHIM-domain interactions between RIPKs		RIPK1 and RIPK3	Inhibits host-cell death	Undefined
MCMV	Murine	vICA, Bax, Bak	M45 disrupting RHIM-domain interactions between DAI and RIPK3		RIPK3	Inhibits host-cell death	Enhanced viral propagation and diminished organism survival
hCMV	Human	vICA, Bax, Bak	IE1		Undefined	Inhibits host-cell death	Enhanced viral propagation and increased cell death.
Yersinia	Murine	Undefined		YopJ	RIPK1	Induces host-cell death	Reduced bacterial propagation, tissue damage, and improved survival.
Salmonella	Murine	Undefined		Salmonella induced IFN-I	RIPK1 and RIPK3	Induces host-cell death	Undetermined
E.coli (EPEC)	Murine and Humans	Undefined	Death domain interactions of Nleb1		RIPK1	Inhibits host-cell death	Undetermined
Clostridium Perferinges	Porcine	Undefined		CPB	RIPK1	Induces host-cell death	Undetermined
Staphylococcus Aureus (Methicillin-Resistant, Strain USA300)	Murine	Undefined		Toxins (Undefined)	RIPK1 and RIPK3	Induces host-cell death	Increased tissue destruction, decreased tissue macrophages, increased bacterial titers.
Mycobacterium tuberculosis	Zebrafish	Undefined		Infection induced TNFα	RIPK1	Induces ROS generation and host-cell death	Undetermined

1.5. Inflammation[3]

Inflammation is an integral part of the host-response (Kumar et al. 2010). RIPK1 and RIPK3 are well-recognized for inducing a necroptosis, a pro-inflammatory form of cell death; however, accumulating evidence suggests that in some cases these enzymes may also regulate inflammation independent of necroptosis. It should be noted that this distinction may be difficult to draw in many cases due to the highly-intertwined nature of cell death and inflammation. The ensuing discussion highlights emerging, but still poorly characterized roles for RIPK1 and RIPK3 in amplifying the host-inflammatory response following cytokine stimulation, activation of innate immune receptors, and microbial infection.

1.5.1. Kinase-independent inflammatory roles of RIPK1

TNFα is well recognized for regulating RIPK1 kinase-dependent cell death; however, TNFα is also a major pro-inflammatory cytokine that promotes Nuclear Factor Kappa B (NFκB) associated inflammation (Christofferson et al. 2012; Vandenabeele, Declercq, et al. 2010; Hitomi et al. 2008; Kelliher et al. 1998). Kinase-independent function of RIPK1 has been linked to NFκB activation in response to TNFα. Expression of kinase-inactive RIPK1 restores defective TNFα-induced NFκB activation in *Ripk1*$^{-/-}$ Jurkat cells (Ting & Pimentel-muiffios 1996). Similarly, analysis of nuclear extracts from embryonic fetal-liver derived transformed pre-B cells demonstrated decreased NFκB-DNA binding in electrophoretic mobility shift assays in *Ripk1*$^{-/-}$ cells (Kelliher et al. 1998). Conspicuously, reports have found that TNFα-induced NFκB activation is associated with covalent modification of RIPK1 (Zhang et al. 2000). These findings

[3] Reprinted from *(Saleh and Degterev 2015, 22-27)* with permission from publisher.

highlight an important role for kinase-independent function of RIPK1 in promoting TNFα-induced NFκB driven inflammation.

Roles for RIPK1-dependent NFκB regulation have also been uncovered downstream of innate immune receptors. In 2004, Tschopp and colleagues noted that RIPK1 promotes NFκB activation downstream of TLR3, the pathogen-recognition-receptor (PRR) for sensing viral double-stranded RNA (Meylan et al. 2004). Activation of NFκB pathway, assessed by phosphorylation of inhibitor of kappa B (IκB), is impaired in MEFs lacking RIPK1 following stimulation with TLR3 agonist, Poly(I:C). Exogenous protein expression in HEK293T cells demonstrated that RIPK1 associates with TLR3 adapter protein, TRIF, by common RHIM-domain interactions. Furthermore, expression of TLR3, TRIF, and RIPK1 in HEK293T cells resulted in their co-immunopreciptation, suggesting that the three factors may complex following receptor activation (Meylan et al. 2004). Similar studies in MEFs demonstrated that RIPK1 is required for NFκB activation following ligation of TLR4 with gram-negative bacteria associated pathogen-associated molecular pattern, lipopolysaccharide (LPS) (Cusson-Hermance et al. 2005). Importantly, LPS-induced NFκB activation also requires TRIF (Cusson-Hermance et al. 2005). Finally, studies found that TRIF-dependent NFκB activation manifested in correlation with increased phosphorylation and ubiquitylation of RIPK1, suggesting importance of post-translational modification in RIPK1-dependent NFκB activation. Together, these results find that RHIM-domain interactions likely facilitate a role RIPK1 in NFκB activation downstream of innate immune receptors, TLR3 and TLR4.

Apart from NFκB signaling, kinase-independent scaffold properties of RIPK1 have also been recognized in PRR activation of the interferon-inducing transcription factor, Interferon Regulatory Factor 3 (IRF3) (Rajput et al. 2011). RIPK1 localizes to mitochondria in association

with cytosolic RNA/DNA sensor RIG-I following viral infection with Sendai Virus (SeV). These events occur in coordination with IRF3 activation and expression of downstream genes. Knockdown of RIPK1 impairs SeV induced IRF3 activation. Moreover, MEFs reconstituted with a non-ubiquitylatable form of RIPK1 at K377 have deficits in SeV-induced IRF3 activation, indicating that ubiquitin conjugation of RIPK1 at K377 is necessary for activation of IRF3 (Rajput et al. 2011). Remarkably, in spite of an abundance of evidence linking ubiquitylation of RIPK1 to NFκB activation, these studies found no changes in NFκB activation following SeV infection. Accordingly, it appears as though RIPK1 may be a versatile regulator in innate immune pathways and precise action of RIPK1 is determined in a context dependent manner.

Few studies have ventured to uncover roles for RIPK1-dependent inflammation in bacterial infection models. However, recent investigation of RIPK1 in *Yersinia* infection discovered that *Ripk1*$^{-/-}$ fetal liver macrophages carried defects in LPS as well as *Yersinia* induced secretion of IL-6, a pyrogen that directs systemic inflammatory responses. Additionally, caspase-1 cleavage was diminished in *Ripk1*$^{-/-}$ fetal-liver macrophages infected with *Yesinia* species, indicating that RIPK1 may be required for caspase-1 driven inflammasome activation and consequently, IL1β and IL-18 secretion (Weng et al. 2014). It is unclear as to whether IL6 secretion and or caspase-1 cleavage requires RIPK1 kinase activity as authors did not report efficacy of RIPK1 kinase-inhibitors; however, the authors did report that IL1β production was blocked in the presence of a RIPK1 kinase inhibitor. Importantly, these observations identify roles for RIPK1 in multiple pro-inflammatory pathways in a model of gram-negative bacterial infection.

1.5.2. Kinase-dependent inflammatory functions of RIPK1

Although kinase activity of RIPK1 has almost exclusively been linked to cell death, a number of recent reports suggested that inflammasome activation by RNA-viruses, including VSV, SeV,

and influenza (Flu), may occur in a RIPK1 kinase-dependent manner. The inflammasome is a molecular complex comprised of the receptor NLRP3 and Caspase-1 that is responsible for the maturation and secretion of pro-inflammatory cytokines, IL1β and IL-18. Nec-1 or knock-down of RIPK1 reduced IL1β secretion in bone-marrow derived macrophages (BMDMs) infected with VSV (Xiaqiong Wang et al. 2014).This regulation was also found to require RIPK3 as *Ripk3*$^{-/-}$ BMDMs also have similar deficits in inflammasome activation following RNA virus infection. It is worthwhile noting that in contrast to these observations, another group found that neither RIPK1 or RIPK3 were required for IL1β production induced by VSV in macrophages (Moriwaki et al. 2016). However, this difference may be attributable to differences in experimental design as Wang and company examined IL1β after a 6 hour infection period whereas Moriwaki et al. examined the same readout after a 2 hour infection period followed by a 4 hour incubation. Indeed, a baseline difference exists in IL1β production in response to VSV infection between the two experimental set ups.

In a physiologic system, *Ripk3*$^{-/-}$ mice produce reduced levels of IL1β and IL-18 in response to infection with RNA viruses (Xiaqiong Wang et al. 2014). Surprisingly, MLKL was not required for inflammasome activity, as ascertained using MLKL knockout (*Mlkl*$^{-/-}$) BMDMs, suggesting that RIPK1 and RIPK3 regulate inflammasome activation independent of necroptosis pathway. Moreover, VSV-induced minimal death in target cells indicating that RIPK1 and RIPK3 were likely not regulating alternative death pathways such as pyroptosis. Mechanistic analysis revealed that RIPK1 and RIPK3 complexed with mitochondrial fission protein, DRP1, and were required for translocation of DRP1 to mitochondria following infection. DRP-1 was required for RNA-virus induced mitochondrial fission, mitochondrial aggregates, ROS generation, and inflammasome activation as well. Poly(I:C), a double-stranded RNA mimic, was found to induce

NLRP3-dependent inflammasome activation in a RIPK1, RIPK3, and DRP1-dependent manner, indicating that viral nucleic acids may be the ignition for RIPK1 and RIPK3-dependent inflammasome activation (Xiaqiong Wang et al. 2014).

Intrinsic kinase-activity of RIPK1 may also underlie certain tissue specific inflammatory processes. Ptpn6^{spin} mice harboring a Tyr208Asn mutation in the non-receptor protein tyrosine phosphatase Src-homology region 2 domain-containing phosphatase-1 (SHP-1) develop foot-pad inflammation that is RIPK1 kinase-dependent (Lukens et al. 2013). Studies revealed that aberrant production of the cytokine IL1α exacerbates inflammation in Ptpn6^{spin}-mediated disease. Nec-1 diminished IL1α expression and ameliorated footpad inflammation in Ptpn6^{spin} mice. Additionally, reconstitution of WT mice with Ptpn6^{spin}/*Ripk1*$^{-/-}$ fetal-liver (hematopoietic precursor) cells abrogated the inflammation produced by transfer of Ptpn6^{spin}/*Ripk1*$^{+/+}$ fetal-liver cells. Notably, Ptpn6^{spin}/*Nlrp3*$^{-/-}$, Ptpn6^{spin}/*Caspase-1*$^{-/-}$, or Ptpn6^{spin}/*Ripk3*$^{-/-}$ mice were not protected from Ptpn6^{spin}-inflammatory disease. The findings suggest a critical role for kinase function of RIPK1 in hematopoietic cells to promote IL1α-dependent inflammation that is independent of inflammasome components and RIPK3 (Lukens et al. 2013).

Similarly, mouse models of RIPK1 and RIPK3 kinase activation, such as tissue-specific caspase-8 deletion in dendritic cells, keratinocytes, and or intestinal epithelium, have spawned inflammatory disease in mice (Kovalenko et al. 2009; Günther et al. 2011; Cuda et al. 2014). Although it may be unclear as to whether inflammation in some of these models is occurring independent of necroptosis, Cuda and colleagues observed that deletion of caspase-8 in dendritic cells (DCs) generated an autoimmune condition in mice that could not be attributed to impaired cell survival or a RIPK3-mediated processes. Caspase-8 deletion in DCs crossed to *Ripk3*$^{-/-}$ mice were not protected from inflammatory pathology. Rather, authors observed that systemic

inflammation was partially dependent on MYD88 and also found that Nec-1 abrogated Toll-like receptor activation-induced expression of TNFα, IL-6, and IL-1β (Cuda et al. 2014). These accounts suggest roles for kinase-function of RIPK1 in regulating Toll-like receptor induced cytokine expression in dendritic cells.

The recent availability of RIPK1 kinase-inactive mouse models has facilitated examination of RIPK1 catalytic activity in directing inflammation. For example, RIPK1 kinase-inactive mice are protected from TNFα induced hypothermia and shock (Polykratis et al. 2014). Another group evaluated kinase-function of RIPK1 in the absence of SHARPIN, a component of the linear ubiquitin assembly complex (LUBAC). SHARPIN-deletion results in gross inflammatory pathology, dermatitis, and diminished organism survival. Authors of this study observed that crossing their independently generated RIPK1 kinase-inactive mice to SHARPIN-deficient mice protected mice from inflammatory pathology and prolonged survival (Berger et al. 2014).

1.5.3. RIPK3 and Inflammation

Work spearheaded by Francis Chan and colleagues has marked RIPK3 as an important component of the host inflammatory response to injury and infection. In one study, the group reported impaired inflammation-associated repair in *Ripk3*$^{-/-}$ mice in the dextran-sodium sulfate (DSS) model of colitis (Moriwaki et al. 2014). Specifically, RIPK3 in hematopoietic cells is required for protection against DSS-colitis; *Ripk3*$^{-/-}$ mice with WT bone-marrow lost less body weight and had reduced inflammation (Moriwaki et al. 2014). Moreover, *Ripk3*$^{-/-}$ mice had reduced circulating levels of IL1β and IL23 and re-supplementation of these cytokines mitigated the extent of colitis. In concordance, bone-marrow derived dendritic cells (BMDCs) had defects in LPS induced expression of cytokines, including, TNFα, IL1b, IL23, and Monocyte Chemotactic Protein-1 (MCP-1) (Moriwaki et al. 2014). It is unlikely that these observations are

linked to differences in cell death or the release of damage-associated molecular patterns as *Ripk3*$^{+/+}$ and *Ripk3*$^{-/-}$ BMDCs did not undergo death in response to LPS. Conversely, these effects were attributed to defects in generation of reactive oxygen species (ROS) and nuclear localization of subunits RelB and p50 in the NFκB pathway (Moriwaki et al. 2014). Similar defects in inflammatory cytokine expression were not observed in BMDMs suggesting that RIPK3 may have a broad functional range that can be employed in a context or cell-specific manner.

Analyses in BMDCs demonstrated that RIPK3 is required for caspase-8 and caspase-1 dependent IL1β processing and secretion. RIPK3 complexation with caspase-8 and Fas-associated death domain (FADD), and caspase-8 cleavage was impaired in *Ripk3*$^{-/-}$ BMDCs stimulated with LPS (Moriwaki et al. 2015). These data suggest that RIPK3 directs LPS-induced IL1β secretion by facilitating maturation of caspase-8. However, kinase activity of RIPK3 appears to be dispensable as RIPK3 kinase-inactive BMDCs did not display a deficit in IL1β production (Moriwaki et al. 2015). Authors also observed that kinase-independent function of RIPK1 may be required as lentiviral CRE-mediated deletion of kinase-inactive RIPK1 in BMDCs reduced LPS-induced caspase-8 maturation; however, no defects were observed in absence of CRE. Paradoxically, RIPK3 kinase inhibitor of necroptosis, GSK'872, augmented LPS-induced IL1β production, suggesting that this regulation may not be controlled by the catalytic activity of RIPK3 *per se*, but may be influenced by the conformation of the kinase domain. Consistent with this model, GSK'872 enhanced recruitment of RIPK1 to RIPK3 and has also been shown to induce RIPK3 dependent apoptosis (Moriwaki et al. 2015; Mandal et al. 2014).

1.5.4. Summary of RIPK1, RIPK3, and Inflammation

Inflammation is a crucial part of the host-response during infection. Notably, RIPK1 and RIPK3 have been identified in critical roles regulating pro-inflammatory transcription factors, cytokine synthesis, and cytokine secretion in response to immunogenic ligands. Moreover, RIPK1 kinase activity and RIPK3 have been linked to tissue specific and systemic inflammation. As discussed, in some instances inflammatory signaling by these proteins can be separated from RIPK1 and RIPK3 kinase-dependent cell death. Accordingly, these factors may emerge as potential therapeutic targets not only in pathologic settings that are driven by significant cell death and tissue loss, but also in disease-states that are primarily inflammatory in nature.

1.6. Summary: Cell death and inflammation as features of the host-response

Cell death and inflammation are critical components of host immune response against invading microbial pathogens. Programmed death of infected cells releases intracellular microbes for clearance by immune cells and restricts microbial proliferation (Lamkanfi & Dixit 2010; Sridharan & Upton 2014). Pathogen associated inflammatory changes modify host-cell programming and activate cell-mediated immunity, both of which promote systemic anti-microbial states. Localized inflammatory responses also promote tissue repair. Notably, manifestations of both of these host-response mechanisms are evident in examples of pro-inflammatory necroptotic cell death, which feature inflammation and tissue repair concurrent with cellular demise (Kaczmarek et al. 2013; Moriwaki et al. 2014).

1.7. Thesis

Macrophages function as a crucial component of the innate immune system in sensing bacterial pathogens and promoting local and systemic inflammation. RIPK1 and RIPK3 are serine/threonine kinases that have been well-characterized as key regulators of programmed necrotic cell death or necroptosis that is dependent on downstream pseudokinase MLKL. The

work presented in the ensuing chapters describes a new function of these kinases as master regulators of cytokine gene expression and the synthesis of inflammatory mediators in primary macrophages activated by LPS, in the absence of caspase-8 activation. RIPK1 and RIPK3 kinase-dependent cytokine production requires the Toll-like receptor 4 (TLR4) adaptor molecule, TRIF, and proceeds independently of MLKL and the well-documented death functions of these kinases. Mechanistically, RIPK1 and RIPK3 kinases promote sustained activation of at least two canonical cytokine response axes: the acute inflammatory response mediated by downstream factors, Erk1/2, c-Fos, and NFκB; and the Type-I interferon (IFN-I) response pathway mediated by TBK1/IKKε and IRF3/7. The evidence summarized here suggests that detergent-insoluble complexes of RIPK1 and RIPK3 (necrosomes) serve as a signaling platform to engage downstream signaling molecules. Using genetic and pharmacologic tools, the data reveal that RIPK1 and RIPK3 kinase functions account for a major fraction cytokine elicited by LPS challenge *in vivo*. Notably, in contrast to the circumstance observed *in vitro*, the regulation *in vivo* did not require exogenous manipulation of caspase-8 activity, suggesting that RIPK1 and RIPK3 kinase-dependent cytokine responses may serve as a feature of the host-inflammatory response in gram-negative bacterial infection.

Intriguingly, in primary macrophages, RIPK1 and RIPK3 kinase-dependent synthesis of IFNβ can be markedly induced by a variety of gram-negative bacterial species (*Yersinia* and *Klebsiella*). Furthermore, data show that RIPK1 and RIPK3 kinase-dependent IFNβ synthesis is strongly induced by avirulent strains of gram-negative bacteria, *Yersinia* and *Klebsiella*, and less-so by their wild-type counterparts. Similarly, RIPK1 kinase-dependent TNFα synthesis is more pronounced following *in vivo* infection with an avirulent strain of *Klebsiella* compared to the wild type.

These data suggest that TRIF-RIPK1-RIPK3 kinase-dependent signaling may be a mechanism of immune-surveillance employed against non-pathogens or commensal bacteria. Conversely, TRIF-RIPK1-RIPK3 signaling may be selectively suppressed by invading microbes to facilitate bacterial pathogenesis. Consistent with this hypothesis, GNB species are armed with specific mechanisms to attenuate RIPK1 and RIPK3 kinase-dependent signaling. As a result, exogenous activation of TRIF-RIPK-RIPK3 kinase-dependent signaling may aid in the clearance of GNB infection. Importantly, the findings reported here identify new drug-targetable activities that may be relevant to infection and/or inflammatory pathologies associated with inappropriate RIPK1 and RIPK3 kinase activation.

Chapter 2

RIPK1 and RIPK3 kinases Promote Cell Death-Independent Inflammation by Toll-like Receptor 4[4]

[4] Najjar M*, Saleh D*, Zelic M, Nogusa S, Shah A, Tai A, Finger JN, Polykratis A, Gough PJ, Bertin J, Whalen M, Pasparakis, Balachandran S, Kelliher M, Poltorak A, Degterev A. 2016. RIPK1 and RIPK3 kinases promote cell death-independent inflammation by Toll-like Receptor 4. *Immunity.* 45: 46-59. *equal contribution.

RIPK1 and RIPK3 kinases promote cell death-independent inflammation by Toll-like receptor 4

Authors

Malek Najjar[1,#], Danish Saleh[2,#], Matija Zelic[3], Shoko Nogusa[4], Saumil Shah[5], Albert Tai[6], Joshua N. Finger[7], Apostolos Polykratis[8], Peter J. Gough[7], John Bertin[7], Michael Whalen[9], Manolis Pasparakis[8], Siddharth Balachandran[4], Michelle Kelliher[3], Alexander Poltorak[6], and Alexei Degterev[1,5,*]

Affiliations

[1]Program in Pharmacology and Experimental Therapeutics, Sackler Graduate School, Tufts University, Boston, MA 02111, USA

[2]Medical Scientist Training Program and Program in Neuroscience, Sackler Graduate School, Tufts University, Boston, MA 02111, USA

[3]Department of Molecular, Cell and Cancer Biology, University of Massachusetts Medical School, Worcester, MA 01605, USA

[4]Blood Cell Development and Function Program, Fox Chase Cancer Center, Philadelphia, PA 19111, USA

[5]Department of Developmental, Molecular & Chemical Biology, Tufts University School of Medicine, Boston, MA 02111, USA

[6]Department of Integrative Physiology and Pathobiology, Tufts University School of Medicine, Boston, MA 02111, USA

[7]Pattern Recognition Receptor Discovery Performance Unit, Immuno-Inflammation Therapeutic Area, GlaxoSmithKline, Collegeville, PA 19426, USA

[8]Institute for Genetics, Center for Molecular Medicine and Cologne Excellence Cluster on Cellular Stress Responses in Aging-Associated Diseases, University of Cologne, 50674 Cologne, Germany.

[9]Neuroscience Center and Department of Pediatrics, Massachusetts General Hospital and Harvard Medical School, Charlestown, MA 02129, USA

#M.N. and D.S. contributed to the manuscript equally

Contact information

[*]Corresponding author at: DMCB, School of Medicine, Tufts University, 136 Harrison Ave, Boston, MA 02111, USA. Email address: alexei.degterev@tufts.edu

Summary

Macrophages are a crucial component of the innate immune system in sensing pathogens and promoting local and systemic inflammation. RIPK1 and RIPK3 are homologous kinases, previously linked to activation of necroptotic death. In this study we have described roles for these kinases as master regulators of pro-inflammatory gene expression induced by lipopolysaccharide, independent of their well-documented cell death functions. In primary macrophages, this regulation was elicited in the absence of caspase-8 activity, required the adaptor molecule TRIF, and proceeded in a cell autonomous manner. RIPK1 and RIPK3 kinases promoted sustained activation of Erk, cFos and NFκB, which were required for inflammatory changes. Utilizing genetic and pharmacologic tools, we showed that RIPK1 and RIPK3 account for acute inflammatory responses induced by lipopolysaccharide *in vivo;* notably, this regulation did not require exogenous manipulation of caspases. These findings identified a new pharmacologically accessible pathway that may be relevant to inflammatory pathologies.

Introduction

RIPK1 and RIPK3 are homologous Ser/Thr kinases, which attracted interest as central inducers of regulated necrotic cell death, termed "necroptosis" (Christofferson & Yuan 2010; Degterev et al. 2005; Linkermann & Green 2014; Pasparakis & Vandenabeele 2015; Silke et al. 2015). A range of triggers, including extracellular factors linked to innate immune regulation, such as ligands for tumor necrosis factor receptor (TNFR), interferon-alpha receptor (IFNαR), and Toll-like receptor (TLR) families, as well as viral infection and genotoxic stressors have been associated with RIPK1 and RIPK3 activation. These stimuli have been shown to induce necroptosis *in vitro* under conditions in which the apical apoptotic cysteine protease, caspase-8, is inhibited pharmacologically or genetically (Degterev et al. 2005; He et al. 2011; Kaiser et al. 2013; Tenev et al. 2011; Thapa et al. 2013; Upton et al. 2010; Upton et al. 2012). Necroptosis is best understood in the context of TNFα signaling and the kinase activity of RIPK3 has been shown to play a central role in its activation (Cho et al. 2009; He et al. 2009; Zhang et al. 2009). RIPK3 functions within an insoluble amyloid-like RIPK1 and RIPK3 "necrosome" complex, formation of which requires catalytic activities of both kinases (Cho et al. 2009), and serves as a signaling platform for the activation of a downstream pseudo-kinase MLKL, a critical mediator of cell lysis and necroptotic death (H. Wang et al. 2014).

In contrast to the well-established roles for kinase activities of RIPK1 and RIPK3 in directing cell death, evidence also hints at the possibility for additional roles for RIPK1 and RIPK3 in the direct regulation of pro-inflammatory signaling (Christofferson et al. 2012; Lukens et al. 2013; McNamara et al. 2013; Wong et al. 2014). Among various inducers of RIPK1 and RIPK3, signaling by TLR3 and TLR4 members of the TLR family of Pattern Recognition Receptors (PRRs) in macrophages engages the RIPK1, RIPK3, and MLKL pathway directly in a manner that

is dependent on the RHIM-containing adaptor protein TRIF in the presence of the pan-caspase inhibitor zVAD.fmk (zVAD) (He et al. 2011; Kaiser et al. 2013; Schworer et al. 2014). Upregulation of inflammatory gene expression by TLR4 is an important component of both physiologic innate immune responses to gram negative bacterial cell membrane component, lipopolysaccharide (LPS), and a contributor to various inflammatory pathologies (Kawai & Akira 2010; Kawai & Akira 2006). Given the challenge of separating pro-inflammatory from pro-necroptotic consequences of RIPK1 and RIPK3 activation, we reasoned that the former regulation might have been overlooked in the previous works.

Here, we report roles for kinase activities of RIPK1 and RIPK3 in LPS-induced expression of inflammatory cytokines that manifest independently from the pro-death functions of these molecules. We have demonstrated that activation of RIPK1 in macrophages by LPS in the presence of zVAD robustly increased expression of a broad range of inflammatory molecules. RIPK3 also contributed to the RIPK1 kinase-dependent inflammation, but in a context dependent manner. We have shown that this regulation is independent of necroptosis and occurs in *Mlkl*$^{-/-}$ macrophages protected from cell death. We have further established that prolonged activation of Erk1/2 MAPK, which may occur through direct engagement by RIPK1 and RIPK3 "necrosome"-like aggregates, is a critical step in directing RIPK1 and RIPK3 kinase-mediated inflammation. Finally, we have extended our observations *in vivo*, affirming the importance of RIPK1 and RIPK3 kinases in the global regulation of acute inflammation induced by a sub-lethal dose of LPS in the absence of exogenous caspase-8 inhibition.

Results

RIPK1 and RIPK3 kinases promote LPS-induced inflammatory gene expression in the absence of caspase-8 activation.

Previously published work suggests that kinase activity of RIPK1 does not contribute to the pro-inflammatory regulation by TLR4 in response to LPS (Cusson-Hermance et al. 2005; Meylan et al. 2004; Newton et al. 2004; Vivarelli 2004). However, the activation of RIPK1 kinase activity and necroptosis also does not occur in LPS-treated macrophages, unless caspases are inhibited using the pan-caspase inhibitor zVAD (Berger et al. 2014; Kaiser et al. 2013; Schworer et al. 2014). Abrogation of the response by a highly selective RIPK1 inhibitor, Nec-1s (also known as 7-Cl-O-Nec-1) (Degterev et al. 2013), and in BMDMs from *Ripk1*$^{D138N/D138N}$ mice, carrying a targeted mutation inactivating the kinase function of RIPK1 (Polykratis et al. 2014), confirmed the response specificity (Fig. 1A, 2A). Additionally, zVAD was required for LPS-induced accumulation of RIPK1, RIPK3 and phosphorylated MLKL in the NP40-insoluble cellular fraction (Fig. 1B), reflecting previously reported formation of detergent-insoluble RIPK1 and RIPK3 necrosomes (Moquin et al. 2013; Ofengeim et al. 2015). Collectively, these observations confirmed the requirement for caspase inhibition for the induction of RIPK1 kinase activity in LPS-treated BMDMs.

Having verified a system to evaluate catalytic function of RIPK1 in BMDMs, we re-examined the role of kinase activity of RIPK1 in LPS-induced inflammatory gene expression. Notably, addition of zVAD robustly increased TNFα mRNA expression and protein secretion in BMDMs treated with LPS (Fig. 1C,D), while only a slight effect was observed when BMDMs were treated with zVAD alone (Fig. 2B). The increase in TNFα synthesis by LPS with zVAD, but not LPS alone was abolished in RIPK1 D138N cells and upon treatment with Nec-1s (Fig. 1C,D).

Examining the kinetics, we observed enrichment of RIPK1, RIPK3, and p-MLKL in the NP40-insoluble cellular fraction reaching a maximum ~1.5 hr after addition of LPS with zVAD (Fig. 2C), followed by increases in TNFα mRNA expression (~2-6 hr) (Fig. 2D,E), which preceded on-set of cell death (>7 hr) (Fig. 2F). We also observed comparable RIPK1 kinase-dependent induction of TNFα mRNA by LPS with zVAD in a different lineage of primary macrophages – thioglycollate-elicited peritoneal macrophages (Fig. 2G,H).

To comprehensively evaluate the RIPK1 kinase-dependent inflammatory profile, we performed a genome-wide microarray analysis on BMDMs stimulated with LPS or LPS with zVAD which revealed a large panel of inflammatory genes whose expression was augmented by zVAD and inhibited by Nec-1s (Fig. 1E). Analysis of a number of these genes in D138N RIPK1 BMDMs confirmed the critical role for RIPK1 kinase activity in promoting their expression after treatment with LPS with zVAD (Fig. 2I).

We also determined that siRNA-mediated silencing of RIPK1 (Fig. 2J) attenuated inflammatory mRNA changes in cells treated with LPS with zVAD (Fig. 2K). In contrast, previous reports suggest that necroptosis induced by LPS with zVAD can efficiently proceed through direct TRIF and RIPK3 activation even in the absence of RIPK1 (Dillon et al. 2014; Kaiser et al. 2013) and, consistently, silencing of RIPK1 expression did not attenuate necroptosis in our hands (Fig. 2L). Thus, RIPK1 is indispensable for the regulation of inflammatory gene expression, unlike its function in necroptosis.

Expectedly, BMDMs expressing a kinase-inactive hypomorphic K51A RIPK3 mutant (*Ripk3*$^{K51A/K51A}$) were protected from cell death induced by LPS with zVAD (Fig. 1F) (Mandal et al. 2014) and were deficient in accumulation of RIPK1, RIPK3, and pMLKL in the detergent insoluble cellular fractions (Fig. 1G). K51A RIPK3 BMDMs also lacked increased inflammatory

gene expression triggered by LPS with zVAD (Fig. 1H and 2M). A similar result was obtained using *Ripk3*$^{-/-}$ BMDMs (Fig. 2N-P) and a selective RIPK3 kinase inhibitor, GSK872 (Fig. 2Q) (Mandal et al. 2014), confirming the role of RIPK3 kinase activity in promoting inflammatory gene expression.

Catalytic activity of caspase-8 regulates activation of RIPK1 and RIPK3 kinases, necrosome formation and the induction of necroptosis (Moquin et al. 2013; O'Donnell et al. 2011). The requirement for zVAD suggests a similar role for caspase-8 in modulating RIPK1 and RIPK3 kinase-dependent inflammatory response. However, because zVAD is known to inhibit all caspases and additional classes of cysteine proteases (Schotte et al. 1999), we sought to confirm the role of caspase-8. Indeed, Cre-mediated deletion of *Casp8* in *Casp8*$^{flox/flox}$ cells (Fig. 2R) promoted both necroptosis in response to LPS alone (Fig. 1I) and induced cytokine expression that was attenuated by Nec-1s (Fig. 1J and 2S). These observations affirmed a specific role for caspase-8 in blocking LPS-induced RIPK1 and RIPK3 kinase-dependent cytokine synthesis *in vitro*.

In sum, these data suggested that activation of RIPK1 and RIPK3 kinases in BMDMs promoted enrichment of these kinases in detergent insoluble cellular fractions followed by an increase in the expression of a range of pro-inflammatory molecules. Notably, these events preceded activation of necroptotic cell death.

Figure 1. Caspase-8 inhibition promotes LPS-induced cytokine gene expression that is dependent on RIPK1 and RIPK3 kinases in macrophages.

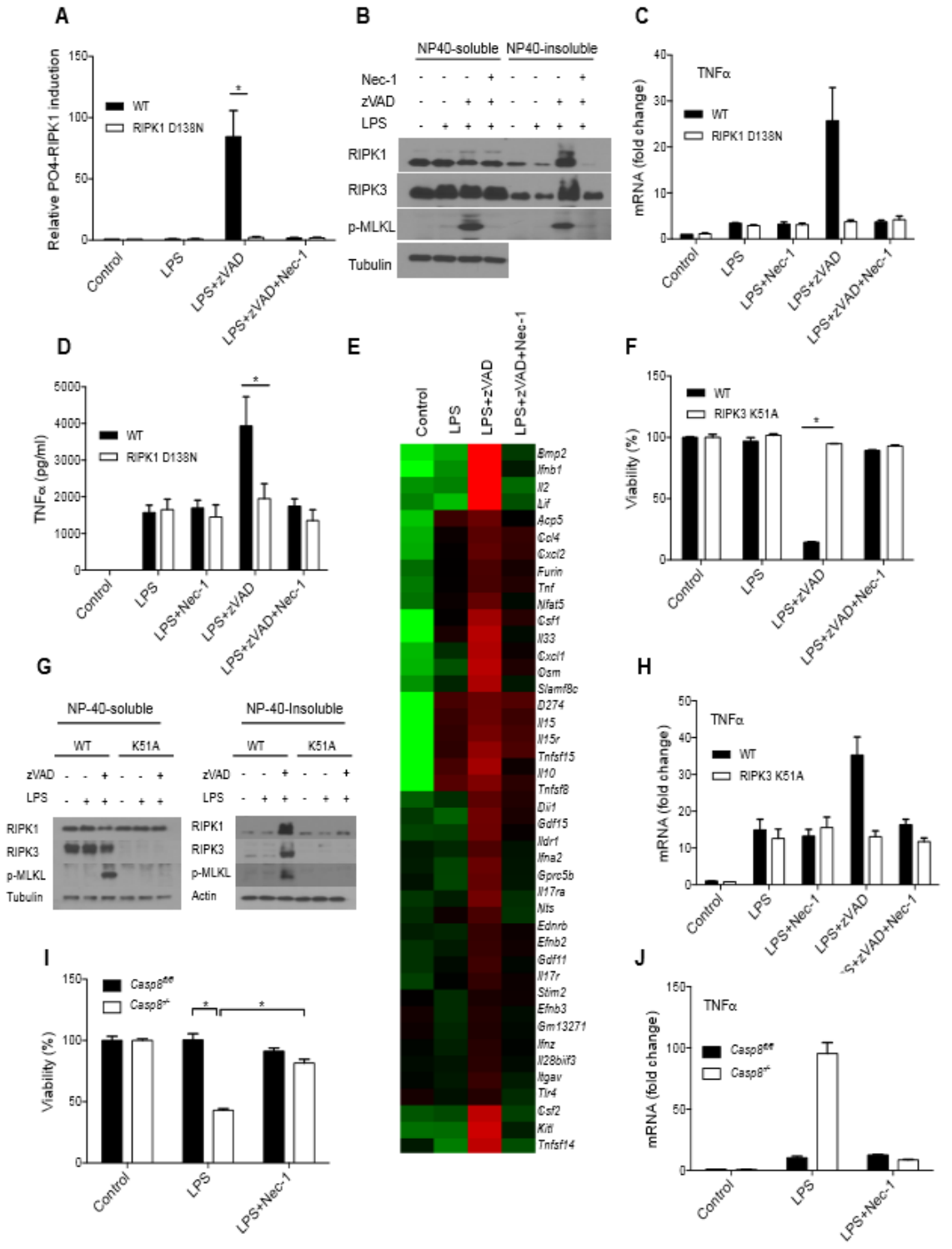

Figure 1: Caspase-8 inhibition promotes LPS-induced cytokine gene expression that is dependent on RIPK1 and RIPK3 kinases in macrophages.

(A) Autophosphorylation of RIPK1 at Ser166 in BMDMs treated for 4 hrs. p-Ser166/total RIPK1 measured by ELISA. (B) Western of NP40-soluble and NP40-insoluble fractions from wild type BMDMs treated for 4 hrs. (C, D) TNF mRNA expression (C) and protein release (D) in BMDMs treated for 7 hrs. (E) Affymetrix gene array expression analysis of inflammatory genes increased by 7 hrs treatment with LPS or LPS with zVAD in BMDMs. (F) Cell viability of BMDMs treated for 24 hrs. (G) Western of NP40-soluble and NP40-insoluble fractions from BMDMs treated for 4 hrs. (H) TNF mRNA expression in BMDMs treated for 7 hrs. (I) Cell viability of BMDMs treated with LPS alone for 24 hrs. (J) TNF mRNA expression BMDMs treated for 7 hrs.

Values represent Mean ± SD. *$p<0.05$. For qRT-PCR and Western blots, data for one representative experiment out of at least three independent repeats are shown. For ELISA, combined data for three independent experiments are shown unless otherwise stated. BMDMs were treated with LPS=10 ng/mL, zVAD=50 μM and Nec-1s=30 μM in all experiments. Use of Nec-1 refers to Nec-1s in this and all other figures.

Contributions: Experiments performed and data analyzed by Malek Najjar and Danish Saleh. Figures prepared by Malek Najjar. Figure legends written by Danish Saleh.

Figure 2. LPS induces RIPK1 and RIPK3 kinase-dependent cytokine production in the absence of Caspase-8 activity in vitro.

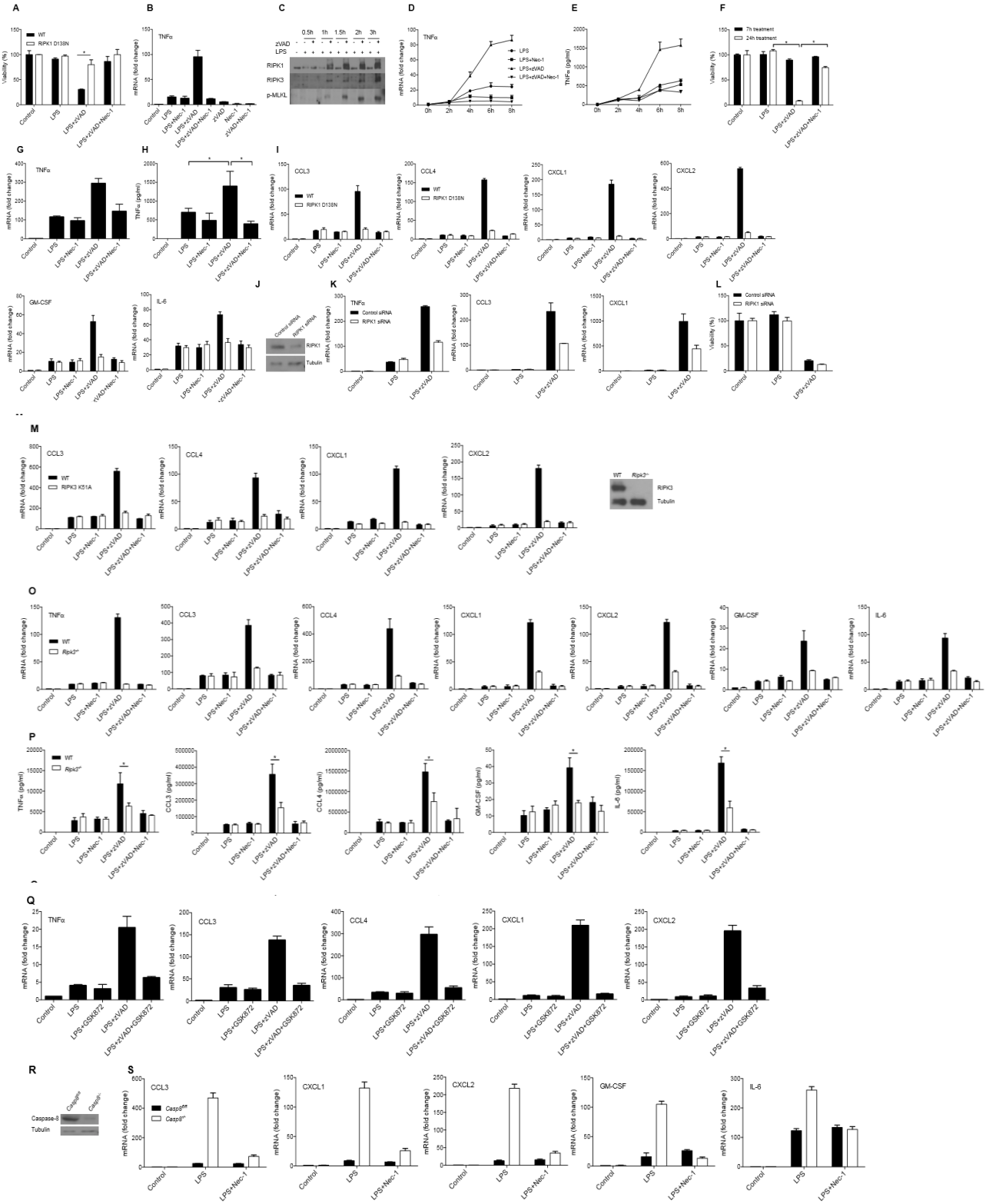

Figure 2. LPS induces RIPK1 and RIPK3 kinase-dependent cytokine production in the absence of Caspase-8 activity in vitro.

(A) Cell viability of wild type and D138N RIPK1 BMDMs treated for 24 hr. (B) qRT-PCR analysis of TNFα mRNA expression in wild type BMDMs treated as indicated for 7 hrs. (C) Western blot analysis of NP40 insoluble fractions probed for RIPK1, RIPK3, and p-MLKL in wild type BMDMs treated for 4 hrs. (D-E) qRT-PCR and ELISA analysis of the time course of TNFα mRNA expression (D) and protein release (E) in wild type BMDMs over 8 hrs. Time course was repeated twice and data are representative. (F) Cell viability of wild type BMDMs treated for 7 or 24 hrs. (G-H) qRT-PCR and ELISA analysis of TNFα mRNA expression (G) and protein release (H) in wild type thioglycollate-elicited peritoneal macrophages treated for 7 hrs. (I) qRT-PCR analysis of mRNA expression of select inflammatory cytokines in wild type and D138N RIPK1 BMDMs treated for 7 hrs. (J-L) Analysis of mRNA expression of select inflammatory cytokines (K, 7 hrs) and cell viability (L, 24 hrs) in BMDMs following siRNA silencing of RIPK1. Silencing of RIPK1 was confirmed by Western blot (J). Scrambled siRNA was used as a control. (M) qRT-PCR analysis of mRNA expression of select inflammatory cytokines in wild type and K51A RIPK3 BMDMs treated for 7 hrs. (N-P) qRT-PCR and ELISA analysis of mRNA expression (O) and protein release (P) of select inflammatory cytokines in wild type and *Ripk3*$^{-/-}$ BMDMs treated for 7 hrs. Loss of RIPK3 protein confirmed by Western blot (N). (Q) qRT-PCR analysis of mRNA expression of select inflammatory cytokines in wild type BMDMs treated for 7 hrs in the presence of RIPK3 kinase inhibitor, GSK872. (R-S) qRT-PCR analysis of mRNA expression of select inflammatory genes in *Casp8*$^{flox/flox}$ BMDMs treated for 7 hrs following Adenoviral-Cre-GFP-mediated excision of *casp8*. Adeno-GFP virus was used as a negative control. Excision of C*asp8* by Adenoviral-Cre-GFP was confirmed by Western blot (R).

For qRT-PCR and Western blots, data for one representative experiment out of at least three independent repeats are shown. For ELISA, combined data for three independent experiments are shown unless otherwise stated. Values represent Mean ± SD. *$p<0.05$. Cells were treated with LPS=10 ng/ml, zVAD=50 μM, Nec-1s=30 μM and GSK872=5 μM.

Contributions: Experiments performed and data analyzed by Malek Najjar and Danish Saleh. Figures prepared by Malek Najjar. Figure legends written by Danish Saleh.

RIPK1 and RIPK3 selectively potentiate TRIF-dependent LPS-induced inflammation in a cell-autonomous manner.

LPS engagement of TLR4 promotes receptor dimerization and engagement of two adapter proteins, MyD88 and TRIF, to initiate downstream signaling events (Yamamoto et al. 2003; Yamamoto et al. 2002). TRIF mediates formation of secondary endosomal complexes, involving additional components including RIPK1 and RIPK3 (Kaiser & Offermann 2005; Meylan et al. 2004). To examine whether RIPK1 and RIPK3 kinase-dependent inflammatory gene expression similarly required TRIF, we analyzed responses to Pam_3CSK_4, an agonist of TLR2 which exclusively engages the adapter MyD88, and poly(I:C), an agonist of TLR3 which exclusively engages the adapter TRIF (Kawai & Akira 2010). Caspase inhibition increased cytokine synthesis induced by LPS and Poly(I:C), but had marginal effect on Pam_3CSK_4, suggesting that RIPK1 and RIPK3 kinase-dependent cytokine synthesis may specifically require TRIF (Fig. 3A and 4A). To confirm this, we examined cytokine responses induced by LPS with zVAD in MyD88 (*Myd88*$^{-/-}$) and TRIF (*Ticam1*$^{-/-}$) deficient BMDMs (Fig. 4B,E). Indeed, increased synthesis and release of multiple inflammatory mediators in response to LPS with zVAD was absent in *Ticam1*$^{-/-}$ BMDMs (Fig. 3B,C and 4C,D), but not affected by the loss of MyD88 (Fig. 4F,G), similar to the specific requirement of TRIF for LPS with zVAD induced cell death (Fig. 3D and 4H). Additionally, LPS with zVAD also potently induced upregulation of IFNβ expression and protein release, which is specifically linked to TRIF, but not MyD88 (Van Lieshout et al. 2015), and this was blocked by Nec-1s (Fig. 4I-K). Overall, these data suggested that RIPK1 and RIPK3 specifically potentiate TRIF-dependent inflammatory signaling downstream of TLR4.

Autocrine TNFα signaling has been previously implicated in the induction of a RIPK1 and RIPK3 dependent inflammatory profile in macrophages upon inhibition of IAPs (Wong et al.

2014). Treatment of BMDMs with a pan-IAP inhibitor, SM164, induced cell death and secondary inflammatory cytokine synthesis that was absent in BMDMs carrying a genetic deletion of TNFR1 (*Tnfr1*$^{-/-}$) and blocked by Nec-1s (Fig. 4L-O). In contrast, cell death and cytokine synthesis induced by LPS with zVAD was not attenuated in *Tnfr1*$^{-/-}$ macrophages (Fig. 3E,F and 4P). Additionally, we found that the combination of TNFα with zVAD is a weak inducer of cytokine synthesis in primary macrophages compared to LPS with zVAD (Fig. 3G and 4Q). To exclude the possibility that autocrine signals may be responsible for RIPK1 and RIPK3 kinase-dependent cytokine synthesis, inflammatory cytokine mRNA synthesis was evaluated in the presence of protein translation inhibitor, cycloheximide (CHX). Increasing doses of CHX abolished TNFα protein synthesis, but failed to block cytokine mRNAs induced by LPS with zVAD (Figure 4R,S). These data indicated that in contrast to the previously described responses to IAP inhibition, induction of cytokine gene expression by LPS with zVAD occurs in a cell-autonomous manner, independent of new protein synthesis and/or autocrine signaling by TNFα.

Figure 3. RIPK1 and RIPK3 kinase-dependent cytokine synthesis and necroptosis require TRIF and manifest in a cell autonomous manner.

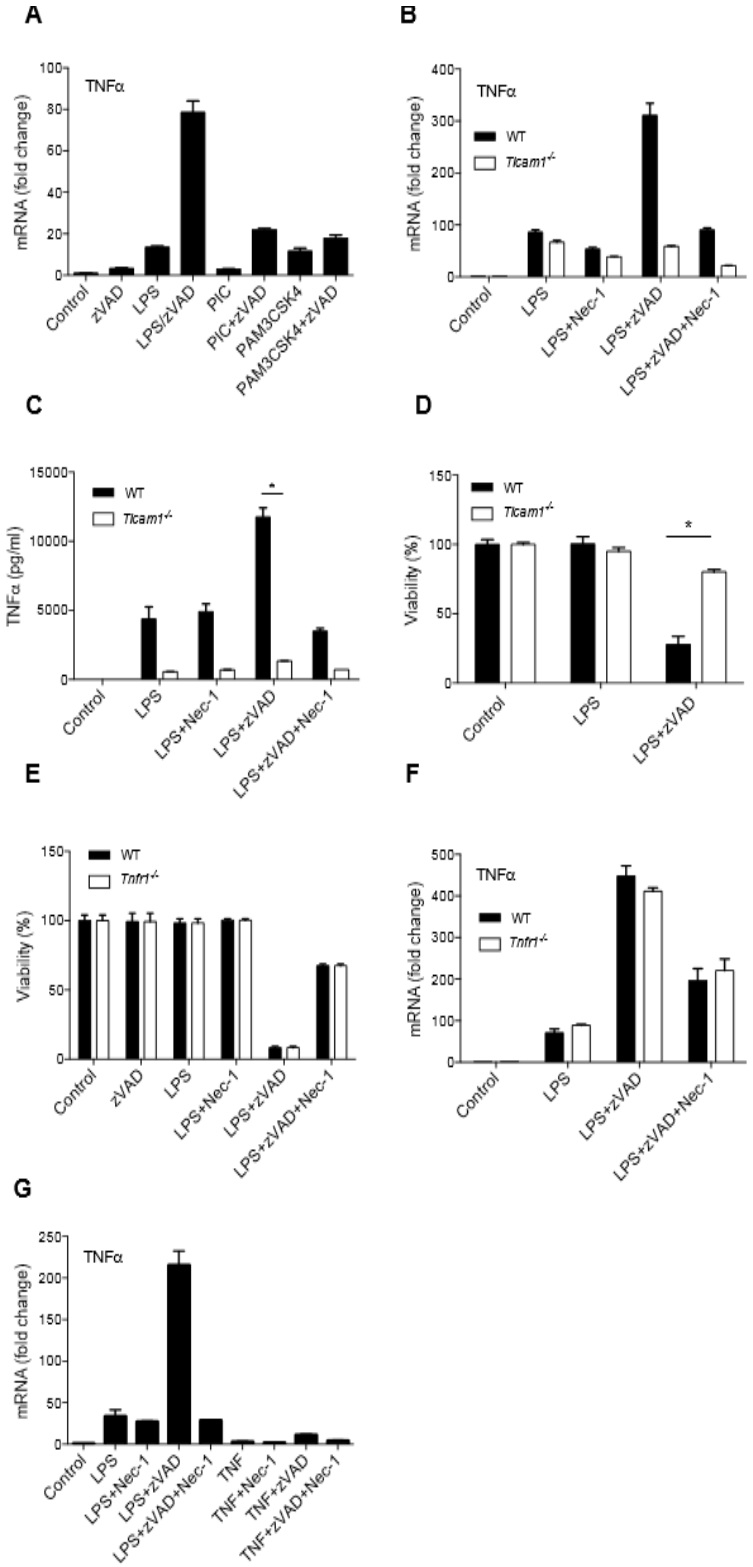

Figure 3: RIPK1 and RIPK3 kinase-dependent cytokine synthesis and necroptosis require TRIF and manifest in a cell autonomous manner.

(A) TNF mRNA expression in wild type BMDMs treated for 7 hrs. (B, C) TNF mRNA expression (B) and protein release (C) in wild type and *Ticam1*$^{-/-}$ BMDMs. (D) Cell viability of wild type and *Ticam1*$^{-/-}$ BMDMs treated for 24 hrs. (E) Cell viability of BMDMs treated for 24 hrs. (F) TNF mRNA expression in BMDMs treated for 7 hrs. (G) TNF mRNA expression in wild type BMDMs treated with LPS with and without zVAD or TNF with and without zVAD for 7 hrs. For qRT-PCR, data for one representative experiment out of at least three independent replicates are shown. For viability, combined data for three independent experiments are shown. Values represent Mean ± SD. *$p<0.05$. BMDMs were treated with LPS=10ng/ml, Poly(I:C)=1μg/mL, Pam_3CSK_4= 1μg/mL, TNFα =10 ng/ml, zVAD=50 μM, and/or Nec-1s=30 μM.

Contributions: Experiments performed, data analyzed Malek Najjar and Danish Saleh. Figures prepared by Malek Najjar. Figure legends written by Danish Saleh.

Figure 4. RIPK1 kinase-dependent cytokine synthesis induced by LPS with zVAD is dependent on TRIF but independent of MyD88 and Tnfr1.

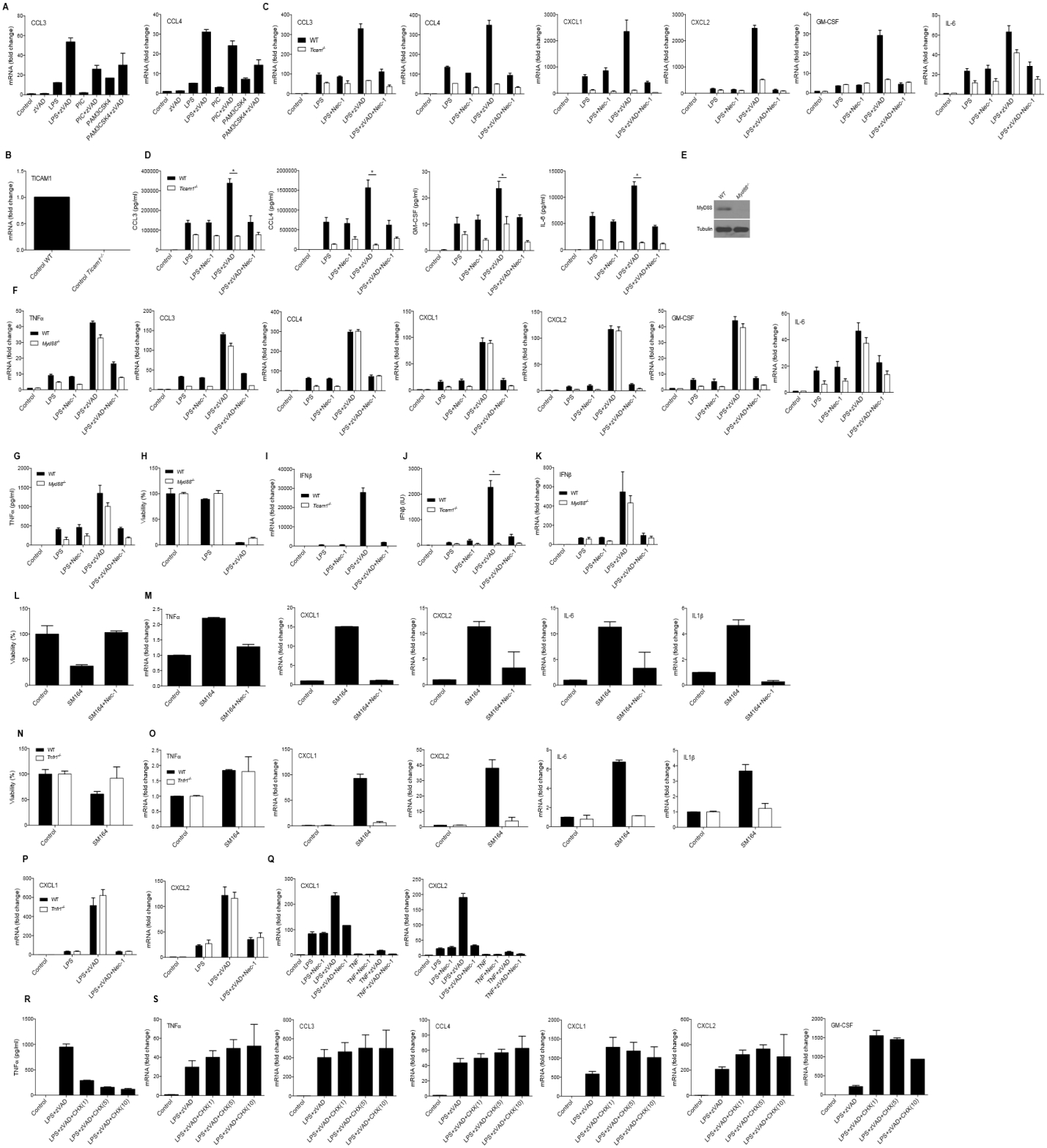

Figure 4. RIPK1 kinase-dependent cytokine synthesis induced by LPS with zVAD is dependent on TRIF but independent of MyD88 and Tnfr1.

(A) qRT-PCR of mRNA expression of CCL3 and CCL4 in wild type BMDMs treated with zVAD and/or TLR4 agonist (LPS), TLR3 agonist (Poly(I:C)), or TLR2 agonist (Pam_3CSK_4), for 7 hrs. (B-D) qRT-PCR and ELISA analysis of mRNA expression (C) and protein release (D) of select inflammatory cytokines in wild type and *Ticam1*$^{-/-}$ BMDMs treated for 7 hrs. Lack of wild type TRIF mRNA expression in *Ticam1*$^{-/-}$ BMDMs was confirmed by qRT-PCR (B) using the recommended protocol by Jackson labs. (E-G) qRT-PCR and ELISA analysis of mRNA expression of select inflammatory cytokines (F) and TNFα protein release (G) in wild type and *Myd88*$^{-/-}$ BMDMs treated for 7 hrs. (E) Loss of Myd88 protein confirmed by Western blot. (H) Cell viability of wild type and *MyD88*$^{-/-}$ BMDMs treated for 24 hrs. (I) qRT-PCR analysis of IFNβ mRNA expression in wild type *Ticam1*$^{-/-}$ BMDMs. (J) ELISA analysis of IFNβ protein release in wild type *Ticam1*$^{-/-}$ BMDMs. (K) qRT-PCR analysis of IFNβ mRNA expression in wild type *MyD88*$^{-/-}$ BMDMs. (L) Cell viability of BALB/C BMDMs treated with SMAC mimetic, SM164, for 9 hours. (M) qRT-PCR analysis of mRNA expression of select inflammatory cytokines in BALB/C BMDMs treated with SM164 for 6 hrs. (N) Cell viability of wild type and *Tnfr1*$^{-/-}$ BMDMs treated with SM164 for 20 hrs. (O) qRT-PCR analysis of mRNA expression of select inflammatory cytokines in wild type and *Tnfr1*$^{-/-}$ BMDMs treated with SM164 for 6 hrs. (P) qRT-PCR of mRNA expression of CXCL1 and CXCL2 in wild type and *Tnfr1*$^{-/-}$ BMDMs treated with LPS or LPS with zVAD for 7 hrs. (Q) qRT-PCR of mRNA expression of CXCL1 and CXCL2 in wild type BMDMs treated with either LPS with zVAD or TNF with zVAD for 7 hrs. (R) ELISA analysis of TNFα protein release in wild type BMDMs treated for 4 hrs. (S) qRT-PCR analysis of select inflammatory cytokines in wild type BMDMs treated with LPS with zVAD in the presence

of increasing concentrations of cycloheximide (CHX) for 4 hrs. For qRT-PCR and Western blots, data for one representative experiment out of at least three independent repeats are shown. For ELISA, combined data for three independent experiments are shown. Values represent Mean ± SD. *$p<0.05$. Experiments using SM164 or CHX were repeated twice and data shown are representative. Cells were treated with LPS=10 ng/mL, zVAD=50 μM, Nec-1s=30 μM, SM164=5 μM, CHX=1, 5, or 10 μg/mL.

Contributions: Experiments performed and data analyzed by Malek Najjar and Danish Saleh. Figures prepared by Malek Najjar. For data featuring use of CHX or SM-164, experiments were performed and figures were prepared by Danish Saleh exclusively. Figure legends written by Danish Saleh.

RIPK1 and RIPK3 kinase-dependent inflammation proceeds independently of MLKL-dependent necroptosis.

As expected, both *Ripk3*$^{-/-}$ and *Mlkl*$^{-/-}$ BMDMs were completely protected from LPS with zVAD induced cell death (Fig. 5A). However, in contrast to the deficiency in RIPK3, we still observed induction of cytokine expression, albeit slightly reduced, in *Mlkl*$^{-/-}$ BMDMs in response to LPS with zVAD (Fig. 5B,C and 6A). Similarly, shRNA silencing of MLKL had no effect on pro-inflammatory signaling, even though it efficiently prevented cell death, in contrast to RIPK3 shRNA, which blocked both responses (Fig. 6B-E). Overall, these data showed that RIPK1 and RIPK3 kinase-dependent induction of cytokine expression still occurred in the cells that did not undergo necroptosis in the absence of MLKL.

To further examine the connection between inflammatory gene expression changes and necroptosis, we evaluated these responses in a different system, using mouse embryonic fibroblasts (MEFs) treated with TNFα, zVAD and a low dose of CHX (Cho et al., 2009; He et al., 2009). As in BMDMs, we found that RIPK1 (*Ripk1*$^{-/-}$ MEFs) was critical for TNFα and IL6 mRNA induction (Fig. 5E,F and 6F), even though it was dispensable for necroptosis (Fig. 5D). Although deletion of RIPK3 prevented necroptosis (Fig. 5G), it did not attenuate TNFα and IL6 induction (Fig. 5H,I and 6G). Consistently, RIPK3 inhibitor, GSK872, also did not inhibit TNFα mRNA expression in wild type MEFs treated with TNFα, zVAD, and CHX at the concentrations that blocked necroptosis (Fig. 6H,I). These data revealed that RIPK1 is indispensable for the upregulation of inflammatory gene expression, while RIPK3 contributes to this regulation in a context-dependent manner and induction of inflammation still occurs in the absence of MLKL-dependent necroptosis.

Figure 5. MLKL is dispensable for cytokine synthesis and the role of RIPK3 is context-specific.

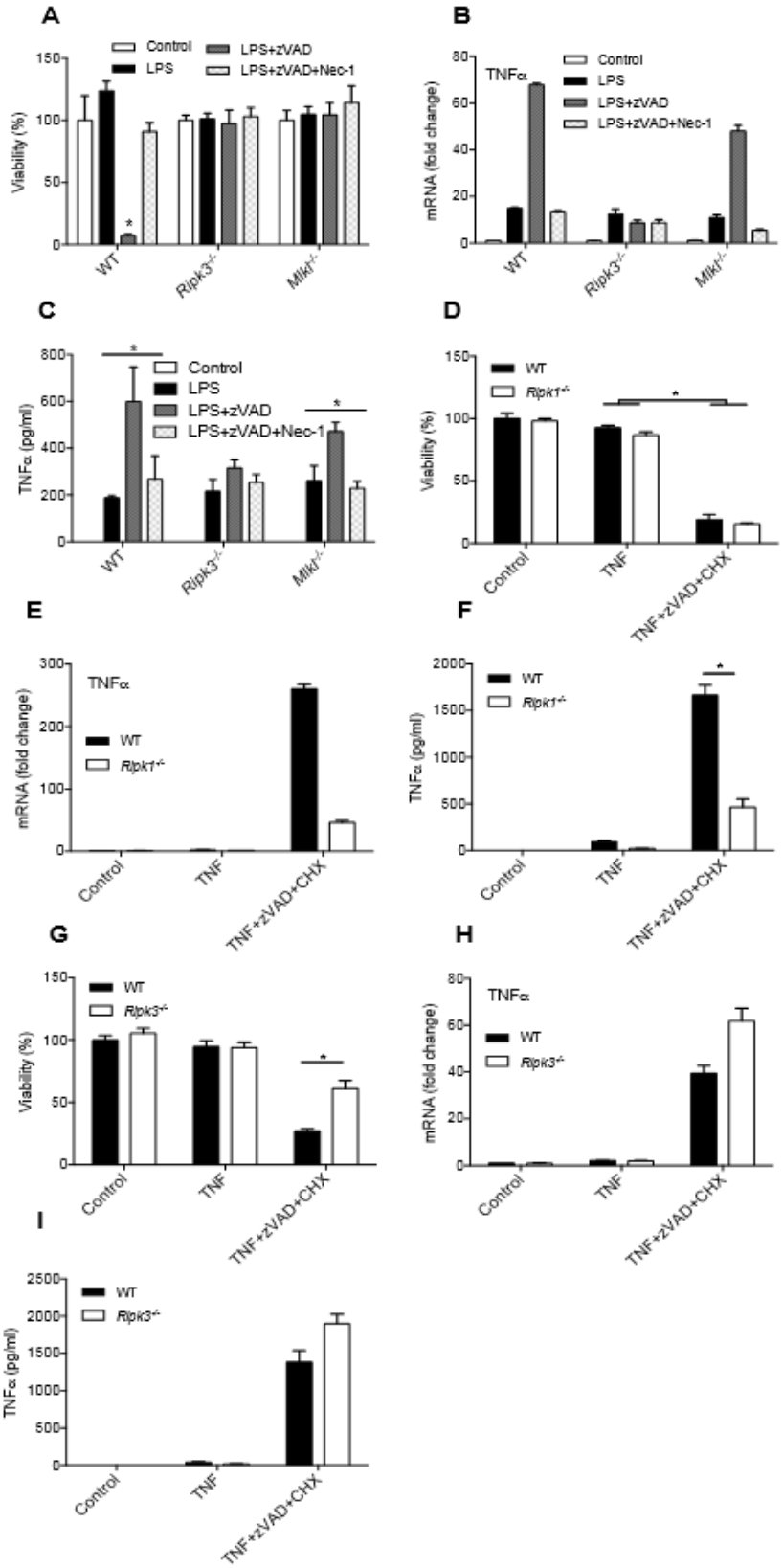

Figure 5: MLKL is dispensable for cytokine synthesis and the role of RIPK3 is context-specific.

(A) Cell viability of BMDMs treated for 24 hrs. (B, C) TNF mRNA expression (B) and protein release (C) in wild type, *Mlkl*$^{-/-}$, and *Ripk3*$^{-/-}$ BMDMs treated for 7 hrs. In (C), statistical significance calculated by one way ANOVA. (D) Cell viability of MEFs treated for 24 hrs. (E, F) TNF mRNA expression (E) and protein release (F) in MEFs treated for 4 hr. (G) Cell viability of MEFs treated for 24 hrs. (H, I) TNF mRNA expression (H) and protein release (I) in MEFs treated for 4 hr. For qRT-PCR, data for one representative experiment out of at least three independent replicates are shown. For viability, combined data for three independent experiments are shown. Values represent Mean ± SD. *$p<0.05$. BMDMs were treated with LPS=10 ng/ml, zVAD=50 μM, and Nec-1s=30 μM. MEFs were treated with TNFα=10 ng/ml, zVAD=25 μM and CHX=1 μg/ml. Contributions: Experiments using TNF+zVAD+CHX were performed by Malek Najjar. Experiments using WT, *Ripk3*$^{-/-}$, and *Mlkl*$^{-/-}$ BMDMs were performed by Malek Najjar and Danish Saleh. Data analyzed and figures prepared by Malek Najjar. Figure legends written by Danish Saleh.

Figure 6. MLKL is dispensable for RIPK1 and RIPK3 kinase-dependent inflammatory cytokine synthesis induced by LPS with zVAD and RIPK3 regulates cytokine production in a context dependent manner.

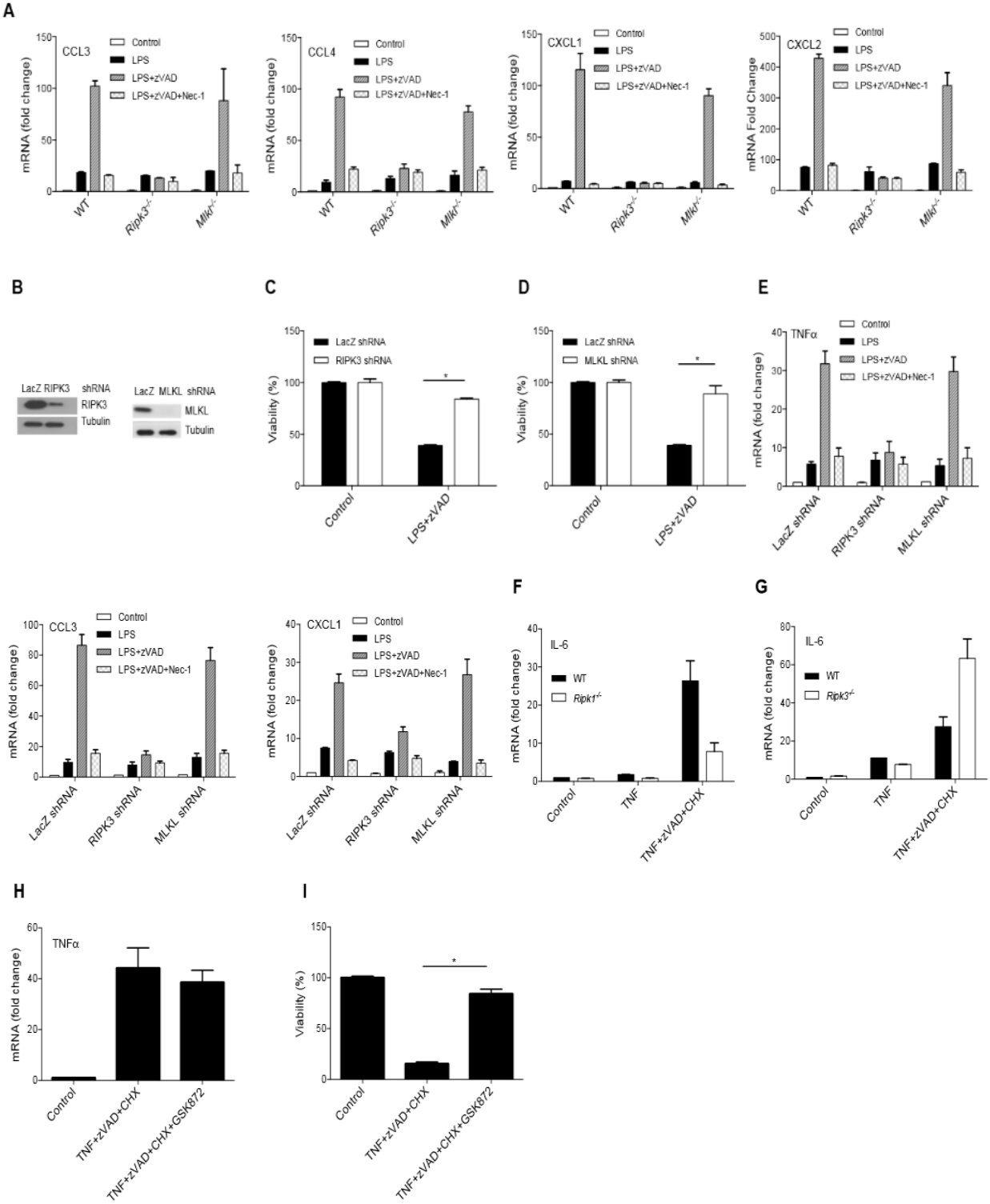

Figure 6. MLKL is dispensable forRIPK1 and RIPK3 kinase-dependent inflammatory cytokine synthesis induced by LPS with zVAD and RIPK3 regulates cytokine production in a context dependent manner.

(A) qRT-PCR analysis of mRNA expression of select inflammatory cytokines in wild type, *Mlkl*$^{-/-}$, and *Ripk3*$^{-/-}$ BMDMs treated for 7 hrs. (B) Silencing of RIPK3 and MLKL using targeted shRNA in iBMMs confirmed by Western blot. (C-D) Cell viability iBMMs expressing RIPK3 (C) and MLKL (D) shRNAs treated with LPS alone LPS with zVAD, or LPS with zVAD and Nec-1 for 24 hours. (E) qRT-PCR analysis of mRNA expression of select inflammatory cytokines in iBMMs expressing RIPK3 and MLKL shRNAs treated for 7 hours. (F-G) qRT-PCR analysis of IL6 mRNA expression in wild type and *Ripk1*$^{-/-}$ MEFs (F) and *Ripk3*$^{-/-}$ MEFs (G) treated with TNFα, zVAD, and CHXfor 4 hrs. (H-I) qRT-PCR analysis of TNFα mRNA expression (H, 4 hrs) and cell viability (I, 24 hrs) analysis in wild type MEFs treated with TNFα, zVAD, and CHX in the presence of GSK872. For qRT-PCR, data for one representative experiment out of at least three independent replicates are shown. For viability, combined data for three independent experiments are shown. Values represent Mean ± SD. *$p<0.05$. BMDMs and iBMMs were treated with LPS=10 ng/ml, zVAD=50 μM, Nec-1s=30 μM and/or GSK872=5 μM. MEFs were treated with TNFα =10 ng/ml, zVAD=25 μM, CHX=1 μg/m and GSK872=5 μM.

Contributions: Experiments using TNF+zVAD+CHX and knockdown experiments were performed by Malek Najjar. Experiments using WT, *Ripk3*$^{-/-}$, and *Mlkl*$^{-/-}$ BMDMs were performed by Malek Najjar and Danish Saleh. Data analyzed and figures prepared by Malek Najjar. Figure legends written by Danish Saleh.

Erk1/2 mediate RIPK1 and RIPK3-dependent inflammatory gene expression changes.

Examining signaling changes, we observed pronounced phosphorylation of MAPK Erk1/2 (Fig. 7A) and increased catalytic activity of the immunoprecipitated protein (Fig. 7B) upon treatment of BMDMs with LPS with zVAD. This response was RIPK1 and RIPK3 kinase-dependent as it was abolished in genetic models of RIPK1 and RIPK3 kinase inactivation and blocked by Nec-1s (Fig. 7A,B and 8A,B).

Importantly, siRNA silencing of Erk1/2 kinases resulted in the pronounced attenuation of multiple gene expression changes and TNFα protein release elicited by LPS with zVAD, without perturbing RIPK1 and RIPK3 kinase-independent responses to LPS alone (Fig. 7C and 8C,D). Furthermore, silencing of Erk1/2 had no effect on cell death induced by LPS with zVAD (Fig. 7D), suggesting that Erk1/2 is a selective transducer of pro-inflammatory signals from RIPK1 and RIPK3. To verify Erk siRNA data, we tested responses in Erk1-deficient (*Mapk3*$^{-/-}$) BMDMs, and similarly observed attenuation of inflammatory responses, but not cell death, in cells treated with LPS with zVAD (Fig. 8E,F).

To elucidate this regulation, we analyzed the effects of two small molecule inhibitors of Erk1/2 pathway. While a direct Erk1/2 inhibitor, SCH772984 (Morris et al. 2013), blocked inflammation induced by LPS with zVAD (Fig. 8G), CL-1040, an inhibitor of upstream Erk1/2 MAPKKs, MEK1 and MEK2, did not reproduce this effect (Fig. 8H), indicating that Erk1/2 regulation by RIPK1 and RIPK3 may not follow a canonical growth factor induced MAPK cascade. This was consistent with the absence of MEK1 and MEK2 activation in BMDMs treated by LPS with zVAD (Fig. 8I). To explore interactions between RIPK1 and Erk1/2, we performed immunoprecipitation of RIPK1 from primary BMDMs, and observed that its association with Erk1/2 was induced in LPS with zVAD stimulated cells and blocked by addition of Nec-1s (Fig.

7E). A reciprocal Erk1/2 IP experiments also confirmed association with RIPK1 (Fig. 8J). Additionally, we observed co-enrichment of phosphorylated Erk1/2 with RIPK1 and RIPK3 in NP40-insoluble cellular fraction in response to LPS with zVAD, which was reduced by Nec-1s and in K51A RIPK3 BMDMs (Fig. 8K,L). Notably, we did not observe MEK1 or MEK2 in the NP40-insoluble fraction (Fig. 8M).

To further investigate constituents of the detergent-insoluble fraction, we probed samples for additional players known to participate in the regulation of RIPK1 and RIPK3 and found TRIF, caspase-8 and CYLD to be similarly enriched (Fig. 9A). Finally, because we previously detected p-MLKL increase in detergent-insoluble aggregates (Fig. 1B), we examined whether Erk1/2 was present in the insoluble fraction from *Mlkl*$^{-/-}$ BMDMs. Indeed, we observed that Erk1/2 co-segregated with RIPK1 and RIPK3 in a MLKL-independent manner (Fig. 9B). These findings suggested that "necrosome"-like detergent insoluble aggregates of RIPK1 and RIPK3 may serve as a signaling platform for engaging Erk1/2 and bypassing MEK1 and MEK2.

Similar to previous data in L929 cells (Christofferson et al. 2012; McNamara et al. 2013), silencing of cJun abrogated inflammatory responses induced by LPS with zVAD in BMDMs (Fig. 9C). However, selective JNK inhibitor VIII did not prevent LPS with zVAD induced gene expression, even though cJun phosphorylation was blocked (Fig. 9D,E), suggesting that cJun phosphorylation by JNK may be co-incidental with RIPK1 and RIPK3 kinase-dependent regulation. The binding partner of cJun in AP1 complex, cFos, is a known direct target of phosphorylation and stabilization by Erk1/2 (Chen et al. 1996; Okazaki & Sagata 1995). Total and phosphorylated cFos were increased upon stimulation with LPS with zVAD in parallel with Erk1/2 in a RIPK1 and RIPK3 kinase-dependent manner (Fig. 7F and 8A,B,). Furthermore, changes in cFos, but not cJun phosphorylation were blocked by Erk1/2 siRNA (Fig. 7G), correlating with

changes in inflammatory gene expression. Silencing of cFos (Fig. 8F) confirmed its requirement for inflammatory gene induction (Fig. 7H and 9G,H). Similar to Erk1/2, cFos only contributed to RIPK1 and RIPK3 kinase-dependent increase after treatment with LPS with zVAD, but was dispensable for LPS induced responses (Fig. 7H) and necroptosis (Fig. 7I), identifying Erk1/2-cFos as a selective axis for inflammatory regulation by RIPK1 and RIPK3.

Along with AP-1, NFκB is established to play a central role in acute inflammatory responses to LPS (Kawai & Akira 2006). As expected, LPS triggered rapid and transient NFκB activation as evidenced by p65 phosphorylation and IκB degradation. This activation was sustained up to 6-9 hr when RIPK1 and RIPK3 kinases became engaged in the presence of zVAD (Fig. 7J and 9I). Unlike cFos siRNA, siRNA silencing of p65 (Fig. 9J) attenuated pro-inflammatory responses to LPS as well as LPS with zVAD; however, similar to cFos silencing, cell death was unperturbed (Fig. 7K,L and 9K,L), reflecting a contribution of NFκB signaling to TRIF-dependent inflammation (Kawai & Akira 2006). Importantly, activation of NFκB was inhibited by siRNA silencing and the small molecule inhibitor of Erk1/2 (Fig. 7G and 9M), but not by cFos siRNA (Fig. 9N) marking these two factors as independent targets of the RIPK1 and RIPK3-Erk1/2 axis that may be activated synergistically to achieve optimal potentiation of the inflammatory responses.

Erk, cFos, and NFκB phosphorylation changes induced by LPS with zVAD were blocked in *Ripk3*$^{-/-}$, RIPK3 K51A and *Ticam1*$^{-/-}$ BMDMs (Fig. 8A,B, 9O), all of which were found to be deficient in inflammatory cytokine production induced by LPS with zVAD (Figs. 1-4). Conversely, these phosphorylation changes were not blocked in *Mlkl*$^{-/-}$ BMDMs, which retained an increased inflammatory response to LPS with zVAD (Fig. 5 and 9P). As further verification of the specificity of this regulation, we determined that phosphorylation of Erk1/2, cFos, and p65,

and degradation of IκB, induced by LPS alone in caspase-8-deficient BMDMs, became sensitive to inhibition by Nec-1s (Fig. 9Q). In sum, these data established the importance of Erk, cFos, and NFκB as mediators of RIPK1 and RIPK3 kinase-dependent inflammatory gene expression.

Figure 7. Erk-cFos and NFkB pathways mediate RIPK1 and RIPK3 kinase-dependent pro-inflammatory signaling induced by LPS with zVAD.

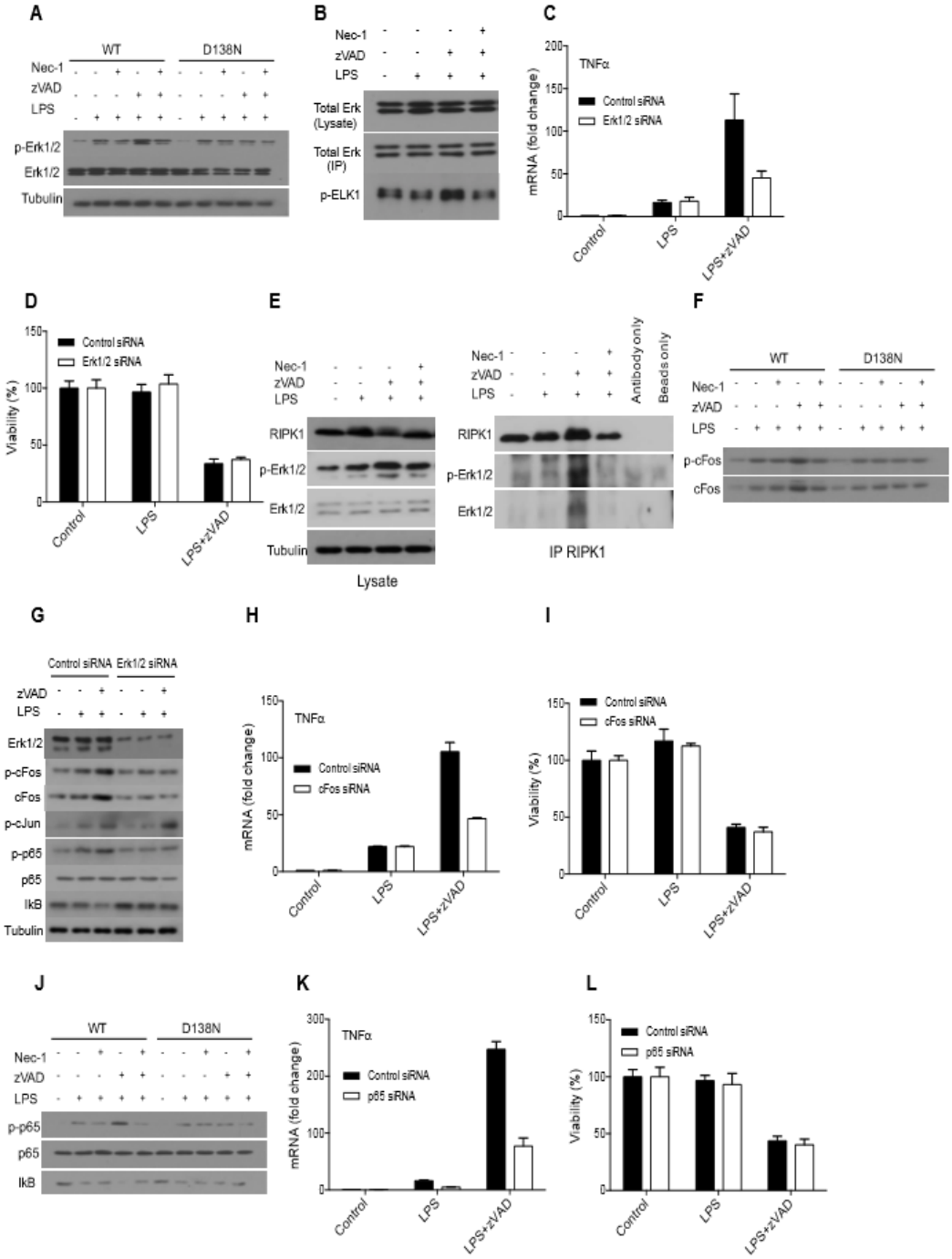

Figure 7: Erk-cFos and NFkB pathways mediate RIPK1 and RIPK3 kinase-dependent pro-inflammatory signaling induced by LPS with zVAD.

(A) Western analysis of Erk1/2 phosphorylation in BMDMs treated for 7 hrs. (B) *In vitro* kinase assay of Erk1/2 protein against Elk1 substrate. Total Erk1/2 was immunoprecipitated from BMDMs treated for 3 hrs. (C-D) TNF mRNA expression (C, 7 hrs) and cell viability (D, 24 hrs) in BMDMs after electroporation with Erk1/2 siRNA. (E) Co-immunoprecipitation of endogenous RIPK1 and Erk1/2 from BMDMs treated for 3 hrs. Western blot analysis for lysate (left panel) and IP (right panel) samples shown. (F) Western analysis in BMDMs treated for 7 hrs. Refer to panel 4A for loading control. (G) Western analysis in wild type BMDMs treated for 7 hrs after electroporation of Erk1/2 siRNA. (H-I) TNF mRNA expression (H, 7 hrs) and cell viability (I, 24 hrs) in BMDMs after electroporation with cFos siRNA. (J) Western analysis in BMDMs treated for 7 hrs. Refer to panel 4A for loading control. (K-L) TNF mRNA expression (K, 7 hrs) and cell viability (L, 24 hrs) in BMDMs after electroporation with p65 siRNA. For qRT-PCR and Western blots, data for one representative experiment out of at least three independent repeats are shown unless otherwise specified. For ELISA, combined data for three independent experiments are shown. Values represent Mean ± SD. *$p<0.05$. BMDMs were treated with LPS=10 ng/ml, zVAD=50 μM, and Nec-1s=30 μM.

Contributions: Contributions: Experiments performed, data analyzed and figures prepared by Malek Najjar. Figure legends written by Danish Saleh.

Figure 8. Inhibition of Erk1/2 blocks cytokine mRNA expression induced by LPS with zVAD.

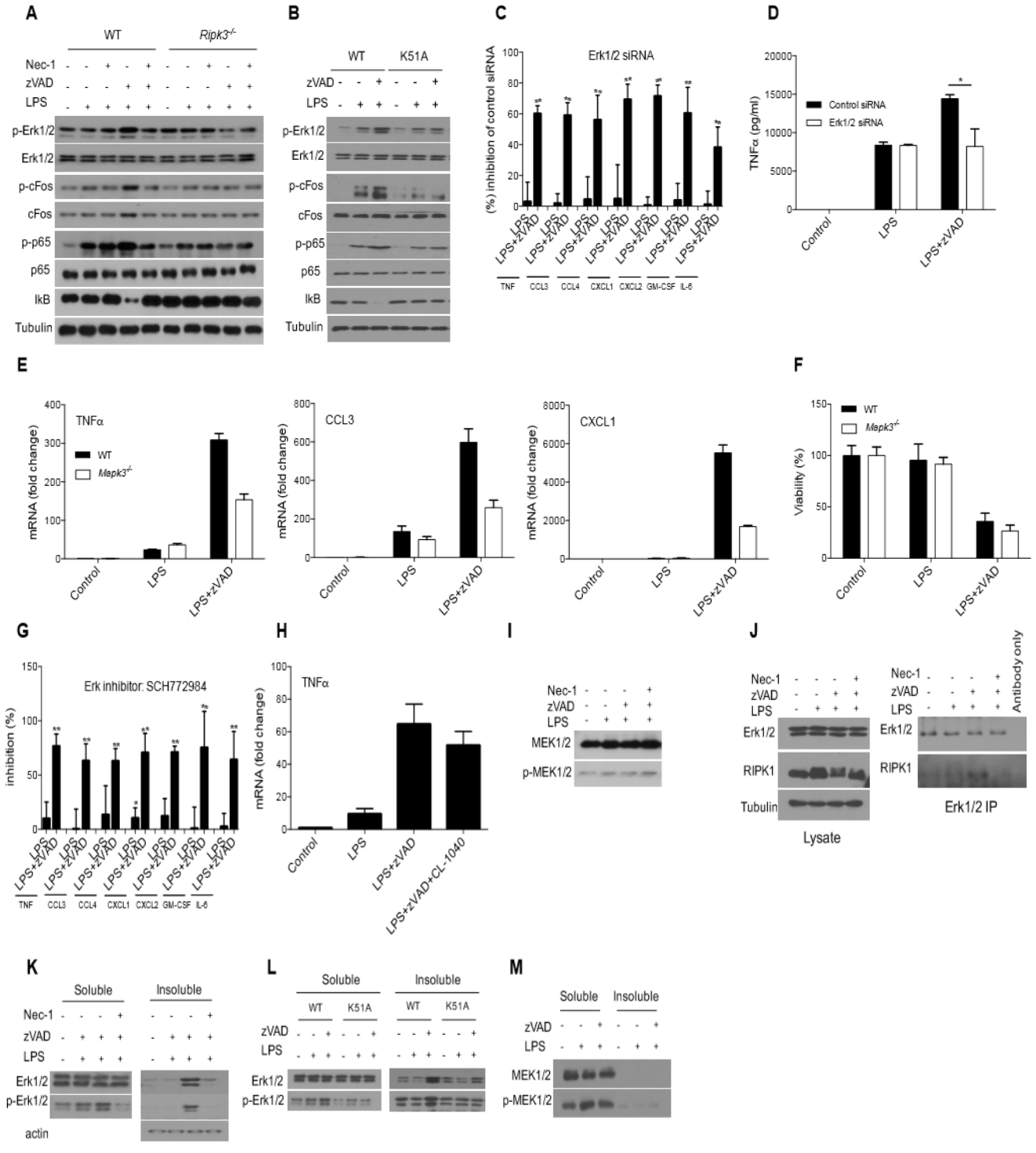

Figure 8. Inhibition of Erk1/2 blocks cytokine mRNA expression induced by LPS with zVAD.

(A-B) Western blot analysis of Erk1/2 phosphorylation in wild type, *Ripk3*$^{-/-}$ (B) and K51A RIPK3 (C) BMDMs treated for 7 hrs. (C) Percent inhibition of mRNA expression of select inflammatory cytokines in BMDMs treated with LPS or LPS with zVAD for 7 hrs following electroporation with Erk1/2 siRNA, evaluated by qRT-PCR. The data reflect the percent inhibition of cytokine mRNA expression in BMDMs electroporated with Erk1/2 siRNA compared to the cells electroporated with control siRNA. Data are the means of three biologic replicates ± SD. *$p<0.05$ and **$p<0.005$. (D) ELISA analysis of TNFα protein release in BMDMs treated for 7 hrs following electroporation with Erk1/2 siRNA. (E) qRT-PCR analysis of mRNA expression of select inflammatory genes in wild type and *Mapk3*$^{-/-}$ BMDMs treated for 7 hrs. (F) Cell viability in wild type and *Mapk3*$^{-/-}$ BMDMs treated for 24 hrs. (G) Percent inhibition of mRNA expression of select inflammatory cytokines in BMDMs treated with LPS or LPS with zVAD for 7 hrs in the presence of Erk1/2 inhibitor (SCH772984), evaluated by qRT-PCR. Data reflect percent inhibition of cytokine mRNA expression in BMDMs treated with Erk1/2 inhibitor over DMSO treated controls. Data are the means of three biologic replicates ± SD. *$p<0.05$ and **$p<0.005$. (H) qRT-PCR analysis of TNFα mRNA expression in BMDMs treated for 7 hrs in the presence of MEK inhibitor (CL-1040). (I) Western blot analysis of MEK1 and MEK2 as well as their phosphorylated forms in wild type BMDMs. (J) Co-immunoprecipitation of endogenous RIPK1 and Erk1/2 from BMDMs stimulated for 3 hrs. Western blot analysis for the lysate (left panel) and Erk1/2 IP (right panel) samples are shown. (K) Western blot analysis of NP40 soluble and NP40 insoluble fractions probed for Erk1/2 and phosphorylated Erk1/2 in wild type BMDMs treated with LPS alone, LPS with zVAD, or LPS with zVAD and Nec-1 for 4 hrs. (L) Western blot analysis of NP40 soluble and NP40 insoluble

fractions probed for Erk1/2 and phosphorylated Erk1/2 in wild type and K51A RIPK3 BMDMs treated with LPS alone, LPS with zVAD, or LPS with zVAD and Nec-1 for 4 hrs. (M) Western blot analysis of NP40 soluble and NP40 insoluble fractions probed for MEK1/2 and phosphorylated MEK1/2 in wild type BMDMs treated with LPS alone or LPS with zVAD for 4 hrs. For qRT-PCR and Western blots, data for one representative experiment out of at least three independent repeats are shown unless otherwise specified. For ELISA, combined data for three independent experiments are shown. Values represent Mean ± SD. BMDMs were treated with LPS=10 ng/ml, zVAD=50 μM, Nec-1s=30 μM, Erk inhibitor SCH772984= 0.5 μM, and MEK inhibitor CL1040=1 μM.

Contributions: Experiments performed, data analyzed and figures prepared by Malek Najjar. Figure legends written by Danish Saleh.

Figure 9. Inhibition of Erk1/2 blocks cytokine mRNA expression induced by LPS with zVAD.

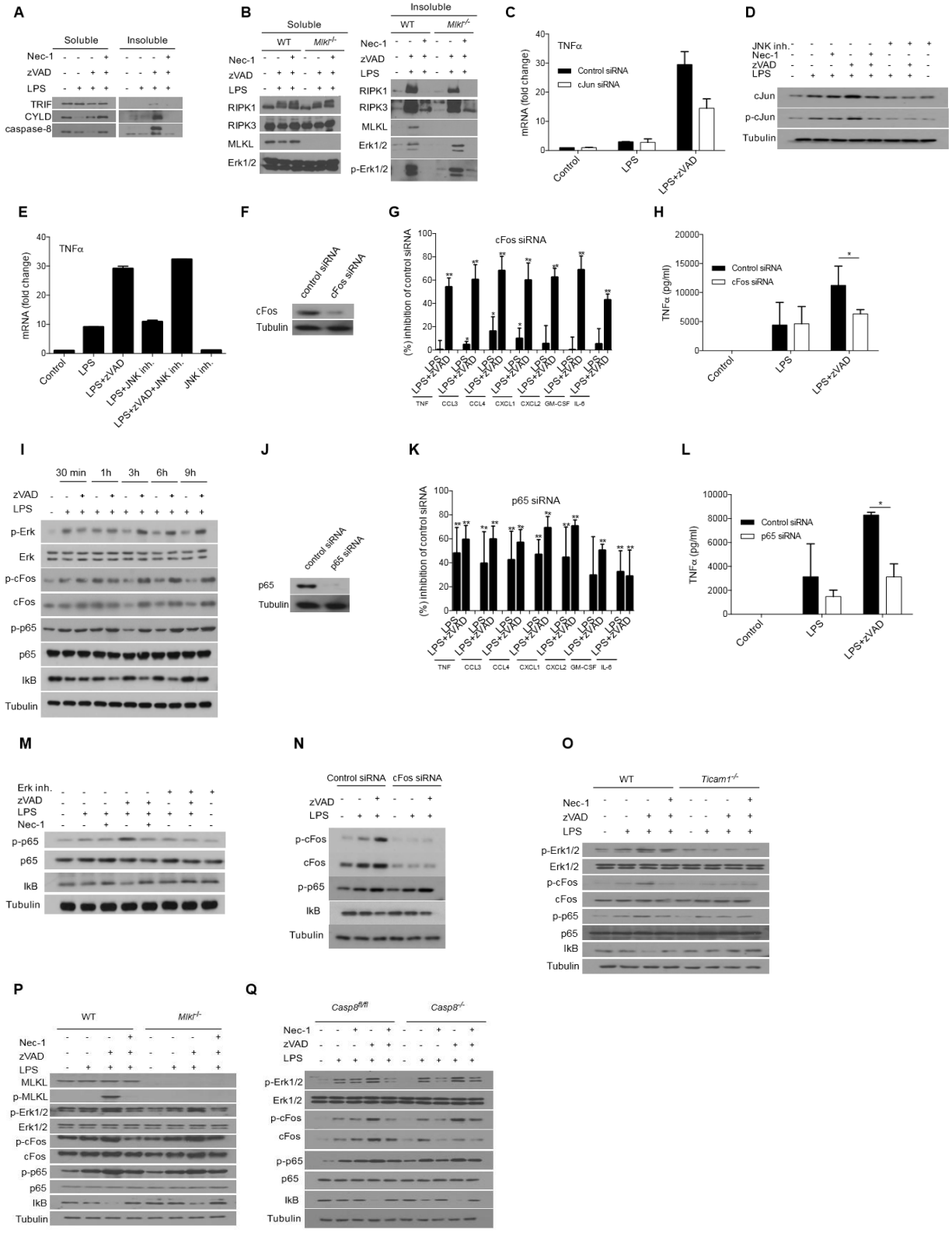

Figure 9. Inhibition of cFos and NFκB pathway blocks cytokine mRNA expression induced by LPS with zVAD.

(A) Western blot analysis of NP40 soluble and NP40 insoluble fractions probed for TRIF, CYLD, and Caspase-8 in wild type BMDMs treated with LPS alone, LPS with zVAD or LPS with zVAD and Nec-1 for 4 hrs. (B) Western blot analysis of NP40 soluble and NP40 insoluble fractions in wild type and *Mlkl*$^{-/-}$ BMDMs treated with LPS alone, LPS with zVAD, or LPS with zVAD and Nec-1 for 4 hrs. (C) qRT-PCR analysis of TNFα mRNA expression in BMDMs treated for 7 hrs following electroporation with cJun siRNA. (D) Western blot analysis of cJun and phosphorylated cJun in BMDMs treated for 7 hrs in the presence of JNK inhibitor VIII. (E) qRT-PCR analysis of TNFα mRNA expression in wild type BMDMs treated for 7 hrs in the presence of JNK inhibitor VIII. (F) Silencing of cFos using targeted siRNA in BMDMs confirmed by Western blot. (G) Percent inhibition of mRNA expression of select inflammatory cytokines in BMDMs treated with LPS or LPS with zVAD for 7 hrs following electroporation with cFos siRNA,evaluated by qRT-PCR. The data reflect the percent inhibition of cytokine mRNA expression in BMDMs electroporated with cFos siRNA compared to the cells electroporated with control siRNA. Data are the means of three biologic replicates ± SD. *$p<0.05$ and **$p<0.005$. (H) ELISA analysis of TNFα protein release in wild type BMDMs treated with LPS with zVAD for 7 hrs following electroporation with cFos siRNA. (I) Western blot analysis of changes in Erk1/2, cFos, p65 and IkB in wild type BMDMs treated with LPS or LPS with zVAD over a 9 hr time course. (J) Silencing of p65 using targeted siRNA in BMDMs confirmed by Western blot. (K) Percent inhibition of mRNA expression of select inflammatory cytokines in BMDMs treated with LPS or LPS with zVAD for 7 hrs following electroporation with p65 siRNA, evaluated by qRT-PCR. The data reflect the percent inhibition of cytokine mRNA expression in BMDMs electroporated with

p65 siRNA compared to the cells electroporated with control siRNA. Data are the means of three biologic replicates ± SD. *$p<0.05$ and **$p<0.005$. (L) ELISA analysis of TNFα protein release in wild type BMDMs treated with LPS with zVAD for 7 hrs following electroporation with p65 siRNA. (M) Western blot analysis in BMDMs treated for 7 hrs in the presence of Erk inhibitor (SCH772984). (N) Western blot analysis in BMDMs treated with LPS alone or LPS with zVAD for 7 hrs following electroporation with cFos siRNA. (O) Western blot analysis in wild type and *Ticam1*$^{-/-}$ BMDMs treated with LPS alone, LPS with zVAD, or LPS with zVAD and Nec-1 for 7 hrs. (P) Western blot analysis in wild type and *Mlkl*$^{-/-}$ BMDMs treated with LPS alone, LPS with zVAD, or LPS with zVAD and Nec-1 for 7 hrs. (Q) Western blot analysis in caspase-8-floxed and caspase-8-deficient BMDMs treated with LPS alone, LPS with zVAD, or LPS with zVAD and Nec-1 for 7 hrs. *Caspase-8* was deleted from *casp8*$^{flox/flox}$ BMDMs by Adenoviral-Cre-GFP mediated excision. For qRT-PCR and Western blots, data for one representative experiment out of at least three independent repeats are shown unless otherwise specified. For ELISA, combined data for three independent experiments are shown. Values represent Mean ± SD. BMDMs were treated with LPS=10 ng/ml, zVAD=50 μM, Nec-1s=30 μM, Erk inhibitor SCH772984= 0.5 μM, and JNK inh. VIII=10 μM.

Contributions: Most experiments performed, data analyzed, and figures prepared by Malek Najjar Data generated from Necrosome isolation assays performed, analyzed, and prepared by Danish Saleh. Figure legends written by Danish Saleh.

RIPK1 and RIPK3 control LPS-induced inflammatory responses *in vivo*.

Induction of necroptosis is characterized by a well-established dichotomy in activation *in vitro*, which in most cases requires inhibition of caspase-8, and *in vivo*, where necroptosis has been observed in a wide range of pathologic injuries in the absence of exogenous caspase inhibition (Duprez et al. 2011; Linkermann & Green 2014). This has been directly illustrated by the activity of the best characterized inducer of necroptosis, TNFα, which requires caspase inhibition for necroptosis *in vitro* in most cellular systems described to date, but efficiently and directly induces RIPK1 and RIPK3 kinase-dependent necroptosis *in vivo* in normal, wild type animals (Duprez et al. 2011). These observations suggest that the strict controls on RIPK1 and RIPK3 kinase activation *in vitro* may be less efficient *in vivo* and prompted us to examine whether RIPK1 and RIPK3 kinases may be involved in the control of inflammatory responses to LPS *in vivo* in the absence of zVAD. To address this question, we injected BALB/c mice intravenously with 30 mg/kg of Nec-1s 15 min prior to intraperitoneal injection with a low dose of LPS (50 µg/kg). Multiple cytokines and chemokines, which were shown to be augmented by zVAD treatment and regulated in a RIPK1 and RIPK3 kinase-dependent manner *in vitro* (Fig. 1: TNFα, CCL3, CCL4, GM-CSF (CSF-2) and IL6), were induced in the circulation by LPS, 1 hr post-injection, and strikingly reduced ~60-80% by Nec-1s (Fig. 10A and 11A). The one hour time point corresponds to the time of maximal TNFα induction (Fig. 11B). Additionally, we observed that Nec-1s decreased mRNA of these molecules in $CD11b^+$ myeloid precursor cells, isolated from the bone marrow of animals (Fig. 10B and 11C). Analysis of additional genes, which were upregulated by LPS with zVAD *in vitro* (Fig. 1), showed similar induction by LPS alone *in vivo* and inhibition by Nec-1s (Table 1). To confirm the role of RIPK1 kinase, we injected wild type and RIPK1 D138N mice with LPS and, similarly, found a robust decrease in circulating inflammatory mediators (Fig.

10C). D138N RIPK1 CD11b^{+} myeloid precursor cells, isolated from the bone marrow of the LPS-injected animals, also displayed greatly reduced mRNA transcripts of inflammatory molecules (Fig. 10D), supporting control of inflammatory gene expression by RIPK1 kinase activity *in vivo*.

To more comprehensively examine the inflammatory profile regulated by RIPK1 kinase, we performed RNA-Seq analysis of the mRNAs from mice treated with vehicle, LPS, and LPS with Nec-1s. Pathway analysis identified multiple innate immune response axes as major pathways induced by LPS *in vivo*, and notably, the same pathways were identified as key targets of Nec-1s in the LPS-injected animals (Table 2). We also evaluated this regulation in CD11b^{+} sorted peritoneal macrophages, a model for mature and activated myeloid cells, and found that intravenous administration of Nec-1s, similarly inhibited LPS-induced TNFα, CCL3 and CCL4 mRNA upregulation 1 hr after LPS injection (Fig. 11D). Overall, these data mark the kinase activity of RIPK1 as an unanticipated master regulator of acute inflammatory responses to LPS *in vivo*.

Our *in vitro* model also pointed to a crucial role for RIPK3 in regulating RIPK1 kinase-dependent cytokine synthesis. Cytokine production was also diminished in the *Ripk3*$^{-/-}$ mice confirming an important role for RIPK3 in LPS-induced inflammation *in vivo* (Fig. 12A). While bone marrow cells provide a limited source for protein analysis, we were able to also observe activation of some of the same signaling pathways *in vivo* that we have linked to RIPK1 and RIPK3 activation *in vitro*, including phosphorylation of Erk, cFos and p65 and degradation of IκB. All of these LPS-induced events were inhibited by Nec-1s (Fig. 12B).

Our *in vitro* data strongly suggested a critical role for RIPK1 and RIPK3 kinases as inducers of cytokine synthesis independent of cell death. Next, we sought to evaluate whether this is also the case *in vivo*. Notably, our studies used low dose of LPS, which is $\leq$10% of what is used

to trigger systemic toxicity. Accordingly, we did not observe cell death in $CD11b^+$ cells that we used for mRNA analysis using AQUA LIVE/DEAD staining (Fig. 11E). Similarly, we did not see any increase in the circulating markers of injury, such as ALT, at either 1 hr or at 7 hrs after LPS injection (Fig. 11F). These data support the notion that RIPK1 regulation of inflammation is not associated with cell death *in vivo*. To examine RIPK1 and RIPK3 kinase-dependent cytokine synthesis in the absence of necroptosis, we assessed the efficacy of Nec-1s in regulating LPS-induced cytokine production in *Mlkl*$^{-/-}$ mice. Consistent with our hypothesis, loss of MLKL did not impair LPS-induced serum cytokines and mRNA expression in $CD11b^+$ cells, and importantly, this induction was still blocked by Nec-1s (Figure 11G,H and 12C,D). Altogether, these data indicate the cell death independent control of inflammation by kinase activity of RIPK1 and RIPK3 *in vivo*, analogous to our data *in vitro*.

We also considered whether TNFα upregulation due to the LPS stimulation might be a contributing factor to the acute RIPK1 and RIPK3 kinase-dependent inflammatory responses. However, administration of TNFα only led to a relatively weak inflammatory response, compared to LPS, and this response was not inhibited by Nec-1s (Fig. 11I). This observation was not surprising as previously published data showed that circulating concentrations of inflammatory mediators, such as IL6, were elevated only several hours after injection of TNFα and this inflammatory response was clearly secondary to the induction of cell death induced by the molecule (Duprez et al. 2011).

Factors that may allow activation of RIPK1 and RIPK3 kinase-dependent injury without perturbation of caspase-8 activity in a variety of mouse models *in vivo* have not yet been addressed comprehensively. One possibility may be lower efficiency of caspase-8 activation *in vivo*. We found that Caspase-Glo caspase-8 activity assay provided a sensitive method to detect caspase-8

activation by LPS alone *in vitro*, and this was inhibited by zVAD (Fig. 11J). Notably, using the same assay, we did not observe caspase-8 activation in bone marrow cells in response to LPS challenge *in vivo*. Only a much higher, toxic dose of LPS was required to elicit robust caspase-8 activation (Fig. 11K). Thus, while development of better and more sensitive tools will be useful for the evaluation of caspase-8 activation, our data suggests the possibility that limitations on caspase-8 activity may explain the direct activation of RIPK1 and RIPK3 signaling by LPS *in vivo*.

Ultimately, these observations suggest that RIPK1 and RIPK3, which are controlled *in vitro* by caspase-8, play a major role in acute inflammatory responses to LPS *in vivo*. Our work revealed a mechanism for this regulation, which is mediated by Erk1/2 in a cell death-independent and cell-autonomous manner.

Figure 10. LPS-induced inflammatory cytokine synthesis requires RIPK1 kinase *in vivo.*

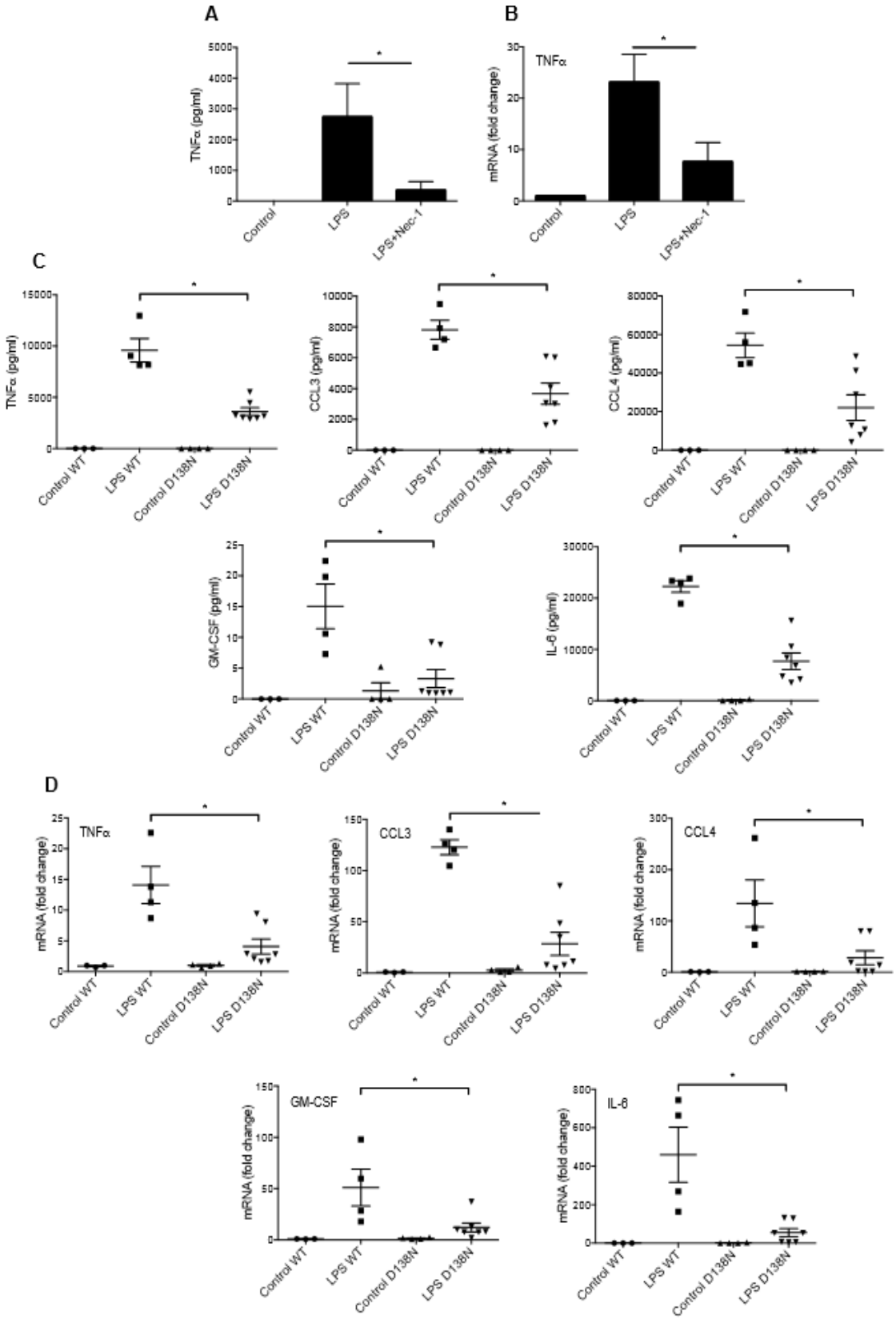

Figure 10: LPS-induced inflammatory cytokine synthesis requires RIPK1 kinase *in vivo.*

(A) Circulating TNFα in wild type mice injected with Nec-1s (iv) 15 min prior to LPS (50μg/kg) (ip) by ELISA. n= 8-9 animals per group and *$p<0.05$. (B) TNF mRNA expression in $CD11b^+$ bone marrow cells isolated from mice post-injection with LPS or LPS/Nec-1s as in (A). n=5-6 animals per group and *$p<0.05$. (C) Multiplexed ELISA analysis of circulating inflammatory mediators in mice injected with LPS (50μg/kg) intraperitoneally. Serum samples evaluated 1 hr thereafter. n=3-6 animals per group and *$p<0.05$. (D) mRNA expression of a panel of inflammatory genes in $CD11b^+$ bone marrow cells isolated from LPS-injected mice as in (C). n= 3-6 animals per group and *$p<0.05$. Values represent Mean ± SD.

Contributions: Experiments performed by Malek Najjar and Danish Saleh. Data analyzed and figures prepared by Malek Najjar. Figure legends written by Danish Saleh.

Figure 11. LPS induced inflammation requires kinase activity of RIPK1 and is independent of cell death in vivo.

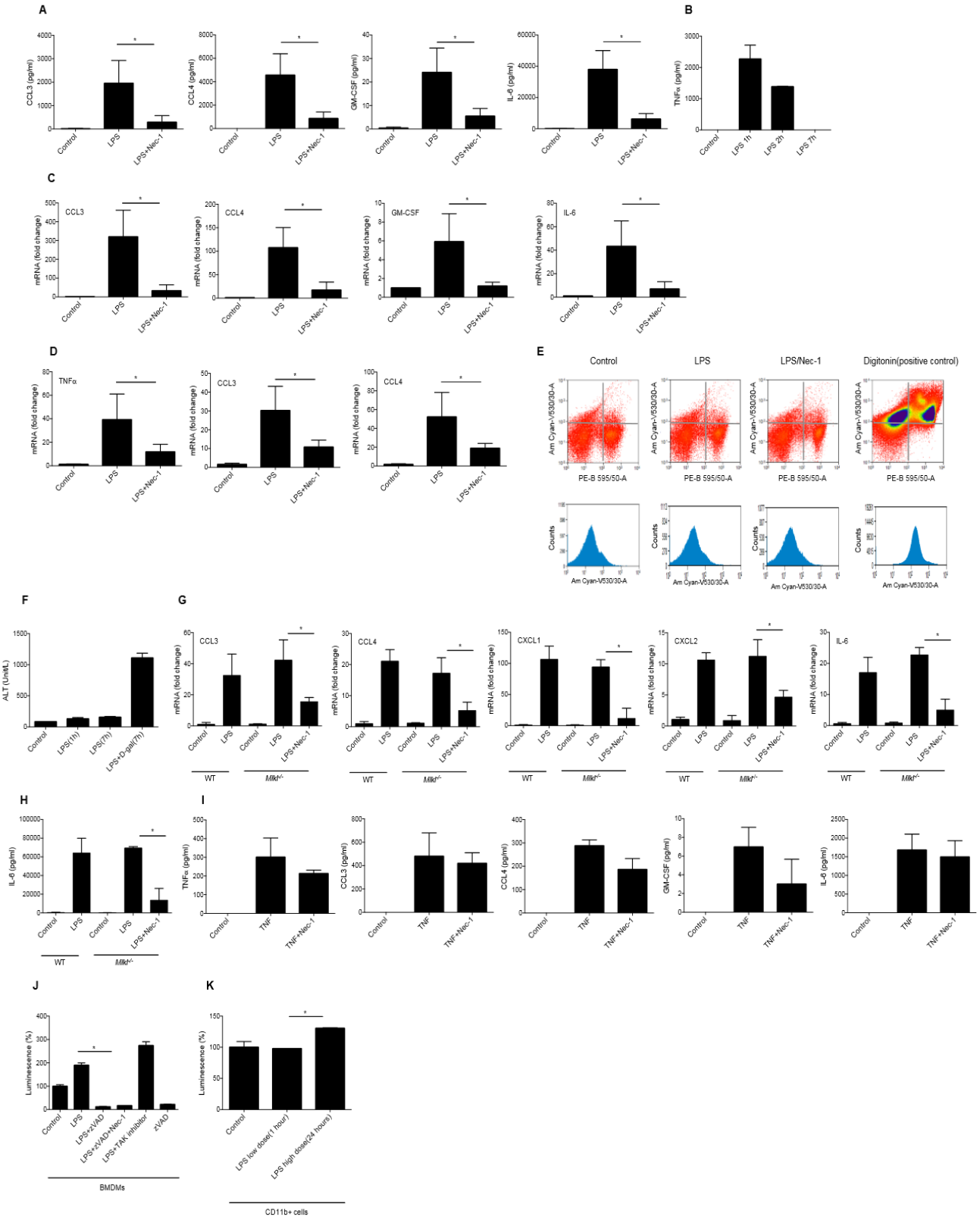

Figure 11. LPS induced inflammation requires kinase activity of RIPK1 and is independent of cell death in vivo.

(A) Multiplexed ELISA analysis of circulating inflammatory cytokines in wild type mice injected with Nec-1s (iv) 15 min prior to LPS (ip). n= 8-9 animals per group and *p<0.05. (B) Serum TNFα was measured 1, 2 and 7 hours after injection with 50 μg/kg LPS alone, n=3 per group. (C) qRT-PCR analysis of mRNA expression of inflammatory genes in $CD11b^+$ bone marrow cells isolated from mice post-injection with LPS or LPS/Nec-1s as in (A). (D) qRT-PCR analysis of mRNA expression of inflammatory genes in $CD11b^+$ thioglycollate-elicited peritoneal macrophages from mice post-injection with LPS or LPS/Nec-1s as in (A). n=3 animals per group and *p<0.05. Values represent Mean ± SD. (E) FACS analysis of $CD11b^+$ cells from bone marrow collected 1 hr after LPS injection. Cell viability was evaluated using LIVE/DEAD AQUA Dead Cell Stain Kit. Post-isolation treatment with digitonin was used as a positive control for cell death. (F) Serum ALT was measured 1 hr and 7 hrs after injection with 50 μg/kg LPS alone or in combination with 800 mg/kg D-gal, n=3-5 per group. (G) qRT-PCR analysis of mRNA expression of inflammatory genes in CD11b+ bone marrow cells isolated from wild type and *Mlkl*$^{-/-}$ mice injected with Nec-1 (iv) 15 min prior to LPS (ip) or LPS (ip) alone. Cells were collected 1 hr after LPS injection. n=3 animals per group and *p<0.05. (H) ELISA analysis of circulating IL6 from wild type and *Mlkl*$^{-/-}$ mice injected with LPS or LPS/Nec-1 as in (G). n=5 animals per group and *p<0.05. (I) Multiplexed ELISA analysis of select circulating inflammatory cytokines after injection of wild type mice with human TNFα (50 μg/kg) or TNFα and Nec-1s (30 mg/kg). Samples were collected 1 hr post-treatment, n=3 per group. (J) Caspase-8 activity assay in wild type BMDMs treated for 3 hours. n=3 biological replicates and *p<0.05. (K) Caspase-8 activity assay in CD11b+ cells, isolated and prepared as in (C and G) and (F). n=3 replicates per group and *p<0.05.

Contributions: Experiments performed and figures prepared by Malek Najjar. Data analyzed by Malek Najjar. Analysis of circulating TNFα in *Mlkl*$^{-/-}$ completed by Danish Saleh. Figure legends written by Danish Saleh.

Figure 12. LPS-induced inflammatory cytokine synthesis requires RIPK3 but not MLKL *in vivo*.

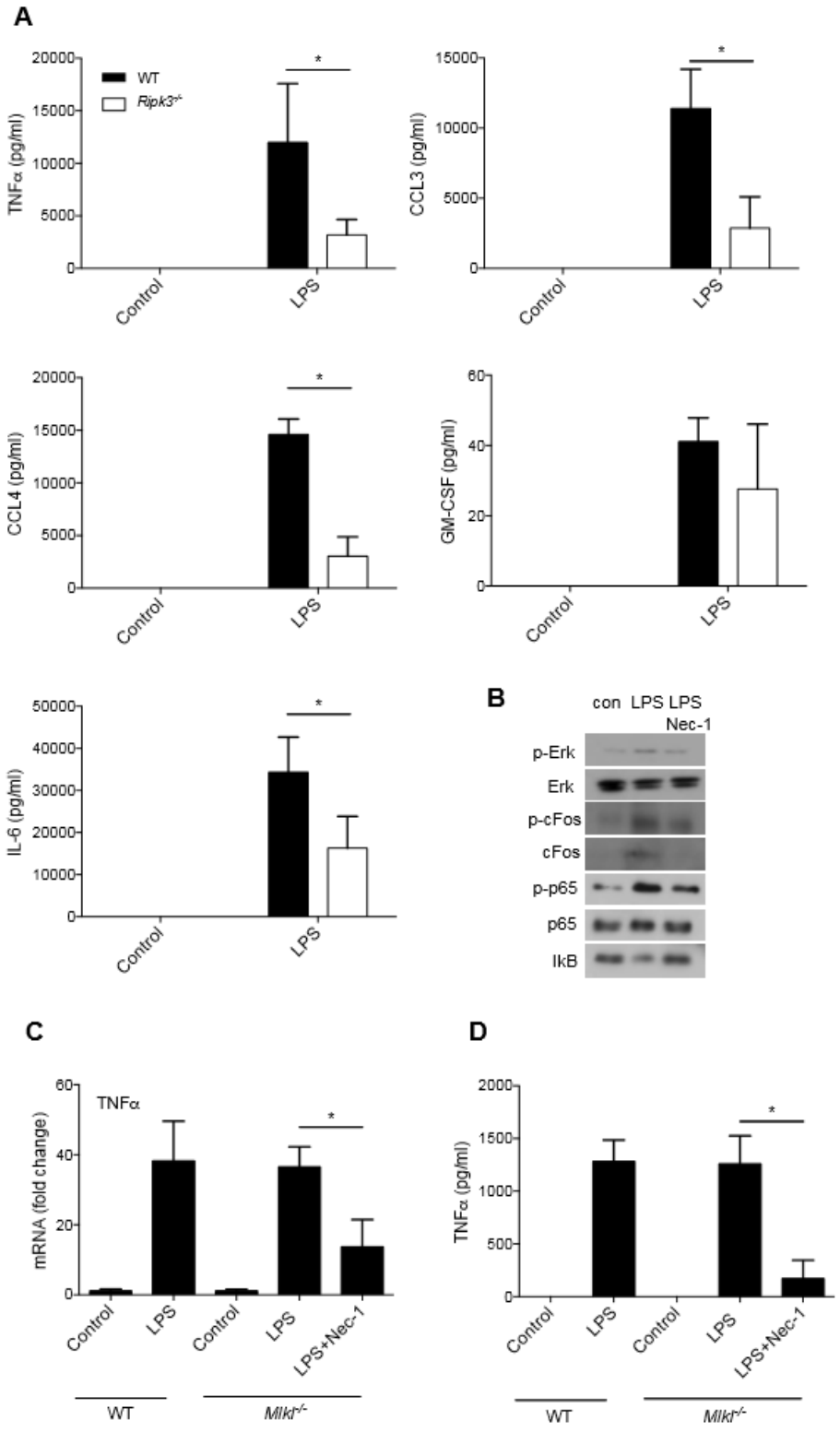

Figure 12: LPS-induced inflammatory cytokine synthesis requires RIPK3 but not MLKL *in vivo*.

(A) Circulating inflammatory mediators in wild type and *Ripk3*$^{-/-}$ mice by ELISA. n= 4 animals per group, *p<0.05. (B) Western analysis in mouse CD11b^{+} bone marrow cells from LPS or LPS and Nec-1s injected animals. Samples from 3 animals per group were pooled for the analysis. (C) TNF mRNA expression in CD11b^{+} bone marrow cells isolated from wild type and *Mlkl*$^{-/-}$ mice injected with Nec-1 (iv) 15 min prior to LPS (ip) (50μg/kg) or LPS (ip) alone. Cells were collected 1 hr after LPS injection. n=3 animals per group and *p<0.05. (D) Circulating TNFα from wild type and *Mlkl*$^{-/-}$ mice injected with LPS or LPS and Nec-1 as in (C). n=5 animals per group and *p<0.05. Also see figure S6.

Contributions: Experiments performed, data analyzed, and figures prepared by Malek Najjar. Figure legends written by Danish Saleh.

Table 1. Similar genes are controlled by RIPK1 in BMDMs *in vitro* and in bone marrow CD11b^{+} following injection of LPS *in vivo*.

	BMDMs *in vitro*		Bone marrow CD11+ *in vivo*	
Gene	Fold induction of LPS/zVAD to LPS alone	Fold reduction by addition of Nec-1s to LPS/zVAD	Fold induction by LPS alone	Fold reduction by addition of Nec-1s
Edn1	19.49	14.77	39.68	12.10
Ifnb1	13.2	9.23	2.97	3.67
Ccl3	11.72	12.6	319.6	9.73
Csf1	9.6	5.85	2.08	1.91
Csl2	8.72	5.59	47.2	3.19
Ccl4	5.28	5.87	107.38	6.22
Cxcl1	4.74	4.65	165.98	3.35
Cxcl2	3.97	3.48	293.1	3.8
Ccl7	2.34	2.09	2.87	3.87
Il6	2.28	3.04	43.29	6.18
Csf2	2.08	2.67	5.92	4.93
Il1b	1.47	5.07	29.4	3.48
Csf	1.45	2.46	3.97	2.38

Table 1: Similar genes are controlled by RIPK1 in BMDMs *in vitro* and in bone marrow CD11b^{+} following injection of LPS *in vivo*.

Gene expression changes in BMDMs and bone marrow samples were evaluated by qRT-PCR. *In vitro,* fold induction by LPS with zVAD relative to LPS alone and fold reduction by LPS with zVAD and Nec-1s relative to LPS with zVAD are shown. *In vivo,* fold induction by LPS relative to vehicle and fold reduction by LPS with Nec-1s relative to LPS alone are shown.

Contributions: Experiments performed by Malek Najjar. Data analyzed and figures prepared by Alexei Degterev. Figure legends written by Danish Saleh.

Table 2. Major pathways induced by LPS and inhibited by Nec-1s in vivo.

Ingenuity pathways inhibited by Nec-1s after LPS injection	p-values
Pattern recognition of bacteria/viruses	$6.3X10^{-17}$
IL10 signaling	$1.2X10^{-13}$
NFkB signaling	$7.9X10^{-12}$
Death receptor signaling	$2X10^{-11}$
Dendritic cells maturation	$7.9X10^{-11}$
Toll-like receptor signaling	$1X10^{-10}$
IL6 signaling	$1.1X10^{-9}$
Activation of IRF3 by cytosolic DNA	$1.5X10^{-12}$

Table 2: Major pathways induced by LPS and inhibited by Nec-1s *in vivo.*

Analysis of the signaling pathways attenuated by Nec-1s in LPS-injected animals. Mice were injected with 20 mg/kg Nec-1s (iv) 15 min prior to 50 μg/kg LPS (ip). Changes in gene expression were analyzed using Ingenuity software and Fisher's exact test for p-value.

Contributions: Experiments performed by Malek Najjar. Data analyzed and figures prepared by Alexei Degterev. Figure legends written by Danish Saleh.

Discussion

Our observations suggest that kinase activity of RIPK1 is a critical component in negotiating acute inflammatory cytokine expression, unlike the role of this kinase in necroptosis, which can be by-passed by direct engagement of RIPK3 (Dannappel et al. 2014; Dillon et al. 2014; Kaiser et al. 2014; Kearney et al. 2015; Rickard et al. 2014; Takahashi et al. 2014; Upton et al. 2010; Upton et al. 2012). In the absence of kinase activity of RIPK1, LPS and LPS with zVAD-induced acute inflammatory changes were attenuated both *in vivo* and *in vitro*, respectively. Similarly, *Ripk3*$^{-/-}$ mice and BMDMs also displayed a significant defect in cytokine production induced by LPS *in vivo* or LPS with zVAD *in vitro*. However, RIPK3, but not RIPK1, was dispensable for inflammatory gene expression changes in TNFα -treated MEFs. These observations distinguish kinase functions of RIPK1 from RIPK3 and suggest that while RIPK3 serves as the requisite cell executioner, RIPK1 may serve as an essential driver of *de novo* cytokine synthesis. Consistent with this framework, recent works from other groups have elucidated additional RIPK1 kinase-dependent inflammatory changes that do not require RIPK3. For example, RIPK1 kinase, but not RIPK3 was responsible for inflammation observed in *Ptpn6*^{spin} mice and caspase-8 deficient dendritic cells (Cuda et al. 2014; Lukens et al. 2013). In another example, work by Yatim et al. showed that chemically enforced RIPK3 oligomerization is insufficient to drive NFκB-dependent cytokine synthesis without RIPK1 (Yatim et al. 2015). Together, our work and that of others suggest an important role for RIPK1 catalytic activity in the regulation of multiple inflammatory pathways.

The precise molecular details of inflammatory signaling by the RIPK1 and RIPK3 necrosome will be important to further understand. Previous work established that TRIF can directly engage RIPK3 (Kaiser et al. 2013) and oligomerization of just RIPK3 is sufficient to

induce necroptosis (Cook et al. 2014; Orozco et al. 2014; Wu et al. 2014). In contrast, our data show that RIPK1 kinase, also a direct binding partner of TRIF (Meylan et al. 2004), is indispensable for TRIF-dependent cytokine synthesis. Evidence also suggests that RIPK1 and RIPK3 form detergent insoluble amyloid-like "necrosome" aggregates (Li et al. 2012) which serve as a signaling platform for MLKL activation by RIPK3. Analogous RIPK1-containing "ripoptosome" complexes were described as a platform for RIPK1-dependent caspase-8 activation (Feoktistova et al. 2011; Tenev et al. 2011). Our data suggest that similar detergent-insoluble RIPK1 and RIPK3 "necrosome"-like aggregates may mediate pro-inflammatory signaling through Erk1/2, bypassing requirement for MEK1 and/or MEK2. However, it remains to be determined whether a singular RIPK1 and RIPK3 complex is formed to carry out distinct pro-inflammatory and pro-death functions or, alternatively, physically and/or compositionally distinct "necrosome"-like complexes are formed to differentially regulate necroptosis and pro-inflammatory gene expression. A comprehensive proteomics analysis of molecular interactions associated with RIPK1 and RIPK3 aggregate formation in BMDMs treated with LPS with zVAD will be needed to further reveal mechanistic details of this regulation.

RIPK1 and RIPK3 have attracted major interest as therapeutic targets for a wide range of pathologies, including ischemia-reperfusion injuries, atherosclerosis, pancreatitis, retinal damage, multiple sclerosis and many others (Linkermann & Green 2014; Ofengeim et al. 2015). While inflammation is often viewed as a consequence of necroptosis (Pasparakis & Vandenabeele 2015; Silke et al. 2015), our findings raise the possibility that the contributions of RIPK1 and RIPK3 to inflammatory pathologies may also reflect cell death-independent regulation of inflammation. Accordingly, it will be critical to consider whether inflammatory pathologies, in which roles for RIPK1 and RIPK3 may not have been closely examined due to the limited influence of cell death,

may involve these proteins in a cell death independent capacity.

Lastly, the dichotomy in RIPK1 and RIPK3 activation *in vivo* and *in vitro* remains to be fully understood. *In vitro*, LPS-induced RIPK1 and RIPK3 kinase-dependent inflammatory cytokine production requires inactivation of caspase-8. However, *in vivo*, LPS-induced RIPK1 and RIPK3 kinase-dependent inflammation proceeds without exogenous manipulation of caspase-8 function. This paradigm is analogous to many other *in vivo* observations, such as the requirement of caspase-8 inhibition *in vitro*, but not *in vivo* for necroptosis activation by TNFα (Duprez et al. 2011). One explanation for these differences may be a discrepancy in the activity of the regulators of RIPKs, such as caspase-8, CYLD, $FLIP_L$, TAK1, and/or A20, resulting in less stringent controls on RIPK activation *in vivo*. Along these lines, while LPS induced caspase-8 activity *in vitro* in our experiments, this was not the case *in vivo,* consistent with the possibility of differences in caspase-8 activation by LPS *in vitro* and *in vivo*. Notably, recent report by Ofengeim et al. similarly suggested deficient activation of caspase-8 in white matter lesions of multiple sclerosis patients are associated with changes in the regulation of RIPK1 and RIPK3 signaling (Ofengeim et al. 2015). Nevertheless, more sensitive and specific methods, especially to assess caspase-8 activity in necroptosis-inhibiting caspase-8 and $FLIP_L$ heterodimeric complex (Oberst et al. 2011), are needed to further address this question in LPS-induced and other *in vivo* models of RIPK1 and RIPK3 kinase regulation.

Author Contributions

M.N., D.S., M.Z., S.N., A.T., J.F. and S.S. performed the experiments. A.P. and M.P. developed RIPK1 D138N mice. M.N., D.S., J.B., P.G., M.W., M.K., S.B., M.P., A.P. and A.D. wrote and revised the manuscript.

Acknowledgments

This work was supported in part by grants from NIH to A.D. (R01GM080356 and R01GM084205), to S.B. and A.D. (R01CA190542), to M.K. (R01AI07118), and to M.W. (R01NS047447). We thank Drs. Vishva Dixit, Stan Krajewski, Katherine Fitzgerald and Sergei Nedospasov for providing the reagents. P.J.G., J.B and J.N.F. are employees of GlaxoSmithKline. A.D. is a consultant for Denali Therapeutics.

Experimental Procedures

Animals

Female BALB/C (Charles River Labs) or C57BL/6 mice 6-8 weeks of age were used for LPS experiments. *Ripk3*$^{-/-}$ (on C57BL/6 background) and matched controls were previously described (Newton et al., 2004) and provided to us by Dr. Vishva Dixit (Genentech). *Ticam1*$^{-/-}$ (C57BL/6J-*Ticam1Lps2*/J) mice, *Myd88-/-* (B6.129-*Myd88*$^{tm1.1Defr/J}$), *Mapk3*$^{-/-}$ (B6.129-*Mapk3*$^{tm1Gela/J}$) mice and corresponding control mice (C57BL/6J, B6.129) were purchased from Jackson labs. *Tnfr1*$^{-/-}$ mice (C56BL/6-*Tnfrsf1*^{tm1Imx}*/J*) on a C57BL/6 background were obtained from Jackson labs. Floxed caspase-8 (*Casp8*$^{fl/fl}$) mice were generated on FVB/N background and were a generous gift of Dr. Stan Krajewski (Burnham institute) (Krajewska et al. 2011). RIPK1 D138N and RIPK3 K51A (*Ripk1*$^{D138N/D138N}$ *and Ripk3*$^{K51A/K51A}$) mice were previously described (Polykratis et al. 2014; Moriwaki et al. 2015). All use of animals was approved by the Tufts University, UMASS and Fox Chase Cancer Center Institutional Animal Care and Use Committees. Mice were maintained in animal facilities in cages with light/dark cycle and experiments were performed according to the protocol with all efforts to minimize the number and suffering of the animals.

Reagents

Lipopolysaccharide (LPS) (*Escherichia coli* 0111:B4) was purchased from Sigma and Mouse TNFα was purchased from Peprotech. Optimized Necrostatin-1 (5-[(7-chloro-1H-indol-3-yl) methyl]-3-methyl-2,4-imidazolidinedione or Nec-1s) was synthesized as previously described (Teng et al. 2005). For *in vivo* administration, Nec-1s was dissolved in PBS containing 25% Polyethylene Glycol 400 (Spectrum labs). Endotoxin free recombinant Human TNFα was purified in Dr. Sergei Nedospasov's lab and injected at 50 μg/kg intra-peritoneal. D-(+)-Galactosamine hydrochloride (D-gal) was purchased from sigma and injected at 800 mg/kg dose

intraperitoneal after dissolved in PBS. RIPK3 inhibitor, GSK872, was also previously described (Mandal et al. 2014). Other inhibitors (and their final concentrations) were as follows: Erk inhibitor, SCH772984 (0.5 μM, Selleck Chemicals), JNK inhibitor VIII (10 μM, Calbiohem), Akt inhibitor VIII (10 μM, Calbiochem), MEK1/2 inhibitors (CL1040, 1 μM, Selleck Chemicals), SM164 (5μM, Apex Bio), pan-caspase inhibitor z-Val-Ala-Asp-FMK (zVAD.fmk, 50 μM, Apex Bio).

Cells

Immortalized C57Bl/6J bone marrow derived macrophages (iBMMs) were a generous gift of Dr. Katherine Fitzgerald (UMASS Medical School). Cells were maintained in DMEM supplemented with 10% fetal bovine serum (FBS) and 1% antibiotic-antimycotic mixture (Invitrogen). 1 X 10^6 iBMMs were seeded for mRNA and western blot experiments into 35 mm^2 dishes and 20,000 cells per well were seeded into 96 well plates for viability. Bone marrow derived macrophages (BMDMs) were prepared from bone marrow cells collected from femurs and tibias of mice. Bone marrow cells were differentiated over 7 days in the presence of conditioned media from L929 cells (30% L929 conditioned media, 20% FBS and 1% antibiotics in RPMI1640) in petri dishes. Media was replenished on day 3. On day 7, adherent cells were collected and reseeded in tissue-culture treated plates for experimentation. After reseeding, cells were maintained in media containing 10% L929 conditioned media, 20% FBS, and 1% antibiotics for 48 hours prior to carrying out experiments. For mRNA and Western blot experiments, 2X10^6 BMDMs were seeded into 35 mm^2 dishes. For cell viability experiments, 50,000 cells per well were seeded in 96-well plates. Thioglycolate-elicited peritoneal macrophages were prepared by priming mice with 1 mL thioglycolate (Remel) intra-peritoneally using an insulin syringe. Mice were euthanized 3 to 4 days after injection, the abdomen was cleaned with 70% ethanol, and the peritoneal cavity was washed

with 5 mL PBS using 18-gauge needle. The wash was added to a 15 ml tube containing DMEM+10%FBS and antibiotics. The contents were spun for 10 minutes at 430g, the supernatant aspirated, the pellet was resuspended in a fresh volume of DMEM+10%FBS+ 1% antibiotics and seeded. Cells were treated for experiments 24 hours post-seeding. For mRNA and Western blot experiments, 2 X 10^6 peritoneal macrophages were seeded into 35 mm^2 dishes. For cell viability experiments, 50,000 cells per well were seeded in 96 well plates. WT, RIPK1$^{-/-}$, and RIPK3$^{-/-}$ MEFs (Cho et al. 2009; Kelliher et al. 1998) were maintained in DMEM, 10% FBS and 1% antibiotics. Cells were seeded in a similar format to BMDMs for experiments.

Western Analysis

For Western analysis data, one representative experiment out of at least three independent replicates are shown. Cells were lysed and harvested in RIPA buffer (Cell Signaling) supplemented with Phenymethanesulfonylfluoride (PMSF) (5 μg/ml, Sigma), leupeptine (1μg/ml), pepstatin (1μg/ml) and aproprotinin (1μg/ml). The protein concentrations were determined using the Pierce 660 nM Protein Assay reagent (Thermo Scientific), and equal amounts of protein were subjected to Western blotting. Samples were separated by SDS/PAGE and transferred to PVDF membranes. Membranes were blocked in Protein-free T20 (TBS) blocking buffer (Fisher Scientific) at room temperature for 1 h, and incubated at 4 °C overnight with primary antibodies (1:1000 dilution in blocking reagent). The following day, membranes were washed and incubated with secondary antibody (1:5000 dilution) at room temperature for 1 h. Signals were developed using Luminata Classico or Forte HRP substrates (Millipore).

Antibodies

The following antibodies acquired from Cell Signaling Technologies were used: NF-κB p65, p-NF- κB p65 (phospho-Ser536), IκB-□, p44/42 MAPK (Erk1/2), p-p44/42 MAPK (p-

Erk1/2)(phospho-Thr202/Tyr204), cFos, p-cFos (phospho-Ser32), caspase-8 mouse specific, MEK1/2, p-MEK1/2(phospho-S217/221), α-Tubulin, anti-mouse IgG HRP-linked antibody, anti-rabbit IgG HRP-linked antibody and RIPK1. RIPK3 antibody was purchased from Prosci, MLKL antibody was purchased from Biorbyt, p-MLKL (pospho-Ser345) antibody was purchased from abcam. p44/42 (Erk1/2) MAP Kinase assay kit # 9800 was purchased from Cell Signaling. CYLD antibody was purchased from Thermo Fisher Scientific. TRIF antibody was purchased from Novus Biologicals. Immunoprecipitation of RIPK1 was carried out using a RIPK1 antibody purchased from BD transduction laboratories. Primary antibodies were used at a dilution of 1:1000 and secondary antibodies were used at a dilution of 1:5000.

Cell Viability Assays

Cells were seeded as described above in 100 µL of media. Typically, cells were treated with 10 ng/ml LPS and 50 □M zVAD for 24 hours. Cell viability was determined using CellTiter-Glo viability assay kit (Promega). Each independent experiment was performed in duplicate and repeated three times. Data shown is a combination of three independent replicates unless otherwise stated. Viability of the cells was analyzed relative to an untreated control.

Measurement of inflammatory molecules by ELISA

Meso Scale Discovery's (MSD) 96-Well MULTI-SPOT mouse multiplex assay was performed according to the manufacturer's instructions to determine the concentrations of TNFα, CCL3, CCL4, GMCSF and IL6 in the serum or cell culture media. Plates were read on MSD sector image 2400. Mouse TNFα was also measured using colorimetric ELISA assay (R&D Systems) according to manufacturer's protocol. Mouse interferon beta (IFN-β) was measured using colorimetric ELISA as following: 96 well plate was kept overnight in 4^0C after coating the wells with 50 µL of monoclonal rat anti-mouse IFN-β (Santa Cruz) captured antibody that was diluted 1:500 in

carbonate buffer (PH 9.5, 1.6 g/L Na_2CO3 and 2.9 g/L NaHCO3). The following day, 200 µL of blocking agent with the diluent buffer (10% FBS in PBS) was added for two hours at 37^0C. Fifty µL of standard and samples were added to the wells and incubated overnight at 4^0C. Fifty µL of polyclonal rabbit anti-mouse IFN-□ detecting antibody (R&D Systems) diluted 1:2000 in 10% FBS diluted in PBS was added to the wells and kept again overnight at 4^0C. Fifty µL of goat anti-rabbit-HRP secondary antibody (Cell Signaling) diluted 1:2000 was added to the wells. Plates were incubated for 2-3 hours at room temperature. Subsequently, 50 µL of the TMB substrate was added. The reaction was stopped by the addition of 50 µL 2N H_2SO_4. Absorbance was measured at 450 nm. Blank values were subtracted. A washing step with buffer (PBS 0.05% TWEEN) was performed after each step and before the addition the substrate and stopping the reaction.

Phospho-RIPK1 ELISA

Lysates were prepared from 3 X 10^6 BMDMs and phospho-RIPK1 ELISAs were performed using multi-array 96 well plates from (Meso Scale Discovery) per the manufacturers guidelines: Capture antibody (anti-RIPK1 mAB, abcam#ab72139) was diluted to 0.5ug/ml in PBS and 35 µL/well were incubated overnight. Plates were blocked in 100µL/well blocker buffer (5% BSA diluted in PBS) while shaking for 2 hours at room temperature (RT). Twenty-five µL of each lysate sample or standard samples (RIPK1 protein, abcam, ab#135220) were added and incubated for 1.5 hour while shaking at RT. Standards were serially diluted 1:2 from 500 pg/µL to 0.122 pg/µg along with a blank. Detection antibody diluted in antibody dilution buffer (1% blocker BSA and 0.1%NP-40) was added at 1µg/mL concentration (either cell signaling RIPK1 or GSK RIPK1 p-Ser166) and incubated for 1.5 hour with shaking at RT. Secondary detection antibody (goat anti-rabbit antibody, sulfo-TAG labeled, Meso Scale Discovery, R32AB-1) diluted in antibody dilution buffer at 1µg/ml was added for 1 hour at RT with shaking Assay was developed using 150µL of MSD

read buffer (R92TC-2) and plates were read on an MSD sector imager 2400.

Stable infection of iBMM cells with shRNAs

To generate retroviral shRNA constructs, shRNAs targeting mouse RIPK3 and MLKL, previously reported by Sun et al. were cloned into pLV-H1-EF1a (Biosettia) according to manufacturer's recommendations. As a control, vector encoding a shRNA against bacterial LacZ was used (Biosettia). Lentiviruses were generated by co-transfecting LentiX 293 cells in 35 mm^2 dishes with 1.28 □g of LP1, 0.64 □g LP2 and 0.8 □g LP3 constructs (Invitrogen) with 1.28 □g pLV vectors using lipofectamine 2000 transfection reagent (Invitrogen). Media (supernatants) were collected three times each 48 hr, filtered through a 0.45 um filter (Millipore) and used to infect macrophages in the presence of 8 □g/ml polybrene. Cells were selected in 1 □g/ml puromycin to create the stable shRNA cell lines.

shRNA sequences:

RIPK1 shRNA: 5'-AAAAGCATTGTCCTTTGGGCAATTTGGATCCAAATTGCCCAAAGGACAATGC-3'.

RIPK3 shRNA 5'-AAAAGCTCTCGTCTTCAACAACTTTGGATCCAAAGTTGTTGAAGACGAGAGC-3'.

LacZ shRNA: 5'-AAAAGCAGTTATCTGGAAGATCATTGGATCCAATGATCTTCCAGATAACTGC-3'

MLKL shRNA: 5'-AAAAGCTGCTTCAGGTTTATCATTTGGATCCAAATGATAAACCTGAAGCAGC-3'.

siRNA silencing

RIPK1, cFos and cJun ON-TARGET PLUS siRNA SMARTpools were purchased from Dharmacon. Erk1, Erk2 and p65 siRNAs was purchased from Cell Signaling. siRNAs were

electroporated using Amaxa mouse macrophage nucleofector kit and Nucleofector II electroporator (Lonza) according to manufacturer's recommendation for primary macrophages. Macrophages were electroporated on day 4 or 5 of culture. After 72 hours, BMDMs were treated with LPS and/or LPS with zVAD for 7 hours. One hundred nM siRNAs were used for RIPK1, cJun, cFos and Erk1/2 (each) and 200 nM for p65, based on the efficiency of silencing evaluated by Western blot.

RNA extraction, cDNA synthesis and qRT-PCR

For RNA extraction, cells were seeded as described above. Cells were stimulated with 10 ng/ml LPS, 50 μM zVAD and 30 μM Nec-1s or other inhibitors as indicated. Total RNA was isolated using RNA MiniPrep kit (ZYMO Research) according to the manufacturer's protocol. 50 ng to 1 □g of RNA was converted to cDNA using iScript cDNA Synthesis Kit (Bio Rad) or ProtoScript M-MuLV First Strand cDNA Synthesis kit (New England Biolabs). qRT-PCR reactions were performed in LightCycler 480 II using using VeriQuest SYBR Green master mix (Affymetrix) and the following program: 50°C for 2 min, 95°C for 10 min, followed by 40 cycles of amplification (95°C for 15 sec, 60°C for 1 min). GAPDH was analyzed as a housekeeping gene.

The primer sequences used to amplify murine genes are as following:

Mouse GAPDH: forward 5'-TGTGTCCGTCGTGGATCTGA-3, reverse: 5'-GGTCCTCAGTGTAGCCCAAG3'.

Mouse TNF: forward 5'-CCCTCACACTCAGATCATCTTCT-3', reverse 5'-GCTACGACGTGGGCTACAG-3'.

Mouse CCL3: forward 5'-TTCTCTGTACCATGACACTCTGC-3', reverse 5'-CGTGGAATCTTCCGGCTGTAG-3'.

Mouse CCL4: forward 5’-TTCCTGCTGTTTCTCTTACACCT-3’, reverse 5’-CTGTCTGCCTCTTTTGGTCAG-3’.

Mouse CXCL1: forward 5’-CTGGGATTCACCTCAAGAACATC-3’, reverse 5’-CAGGGTCAAGGCAAGCCTC-3’.

Mouse CXCL2: forward 5’-CCACCACCAGGCTAGAGG-3’, reverse 5’-GCGTCACACTCAAGCTCTG-3’.

Mouse GMCSF (CSF-2): forward 5’-GGCCTTGGAAGCATGTAGAGG-3’, reverse 5’-GGAGAACTCGTTAGAGACGACTT-3’.

Mouse IL6: forward 5’-TAGTCCTTCCTACCCCAATTTCC-3’, reverse 5’-TTGGTCCTTAGCCACTCCTTC-3’.

TRIF: forward 5’-GGACCTCAGCCTCTCATTATTC-3’, reverse 5’-GGTTCTCCGAACACTCAGTC-3’.

Mouse CSF1: forward 5’-GGCTTGGCTTGGGATGATTCT-3’, reverse 5’-GAGGGTCTGGCAGGTACTC-3’.

Mouse CSF3: forward 5’-ATGGCTCAACTTTCTGCCCAG-3’, reverse 5’-CTGACAGTGACCAGGGGAAC-3’.

Mouse IFNb1: forward 5’-CAGCTCCAAGAAAGGACGAAC-3’, reverse 5’-GGCAGTGTAACTCTTCTGCAT-3’.

Mouse CCL7: forward 5’-GCTGCTTTAAGCATCCAAGTG-3’, reverse 5’-CCAGGGACACCGACTACTG-3’.

Microarray analysis

For Affymetrix gene chip analysis, BMDMs were treated with 10 ng/ml LPS, 50 □M zVAD and 30 □M Nec-1s for 6 hr. Total RNA was isolated using Qiagen RNeasy kit. Samples were submitted

to Keck DNA microarray facility (Yale University) for hybridization and analysis using GeneChip Mouse Gene 1.0 ST Array. Functional annotation clustering of the genes, increased ≥ 1.5-fold in LPS with zVAD vs. LPS treated cells, was performed using NIH DAVID. Hierarchical clustering of the identified cytokine and/or chemokine cluster was performed using Cluster3-TreeView within R platform. Red – upregulation.

http://www.ncbi.nlm.nih.gov/geo/query/acc.cgi?acc=GSE72797

Co-immunoprecipitation

Co-IP of endogenous RIPK1 and Erk1/2 was performed using $1x10^7$ BMDM cells per condition in 10 cm^2 dishes. Cells were lysed in a buffer composed of 30mM TrisHCl (pH7.4), 150 mM NaCl, 10%(v/v) glycerol, 10%(v/v) Triton X-100, 5 mM NaF, 10 mM sodium pyrophosphate, 175mM □-glycerol phosphate, 50µg/ml PMSF,1µg/ml leupeptine, 1µg/ml pepstatin and 1µg/ml aprotinin. Lysates were incubated overnight with 1.25 µg mouse monoclonal anti-RIPK1 antibody (BD Biosciences) or Erk1/2 antibody (cell signaling) at 4°C. Following, lysates were incubated with 20 □L of protein G Dynabeads per reaction (Invitrogen) for 3-4 hours. Bead-protein-antibody mixtures were washed 3 times using lysis buffer with higher NaCl (500 mM). Bound proteins were eluted using SDS then heating up the samples for 5 min. Beads were retrieved using magnetic stand and solubilized protein were analyzed by Western blotting.

Necrosome formation assay

Isolation of NP40 soluble and insoluble fractions was performed as previously described (Moquin et al. 2013; Li et al. 2012). Cells were seeded into 35 cm^2 dishes at 2 X 10^6 cells/well and stimulated with 10 ng/ml LPS, 50 □M zVAD and 30 □M Nec-1s for up to 3 hr. Cells were lysed in 1%NP-40 lysis buffer (150mM NaCl, 20mM Tris-Cl (pH 7.5), 1% NP-40, 1mM EDTA, 3mM Na-fluoride, 1mM B-glycerophosphate, 1mM Sodium Orthovanadate, 5uM Idoacetamide, 2uM N-

ethylmaleimide and 5μg/ml PMSF and 1μg/ml leupeptine, 1μg/ml pepstatin and 1μg/ml aprotinin. Lysates were flash frozen on dry-ice, thawed on ice and vortexed for 10 sec followed by centrifugation at 1000g for 10 minutes to remove nuclear pellets. Supernatants were collected and centrifuged at 34400g for 15 minutes in the refrigerated table-top centrifuge. Resultant supernatants were collected (NP-40 soluble fractions) and pellets (NP-40 insoluble) were boiled in 1x SDS-PAGE buffer.

Generation of *Casp8*$^{-/-}$ BMDMs using GFP-CRE adenovirus

Recombinant adenovirus expressing Cre recombinase was purchased from SignaGen Laboratories. Casp8$^{fl/fl}$ BMDMs were infected at 100-1000 MOI on Day 3. Amount of adenovirus required for complete deletion of caspase-8 (*Casp8*$^{-/-}$) (Western blot) and 100% infection efficiency (GFP fluorescence) was determined in preliminary titration experiments. Media containing virus was then removed and fresh culture media was added. Twenty-four hours later, the second infection (day 5) was done. Culture media was changed again after 24 hours and cells were treated on day 7 of BMDM differentiations. A recombinant control adenovirus expressing just GFP was used as a control. Detection of infected cells was monitored by manual visualization of GFP-positive cells using fluorescence microscopy.

***In vivo* LPS challenge and Nec-1s treatment**

Mice were injected intravenously via tail vein with 100μL of 30 mg/kg optimized Nec-1s (7-Cl-O-Nec-1), (Degterev et al. 2013) 15 min prior to intraperitoneal injection of 50 □g/kg LPS (Sigma) dissolved in 500μL PBS. Nec-1s was dissolved in PBS containing 25% Polyethylene Glycol 400 by water sonication for 15 min. Blood was collected 1 hour after LPS injection and cytokines were measured using multiplexed ELISA assay (Meso Scale Discovery) or colorimetric ELISA assay. Bone marrow cells were flushed from femurs and tibias with PBS, centrifuged at 430g,

resuspended/blocked with 1 □M EDTA and 2% BSA in PBS for 45 min at 4^0C, and stained using anti-$CD11b^+$-PE antibody (Biolegend, clone M1/70, 1:500) for 60 min at 4^0C. CD11b+ cells were sorted by fluorescence-activated cell sorting (FACS) using MoFlo sorter (Beckman-Coulter).

Measurement of cell death of CD11b+ cells

LIVE/DEAD® Fixable Aqua Dead Cell Stain Kit (Invitrogen, L34957) was used. $CD11b^+$ cells were collected as described previously (see: LPS Challenge), and then aqua stain was added according to manufacturer's guidelines. Cell death analysis was carried out by flow cytometry to quantify dye uptake by $CD11b^+$ cells.

Measurement of plasma alanine aminotransferase

Serum was obtained from whole blood samples centrifuged at 16500 g for 10 minutes at room temperature. Serum alanine aminotransferase (ALT) was measured to assess hepatic tissue damage using the pointe scientific, INC kit according to the recommended protocol.

Caspase-Glo Assay system

Cells were seeded in 384 well plate in 40µL of media; BMDMs were seeded at 20,000 cells per well for BMDMs and $CD11b^+$ cells were seeded at 200,000 cells per well. Luminescent assay was determined using 15 uL of Caspase-Glo reagent (Promega) after 45 min. For BMDMs, each independent experiment was performed in triplicate and repeated three times. $CD11b^+$ Caspase-Glo luminescent assay was performed with three replicates. Luminescence was analyzed relative to untreated controls.

Next Generation Sequencing

For RNA-Seq analysis, mice were divided into 3 groups - control (n=2), LPS (n=2) and LPS/Nec-1s (n=2). Bone marrow cells were isolated by FACS as described for qPCR analysis. Total RNAs were isolated using Qiagen RNeasy kit according to the manufacturer's protocol. Input RNA

samples were analyzed by an Agilent BioAnalyzer 2100 to assess the integrity and quantity of sample. RNA samples were then amplified using NuGen Ovation RNA System V2. The resulting cDNA samples were fragmented on Covaris M220 Focused Solicitor, followed by purification and concentration with a Qiagen MiniElulte Spin Column. Following this step, S1 Nuclease (Promega) was used according to the manufacture's protocol. Resulting amplified and fragmented cDNA samples from RNA amplification were used as input for library preparation, using Illumina TruSeq DNA Sample Preparation Kit per the manufacturer's instruction. The resultant libraries were quantified and pooled at equal molar concentration for sequencing. Sequencing was done on a lane of High Output single read 100 bases on an Illumina HiSeq 2500 using SBS V3 chemistry. The base calling and demultiplexing was performed with CASAVA v1.8. Resulting data were aligned to mouse mm10 reference genome with Tophat 2 and different gene expression analysis with Cuffdiff.

Gene expression profiles were analyzed using Ingenuity pathway analysis (IPA) software to identify pathways regulated by LPS and Nec-1s.

http://www.ncbi.nlm.nih.gov/geo/query/acc.cgi?acc=GSE73836

Statistics

Statistics were reported for all experiments with 3 or more biological replicates, and analyzed by two-tailed Student t-test or one-way ANOVA, where specified. Statistical significance was determined using an alpha value of 0.05. All experiments were repeated with three independent biological replicas. For qRT-PCR data, one representative data set is typically shown due to the variability in responses to LPS and/or LPS with zVAD in independent BMDM preparations.

Chapter 3

Kinase Activities of RIPK1 and RIPK3 Can Direct IFNβ Synthesis Induced by Lipopolysaccharide[5]

[5] **Saleh, D.,** Najjar, M., Zelic, M., Shah, S., Nogusa, S., Polykartis, A., … Degterev, A. (2017). Kinase Activities of RIPK1 and RIPK3 Can Direct IFN-β Synthesis Induced by Lipopolysaccharide. *The Journal of Immunology.*198(10).
Reprinted here with permission of publisher.

Kinase activities of RIPK1 and RIPK3 can direct IFNβ synthesis induced by lipopolysaccharide

Authors

Danish Saleh[1], Malek Najjar[2], Matija Zelic[3], Saumil Shah[4], Shoko Nogusa[5], Apostolos Polykratis[6], Michelle K. Paczosa[7], Peter J. Gough[8], John Bertin[8], Michael Whalen[9], Katherine Fitzgerald[10], Nikolai Slavov[11], Manolis Pasparakis[6], Siddharth Balachandran[5], Michelle Kelliher[3], Joan Mecsas[12], and Alexei Degterev[1,2,4*]

Affiliations

[1]Medical Scientist Training Program and Program in Neuroscience, Sackler School of Graduate Biomedical Sciences, Tufts University School of Medicine, Boston, MA 02111, USA

[2]Graduate Program in Pharmacology and Experimental Therapeutics, Sackler School of Graduate Biomedical Sciences, Tufts University School of Medicine, Boston, MA 02111, USA

[3]Department of Molecular, Cell and Cancer Biology, University of Massachusetts Medical School, Worcester, MA 01605, USA

[4]Department of Developmental, Molecular & Chemical Biology, Tufts University School of Medicine, Boston, MA 02111, USA

[5]Blood Cell Development and Function Program, Fox Chase Cancer Center, Philadelphia, PA 19111, USA

[6]Institute for Genetics, Center for Molecular Medicine and Cologne Excellence Cluster on Cellular Stress Responses in Aging-Associated Diseases, University of Cologne, 50674 Cologne, Germany

[7]Program in Immunology, Tufts University School of Medicine, Sackler School of Biomedical Sciences, Boston, MA 02111, USA

[8]Pattern Recognition Receptor Discovery Performance Unit, Immuno-Inflammation Therapeutic Area, GlaxoSmithKline, Collegeville, PA 19426, USA

[9]Department of Pediatric Critical Care Medicine, Neuroscience Center, Massachusetts General Hospital and Harvard Medical School, 149 13th Street, Charlestown, MA 02129, USA

[10]Division of Infectious Disease and Immunology, Department of Medicine, University of Massachusetts Medical School, 364 Plantation Street, Worcester, MA 01605, USA

[11]Department of Bioengineering and Biology, Northeastern University, Boston, MA 02115, USA

[12]Department of Molecular Biology and Microbiology, Tufts University School of Medicine, Sackler School of Biomedical Sciences, Boston, MA 02111, USA

Contact information

[*]Corresponding author at: Department of Developmental, Molecular & Chemical Biology, School of Medicine, Tufts University, M&V716, 136 Harrison Ave, Boston, MA 02111, USA. Fax: +1-617-636-2409. Email address: alexei.degterev@tufts.edu

Abstract

The innate immune response is a central element of the initial defense against bacterial and viral pathogens. Macrophages are key innate immune cells that upon encountering pathogen associated molecular patterns respond by producing cytokines, including Interferon-β (IFNβ). In this study, we identify a novel role for RIPK1 and RIPK3, a pair of homologous serine/threonine kinases previously implicated in the regulation of necroptosis and pathologic tissue injury, in directing IFNβ production in macrophages. Using genetic and pharmacologic tools we show that catalytic activity of RIPK1 directs IFNβ synthesis induced by lipopolysaccharide (LPS) in mice. Additionally, we report that RIPK1 kinase-dependent IFNβ production may be elicited in an analogous fashion using LPS in bone-marrow derived macrophages (BMDMs) upon inhibition of caspases. Notably, this regulation requires kinase activities of both RIPK1 and RIPK3, but not the necroptosis effector protein, MLKL. Mechanistically, we provide evidence that a necrosome-like RIPK1 and RIPK3 aggregates facilitate canonical TRIF-dependent IFNβ production downstream of the LPS receptor TLR4. Intriguingly, we also show that RIPK1 and RIPK3 kinase-dependent synthesis of IFNβ is markedly induced by avirulent strains of gram-negative bacteria, *Yersinia* and *Klebsiella*, and less-so by their wild-type counterparts. Overall, these observations identify unexpected roles for RIPK1 and RIPK3 kinases in the production of IFNβ during the host inflammatory responses to bacterial infection and suggest that the axis in which these kinases operate may represent a target for bacterial virulence factors.

Introduction

Receptor-Interacting Protein Kinases 1 and 3 (RIPK1 and RIPK3) are homologous serine/threonine kinases that are critical regulators of necroptosis, a form of necrotic cell death associated with pathologic tissue injury (Degterev et al. 2008; Christofferson et al. 2014; Kaczmarek et al. 2013; Vanden Berghe et al. 2014; Linkermann & Green 2014; Pasparakis & Vandenabeele 2015). RIPK1 and RIPK3 are components of the signaling machinery downstream of innate immune pathogen recognition receptors (PRRs), Toll-like receptors 3 and 4 (TLR3 and TLR4) (Cusson-Hermance et al. 2005; Meylan et al. 2004; Kaiser et al. 2013; Kaiser & Offermann 2005; Vivarelli 2004). Catalytic activity of these kinases, induced by activation of TLR3 or TLR4 in the presence of pan-caspase inhibitor, zVAD.fmk (zVAD), promote necroptosis in primary macrophages (Schworer et al. 2014; Kaiser et al. 2013; He et al. 2011; Najjar et al. 2016). This regulation is dependent on the TLR3/4 Rip-Homotypic Interacting Motif (RHIM)-domain containing adapter protein, Toll-interleukin-receptor-domain-containing-adapter-inducing-Interferon-β (TRIF) (Schworer et al. 2014; Kaiser et al. 2013; He et al. 2011; Najjar et al. 2016). Upon activation, RIPK1 and RIPK3 form insoluble cellular aggregates, termed 'necrosomes,' which function to allow phosphorylation and activate of the target pseudokinase, MLKL, by RIPK3 (Li et al. 2012; Cho et al. 2010; Cook et al. 2014; Orozco et al. 2014). Phosphorylation of MLKL promotes its oligomerization and translocation to the cell surface where it functions to increase membrane permeability and facilitate necrotic cell death through a mechanism that is not yet fully understood (Murphy et al. 2013; Cai et al. 2014; Sun et al. 2012; Wu et al. 2013; Hildebrand et al. 2014).

New evidence suggests existence of direct links of RIPK1 and RIPK3 to inflammation that occur independently of cell death. For example, *in vitro*, RIPK1 kinase activation has been linked

to TNFα production in contexts of caspase inhibition and DNA damage (Christofferson et al. 2012; Biton & Ashkenazi 2011; Hitomi et al. 2008; McNamara et al. 2013). We have recently demonstrated the existence of a TRIF-mediated cell death-independent signaling pathway downstream of RIPK1 and RIPK3 that involves activation of Erk1/2 and NFκB and directs synthesis of acute inflammatory cytokines, including TNFα, following TLR4 activation (Najjar et al. 2016). In another example, RIPK1 kinase-dependent IL-1α expression and tissue inflammation, occurring in the absence of necroptosis, was reported in the Ptpn(spin) model of human neutrophilic dermatitis (Lukens et al. 2013). In macrophages, RIPK3 is required for activation of NFκB and IL-1β release both in kinase-independent and dependent manner conditional on caspase-8 inhibition (Moriwaki et al. 2014; Moriwaki et al. 2015; Lawlor et al. 2015).

Here, we report a novel role for the kinase activity of RIPK1 in directing lipopolysaccharide (LPS) induced IFNβ synthesis in mice and *in vitro* in primary mouse macrophages when caspases are inhibited. We report that this regulation requires TRIF and occurs by way of a canonical Type I interferon (IFN-I) response pathway, requiring TBK1, IKKε, and IRF3/7. These canonical IFN-I inducing factors co-localize to RIPK1/RIPK3 kinase containing detergent-insoluble cellular fractions following TLR4 activation, and this localization was disrupted by the selective RIPK1 kinase inhibitor, Nec-1s. Together, these data demonstrate that a necrosome-like RIPK1 and RIPK3 signaling platform mediates TRIF-dependent IFNβ production. Moreover, enhanced RIPK1 and RIPK3 kinase-dependent IFNβ synthesis was observed after challenge with attenuated mutant strains of *Yersinia pseudotuberculosis* and *Klebsiella pneumoniae* in the presence of caspase inhibition, suggesting that this pathway may represent a new target of bacterial virulence factors.

Results

Kinase activity of RIPK1 is required for IFNβ synthesis induced by LPS in mice.

In a previous study, we reported that kinase activity of RIPK1 was required for acute inflammatory cytokine production induced by LPS in mice, including TNFα, IL6, CCL3/4 and CXCL1/2, suggesting that the catalytic activity of RIPK1 might serve an important role in the innate immune response induced by TLR4 (Najjar et al. 2016). Synthesis of Type I interferons, including Interferon-beta (IFNβ) (Doyle et al. 2002; Sakaguchi et al. 2003; Power et al. 2007), is elicited by TLR4 activation and plays an important role in innate and adaptive immunity against infections (Ivashkiv & Donlin 2013). To inquire whether the catalytic activity of RIPK1 may also be required for LPS-induced IFNβ synthesis, we first tested the effect of the selective RIPK1 inhibitor, Nec-1s, on this process. Nec-1s injection prior to the challenge with LPS abolished IFNβ mRNA synthesis in $CD11b^+$ monocytic cells *in vivo* (Figure 1a). In addition, we observed that LPS-driven induction of a panel of interferon-stimulated genes (ISGs) was similarly abolished by Nec-1s in $CD11b^+$ cells (Figure 1b). LPS-induced IFNβ synthesis was also attenuated in monocytic $CD11b^+$ cells from D138N RIPK1 kinase-inactive mice (D138N RIPK1 or $Ripk1^{D138N/D138N}$) (Figure 1c). Together, these pharmacologic and genetic approaches suggest that RIPK1 kinase is indeed required for LPS-induced upregulation of IFNβ expression *in vivo*.

Figure 1. LPS induced IFN-I production is dependent on kinase-activity of RIPK1.

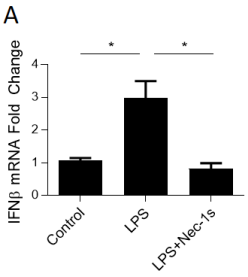

B

Gene	Fold Induction LPS v. Control (p-value)	Fold Induction LPS+Nec-1s v. Control (p-value)
Mx2	30.28 (<0.01)	1.26 (1.00)
Ifit1	22.26 (<0.01)	0.55 (0.02)
Mx1	13.12 (<0.01)	0.63 (1.00)
Isg15	10.96 (<0.01)	0.56 (0.07)
Ifi205	8.54 (<0.01)	1.33 (0.23)
Trex1	5.46 (<0.01)	1.11 (0.57)
Ifit3	4.42 (<0.01)	0.32 (0.01)
Ifih1	4.00 (<0.01)	0.88 (0.51)
Slc15a3	3.28 (<0.01)	1.00 (0.91)
Eif2ak2	3.04 (<0.01)	1.09 (0.53)
Isg20	2.98 (<0.01)	0.71 (0.11)
Ifit2	2.86 (<0.01)	0.87 (0.51)

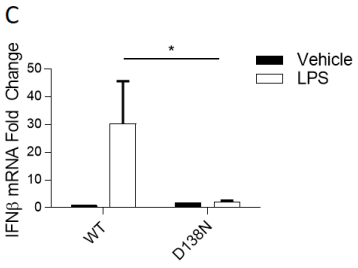

Figure 1: LPS induced IFN-I production is dependent on kinase-activity of RIPK1.

(A) qRT-PCR analysis of *Ifnb* mRNA expression in wild type (WT) mice injected with Nec-1s (iv) 15 min prior to LPS (ip). n= 6 animals per group and *p<0.05. Values reflect mean ± SE. (B) RNA seq analysis of a panel of IFN-I response genes in CD11b+ cells isolated from mice injected as in (A). Values reflect mean. P values marked in parentheses. GSE73836. (C) qRT-PCR analysis of *Ifnb* mRNA expression WT and D138N mice injected with LPS (ip). n= 3-7 animals per group and *p<0.05. Values reflect mean across biological variants and error bars reflect SE.

Contributions: Experiments performed and data analyzed by Danish Saleh, Malek Najjar, and Alexei Degterev. Figures prepared, and figure legends written by Danish Saleh.

LPS with zVAD.fmk induces RIPK1 kinase-dependent IFNβ synthesis in BMDMs.

Deletion of caspase-8 or use of pan-caspase inhibitor, zVAD, is sufficient to facilitate RIPK1 kinase activation by LPS *in vitro* (Schworer et al. 2014; He et al. 2011; Kaiser et al. 2013; Najjar et al. 2016). Within 24 hours, LPS and zVAD treatment, but not LPS alone induced RIPK1 kinase-dependent cell death in bone marrow derived macrophages (BMDMs) (Figure 2a and 2b). Requirement for caspase inhibition for RIPK1 activation *in vitro* is also supported by our previously published phopsho-RIPK1 ELISA data (Najjar et al. 2016). To address the possible role of RIPK1 in IFN-I production, we first examined whether zVAD promoted LPS-induced IFNβ synthesis in BMDMs. Indeed, LPS paired with zVAD greatly increased synthesis of IFNβ compared to LPS alone over an 8 hour time course (Figure 3a). Similarly, mRNA expression of interferon stimulated genes (ISGs), MX2 and IFIT1, was augmented by LPS with zVAD compared to LPS alone (Figure 3b, 3c).

Next, to evaluate whether this regulation was dependent on the catalytic activity of RIPK1 kinase, we examined IFNβ synthesis in BMDMs generated from two different mouse strains expressing kinase-dead mutants of RIPK1 (D138N RIPK1 or K45A RIPK1 (*Ripk1*$^{K45A/K45A}$) mice (Berger et al. 2014; Polykratis et al. 2014). Consistent with our hypothesis, we observed that in the absence of the kinase activity of RIPK1, increases in IFNβ mRNA synthesis and protein release in response to LPS with zVAD was abolished or attenuated, respectively (Figure 3d-g). Nec-1s also blocked IFNβ production by LPS with zVAD (Figure 3d-g). Conversely, catalytic activity of RIPK1 was not essential for the responses to LPS alone, confirming that activation of RIPK1 in the presence of caspase inhibition greatly promotes IFNβ synthesis in BMDMs.

Figure 2. LPS with zVAD induces RIPK1 kinase-dependent cell death.

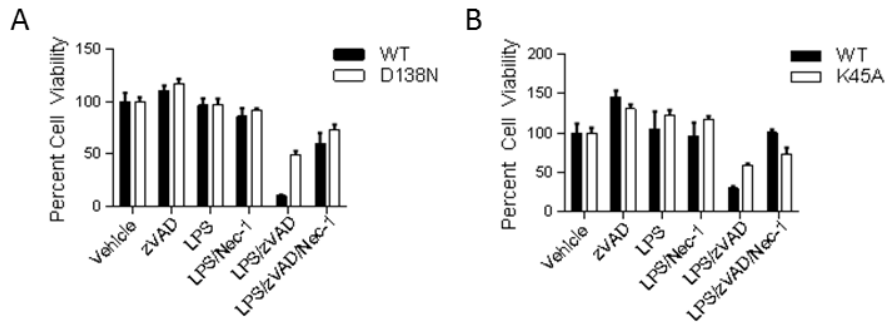

Figure 2. LPS with zVAD induces RIPK1 kinase-dependent cell death. (A) Cell viability of wild type (WT) and D138N RIPK1 BMDMs (D138N) treated for 24 hours and evaluated by ATP assay. (B) Cell viability of WT and K45A RIPK1 BMDMs (K45A) treated for 24 hours and evaluated by ATP assay. Presented data are representative datasets from experimental observations made at least 3 times. Error bars reflect SD from the mean. BMDMs were treated with LPS=10 ng/mL, zVAD=50 μM, and/or Nec-1s=30μM where indicated.

Contributions: Experiments performed by Danish Saleh and Malek Najjar. Data analyzed, figures prepared, and figure legends written by Danish Saleh.

Figure 3. LPS with zVAD induces IFNβ synthesis in a RIPK1 kinase-dependent manner.

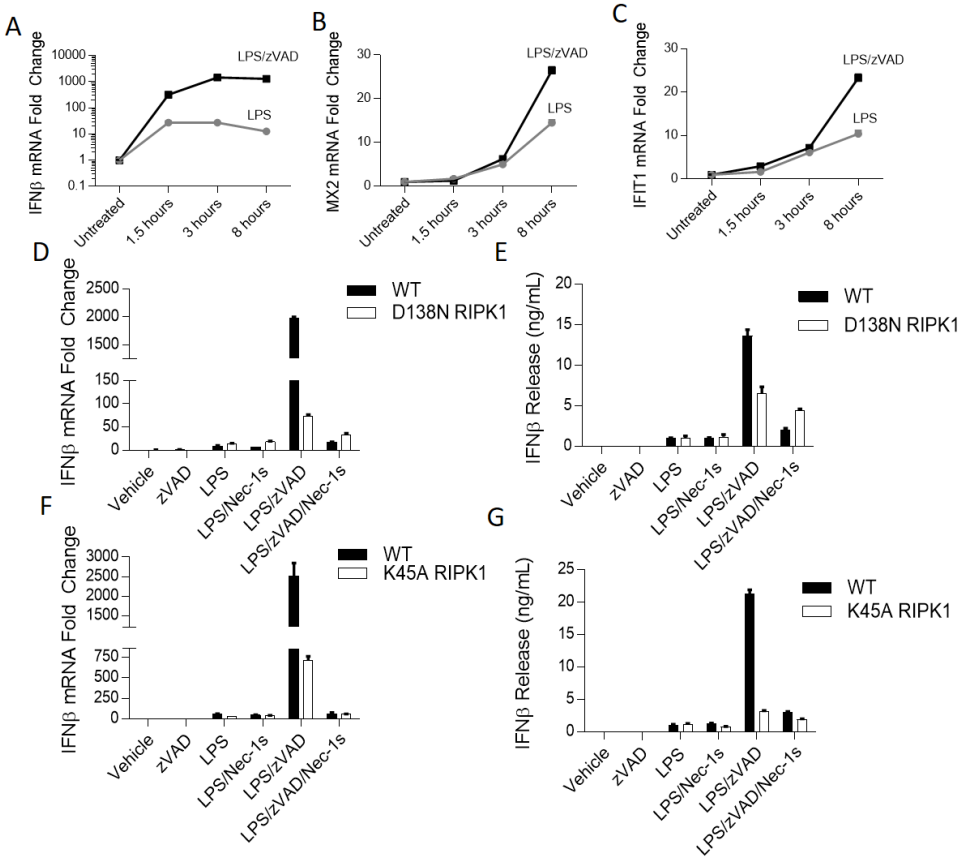

Figure 3: LPS with zVAD induces IFNβ synthesis in a RIPK1 kinase-dependent manner.

(A-C) Time course of mRNA expression changes in *Ifnb* (A), *Mx2* (B), and *Ifit1* (C) evaluated by qRT-PCR in wild type BMDMs. Black squares – LPS/zVAD; Grey circles – LPS. (D-E) qRT-PCR and ELISA analysis of *Ifnb* mRNA expression and IFNβ protein release in WT and D138N BMDMs treated for 5-7 hrs. (F-G) qRT-PCR and ELISA analysis of *Ifnb* mRNA expression and IFNβ protein release in WT and K45A BMDMs treated for 5-7 hrs. Presented data are representative datasets from experimental observations made at least 3 times. ELISA using K45A RIPK BMDMs and the formal timecourse were repeated 2 times. Error bars reflect SD from the mean. BMDMs were treated with LPS=10 ng/mL, zVAD=50 μM, and/or Nec-1s=30μM where indicated.

Contributions: Experiments performed by Danish Saleh and Malek Najjar. Data analyzed, figures prepared, and figure legends written by Danish Saleh.

IFNβ synthesis induced by LPS with zVAD requires kinase activity of RIPK3 but not MLKL. RIPK3 is a central component of the necroptosis signaling cascade and is required for necroptosis induced by LPS with zVAD (Kim & Li 2013). Catalytic activity of RIPK3 is required for the formation of detergent-insoluble RIPK1-RIPK3 'necrosome' complexes and consequent phosphorylation of MLKL, which ultimately leads to the execution of necroptosis (Murphy et al. 2013; Cai et al. 2014; Hildebrand et al. 2014; Vanden Berghe et al. 2014; Zhao et al. 2012; Cook et al. 2014; Najjar et al. 2016). Consistently, we observed that K51A RIPK3 BMDMs *(Ripk3*$^{K51/K51A}$*)*, expressing low levels of a kinase-dead mutant of RIPK3 (Mandal et al. 2014), and RIPK3 knockout (*Ripk3*$^{-/-}$) BMDMs were protected from cell death induced by LPS with zVAD (Figure 4a, Fig 4b).

We next sought to determine whether RIPK1 kinase-dependent IFNβ production required these additional necroptotic factors. Stimulation of RIPK3 K51A BMDMs by LPS with zVAD failed to induce IFNβ production above the response by LPS alone, indicating that RIPK3 was required for RIPK1 kinase-dependent IFNβ production (Figure 5a). To further evaluate the role of catalytic activity of RIPK3, we used the specific RIPK3 kinase-inhibitor GSK'872 (Kaiser et al. 2013; Mandal et al. 2014). We observed that GSK'872 blocked IFNβ synthesis induced by LPS with zVAD, confirming that the catalytic activity of RIPK3 is also required for RIPK1 kinase-dependent IFNβ production in BMDMs (Figure 5b). In contrast, deletion of *Mlkl* only minimally impaired IFNβ mRNA synthesis induced by LPS with zVAD, even though these BMDMs were, expectedly, completely resistant to necroptosis (Figure 5c, 5d) (Najjar et al. 2016). These observations demonstrated that RIPK1 and RIPK3 kinase-dependent IFNβ synthesis is independent of necroptosis pathway and that bifurcation of the respective signaling cascades occurs upstream of MLKL. Furthermore, given the paucity of known targets of RIPK1 and RIPK3,

these findings highlight the possibility of new cell death-independent enzymatic targets for these kinases that remain to be defined.

Figure 4. RIPK3 is required for cell death induced by LPS with zVAD.

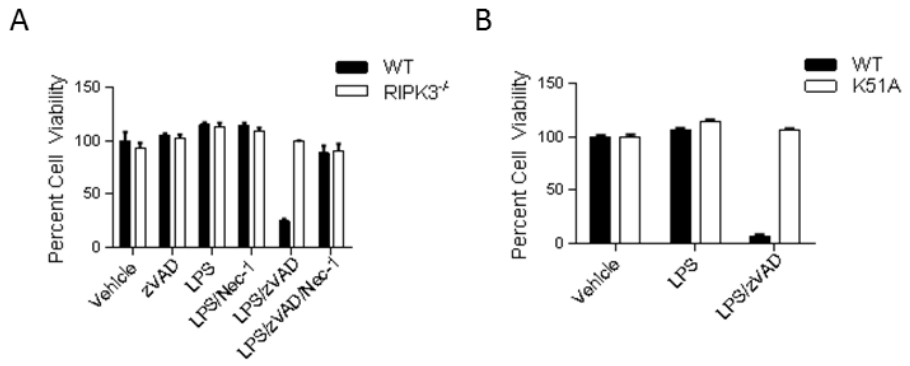

Figure 4. RIPK3 is required for cell death induced by LPS with zVAD. (A) Cell viability of wild type (WT) and RIPK3 knockout (*Ripk3*$^{-/-}$) BMDMs treated for 24 hours and evaluated by ATP assay. (B) Cell viability of WT and K51A RIPK3 BMDMs (K51A) treated for 24 hours and evaluated by ATP assay. Presented data are representative datasets from experimental observations made at least 3 times. Error bars reflect SD from the mean. BMDMs were treated with LPS=10 ng/mL, zVAD=50 μM, and/or Nec-1s=30μM where indicated.

Contributions: Experiments performed by Danish Saleh and Malek Najjar. Data analyzed, figures prepared, and figure legends written by Danish Saleh.

Figure 5. Kinase-activity of RIPK3, but not MLKL, is required for RIPK1 kinase-dependent IFNβ synthesis.

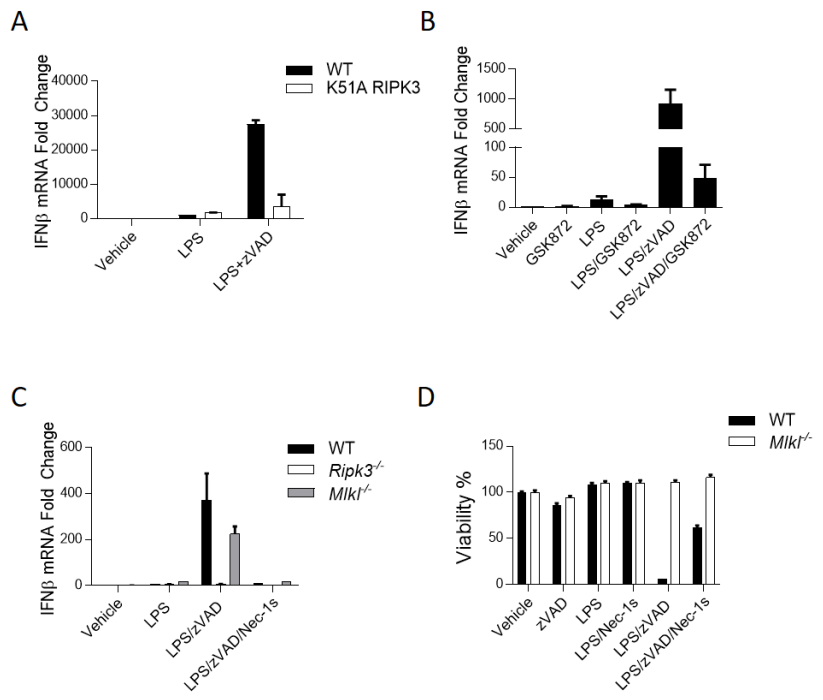

Figure 5: Kinase-activity of RIPK3, but not MLKL, is required for RIPK1 kinase-dependent IFNβ synthesis.

(A) qRT-PCR analysis of *Ifnb* mRNA expression in WT and K51A BMDMs treated for 5-7 hrs. (B) qRT-PCR of *Ifnb* mRNA expression in wild type BMDMs treated with RIPK3 kinase inhibitor (GSK872= 5μM) for 5-7 hrs. (C) qRT-PCR of *Ifnb* mRNA expression in wild type (WT), RIPK3 knockout (*Ripk3*$^{-/-}$) and MLKL knockout (*Mlkl*$^{-/-}$) BMDMs treated for 7 hrs. (D) Cell viability of WT and *Mlkl*$^{-/-}$ BMDMs treated for 24 hours and evaluated by CellTiterGlo ATP assay. Presented data are representative datasets from experimental observations made at least 3 times. Error bars reflect SD from the mean. BMDMs were treated with LPS=10 ng/mL, zVAD=50 μM, GSK'872=5μM, and/or Nec-1s=30μM where indicated.

Contributions: Experiments performed by Danish Saleh and Malek Najjar. Data analyzed, figures prepared, and figure legends written by Danish Saleh.

IFNβ production by LPS with zVAD requires TRIF, STING, TBK1/IKKε, and IRF3/7.

IFNβ production, induced by LPS alone, is dependent on a number of key intermediaries starting with the adapter protein TRIF, which mediates signaling through canonical downstream IFN-I pathway intermediaries, including homologous kinases TANK-binding kinase (TBK1), and Inhibitor of Kappa b Kinase ε (IKKε); and the transcription factors, Interferon Regulatory Factors (IRFs) (Yamamoto et al. 2003; Solis et al. 2007; Fitzgerald et al. 2003; Gatot et al. 2007; Doyle et al. 2002). As TRIF (*Ticam 1*) is required for RIPK1 and RIPK3 dependent necroptosis (He et al. 2011), we evaluated IFNβ mRNA synthesis in *Ticam1*$^{-/-}$ BMDMs to examine whether TRIF is similarly required for the RIPK1 and RIPK3 kinase-dependent IFNβ synthesis. Not surprisingly, in the absence of TRIF, neither LPS nor LPS with zVAD induced IFNβ mRNA synthesis (Figure 6a). Therefore, next we sought to determine whether increased IFNβ synthesis upon RIPK1 and RIPK3 activation, reflects induction of the canonical IFN-I axis (TBK1, IKKε, and IRF3) or whether a new TRIF-dependent signaling mechanism is engaged by RIPK1 and RIPK3. Over an extended timecourse, we found that LPS with zVAD enhanced phosphorylation of TBK1, IKKε, and IRF3 compared to LPS alone, suggesting IFN-I pathway hyper-activation (Figure 6b, 7a-c). Additionally, TBK1, IKKε, and IRF3 phosphorylation in the cells stimulated with either LPS alone or LPS with zVAD was reduced in *Ticam1*$^{-/-}$ BMDMs, confirming that TRIF was required for IFN-I pathway activation by LPS and zVAD (Figure 6c). By comparison, early TRIF-dependent activation of the IFN-I pathway (1 hour post-treatment) was not affected by zVAD or blocked by Nec-1s, suggesting that the catalytic function of RIPK1 is not required for early signaling events in this pathway (Figure 6d). A recent study demonstrated that TRIF directly associated with STING, an intracellular nucleotide sensor, and was also required for STING dependent IFN-I synthesis (Wang et al. 2016). Consistent with a role for STING as a co-driver for TRIF-dependent

IFNβ synthesis, we found that STING was also required for TRIF/RIPK1-dependent IFNβ synthesis by LPS with zVAD (Figure 6e).

To test the functional roles of TBK1 and IKKε in RIPK1 and RIPK3 kinase-dependent IFNβ synthesis, two dual TBK1/IKKε inhibitors (MRT67307 and BX795) were used (Clark et al. 2011; Clark et al. 2009). These inhibitors blocked both LPS and LPS with zVAD induced IFNβ mRNA synthesis (Figure 6f and 7d), and we confirmed that MRT67307 also blocked phosphorylation of IRF3 induced by LPS and LPS with zVAD (Figure 6g).

To examine the contribution of IRFs to RIPK1 and RIPK3 kinase-dependent IFNβ production, we evaluated responses in *Irf3*$^{-/-}$/*Irf7*$^{-/-}$ BMDMs. Again, IFNβ mRNA synthesis induced by LPS or LPS with zVAD were completely abolished in the absence of IRF3 and IRF7, demonstrating the IRFs are also required for RIPK1 and RIPK3 kinase-dependent IFNβ synthesis (Figure 6h). Altogether, these data suggest that TRIF plays a dual role in promoting both signaling by RIPK1 and RIPK3 kinases and TBK1/IKKε as well as allows cross-talk between the two pathways to enhance activation of the TBK1, IKKε, and IRF3 signaling cascade.

Lastly, we examined whether activation of IFN-I pathway intermediaries was also regulated by catalytic activities of RIPK1 and RIPK3. Importantly, phosphorylation of TBK1, IKKε, and IRF3 was attenuated in K45A RIPK1 BMDMs and D138N RIPK1 BMDMs and inhibited by Nec-1s in wild-type BMDMs, confirming the requirement for RIPK1 kinase in this regulation (Figure 8a and 8b). Similarly, these events were abolished in K51A RIPK3 BMDMs, in *Ripk3*$^{-/-}$ BMDMs and by GSK'872 (Figure 8c, 8d and 9). Notably, RIPKI kinase was specifically required for TRIF-dependent signaling events that were augmented by LPS with zVAD as early activation of TBK1, IKKε, and IRF3 at 1 hour post-treatment did not require RIPK1 kinase (Figure 4d). Together, these observations suggest that RIPK1 and RIPK3 kinase-dependent IFNβ synthesis

is mediated by the canonical TBK1/IKKε/IRF signaling cascade and that this regulation is also dependent on the adapter TRIF.

Figure 6. RIPK1 kinase-dependent IFNβ synthesis requires TRIF, STING, TBK1/IKKε, and IRF3/7.

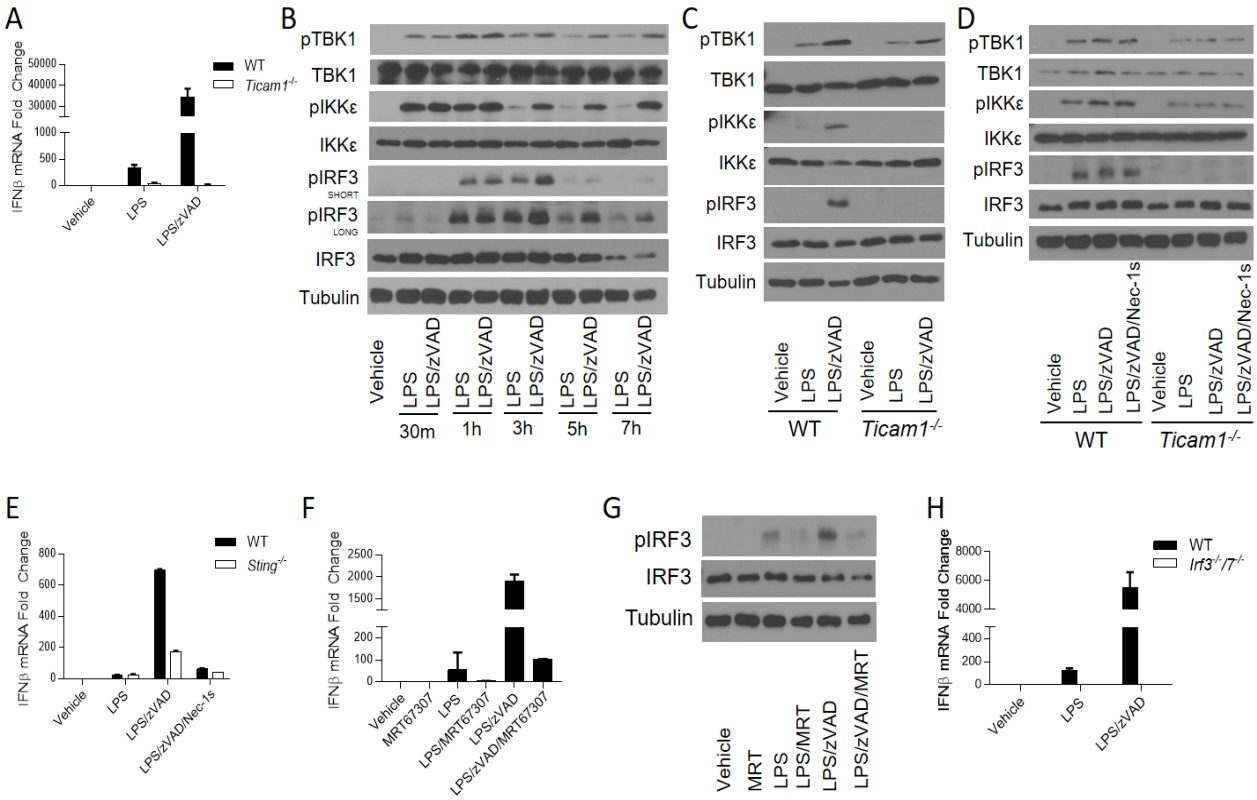

Figure 6: RIPK1 kinase-dependent IFNβ synthesis requires TRIF, STING, TBK1/IKKε, and IRF3/7.

(A) qRT-PCR of *Ifnb* mRNA expression in WT and *Ticam1*$^{-/-}$ BMDMs treated for 5-7 hrs. (B) Time course of TBK1, IKKε, and IRF3 phosphorylation evaluated by Western analysis in wild type BMDMs. (C) Western analysis of TBK1, IKKε, and IRF3 phosphorylation in wild type (WT) and *Ticam1*$^{-/-}$ BMDMs treated for 3-4 hours. (D) Western analysis of TBK1, IKKε, and IRF3 phosphorylation in wild type (WT) and *Ticam1*$^{-/-}$ BMDMs treated for 1 hour. (E) qRT-PCR analysis of Ifnb mRNA expression in WT and *Sting*$^{-/-}$ BMDMs treated for 5-7 hrs. (F) qRT-PCR of *Ifnb* mRNA expression in wild type BMDMs treated with TBK1/IKKε inhibitor (MRT67307, 2μM) for 5-7 hrs. (G) Western analysis of IRF3 phosphorylation in wild type BMDMs treated with

MRT67307 for 3-4 hrs. (H) qRT-PCR of *Ifnb* mRNA expression in WT and *Irf3*$^{-/-}$*7*$^{-/-}$ BMDMs treated for 5-7 hours. Presented data are representative datasets from experimental observations made at least 3 times; experiments using *Sting*$^{-/-}$ BMDMs were repeated 2 times. Error bars reflect SD from the mean. BMDMs were treated with LPS=10 ng/mL, zVAD=50 μM, Nec-1=30μM and/or MRT67307=2μM where indicated.

Contributions: Experiments performed by Danish Saleh and Malek Najjar. Data analyzed, figures prepared, and figure legends written by Danish Saleh.

Figure 7. TRIF, TBK1/IKKε, and IRF3 are important for LPS/zVAD induced IFNβ synthesis.

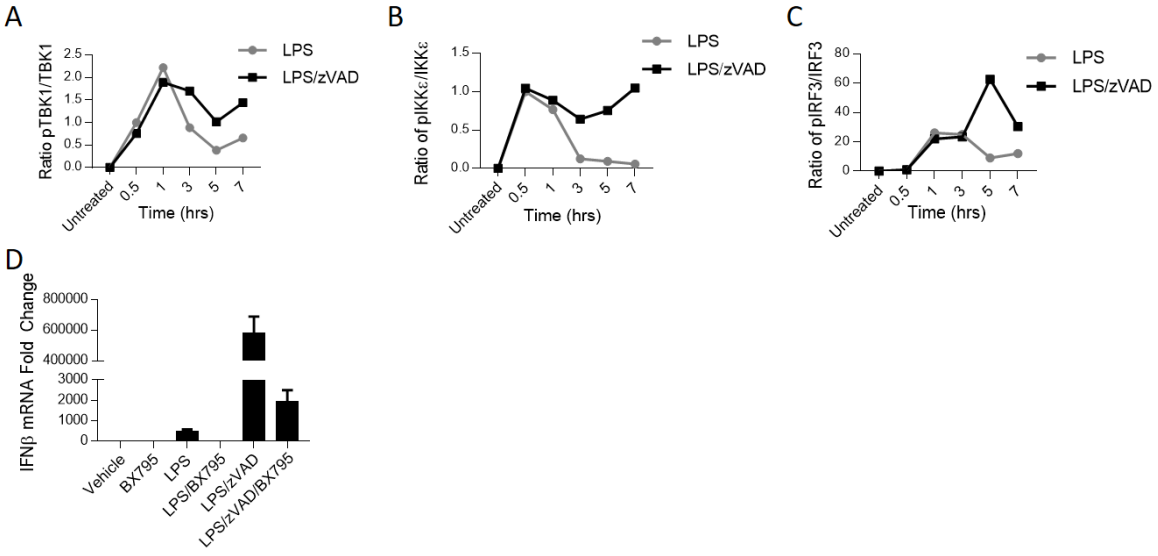

Figure 7. TRIF, TBK1/IKKε, and IRF3 are important for LPS/zVAD induced IFNβ synthesis.

(A-C) Densitometry analysis Western blot timecourse phosphorylation of TBK1 (A), IKKε (B), and IRF3 (C) in wild type BMDMs. (D) qRT-PCR of *Ifnb* mRNA expression in wild type BMDMs treated with TBK1/IKKε inhibitor (BX795) for 5-7 hrs. Presented data are representative datasets from experimental observations made at least 3 times. Error bars reflect SD from the mean. BMDMs were treated with LPS=10 ng/mL, zVAD=50 μM, Nec-1s=30μM and/or BX795=1μM where indicated.

Contributions: Experiments performed by Danish Saleh and Malek Najjar. Data analyzed, figures prepared, and figure legends written by Danish Saleh.

Figure 8. IFN-I pathway activation by LPS with zVAD is RIPK1 and RIPK3 kinase-dependent.

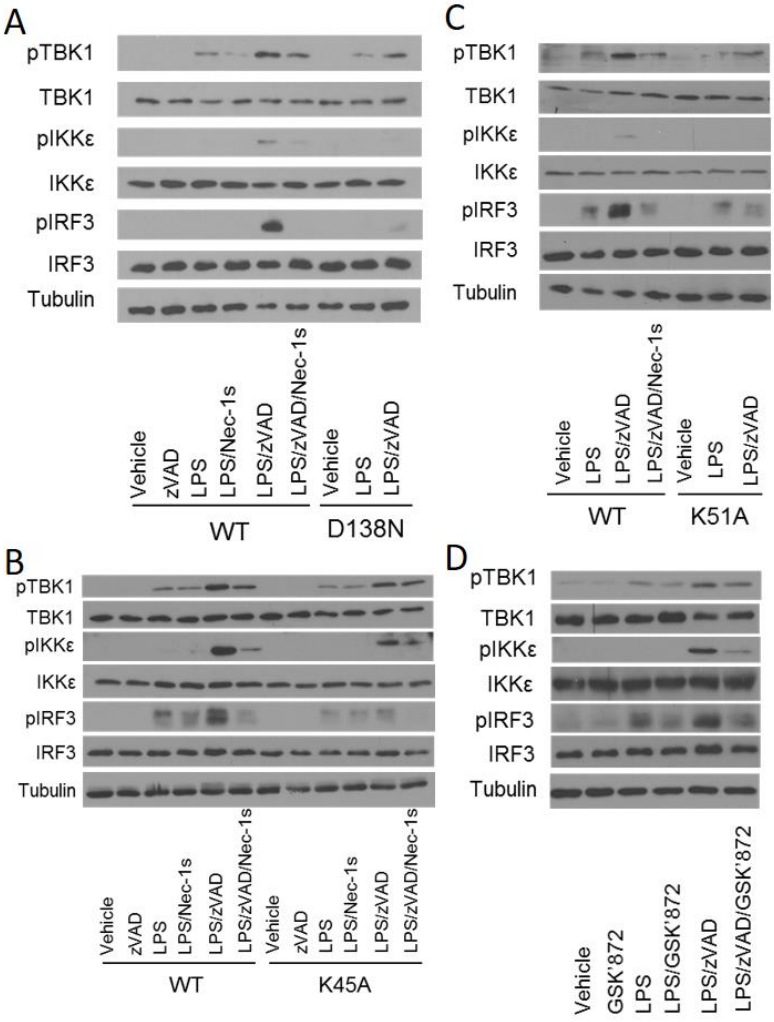

Figure 8: IFN-I pathway activation by LPS with zVAD is RIPK1 and RIPK3 kinase-dependent.

(A) Western analysis of TBK1, IKKε, and IRF3 phosphorylation in wild type (WT) and D138N RIPK1 (D138N) BMDMs treated for 3-4 hrs. (B) Western analysis of TBK1, IKKε, and IRF3 phosphorylation in wild type (WT) and K45A RIPK1 (K45A) BMDMs treated for 3-4 hrs. (C) Western analysis of TBK1, IKKε, and IRF3 phosphorylation in wild type (WT) and K51A RIPK3 (K51A) BMDMs treated for 3-4 hrs. (D) Western analysis of TBK1, IKKε, and IRF3

phosphorylation in wild type BMDMs treated with RIPK3 kinase inhibitor (GSK'872) for 3-4 hrs. Presented data are representative datasets from experimental observations made at least 3 times. BMDMs were treated with LPS=10 ng/mL, zVAD=50 μM, Nec-1=30μM and/or GSK'872=5μM where indicated.

Contributions: Experiments performed by Danish Saleh and Malek Najjar. Data analyzed, figures prepared, and figure legends written by Danish Saleh.

Figure 9. IFN-I pathway activation by LPS with zVAD is dependent on RIPK3.

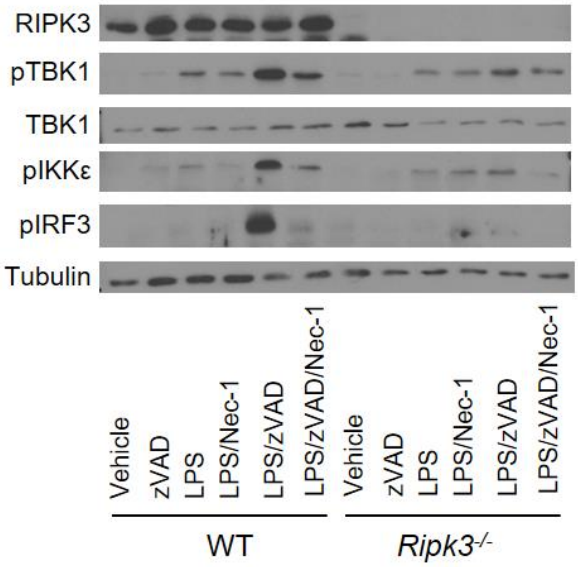

Figure 9. IFN-I pathway activation by LPS with zVAD is dependent on RIPK3. Western analysis of TBK1, IKKε, and IRF3 phosphorylation in wild type (WT) and *Ripk3*$^{-/-}$ BMDMs treated for 3-4 hours. Presented data are representative datasets from experimental observations made at least 3 times. BMDMs were treated with LPS=10 ng/mL, zVAD=50 μM, and/or Nec-1s=30μM where indicated.

Contributions: Experiments performed by Danish Saleh and Malek Najjar. Data analyzed, figure prepared, and figure legend written by Danish Saleh.

LPS with zVAD promotes localization and activation of TBK1, IKKε, and IRF3 in RIPK1 and RIPK3-containing detergent-insoluble cellular fractions.

Observing that IFN-I pathway intermediaries were required for RIPK1 and RIPK3 kinase-dependent IFNβ synthesis, we considered the possibility that these intermediaries associate with RIPK1 and RIPK3 'necrosomes'. Activation of RIPK1 and RIPK3 kinase-dependent cell death is associated with post-translational modification and enrichment of the kinases in detergent insoluble cellular fractions, representing necrosome complexes (Li et al. 2012; Moquin et al. 2013; Ofengeim et al. 2015; Najjar et al. 2016). LPS and zVAD treatment of BMDMs resulted in the co-enrichment of modified forms of RIPK1 and RIPK3 in detergent insoluble cellular fractions that was blocked by Nec-1s (Figure 10a), consistent with our previous report of the formation of detergent-insoluble necrosome-like aggregates in LPS and zVAD-treated BMDMs (Najjar et al. 2016). We next analyzed co-enrichment of IFN-I pathway intermediaries with RIPK1 and RIPK3 under these conditions. Notably, we observed that TBK1, IKKε, and IRF3 were enriched in detergent insoluble fractions (Figure 10b). Moreover, we found that phosphorylated or activated forms of these intermediaries were enriched in these cellular compartments (Figure 10b). This regulation was dependent on the catalytic function of RIPK1 and RIPK3 as enrichment of these factors was abolished in the presence of Nec-1s or in K51A RIPK3 BMDMs (Figure 10b,c). We further examined co-enrichment with RIPK1 and RIPK3 using additional high molecular weight protein complex fractionation by sucrose-gradient-based velocity sedimentation. These experiments were performed in an immortalized macrophage cell line (RAW264.7 cells), providing a more abundant source of material than BMDMs, using an optimized pan-caspase inhibitor, IDN6556 (Brumatti et al. 2016). RIPK1 and RIPK3 were enriched in fractions 12 and 13, indicating the formation of a high molecular weight complex, when cells were treated by LPS

and a pan-caspase-inhibitor that was abolished in the presence of Nec-1s (Figure 10d). Consistent with the previous data, TBK1, IKKε, and IRF3 were again co-enriched in these same fractions (Figure 10d). Intriguingly, additional co-immunoprecipitation studies revealed that TBK1 and IKKε directly complexed with RIPK1, as did RIPK3, when cells were treated with LPS with IDN and this was abolished in the presence of Nec-1s (Figure 10e). We also found that TRIF association with IKKε was not modified in a RIPK1 kinase-dependent manner, suggesting that RIPK1 kinase-dependent signaling may be mediated by post-translational modification as opposed changes in molecular association (Figure 10f). Lastly, to confirm that RIPK1 and RIPK3 kinase-dependent IFN-I pathway signaling did not also require MLKL, we examined enrichment of IFN-I pathway intermediaries in detergent-insoluble fractions in *Mlkl*$^{-/-}$ BMDMs. Consistent with our previous observation that MLKL was not required for RIPK1 and RIPK3 kinase-dependent IFNβ synthesis, we observed that MLKL was also dispensable for co-enrichment and activation of TBK1, IKKε, and IRF3 in necrosome containing cellular fractions (Figure 10g). Together, these data support the model that IFN-I pathway intermediaries may be recruited and directly activated by RIPK1 and RIPK3 necrosome complexes.

Figure 10. Kinase activity of RIPK1 and RIPK3 are required for localization and activation of IFN-I pathway intermediaries in detergent-insoluble cellular fractions.

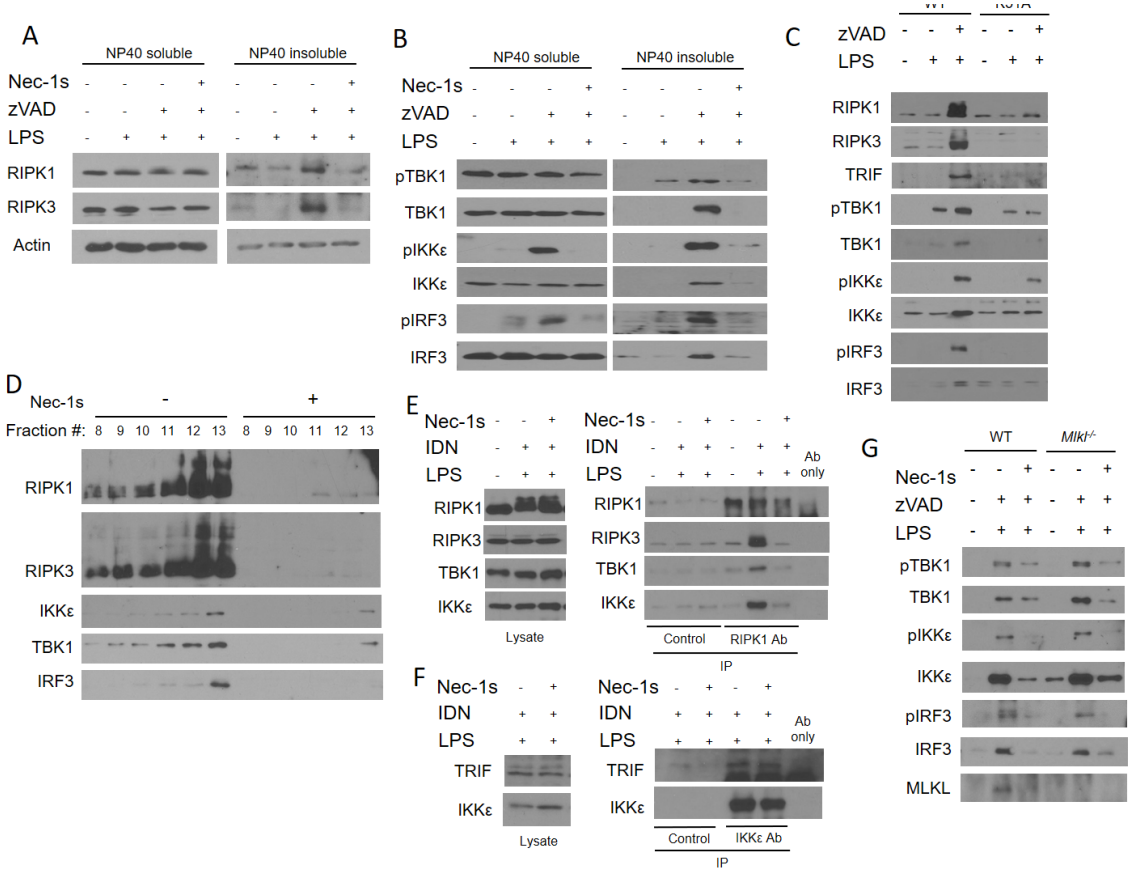

Figure 10: Kinase activity of RIPK1 and RIPK3 are required for localization and activation of IFN-I pathway intermediaries in detergent-insoluble cellular fractions.

(A) Western analysis of localization and modification of RIPK1 and RIPK3 in NP40-soluble and NP40-insoluble fractions from wild type BMDMs treated for 3-4 hrs. (B) Western analysis of localization and phosphorylation of TRIF, TBK1, IKKε, IRF3 in NP40-soluble and NP40-insoluble fractions from wild type BMDMs treated for 3-4 hrs. (C) Western analysis of RIPK1, RIPK3, TRIF, TBK1, IKKε, and IRF3 in NP40-insoluble fractions from wild type (WT) and K51A RIPK3 (K51A) BMDMs treated for 3-4 hrs.(D) Western analysis of RIPK1, RIPK3, TBK1, IKKε, and IRF3 in RAW264.7 macrophages treated with LPS and IDN6556 (10μM) +/- Nec-1s for 3-4 hrs. Lysates were fractionated on a linear sucrose-gradient by velocity sedimentation and protein

was collected following chloroform-methanol precipitation. (E) Co-immunoprecipitation analysis of RIPK3, TBK1, and IKKε following immunoprecipitation of RIPK1 from RAW264.7 macrophages treated for 3-4 hrs. (F) Co-immunoprecipitation analysis of TRIF following immunoprecipitation of IKKε from RAW264.7 macrophages treated for 3-4 hrs. Control=Beads only. (G) Western analysis of RIPK1, RIPK3, TRIF, TBK1, IKKε, and IRF3 in NP40-insoluble fractions from wild type (WT) and *Mlkl*$^{-/-}$ BMDMs treated for 3-4 hrs. Presented data are representative datasets from experimental observations made at least 3 times. TBK1 co-IP with RIPK1 was observed 2 times. BMDMs were treated with LPS=10 ng/mL, zVAD=50 μM, IDN6556=10μM, and/or Nec-1s=30μM where indicated.

Contributions: Experiments performed, data analyzed, figures prepared, and figure legends written by Danish Saleh.

RIPK1 and RIPK3 kinase-dependent IFNβ synthesis in macrophages is induced by avirulent strains of gram-negative bacteria.

Several studies have demonstrated that TRIF-dependent IFNβ production is an important feature of the host-response that aids in the resolution of gram negative bacterial infections (Cai et al. 2009; Sotolongo et al. 2011; Ruiz et al. 2016). However, gram negative bacteria pathogens such as *Yersinia* and *Klebsiella* have evolved an armament of virulence factors to manipulate host-responses and facilitate their pathogenesis. In case of *Yersinia,* Type-III Secretion System (T3SS) Yop proteins are injected directly into host cells (Davis et al. 2010; Viboud & Bliska 2005; Zhang et al. 2011). Several of these Yops impede host-cell defenses by blocking host pro-inflammatory signaling. Similarly, *Klebsiella* is equipped with an outer polysaccharide capsule that facilitates immune evasion and enhances bacterial virulence (Lawlor et al. 2006; Lawlor et al. 2005). We evaluated whether these pathogens use their virulence factors to dampen sensing of their LPS and subsequent IFNβ induction by RIPK1 and RIPK3.

We examined IFNβ mRNA synthesis in the presence of zVAD following infection with WT or avirulent forms of *Yersinia pseudotuberculosis (Yptb)* and *Klebsiella pneumonia (Kp)*. Notably, the avirulent strain of *Yptb*, lacking the ability to inject Yops into host cells (*ΔyscF),* and the avirulent strain of *Kp (ΔcpsB),* unable to produce an outer polysaccharide capsule, induced a robust increase in IFNβ mRNA synthesis compared to WT or pathogenic counterparts in the presence of zVAD (Figure 11a, 11b). To verify that IFNβ induction was dependent on RIPK1 and RIPK3 kinases, we also determined that the response was absent in K45A RIPK1 and K51A RIPK3 BMDMs (Figure 11a, 11b). Furthermore, consistent with the previous data, we again observed robust RIPK1 kinase activity-dependent co-accumulation of RIPK1, RIPK3 and IFN-I pathway components in the insoluble fractions of cells infected with *ΔyscF* or *ΔcpsB* in the

presence of zVAD (Figure 11c, 11d). In sum, these data provide direct demonstration that gram negative bacteria are capable of inducing RIPK1 and RIPK3 kinase-dependent IFNβ synthesis *in vitro* in the presence of zVAD, and that this induction may be under negative regulation by bacterial virulence factors. Accordingly, these data, paired with our *in vivo* observations of LPS-induced RIPK1 kinase-dependent IFNβ synthesis, suggest a potential role for RIPK1 kinase-dependent IFNβ synthesis as part of a physiologic host-response in bacterial infection.

Figure 11. RIPK1 and RIPK3 kinase-dependent IFNβ synthesis is augmented by attenuated strains of *Yersinia pseudotuberculosis* and *Klebsiella pneumonia*.

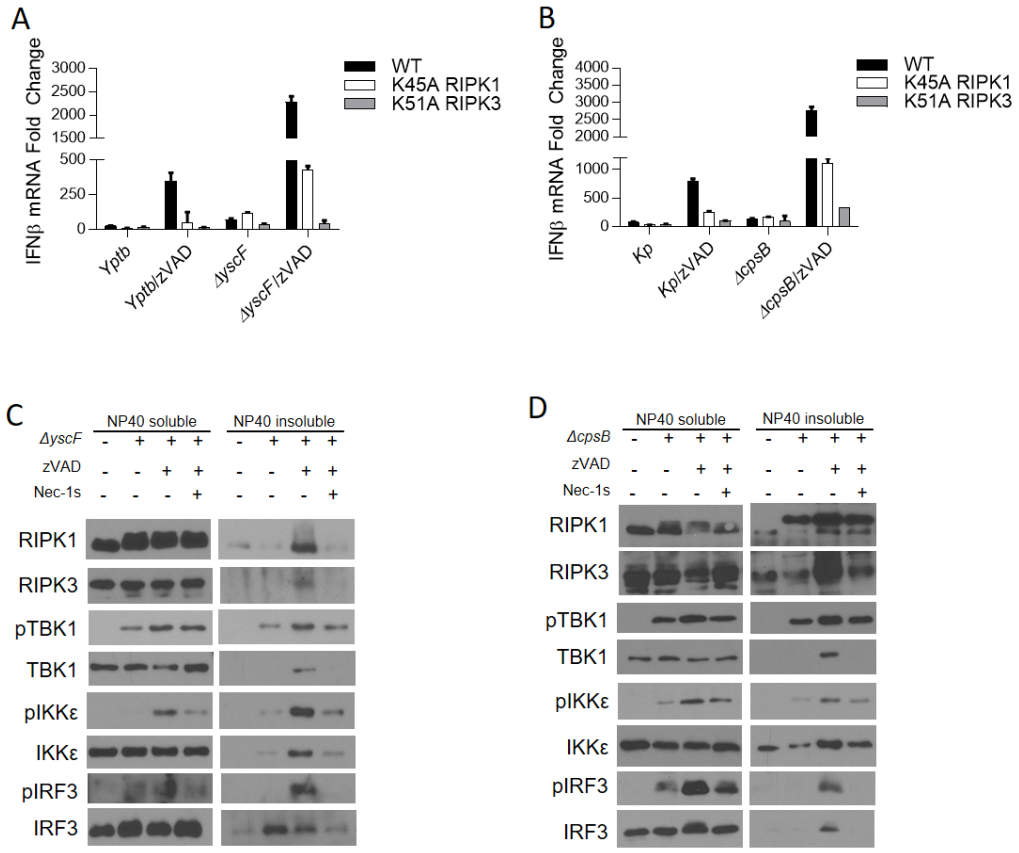

Figure 11: RIPK1 and RIPK3 kinase-dependent IFNβ synthesis is augmented by attenuated strains of *Yersinia pseudotuberculosis* and *Klebsiella pneumonia*.

(A) qRT-PCR of *Ifnb* mRNA expression in wild type (WT), K45A RIPK1 (K45A), and K51A RIPK3 (K51A) BMDMs infected with wild type *Yersinia pseudotuberculosis (Yptb)* or a mutant strain unable to inject pathogenicity factors into macrophages *(ΔyscF)*, at an MOI of 40-60. (B) qRT-PCR of *Ifnb* mRNA expression in WT, K45A, and K51A BMDMs infected with wild type *Klebsiella pneumonia (Kp)*, or a mutant strain lacking its out polysaccharide capsule virulence factor *(ΔcpsB)* at an MOI of 40-60. (C) Western analysis of localization and phosphorylation of

TRIF, TBK1, IKKε, IRF3 in NP40-soluble and NP40-insoluble fractions from wild type BMDMs treated as described in (A). (D) Western analysis of localization and phosphorylation of TRIF, TBK1, IKKε, IRF3 in NP40-soluble and NP40-insoluble fractions from wild type BMDMs treated as described in (B). Presented data are representative datasets from experimental observations made at least 3 times. Error bars reflect SD from the mean. BMDMs were treated with zVAD=50 μM and/or Nec-1s=30μM where indicated. Gentamicin (100μg/mL) was added 2 hours post-infection in each experiment.

Contributions: Experiments performed, data analyzed, figures prepared, and figure legends written by Danish Saleh.

Discussion

RIPK1 and RIPK3 activation and necrosis are generally believed to be associated with acute and pathologic injury; however, emerging evidence suggests RIPK1 and RIPK3 may play significant roles in physiologic host-defense responses to viral and bacterial infections (Saleh & Degterev 2015; Sridharan & Upton 2014). To date, studies have focused on the roles of RIPK1 and RIPK3 in the context of pathogen-induced cell death. For example, RIPK1 and caspase-8-dependent apoptosis has been described as a central feature of the innate immune response to gram-negative bacterial pathogen, *Yersinia* (Weng et al. 2014; Philip et al. 2014). Similarly, RIPK1 and RIPK3 kinase-dependent necroptosis have been implicated in macrophage cell death by *Salmonella* and local-tissue damage in necrotizing pneumonia caused by *Methicillin-Resistant Staphylococcus Aureus (MRSA)* (Kitur et al. 2015; Robinson et al. 2012). However, inflammatory signaling is also a critical component of the initial innate immune response that has not been as closely examined in RIPK1 and RIPK3 biology.

Previous work suggested that kinase activities of RIPK1 and RIPK3 may not contribute to cytokine synthesis downstream of TLR3 and TLR4 (Cusson-Hermance et al. 2005; Kelliher et al. 1998; Meylan et al. 2004; Newton et al. 2004). However, these studies were performed in the absence of caspase inhibition, which is a requisite to elicit kinase functions of RIPK1 and RIPK3 *in vitro* (Schworer et al. 2014; Kaiser et al. 2013; He et al. 2011; Najjar et al. 2016). In contrast, data in this study as well as other recent reports (Wong et al. 2014; Christofferson et al. 2012; McNamara et al. 2013; Najjar et al. 2016) describe RIPK1 and RIPK3 kinase-dependent cytokine responses that manifest independent of MLKL-dependent cell death signaling. In a prior study we reported that RIPK1 and RIPK3 kinase-dependent cytokine profile evaluated *in vitro*, in the presence of zVAD, correlated strongly with the inflammatory profile observed *in vivo*, in the

absence of exogenous caspase manipulation (Najjar et al. 2016). We observed the dichotomy between RIPK1 kinase regulation *in vitro* and *in vivo* was linked to limited caspase-8 activation in bone marrow monocytic cells collected from mice injected with LPS (Najjar et al. 2016). Similarly, in this study we find that exogenous inhibition of caspases is not requisite for RIPK1 and RIPK3 kinase-dependent IFNβ synthesis *in vivo* following LPS challenge. These findings suggest that use of zVAD *in vitro* may aid in uncovering new pro-inflammatory roles for RIPK1 and RIPK3 *in vivo*.

In vitro observation of detergent-insoluble, amyloid-like, RIPK1 and RIPK3 complexes, also known as necrosomes, have been linked to RIPK1 and RIPK3 kinase-dependent signaling (Li et al. 2012; Moquin et al. 2013; Najjar et al. 2016). Indeed, it is well established that caspase inhibition is essential the induction of necroptosis and that MLKL is recruited to necrosome signaling platforms (Najjar et al. 2016; Schworer et al. 2014; He et al. 2011; Kaiser et al. 2013) . Similarly, in the presence of caspase inhibition, we also observe enrichment and activation of IFN-I pathway intermediaries in necrosome containing cellular fraction and, remarkably, this did not require MLKL. Although the necrosome was originally defined as a cell-death signaling complex, our data here and in our previous study suggest that the necrosome may additionally serve as a signaling platform for the induction of IFNβ and other cytokines (Najjar et al. 2016; Saleh et al. 2017). It is important to note that the precise details of necrosome signaling are poorly understood and it remains to be determined whether a singular 'necrosome' platform is capable of driving cytokine and pro-death signaling independent of one another. Alternatively, the 'necrosome' might reflect physically and/or compositionally heterogenous RIPK1 and RIPK3 containing platforms that are defined and influenced by their immediate molecular context to promote cytokine synthesis or pro-death signaling.

Our data found that STING contributes to TRIF/RIPK1-dependent IFNβ synthesis (Fig. S4e). Recent work by Wang X. et al. suggested that TRIF is required for STING to activate IFNβ synthesis. Thus, it is possible that STING and TRIF may similarly cooperate in promoting RIPK1 activation and IFNβ synthesis. STING has also been proposed to respond to damaged DNA to induce IFNβ synthesis. This might serve as an indirect mechanism of STING participation in TRIF-RIPK1 kinase-dependent events. However, we believe this latter regulation is unlikely to be a major mechanism contributing RIPK1 kinase-dependent IFNβ synthesis because we observe considerable induction in IFNβ by LPS with zVAD in *Mlkl*$^{-/-}$ BMDMs, a system without measurable loss in cell viability (Figure 5c, 5d). Nevertheless, further experiments are needed to further clarify the mechanism of STING involvement.

Protective host defenses mediated specifically by TRIF have been described in response to several gram-negative bacterial pathogens (Cai et al. 2009; Sotolongo et al. 2011; Ruiz et al. 2016). For instance, pulmonary infection by *Klebsiella* has been found to become significantly more deadly in TRIF-deficient mice (Cai et al. 2009). Conversely, pre-administration of TLR3 agonist, poly(I:C), which engages TRIF-dependent signaling exclusively, has been shown to promote clearance of gram negative bacterial pathogens (Ruiz et al. 2016). Given these observations, our data raise the question as to whether previously described TRIF-dependent protective host responses are mediated by RIPK1/RIPK3 *in vivo*. Furthermore, our studies in macrophages suggest that TRIF/RIPK1/RIPK3-dependent responses may be either broadly or specifically targeted by bacterial virulence factors. While this has been addressed in various viral infections (Huang et al. 2015; Xing Wang et al. 2014; Guo et al. 2015; Upton et al. 2012; Omoto et al. 2015), the regulation of RIPK1 and RIPK3 signaling by gram negative bacterial pathogen virulence factors is still poorly understood.

Accordingly, to our knowledge, our work is the first to demonstrate the capacity of RIPK1 and RIPK3 kinases to induce cytokine synthesis in response to gram negative bacteria. We report activation of RIPK1 and RIPK3 kinase-dependent IFNβ synthesis by *Klebsiella* and *Yersinia* mutants *in vitro* in the presence of zVAD. This observation is analogous to the regulation of RIPK1 previously noted in viral-induced RIG-I signaling in which caspase-8-dependent cleavage of RIPK1 attenuated IRF3 activation and IFN-I production (Rajput et al. 2011). However, significantly, our data additionally reveals the propensity of avirulent bacterial strains to promote more efficient RIPK1 and RIPK3 kinase-dependent IFNβ induction compared to their wild type pathogenic counterparts *in vitro*.

Data by Nogusa et al. showed that RIPK3 was dispensable for the IFN-I transcriptional response induced by RIG-like receptor (RLR) activation or Influenza virus infection in mouse embryonic fibroblasts (Nogusa, Slifker, et al. 2016), in contrast to the central role of this protein in cell-death induction during influenza infection in the same cell types (Nogusa, Thapa, et al. 2016). These data suggest that there may be important differences in the activation and consequence of the RIPK1 and RIPK3 kinase-dependent cytokine responses in cases of gram-negative bacterial infections, which often occur extracellularly, versus intracellular viral infections, where cell death may be necessary to eliminate infected host cells and prevent viral replication. However, broader sets of pathogens and the roles of cell type specific factors remain to be examined.

In this study we describe a novel role for RIPK1 kinase in directing IFNβ synthesis in response to LPS *in vivo*. We find that RIPK1 kinase-dependent IFNβ synthesis may be elicited in analogous fashion in BMDMs using LPS with zVAD. Notably, we observed that RIPK1 kinase-dependent IFNβ synthesis in BMDMs also required RIPK3 kinase but not MLKL, a requisite

executioner of necroptosis pathway. Conversely, RIPK1 kinase-dependent IFNβ synthesis required the TLR4 adapter protein, TRIF, and downstream canonical IFN-I pathway intermediaries, including TBK1, IKKε and IRF3. It is important to note that RIPK1 and RIPK3 kinase-dependent IFN-I pathway activation *in vitro* was a delayed feature of TRIF-dependent signaling, suggesting that RIPK1 and RIPK3 kinases are not required for early endosomal translocation of TLR4 (Kagan et al. 2008) (Figure 12). Interestingly, we also noted that the intracellular nucleotide sensor, STING, likely participates in this regulation. Examination of detergent-insoluble cellular fractions or 'necrosome'-like fractions in RIPK1 kinase-activating conditions suggested that the 'necrosome' may represent a scaffold for the TRIF-IRF3 signaling axis, and/or that one or multiple IFN-I pathway intermediaries might be direct targets of RIPK1 and/or RIPK3. These data were further supported by co-immunoprecipitation studies. Finally, our observation that avirulent bacteria are capable of inducing RIPK1 and RIPK3 kinase-dependent IFNβ synthesis to a greater extent than their pathogenic counterparts *in vitro*, prompts further examination of the role that RIPK1 and RIPK3 kinase-dependent IFNβ synthesis may play in the host response against bacterial infection.

Figure 12. RIPK1 and RIPK3 kinases engage the IFN-I pathway downstream of the adapter protein TRIF.

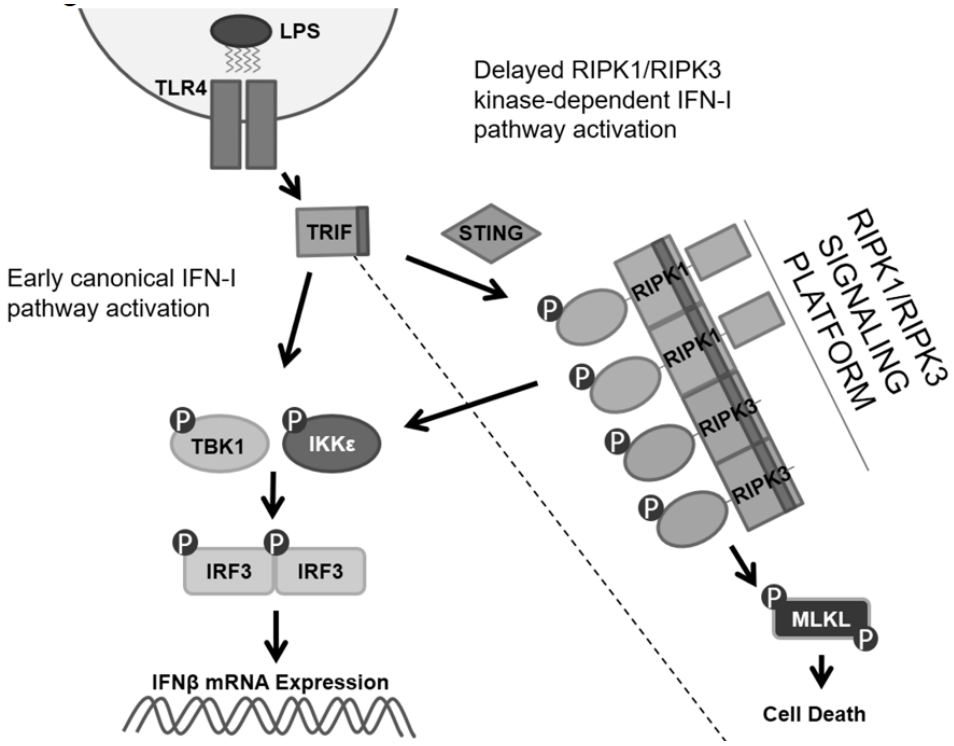

Figure 12: RIPK1 and RIPK3 kinases engage the IFN-I pathway downstream of the adapter protein TRIF.

Contributions: Figure prepared by Danish Saleh.

Author Contributions

D.S. performed cell viability, Western analyses, and ELISAs. M.N., D.S., and S.S. performed RNA work and qRT-PCRs. D.S., M.N. and M.Z. performed *in vivo* experiments. D.S. and N.S. fractionated lysates using sucrose gradient and velocity sedimentation. A.T. performed the RNA-Seq analysis. D.S. prepared the fractionation samples. J.B. and P.G. generated and provided the K45A RIPK1 and K51A RIPK3 mice. A.P. and M.P. developed RIPK1 D138N mice. M.Z., M.P., and M.K. provided the D138N RIPK1 cells. M.W. provided *Ripk3*$^{-/-}$ cells. S.N. and S.B. provided *Mlkl*$^{-/-}$ cells. K.F provided *Irf3*$^{-/-}$/*Irf7*$^{-/-}$ cells. J.M. and M.P. provided bacterial strains. M.Z., J.B., P.G, M.P., K.F., N.S., S.B., and J.M. helped revise the manuscript. D.S. and A.D. wrote and revised the manuscript.

Acknowledgments

We thank Drs. Vishva Dixit, Stan Krajewski, Sergei Nedospasov, and Alexander Poltorak for providing the reagents. We thank Dr. Albert Tai for helping with analysis of RNA sequencing data. P.J.G. and J.B are employees of GlaxoSmithKline. A.D. is a consultant for Denali Therapeutics.

Experimental Procedures

Animals

Female Balb/c mice at 6-8 weeks of age were used for LPS experiments (Charles River Labs). *Ripk3*$^{-/-}$ (on C57BL/6 background) and matched controls were previously described (Newton et al., 2004) and provided to us by Dr. Vishva Dixit (Genentech). *Sting*$^{-/-}$ mice were a gift from Dr. Alexander Poltorak. TRIF$^{-/-}$ *(Ticam1*$^{-/-}$*)* (C57BL/6J-*Ticam1Lps2*/J) mice and corresponding control mice (C57BL/6J, B6.129P2) were purchased from Jackson labs. *D138N RIPK1, K45A RIPK1, K51A RIPK3, and Mlkl*$^{-/-}$ mice were previously described (Berger et al. 2014; Polykratis et al. 2014; Moriwaki et al. 2015; Nogusa, Thapa, et al. 2016).

All use of animals was approved by the Tufts University, UMASS, and Fox Chase Cancer Center Institutional Animal Care and Use Committees. Mice were maintained in Tufts animal facility in cages with light/dark cycle and experiments performed according to the protocol with all efforts to minimize the number and suffering of the animals.

Bacteria

Yersinia strains (*Yptb* and *ΔyscF*) were on the IP2666 background and have been previously described (Davis & Mecsas 2007). *Yersinia* bacteria were cultured overnight in 2XYT at 26C. On the day of infection, cultures were diluted 1:40 in 5mM $CaCl_2$ containing 2XYT for 2 hours and then moved to 37C for two hours prior to infection. *Klebsiella* strains (*Kp* and *ΔcpsB*) were on the *Kp* ATCC 43816 background. *ΔcpsB* was generated and gifted by Michelle Paczosa and will be reported in a future publication. *Klebsiella* bacteria were grown overnight at 37C in L broth.

Infections

Macrophages were infected in antibiotic free media (10% L929 conditioned media + 10% FBS in RPMI) bacteria at an MOI of 40-60 and bacterial were spun down at 300g for 3 minutes. Two

hours post-infection, 100μg/mL Gentamicin was administered and macrophages were harvested 6 hours post-infection. Prior to infection, bacterial counts were estimated using an optical density read-out and confirmed by colony-forming unit assay.

***In vivo* LPS challenge and Nec-1s treatment**

Mice were injected intravenously or intraperitoneally with 30 mg/kg optimized Nec-1s (7-Cl-O-Nec-1) (Degterev et al. 2013), 15 min prior to intraperitoneal injection of 50 μg/kg LPS (Sigma). $CD11b^+$ bone marrow cells were collected 1 hour post-injection from femurs and stained at a dilution of 1:300 using PE conjugated anti-mouse/human $CD11b^+$ (BioLegend, 101207) for 1 hour in FACS buffer (2% FBS and 1μM EDTA in PBS). 20-40% of total cells were $CD11b^+$ and these were sorted by FACS. Sorted cells were used for qRT-PCR or RNA-Seq.

Reagents

Lipopolysaccharide (LPS) (*Escherichia coli* 0111:B4) was purchased from Sigma. Optimized Necrostatin-1s (Nec-1s) (5-[(7-chloro-1H-indol-3-yl) methyl]-3-methyl-2,4-imidazolidinedione) was synthesized as previously described (Teng et al., 2005). For *in vivo* administration, Nec-1s was dissolved in PBS containing 25% Polyethylene Glycol 400 (Spectrum labs). RIPK3 inhibitor, GSK'872, was also previously described (Mandal et al. 2014; Kaiser et al. 2013). TBK1/IKKε inhibitors, MRT67307 and BX795 were previously described (Clark et al. 2011; Clark et al. 2009). IDN6556 was previously described (Brumatti et al. 2016). zVAD.fmk was purchased from ApexBio.

Cells

Bone marrow derived macrophages (BMDMs) were prepared by flushing bone marrows from femurs and tibias. BMDMs were allowed to differentiate for 7 days in the presence of conditioned media from L929 cells, containing Macrophage Colony Stimulating Factor (M-CSF) - 30% L929

media, 20% FBS and 1% PSA (penicillin/streptomycin/antimycotic solution) in RPMI1640. Medium was replenished on day 3. 48 hours before treating the cells, the medium was exchanged to 10% L929 media, 10% FBS and 1% PSA in RPMI1640. On day 7, the adherent cells were collected using PBS and centrifuged at 430 g for 5 min and replated for the experiments. For mRNA and Western blot experiments, 2 X 10^6 BMDMs were seeded into 35 mm^2 dishes. For cell viability experiments, 50,000 cells per well were seeded in 96 well plates. RAW cells (RAW264.7) were grown in DMEM containing 10% FBS and 1% PSA. For experiments, cells were treated with all reagents (stimulants and inhibitors) simultaneously. For example, inhibitors (ie: Nec-1s) were added to cells with LPS and zVAD or IDN at time zero.

Western blotting

Cells were lysed and harvested in RIPA buffer (Cell Signaling) supplemented with Phenymethanesulfonylfluoride (PMSF) (5 μg/ml, Sigma), leupeptine (1μg/ml), pepstatin (1μg/ml) and aproprotinin (1μg/ml). The protein concentrations were determined using Bio-Rad Protein Assay reagent, and equal amounts of protein were subjected to Western blotting. Samples were separated by SDS/PAGE and transferred to PVDF membranes. After being blocking in Protein-free T20 (TBS) blocking buffer (Fisher Scientific) at room temperature for 1 h, the membranes were rinsed with TBST (0.1%) and incubated at 4 °C overnight with primary antibodies (1:1000 dilution). The membranes were washed and incubated with secondary antibody (1:5000 dilution) at room temperature for 1 h. Signals were developed using Luminata Classico or Forte HRP substrates (Millipore).

Antibodies

The following antibodies acquired from Cell Signaling Technologies were used: TBK1 (#3504), p-TBK1 (#5483), IKKε (#3416), p-IKKε (#8766), IRF3 (#4302), and p-IRF3 (4947), RIPK1

(#3493), αTubulin (#3873), anti-mouse IgG HRP-linked antibody, and anti-rabbit IgG HRP-linked antibody. RIPK3 antibody was purchased from Prosci (#2283). Primary antibodies were used at a dilution of 1:1000 and secondary antibodies were used at a dilution of 1:5000.

Cell Viability Assays

The cells were seeded as described above in 100 µL of media. Typically, cells were treated with 10 ng/ml LPS and 50 µM zVAD for 24 hours. Cell viability was determined using CellTiter-Glo viability assay kit (Promega). Each independent experiment was performed in duplicate and repeated three times. Viability of the cells, relative to an untreated control, was determined and plotted.

Measurement of IFNβ by ELISA

Mouse interferon beta (IFNβ) was measured using colorimetric ELISA. 96 well plate was incubated at 4C overnight after coating wells with 50 µL of monoclonal rat anti-mouse IFNβ (Santa Cruz, SC-57201) diluted 1:500 (final concentration: 0.2µg/mL) in 0.1M carbonate buffer. The following day, wells were incubated with 200 µL of blocking buffer (10% FBS in PBS) for 2 hours at 37C. After blocking, wells were incubated with 50µL of standard or sample (diluted 1:1, 1:5, and/or 1:25 in blocking buffer) and incubated overnight at 4C. Interferon-beta protein purchased from PBL (product number: 12400) and standard curves were generated using concentrations 0-1000IU/mL (0-2ng/mL). The following day, wells were incubated with 50µL of polyclonal rabbit anti-mouse IFN-β detecting antibody from PBL (product number: 32400) diluted 1:2000 (final concentration: 0.5µg/mL) in blocking buffer and incubated overnight at 4C. The following day, 50µL of goat anti-rabbit-HRP secondary antibody (Cell Signaling) diluted 1:2000 was added to the wells. Plates were incubated for 2-3 hours at room temperature. Subsequently, 50 µL of the TMB substrate was added. The reaction was stopped by the addition of 50 µL 2N H_2SO_4.

Absorbance was measured at 450 nM. A washing step with buffer (PBS 0.05% TWEEN) was performed after each step and before the addition the substrate.

RNA extraction, cDNA synthesis and qRT-PCR

For RNA extraction, cells were seeded as described above. Cells were stimulated with 10 ng/ml LPS, 50 µM zVAD and 30 µM Nec-1s or other inhibitors as indicated. Total RNA was isolated using RNA MiniPrep kit (ZYMO Research) according to the manufacturer's protocol. 50 ng to 1 µg of RNA was converted to cDNA using iScript cDNA Synthesis kit (BioRad). 1 µL of cDNA was used with 500 pM primers in 20 µL qPCR reactions using VeriQuest SYBR Green master mix (Affymetrix). qRT-PCR reactions were performed in LightCycler 480 II using the following program: 50°C for 2 min, 95°C for 10 min, followed by 40 cycles of amplification (95°C for 15 sec, 60°C for 1 min). GAPDH was analyzed as a housekeeping gene.

The primer sequences used to amplify murine genes are as following:

Mouse GAPDH: forward 5'-TGTGTCCGTCGTGGATCTGA-3', reverse: 5'-GGTCCTCAGTGTAGCCCAAG3'.

Mouse IFNb1: forward 5'-CAGCTCCAAGAAAGGACGAAC-3', reverse 5'-GGCAGTGTAACTCTTCTGCAT-3'.

Mouse MX2: forward 5'-GAGGCTCTTCAGAATGAGCAA -3', reverse 5'-CTC TGCGGTCAGTCTCTCT-3'.

Mouse IFIT1: forward 5'- CTGAGATGTCACTTCACATGG AA -3', reverse 5'-GTGCATCCCCAATGGGTTCT -3'.

Necrosome formation assay

Isolation of NP40 soluble and insoluble fractions was performed as previously described (Li et al. 2012; Moquin et al. 2013). Cells were seeded into 35 cm^2 dishes at 2 X 10^6 cells/well and

stimulated with 10 ng/ml LPS, 50 μM zVAD and 30 μM Nec-1s for up to 3 hr. Cells were lysed in 1%TritonX100 or 1%NP-40 lysis buffer (150mM NaCl, 20mM Tris-Cl (pH 7.5), 1% TritonX100 or 1%NP-40, 1mM EDTA, 3mM Na-fluoride, 1mM B-glycerophosphate, 1mM Sodium Orthovanadate, 5uM Idoacetamide, 2uM N-ethylmaleimide and Phosphatase and 5μg/ml PMSF and 1μg/ml leupeptine, 1μg/ml pepstatin and 1μg/ml aprotinin. Lysates were flash frozen on dry-ice, thawed on ice and vortexed for 10 sec followed by centrifugation at 1000g for 15 minutes in the refrigerated table-top centrifuge to remove nuclei. Supernatants were collected and centrifuged at 34,400g for 15 minutes to precipitate detergent-insoluble cellular fraction (NP40 or Triton insoluble). Supernatants were collected (NP40 or Triton soluble fractions) and pellets were boiled in 1x SDS-PAGE buffer.

Sucrose-gradient velocity sedimentation

RAW264.7 macrophages were treated for 3-4 hrs and lysates collected as in the necrosome formation assay. Samples were flash frozen, thawed, and nuclei were precipitated and discarded as in necrosome formation assay. Protein concentration normalized, and placed upon a 10-50% linear sucrose gradient. Samples were subject to velocity sedimentation at ~250,000g for 2.5-3 hours and samples were collected in 13-14 x 1 mL aliquots. Samples were subjected to Chloroform/Methanol protein precipitation to eliminate sucrose and/or concentrate protein samples prior resuspension in Laemmli buffer for Western Analysis.

Co-immunoprecipitation studies

RAW264.7 macrophages were treated for 3-4 hrs and lysates collected as in the necrosome formation assay. Samples were vortexed and incubated on ice prior to precipitating nuclei. Lysate protein concentration was normalized to 2mg/mL across samples and lysates were incubated overnight with Rabbit anti-RIPK1 or Rabbit anti-IKKε antibody. Antibody bound protein was

captured using Protein A-conjugated magnetic beads per sample (ThermoFisher Scientific, Pierce Protein A Magnetic Beads #88845) and eluted by boiling in 1x Laemmli buffer for 5 min.

RNA Sequencing

For RNA-Seq analysis, mice were divided intro 3 groups - control (n=2), LPS (n=2) and LPS/Nec-1s (n=2). Bone marrow cells were isolated by FACS as described for qPCR analysis. Total RNAs were isolated using Qiagen RNeasy kit according to the manufacturer's protocol. Input RNA samples were first analysis by Agilent BioAnalyzer 2100 to asset the integrity and quantity. The RNA samples were then amplified using NuGen Ovation RNA System V2. The resulting cDNA samples were fragmented on Covaris M220 Focused Solicitor, followed by purification and concentration with a Qiagen MiniElulte Spin Column. Following this step, S1 Nuclease (Promega) was used according to the manufacture's protocol. Then, the amplified and fragmented cDNA samples from RNA amplification was used as input for library preparation, using Illumina TruSeq DNA Sample Preparation Kit per the manufacturer's instruction. The resulted libraries were quantified and pooled at equal molar concentration for sequencing. The sequencing was done on a lane of High Output single read 100 bases on an Illumina HiSeq 2500 using SBS V3 chemistry. The base calling and demultiplexing was performed with CASAVA v1.8. The resulting data were then aligned to mouse mm10 reference genome with Tophat 2 and different gene expression analysis with Cuffdiff. Gene expression profiles were analyzed using Ingenuity pathway analysis (IPA) software to identify pathways regulated by LPS and Nec-1s.

http://www.ncbi.nlm.nih.gov/geo/query/acc.cgi?acc=GSE73836

Statistics

For *in vivo* studies, statistics were analyzed by two-tailed Student t-test and significance was determined using an alpha value of 0.05. Error bars reflect standard error (SE) from the mean. For

in vitro studies, experiments were repeated with at least 2, but in most cases 3 biological replicates. In each figure, one representative dataset is shown due to the variability in the general responsiveness to LPS in independent cell preparations. Error bars reflect standard deviation (SD) from the mean with measurements made in duplicate.

Chapter 4

Discussion

4.1 Summary

Data presented in the preceding chapters suggest a novel role for the catalytic functions of RIPK1 and RIPK3 in directing innate immune cytokine production by mechanisms distinct from their previously described roles in directing cell death. *In vivo* studies utilizing pharmacologic and genetic tools establish the kinase function of RIPK1 and RIPK3 as mediators of the cytokine profile induced by LPS. *In vitro*, this observation is examined closely using LPS in the context of caspase inhibition to delineate two novel TRIF-dependent signaling axes (Erk1/2-cFos/p65 and TBK1/IKKε-IRF3) that operate downstream of the 'necrosome' to promote synthesis of acute inflammatory cytokines (TNFα, IL6, CCL3, CCL4, CXCL1, and CXCL2) and IFNβ. This regulation likely manifests independent of necroptosis pathway as cytokine synthesis can be elicited in a RIPK1 kinase-dependent manner *in vivo* in the absence of MLKL. Similarly, *in vitro*, RIPK1 and RIPK3 kinase-dependent cytokine synthesis and necrosome formation occur in the absence of MLKL (Figure 1).

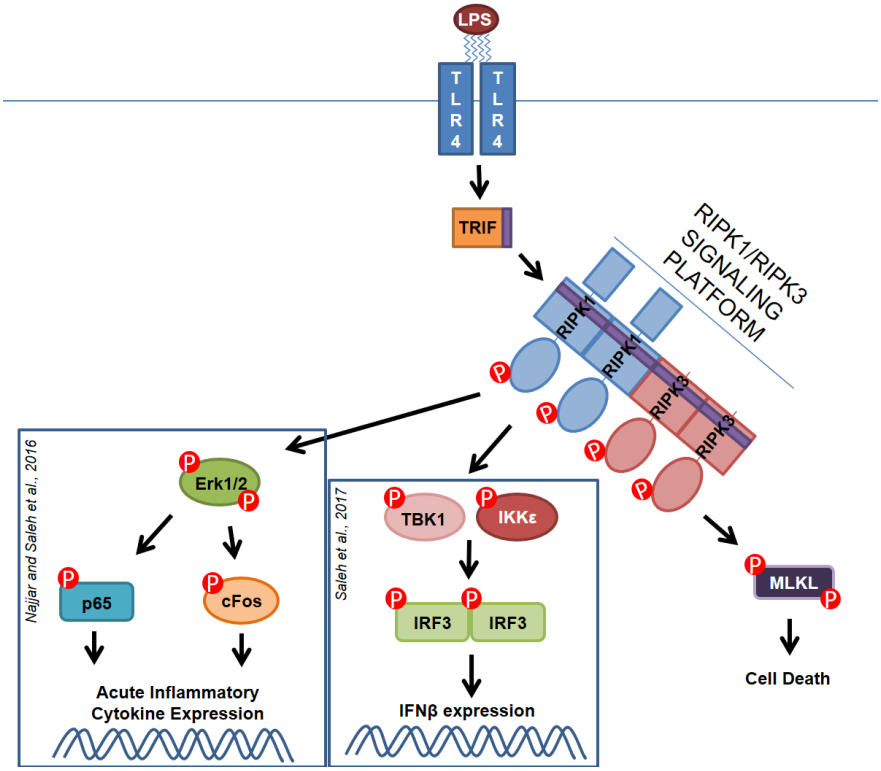

Figure 1. RIPK1 and RIPK3 kinase-dependent cytokine synthesis pathways.
*Figure Prepared by Danish Saleh

4.2 The RIPK1 and RIPK3 signaling platform

Intracellular molecular complexes by which RIPK1 and RIPK3 execute their regulation have long been characterized as detergent-insoluble, filamentous, amyloid-like, protein aggregates also termed

‘necrosomes’ (Li et al. 2012). In this description, the necrosome is defined by chemical and physical properties; however, the molecular composition of this signaling platform is poorly understood. In general, the ‘necrosome’ refers to the RIPK1 and RIPK3 signaling platform that engages downstream pathways, historically marked by the phosphorylation and activation of MLKL exclusively. Our work identifies additional putative downstream kinases, including Erk1/2 and TBK1/IKKε, as phosphorylation and activation of these molecules is mediated in a RIPK1 and RIPK3 kinase-dependent manner. We applied detergent-based cellular fractionation to examine detergent-insoluble cellular compartments to further delineate signaling associated with RIPK1 and RIPK3 kinase activation (Moquin et al. 2013; Ofengeim et al. 2015). Indeed, we observed that our putative targets (Erk1/2 and TBK1/IKKε) and their phosphorylated or activated forms, were enriched in detergent-insoluble cellular fractions in a RIPK1 and RIPK3 kinase-dependent manner. To verify these initial observations, we examined RIPK1 and RIPK3 signaling complexes applying different approaches, including velocity-sedimentation and sucrose-gradient fractionation as well as RIPK1 co-immunoprecipitation (Saleh and Degterev, *Unpublished*). The application of velocity-sedimentation and sucrose-gradient fractionation revealed that modified forms of RIPK1 and RIPK3 were enriched in molecular weight fractions alone with downstream signaling proteins (Erk1/2 (not shown), TBK1, IKKε, and IRF3) and this regulation manifested in a RIPK1 kinase-dependent manner. Co-immunoprecipitation studies also found that kinases Erk1/2, TBK1, and IKKε, specifically associated with RIPK1 in RIPK1 and RIPK3 activating conditions *in vitro*.

The physical organization, stoichiometry, and kinetics of the RIPK1 and RIPK3 signaling platform remain to be understood. Specifically, it is unclear if the term ‘necrosome’ identifies a single molecular complex that engages diverse downstream signaling axes independent of one another. Alternatively, the ‘necrosome’ might refer to a series of heterogeneous molecular complexes that share similar chemical and physical properties, attributable to a common RIPK1 and RIPK3 molecular core. According to this latter model, the capacity for RIPK1 and RIPK3 to promote pro-death versus cytokine synthesis pathways may be defined by upstream signaling and the immediate molecular environment. The latter is also supported

by studies demonstrating that homodimerization or oligomerization of RIPK3 is sufficient to induce cell death, whereas, Yatim et al. demonstrated that forced oligomerization of RIPK3 required RIPK1 in order to also promote NFκB-dependent cytokine production in $CD8^+$ T cells (Yatim et al. 2015; Wu et al. 2014). Similarly, over expression of RIPK1 in target cells can induce cell death that is either apoptotic or necroptotic – cellular processes that are likely defined by molecular target availability (Cook et al. 2014).

4.3 RIPK1 and RIPK3 kinase-dependent cytokine synthesis in bacterial infection

Preliminary attempts at examining this regulation in gram-negative bacterial infection models yielded promising results. RIPK1 and RIPK3 kinase-dependent IFNβ synthesis has reliably been elicited in *Yersinia* and/or *Klebsiella* infection of primary macrophages using the pan-caspase inhibitor zVAD. Notably, this induction of IFNβ was more pronounced by attenuated strains of these species, suggesting that the TRIF-RIPK1-RIPK3 signaling pathway might be a targeted and/or suppressed by gram-negative bacterial species to facilitate their pathogenesis. Moreover, these are not the only gram-negative bacterial species primed to disengage RIPK1 kinase-dependent signaling. Recent work has shown that *Porphorymonas gingivalis* directly cleaves RIPK1 kinase and thereby dampens TNFα-induced production of inflammatory cytokines (Barth & Genco 2016; Madrigal et al. 2012).

In vivo experiments using RIPK1 and RIPK3 kinase-inactive double knock-in mice, carrying targeted mutations rendering both kinases catalytically inactive, revealed that induction of circulating TNFα in mice infected with the attenuated capsular-deficient (*ΔcpsB*) of *Klebsiella* was regulated in a RIPK1 and RIPK3 kinase-dependent manner. By comparison, the wild-type strain (*Kp*) induced circulating TNFα to a lower level and this was not dependent on RIPK1 and RIPK3 kinases (Figure 2). These data are consistent with our hypothesis that RIPK1 and RIPK3 kinase-dependent cytokine synthesis might be selectively targeted or suppressed by pathogens in order to subvert the host-response and facilitate pathogenesis.

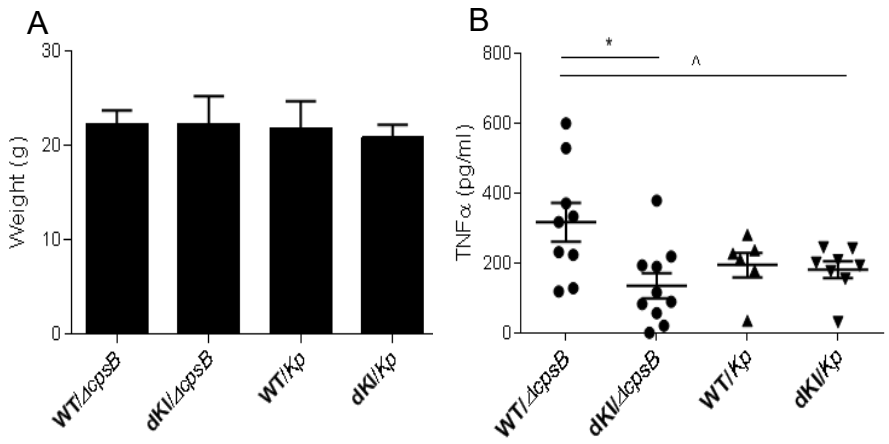

Figure 2. Attenuated Klebsiella pneumonia (ΔcpsB) induces circulating levels of TNFα in a manner that is dependent on kinase activities of RIPK1 and RIPK3 *in vivo*. (A) Body weights and (B) Circulating TNFα from wild-type (WT) and double kinase-inaction (dKI; K45A RIPK1 and K51A RIPK3 kinase inactive) mice infected with an attenuated mutant of *Klebsiella pneumonia (ΔcpsB)*, unable to produce an outer polysaccharide capsule virulence factor, or wild-type *Klebsiella pneumonia (Kp)*, with 10^7 colony forming units intraperitoneally. *signifies p<0.05 by 2-tailed student T-test. ^signifies p<0.05 by One-way ANOVA.
*Experiments performed, data analyzed, and figures prepared by Danish Saleh.

Nevertheless, we have failed to reliably observe RIPK1 and RIPK3 kinase-dependent acute inflammatory cytokine production (TNFα, IL6, CCL3, CCL4, CXCL1, CXCL2) in our *in vitro* infection models using *Yersinia* and/or *Klebsiella* (data not shown). This stands in marked contrast to our *in vitro* experiments performed using LPS. Specifically, it is peculiar that we observe acute inflammatory cytokine synthesis as well as IFNβ synthesis induced by LPS with zVAD *in vitro*, but only RIPK1 and RIPK3 kinase-dependent IFNβ synthesis can be detected upon infection with bacteria in the presence of zVAD. In reconciling this difference, one might consider that bacteria are complex organisms that engage and activate multiple pathogen-recognition patterns receptors during infection. From this vantage point, one might speculate that bacterial induced TRIF-dependent acute inflammatory cytokine synthesis is small compared to the aggregate of TRIF-independent cytokine production. Consider the relatively meager induction of TRIF-RIPK1-RIPK3 kinase dependent TNFα synthesis by LPS (~2-4 fold comparing LPS+zVAD to LPS alone) to the substantially more pronounced effect on IFNβ synthesis by the TRIF-RIPK1-RIPK3 kinase pathway (~100-1000-fold comparing LPS+zVAD to LPS alone). It follows that in the context of bacterial infection, where multiple TRIF-RIPK1-RIPK3 kinase-independent cytokine synthesis pathways are activated, the fold induction in RIPK1 and RIPK3 kinase-dependent IFNβ might still be appreciated whereas the induction of RIPK1 and RIPK3 kinase-dependent TNFα synthesis might be obscured.

4.4 RIPK1 and RIPK3 in Host Immunity

Emerging evidence presented throughout this thesis illuminate roles for RIPK1 and RIPK3 in fortifying host-immune responses against microbial pathogens. The introduction to this thesis included a literature review on the subject of RIPK1 and RIPK3 dependent cell death in host-immune cells to mitigate viral dissemination and promote host-survival during viral infection. Additionally, a summary of roles for RIPK1 and RIPK3 cell death in bacterial pathogenesis were also examined. And lastly, the introduction summarized evidence marking these kinases as important drivers of cytokine production and inflammation in kinase-independent pathways as well as kinase-dependent pathways.

Nevertheless, the roles of RIPK1 and RIPK3 in host-immunity may not exclusively be limited to cell death and inflammation of host-immune cells. Regulation of cell death and inflammation that is dependent on RIPK1 and RIPK3 have also been found to play critical roles in epithelial integrity and barrier function, an important first-line defense against microbial pathogens.

4.4.1 Epithelial Barrier Function[6]

The intestinal epithelia and skin are first line defenses against infection by commensal and pathogenic microbial flora (Kumar et al. 2010; Bonnet et al. 2011; Kaser et al. 2010; Macdonald & Monteleone 2005). Destruction of critical epithelial barriers predispose to microbial-induced infection and the generation of tissue-inflammation. The literature has illuminated crucial roles for RIPK1 and RIPK3 in maintaining barrier tissues. For example, kinase-independent function of RIPK1 has been found to be essential in preserving intestinal epithelial integrity and skin homeostasis. Conversely, kinase-activity of RIPK1 and activation of RIPK3-dependent necroptosis have been associated with epithelial tissue destruction. The following discussion explores these opposing roles of RIPK1 and RIPK3 in barrier tissue biology.

---

[6] Reprinted from *(Saleh and Degterev 2015, pages 17-22)* with permission from publisher.

4.4.1.1. Intestinal Epithelia

4.4.1.1.1 Kinase-independent functions of RIPK1

Two groups have reported roles for RIPK1 in maintaining epithelial integrity using independently generated mouse models of RIPK1 deletion in intestinal epithelial cells ($RIPK1^{IEC}$). Grossly, weight-loss and diminished survival was observed in mice lacking epithelial-specific RIPK1. Histological evaluation of gastrointestinal tissue revealed atypical cell death of intestinal epithelial cells, and features of inflammatory injury, including, leukocyte infiltration and abnormal tissue architecture (Dannappel et al. 2014; Takahashi et al. 2014).

Loss of RIPK1 in intestinal epithelia sensitized mice to microbial injury. Takahashi and colleagues reported that broad-spectrum antibiotic treatment prevented weight-loss and improved survival in animals. Antibiotics treatment also protected against cellular apoptosis in intestinal tissue as well as signs of local tissue and systemic inflammation, shortened colon length and splenic enlargement, respectively. Conversely, Dannappel and colleagues found antibiotic treatment was ineffective at reversing histological findings of cellular apoptosis; however, these differences may be attributed to variations in antibiotic regimens and treatment schedules.

RIPK1 deletion in intestinal epithelia was associated with increased sensitivity to inflammation-associated cell death. TNFα treatment resulted in increased apoptosis of $RIPK1^{IEC}$ organoids (Takahashi et al. 2014). In addition, deletion RIPK1 associated with increased death induced by innate immune ligand, polyinosinic:polycytidylic acid (Poly(I:C)), as well as the cytokines, interferon-β (IFNβ) and interferon-γ (IFNγ) (Kaiser et al. 2014; Dillon et al. 2014). Similarly, deletion of TNF Receptor ($Tnfr^{-/-}$) prolonged survival and ameliorated intestinal apoptosis in $RIPK1^{IEC}$ mice. Although Takahashi and colleagues appreciated improved survival in $RIPK1^{IEC}$ mice upon deletion of MYD88, a key adaptor in innate-immune inflammatory signaling and downstream of multiple Toll-like receptor family members, these findings could not be affirmed by Dannappel et al. Nevertheless, together, these observations

suggest that deletion of RIPK1 in intestinal epithelia increased tissue sensitivity to death by innate-immune signals and cytokines.

Whole-body RIPK1 deletion results in unbridled postnatal inflammation and lethality. Notably, embryonic development is unaffected by RIPK1 deletion, highlighting the importance of RIPK1 in post-embryonic life, when the body is exposed to a variety of external factors, in particular, skin and gut colonization by microbial flora (Takahashi et al. 2014; Dannappel et al. 2014; Polykratis et al. 2014; Berger et al. 2014).

The role for RIPK1 is not exclusively limited to early development as acute deletion of RIPK1 in intestinal epithelia of adult mice also resulted in rapid death associated with apoptosis of intestinal epithelia (Takahashi et al. 2014). Moreover, the protective role of RIPK1 in intestinal epithelia was credited to its kinase-independent function or scaffold function because mouse models of RIPK1 kinase-inactivation have normal survival and fail to exhibit pathologic features associated with RIPK1 deletion (Takahashi et al. 2014; Dannappel et al. 2014; Polykratis et al. 2014; Berger et al. 2014).

RIPK1 was previously thought to regulate pro-inflammatory and pro-survival signaling by regulation of downstream transcription factor NFκB (Cusson-Hermance et al. 2005; Meylan et al. 2004). However, counter to the dogma, Takahashi and Dannappel both reported that NFκB signaling was not impaired in $RIPK1^{IEC}$ epithelia. Specifically, inhibitor of kappa-B (IκB) degradation was unchanged in $RIPK1^{IEC}$ organoids stimulated with TNFα.

Epithelial cell death and inflammatory sequelae were attributed to caspase-8 and FADD-dependent apoptosis and or RIPK3-dependent necroptosis. These insights were gleaned using intestinal epithelia specific knock-outs of caspase-8 ($Casp8^{IEC}$) or FADD ($FADD^{IEC}$) and RIPK3 deletion mutant mice in conjunction with $RIPK1^{IEC}$ mice. Caspase-8^{IEC}/$RIPK1^{IEC}$ mice were completely protected against early lethality and histological features of intestinal pathology (Takahashi et al. 2014). By comparison, $FADD^{IEC}$/$RIPK1^{IEC}$ mice has increased cleaved-caspase 3 negative dying cells and exhibited altered

intestinal pathology that resembled necroptotic intestinal disease observed in FADD^{IEC} mice (Dannappel et al. 2014). RIPK1^{IEC} /*Ripk3*$^{-/-}$ were also not protected from inflammatory changes in the intestinal tissue and had diminished survival. Nevertheless, inflammatory histopathology and survival were completely rescued in RIPK1^{IEC}/FADD^{IEC}/*Ripk3*$^{-/-}$ indicating that both FADD (apoptosis) and RIPK3 (necroptosis) were important for pathologic changes in the tissue in the absence of RIPK1 (Dannappel et al. 2014).

Dannappel and colleagues also suggested that RIPK1 maintained intestinal epithelial integrity by preserving the pro-survival or anti-apoptotic proteins, cIAP1, TRAF-2, and c-FLIP. In MEFs, TNFα stimulation resulted in rapid degradation of cIAP1, TRAF-2, and c-FLIP in RIPK1 knockout (*Ripk1*$^{-/-}$) but not RIPK1 kinase-inactive cells. Moreover, tamoxifen-induced deletion of RIPK1 in organoid cultures was associated with reduced expression of these anti-apoptotic proteins and rapid organoid death (Dannappel et al. 2014).

4.4.1.1.2. Kinase-dependent regulation by RIPK1 and the role of RIPK3

Loss of caspase-8 or death-receptor adaptor protein, Fas-associated death domain (FADD), has been shown to sensitize cells to necroptotic cell death (Zhang et al. 2009; He et al. 2009; Osborn et al. 2010; Vandenabeele, Galluzzi, et al. 2010; Kim & Li 2013). Several groups analyzed the consequences of genetic deletion of these factors on the integrity of the intestinal epithelium.

In 2011, Welz et al. reported that RIPK3 was required for intestinal-epithelial cell loss and intestinal disease in FADD^{IEC} mice which exhibited diminished survival, reduced weight, and diarrhea (Welz et al. 2011). Evaluation of gastrointestinal tissue revealed necrotic loss of intestinal epithelia or enterocytes, enteric and colonic inflammation, and destruction of antimicrobial Paneth cells of crypts found in the small intestine. Conspicuously, FADD^{IEC}/*Ripk3*$^{-/-}$ mice developed normally and were protected from intestinal epithelial cell loss, Paneth cell loss, and signs of inflammation, affirming an important role for RIPK3-dependent intestinal epithelial cell loss in the generation of gastrointestinal inflammatory disease (Welz et al. 2011). Moreover, the same group also observed that intestinal-epithelial inactivation of

CYLD, a cellular deubiquitinase reported to promote RIPK1 and RIPK3-dependent necroptosis, protected animals from developing gastrointestinal inflammation (Moquin et al. 2013). Significantly, antibiotic treatment, germ-free rearing, or concomitant deletion of MYD88 or TNF, ameliorated or abolished signs of intestinal inflammatory disease, emphasizing the importance of gut flora and innate immune responses in the development of gastrointestinal disease upon loss of intestinal epithelia (Welz et al. 2011). Collectively, these observations suggest that activation of RIPK3-dependent necroptosis may promote intestinal epithelial cell loss and bacterial-associated gastrointestinal inflammation.

RIPK3-dependent intestinal tissue damage was also observed upon the genetic deletion of caspase-8. Weinlich and colleagues administered oral tamoxifen gavage to Rosa-CRE expressing mice that were crossed to Caspase-8 floxed ($Casp8^{fl/fl}$) mice to generate mice lacking caspase-8 in adult gastrointestinal tissue ($Casp8^{GI}$) (Weinlich et al. 2013). In an alternative approach, Günther and colleagues generated mice lacking caspase-8 in intestinal epithelial cells ($Casp8^{IEC}$) by breeding $Casp8^{fl/fl}$ mice with mice expressing CRE-recombinase under the regulation of intestinal epithelial-specific villin promoter.

Acute deletion of caspase-8 in $Casp8^{GI}$ mice treated with tamoxifen promoted rapid weight-loss and diminished survival (Weinlich et al. 2013). These mice also manifested with histological features of intestinal inflammation, marked by cell death of enterocytes, tissue inflammation, and infiltration of immune cells. Importantly, concomitant deletion of RIPK3 protected mice from intestinal disease noted in $Casp8^{GI}$ mice. $Casp8^{GI}$/*Ripk3*$^{-/-}$ mice maintained body weight, had normal survival, fewer dying enterocytes, and intact gastrointestinal tissue architecture, indicating that intestinal damage was likely a consequence of RIPK3-dependent enterocyte death in $Casp8^{GI}$ mice (Weinlich et al. 2013). Similarly, $Casp8^{IEC}$ mice were found to have spontaneous inflammatory lesions in the terminal ileum, marked by bowel wall thickening, loss of intestinal crypts, and increased cellularity, suggesting immune cell infiltration. Notably, $Casp8^{IEC}$ mice had increased epithelial cell death associated with necrotic features. The authors also observed loss of specialized epithelial cells, specifically goblet and Paneth cells, which protect enteric epithelia and aid immunity by producing mucus and secreting antimicrobial peptides,

respectively (Günther et al. 2011). Not surprisingly, intestinal epithelia of these mice had increased sensitivity to TNFα-induced necroptosis. Intravenous TNFα resulted in high lethality associated with severe destruction of the small-bowel and an increased number of dying epithelial cells that were negative for cleaved caspase-3. Significantly, inhibition of RIPK1 kinase-dependent cell death using Nec-1 blocked TNFα-induced lethality and destruction of the small bowel (Günther et al. 2011).

Together, these studies demonstrate that activation of necroptosis in intestinal epithelia leads to loss of intestinal barrier integrity and induction of tissue inflammation. These phenotypes may be associated with commensal bacterial-induced innate immune responses. The data also suggest that inappropriate activation of RIPK3-dependent signaling in human intestinal epithelia may be linked to chronic inflammatory diseases of the bowel, namely, Crohn's disease. Immunohistochemical analysis of tissue samples from human patients revealed increased RIPK3 expression in Paneth cells of the distal small bowel. Diseased tissue specimens also had decreased numbers of Paneth cells and increased Paneth cell death with necrotic features as determined by electron microscopy. Moreover, Paneth cells from the tissue biopsies of the patients with Crohn's disease were susceptible to TNFα-induced cell death that could be blocked with Nec-1 (Günther et al. 2011). These data suggest that aberrant activation of necroptosis and subsequent loss of barrier function may be an important factor underlying chronic inflammation in the gut.

4.4.1.2. Skin

4.4.1.2.1. Kinase-independent functions of RIPK1

Similar to the intestinal epithelia, RIPK1 in keratinocytes and epidermal tissue is important for homeostasis of the skin. RIPK1 deficient primary keratinocytes have increased susceptibility to TNFα-induced apoptosis; however, injury *in vivo* appears entirely dependent on necroptosis as RIPK3 deletion protects against pathological features of skin inflammation. Moreover, ablation of RIPK1 in epithelia ($RIPK1^{E}$) results in a pro-inflammatory phenotype with increased epidermal thickness and inflammation

(Dannappel et al. 2014). Localized inflammation of the skin may disrupt integrity of the organ, thereby increasing susceptibility to infection and exacerbating inflammatory pathology. This theory is supported by the observation that RIPK1^{E} mice also lacking the Toll-like receptor adaptor protein, TRIF, were partially protected from inflammatory injury of the skin, likely due to decreased activation of innate-immune pathways by microbial flora (Dannappel et al. 2014). Additionally, much of the inflammatory injury observed in epithelial deletion of RIPK1 may be attributed to increased sensitivity to TNFα signaling similar to observations made in the intestinal epithelia. RIPK1^{E}/*Tnfr*$^{-/-}$ mice are protected from inflammation of the skin, including epidermal thickness (Dannappel et al. 2014). Analogous to observations made in intestinal epithelia, anti-apoptotic ubiquitin-ligase, cIAP1, is rapidly diminished following TNFα exposure to RIPK1^{E} to primary keratinocytes (Dannappel et al. 2014). Lastly, inflammatory phenotypes associated with RIPK1 deletion in the epithelia appear to be independent of kinase-activity of RIPK1 as kinase-inactive models of RIPK1 have not been found to manifest with spontaneous inflammation of the skin (Berger et al. 2014; Polykratis et al. 2014).

4.4.1.2.2. The role of RIPK3

Deletion of FADD in epidermal keratinocytes resulted in development of RIPK3-dependent skin lesions and early death (Bonnet et al. 2011). Histologically, these mice displayed patchy pathologic skin signs, marked by epidermal hyperplasia and thickening, keratinocyte death, and immune cell accumulation. Importantly, keratinocyte death appeared to be caspase-independent, as a large fraction of dying keratinocytes did not contain active caspase-3 but showed necrotic morphology by electron microscopy. Similar to FADD deficiency in intestinal epithelium, FADD^{E}/*Ripk3*$^{-/-}$ mice neither exhibited early lethality nor developed skin lesions during development and into adulthood. In fact, FADD^{E}/*Ripk3*$^{-/-}$ mice had normal skin, with normal epidermal thickness and an absence of dying keratinocytes and pathologic inflammatory infiltrates, indicating that inflammatory disease observed in FADD^{E} mice was dependent on RIPK3-mediated cell death. Concordantly, FADD^{E} mice with concomitant deletion of TNFα-receptor, MYD88, or an inactivating mutation of CYLD, had delayed onset of inflammatory skin lesions, stressing

that compromise of barrier function and microbial-associated innate-immune activation may be responsible for the disease pathogenesis (Bonnet et al. 2011).

Constitutive loss caspase-8 in epidermal keratinocytes produced an inflammatory skin disorder with epidermal hyperplasia, dermal inflammatory cell infiltration, and premature lethality in mice (Kovalenko et al. 2009). These findings were corroborated by studies in which acute deletion of caspase-8 in adult murine skin by application 4-hydroxytamoxifen to Rosa-CRE, $Casp8^{fl/fl}$ mice, resulted in local tissue inflammation and damage (Welz et al. 2011). Importantly, 4-hydroxytamoxofen treatment of Rosa-CRE, $Casp8^{fl/fl}$, $Ripk3^{-/-}$ mice resulted in minimal dermal inflammation, epidermal hyperplasia, and keratinocyte death (Welz et al. 2011). In accord, it becomes apparent that RIPK3-dependent signaling promoted skin inflammation and injury upon deletion of caspase-8 in epidermal tissue. The role of RIPK1 has not been specifically established in these studies; however, it might be hypothesized that RIPK1 kinase activity may be important as an inducer of RIPK3-dependent cell death.

4.4.1.3. Summary of Roles of RIPK1 and RIPK3 in epithelial barrier function

Loss of essential barrier cells lends the organism to infection by commensal microbiological flora, tissue injury, and diminished survival. The studies described above highlight an important role for kinase-independent function of RIPK1 in maintaining epithelial homeostasis of the intestinal tract as well as in the skin. RIPK1 serves this function by two apparent means that may be fundamentally intertwined. First off, the presence of RIPK1 directly prevents uncontrolled activation of caspase 8-FADD associated apoptosis and RIPK3-dependent necroptosis at the epithelial surface. Secondly, RIPK1 promotes a survival-like state in the presence of pro-inflammatory and pro-injury signals such as TNFα, IFNβ, and other ligands associated with infection. Indeed, dual roles of RIPK1 in both activating and inhibiting necroptotic cell death has been described in the literature (Kearney et al. 2014; Orozco et al. 2014). Furthermore, evidence reported here also demonstrates that aberrant or inappropriate activation of necroptosis, driven by RIPK1-kinase function or RIPK3, can result in loss of barrier function in the skin

and intestinal epithelia. Deletion of caspase-8 or FADD in barrier tissue sensitizes cells to necrotic death and chronic inflammatory disease that may be attributed to microbial activation of the innate immune host-response.

4.5. Significance and Future Directions

Initial interest in pathophysiologic roles for RIPK1 and RIPK3 stemmed from the close association of cell death with inflammation in disease. Available evidence defines critical roles for these proteins in driving inflammation associated pathology in a variety of disease models, including dermatitis, colitis, multiple sclerosis, amylotropic lateral sclerosis (ALS), ischemia-reperfusion injury, neoplastic disease, stroke, cortical injury, and many others (Linkermann & Green 2014; Ito et al. 2016; Ofengeim et al. 2015; Kovalenko et al. 2009; Lukens et al. 2013; Degterev et al. 2005; You et al. 2008; Günther et al. 2011; Seifert et al. 2016). Although the novelty of the work presented in this thesis is contextualized as a physiologic process that manifests as a feature of the host-response against invading pathogens, the precedent of cell-death independent cytokine production by RIPK1 and RIPK3 and associated mechanisms have implications for the understanding of these two kinases in clinical pathophysiology as well. For example, RIPK1 and RIPK3 necrosome formation and necroptosis in a model of pancreatic ductal adenocarcinoma (PDA) is associated with CXCL1 expression that promotes an immuno-suppressive tumor environment (Seifert et al. 2016). Evidence presented here suggests that necrosome-associated CXCL1 expression may be selectively targeted and separated, therapeutically, from RIPK1 and RIPK3 kinase-dependent necroptosis, to minimize tumor-suppressive processes and control tumor growth by cell death processes for the management of PDA. Inhibitors of Erk1/2 pathway might be an appropriate tool to diminish production of CXCL1 while leaving cell death regulation unperturbed. In another example, RIPK1 kinase-dependent necroptosis has also been reported in models of ischemic injury and stroke (Degterev et al. 2005; Kaczmarek et al. 2013). Controlling the loss of cellular mass is an important goal in the management of ischemic disease to preserve tissue function. However, cytokine production and pro-inflammatory ligands released from damaged cells may be important in resolving

tissue loss and promoting tissue repair in a timely manner. With our expanded understanding of necroptosis and RIPK1 and RIPK3 kinase-dependent cytokine production, in lieu of targeting RIPK1 and RIPK3 directly to control limit necrotic injury, one might propose therapeutic regimens that block death signaling downstream of RIPK1 and RIPK3 (ie: MLKL), to preserve pro-inflammatory signaling driven by these proteins during injury.

The current dogma professes that cell death or necroptosis associated inflammation stems from the release of intracellular DAMPs that activate inflammatory cells and promote tissue infiltration (Kaczmarek et al. 2013). However, this model fails to consider the possibility of cell-intrinsic cytokine production by cell death machinery in driving inflammation and ultimately cell death. For example, this thesis describes a cell autonomous axis by which RIPK1 and RIPK3 kinases drive the production of TNFα, a pro-inflammatory cytokine well-described as a driver of apoptosis and/or necroptosis in target cells. This raises an interesting question of whether inflammation is preceding and driving cell death or whether cell death is the underlying pathologic factor. We can examine this possibility by considering Multiple Sclerosis, a chronic inflammatory disease of the central nervous system (CNS) that has been associated with upregulation of RIPK1 and RIPK3 as well has hyperactivation of necroptosis (Ofengeim & Yuan 2013). Examination of disease progression in mouse models of CNS inflammation have demonstrated that inhibition of RIPK1 or ablation of RIPK3 serve to attenuate pathology and cell death. Additionally, it is worth noting that treatment of mice with Nec-1s prior to clinical disease onset conferred greater benefit over the disease course than late treatment (Ofengeim et al. 2015). Accordingly, one might be compelled to inquire whether early disease is marked by subclinical inflammation that may be driven RIPK1 and RIPK3 prior to the induction of tissue injury, death, and clinical disease onset. Indeed, a similar hypothesis has been proposed to account for disease progression in Alzheimer's disease, another degenerative disease of the central nervous system that manifests with cell death and inflammation (Vom Berg et al. 2012). In a second example, You et al., report that Nec-1 attenuates neuronal cell death and inflammation following controlled cortical impact. Here, administration of Nec-1 also serves to confer a

functional benefit in memory as mice perform better in the Morris Water Maze test with Nec-1. In this model, as others, it remains to be determined how and to what extent pro-inflammatory cytokine expression, independent of RIPK1 kinase-dependent cell death, contributes to tissue injury and long-term behavioral outcomes (You et al. 2008). Our findings suggest that inflammation ought to be examined more closely as RIPK1 kinase-dependent cytokine production exacerbates cell death in the brain in this injury model.

In addition to reporting a new role for the catalytic functions of RIPK1 and RIPK3, this work provides a summary of the available literature highlighting roles for RIPK1 and RIPK3 in regulating inflammatory pathways in response to cytokine signals, innate immune ligands, and microbial species. Similar to the inquiry of roles of RIPK1 and RIPK3 kinases in the pathophysiology of disease discussed above, it remains to be understood how cell-autonomous RIPK1 and RIPK3 kinase-dependent cytokine synthesis pathways influence infection models and the host-response to microbial pathogens, independent of their roles in cell death. To date, many of the available studies fail to employ the appropriate tools to discriminate cell-death dependent processes from those that are cell-death independent. Understandably, scientists may shy away from these ventures because of the specter of underlying cell death in experimental models and the clearly established pro-inflammatory nature of cell death processes; however, these confounding factors can be addressed experimentally. For example, evaluating RIPK1 and RIPK3 dependent inflammation on a *Mlkl*$^{-/-}$ background may provide interesting insights into necroptosis-independent functions of RIPK1 and RIPK3. Alternatively, infection-associated RIPK1 and RIPK3 activity may be evaluated in models of cytokine depletion and inflammatory attenuation. Indeed, efforts are underway to discriminate RIPK1 and RIPK3 dependent inflammation from cell death (Kang et al. 2014). Importantly, it is necessary to recognize that these answers will be important in ultimately addressing the significance of RIPK1 and RIPK3 kinase-dependent inflammation in the host-response. Moreover, as described above for other pathophysiologic states, this knowledge will inform management strategies for patients being treated for infections ranging in severity from mild-acute cases to chronic

infection and sepsis. For example, from a therapeutic standpoint, it might seem worthwhile to permit RIPK1 and RIPK3 kinase-dependent cytokine synthesis while impeding RIPK1 and RIPK3 kinase-dependent cell death in innate immune cells to expedite the clearance of certain infections.

4.6. TRIF-RIPK1-RIPK3 axis as a therapeutic target in infection

Emerging roles of RIPK1 and RIPK3 kinases in innate immunity need to be considered when evaluating the therapeutic potential of these targets. Certainly, involvement of RIPK1 and RIPK3 in response to pathogens *per se* should enhance enthusiasm for developing therapeutic strategies which target RIPK1 and RIPK3 signaling. While our data suggests that RIPK1 and RIPK3 might regulate the robustness of innate immune responses, it is unclear whether inhibition of this axis may truly change the outcome of infection as opposed to just changing the kinetics of cell death and, ultimately, the death of the organism. Theoretically, the TRIF-RIPK1-RIPK3 signaling axis may be engaged by pharmacologic tools for the purposes of enhancing host-responses and aiding in the resolution of infection. This may be employed prophylactically by using ligands that activate TRIF-dependent pathways specifically, such as Poly(I:C) or RIPK1 and RIPK3 activators such as SMAC-mimetics. On the other hand, in cases of patients with acute-bacterial infection who are at risk for sepsis, when cell death and inflammation are the reason for high mortality, these pathways may be pharmacologically dampened to transiently attenuate the intensity of the host-responses, thereby, improving patient outcomes. This strategy may be particularly useful when alternative therapeutic options, such as antibiotics, are available to ultimately eradicate pathogens. Needless to say, before these therapeutic strategies can be examined in earnest, precedents clearly demonstrating the importance of RIPK1 and RIPK3 kinase-dependent inflammation in microbial infection will be required.

Chapter 5

Bibliography

Albrecht, M.E., 2014. Epidemiology, clinical manifestations, and diagnosis of genital herpes simplex virus infection. *Uptodate*. Available at: http://www.uptodate.com/contents/epidemiology-clinical-manifestations-and-diagnosis-of-genital-herpes-simplex-virus-infection?source=search_result&search=HSV-2&selectedTitle=1~68.

Alpuche-aranda, B.C.M. et al., 1994. Stimulate Macrophage Macropinocytosis and Persist within Spacious Phagosomes By Celia M. Alpuche-Aranda,* Esther L. gacoosin,~ Joel A. Swanson,~ and Samuel I. Miller*. , 179(February).

Autheman, D. et al., 2013. Clostridium perfringens beta-toxin induces necrostatin-inhibitable, calpain-dependent necrosis in primary porcine endothelial cells. *PloS one*, 8(5), p.e64644. Available at: http://www.pubmedcentral.nih.gov/articlerender.fcgi?artid=3667183&tool=pmcentrez&rendertype=abstract [Accessed April 24, 2015].

Barth, K. & Genco, C.A., 2016. Microbial Degradation of Cellular Kinases Impairs Innate Immune Signaling and Paracrine TNFα Responses. *Scientific reports*, 6(October), p.34656. Available at: http://www.ncbi.nlm.nih.gov/pubmed/27698456.

Behnsen, J. et al., 2015. Exploiting host immunity: the Salmonella paradigm. *Trends in Immunology*, 36(2), pp.112–120. Available at: http://linkinghub.elsevier.com/retrieve/pii/S1471490614002282 [Accessed January 12, 2015].

Vom Berg, J. et al., 2012. Inhibition of IL-12/IL-23 signaling reduces Alzheimer's disease-like pathology and cognitive decline. *Nature medicine*, 18(12), pp.1812–9. Available at: http://www.nature.com/nm/journal/v18/n12/full/nm.2965.html%5Cnhttp://www.nature.com/nm/journal/v18/n12/pdf/nm.2965.pdf%5Cnhttp://www.ncbi.nlm.nih.gov/pubmed/23178247.

Berger, A.K. & Danthi, P., 2013. Reovirus activates a caspase-independent cell death pathway. *mBio*, 4(3), pp.e00178-13. Available at: http://www.pubmedcentral.nih.gov/articlerender.fcgi?artid=3656442&tool=pmcentrez&rendertype=abstract [Accessed April 24, 2015].

Berger, S.B. et al., 2014. Cutting Edge: RIP1 Kinase Activity Is Dispensable for Normal Development but Is a Key Regulator of Inflammation in SHARPIN-Deficient Mice. *Journal of immunology (Baltimore, Md. : 1950)*. Available at: http://www.ncbi.nlm.nih.gov/pubmed/24821972 [Accessed May 28, 2014].

Vanden Berghe, T. et al., 2010. Necroptosis, necrosis and secondary necrosis converge on similar cellular disintegration features. *Cell death and differentiation*, 17(6), pp.922–930. Available at: http://dx.doi.org/10.1038/cdd.2009.184%5Cnhttp://www.ncbi.nlm.nih.gov/pubmed/20010783%5Cnhttp://www.nature.com/cdd/journal/v17/n6/pdf/cdd2009184a.pdf.

Vanden Berghe, T. et al., 2014. Regulated necrosis: the expanding network of non-apoptotic cell death pathways. *Nature reviews. Molecular cell biology*, 15(2), pp.135–47. Available at: http://www.ncbi.nlm.nih.gov/pubmed/24452471 [Accessed July 9, 2014].

Bertin, J. et al., 1997. Death effector domain-containing herpesvirus and poxvirus proteins inhibit both Fas- and TNFR1-induced apoptosis. *Proceedings of the National Academy of Sciences*, 94(February), pp.1172–1176.

Best, S.M., 2008. NIH Public Access. , pp.171–192.

Birnbaum, M.J., Clem, R.J. & Miller, L.K., 1994. An Apoptosis-Inhibiting Gene from a Nuclear Polyhedrosis Virus Encoding a Polypeptide with Cys / His Sequence Motifs. , 68(4), pp.2521–2528.

Bischofberger, M., Iacovache, I. & van der Goot, F.G., 2012. Pathogenic pore-forming proteins: function and host response. *Cell host & microbe*, 12(3), pp.266–75. Available at: http://www.ncbi.nlm.nih.gov/pubmed/22980324 [Accessed February 22, 2015].

Biton, S. & Ashkenazi, A., 2011. NEMO and RIP1 control cell fate in response to extensive DNA damage via TNF-α feedforward signaling. *Cell*, 145(1), pp.92–103. Available at: http://www.ncbi.nlm.nih.gov/pubmed/21458669 [Accessed January 29, 2014].

Bliska, J.B., 2003. The Ability To Replicate in Macrophages Is Conserved between Yersinia pestis and Yersinia pseudotuberculosis. , 71(10), pp.5892–5899.

Bonnet, M.C. et al., 2011. The adaptor protein FADD protects epidermal keratinocytes from necroptosis in vivo and prevents skin inflammation. *Immunity*, 35(4), pp.572–82. Available at: http://www.ncbi.nlm.nih.gov/pubmed/22000287 [Accessed May 10, 2015].

Boyden, E.D. & Dietrich, W.F., 2006. Nalp1b controls mouse macrophage susceptibility to anthrax lethal toxin. *Nature genetics*, 38(2), pp.240–4. Available at: http://www.ncbi.nlm.nih.gov/pubmed/16429160 [Accessed April 24, 2015].

Brumatti, G. et al., 2016. The caspase-8 inhibitor emricasan combines with the SMAC mimetic birinapant to induce necroptosis and treat acute myeloid leukemia. , 8(339), pp.1–12.

Cai, S. et al., 2009. Both TRIF- and MyD88-dependent signaling contribute to host defense against pulmonary Klebsiella infection. *Journal of immunology (Baltimore, Md. : 1950)*, 183(10), pp.6629–38. Available at: http://www.pubmedcentral.nih.gov/articlerender.fcgi?artid=2777750&tool=pmcentrez&rendertype=abstract [Accessed October 26, 2014].

Cai, Z. et al., 2014. Plasma membrane translocation of trimerized MLKL protein is required for TNF-induced necroptosis. *Nature cell biology*, 16(1), pp.55–65. Available at: http://www.ncbi.nlm.nih.gov/pubmed/24316671 [Accessed April 25, 2015].

Chen, R. et al., 1996. Phosphorylation of c-Fos at the C-terminus enhances its transforming activity. *Oncogene*, 12(7), pp.1493–502.

Chen, W. et al., 2013. Diverse sequence determinants control human and mouse receptor interacting protein 3 (RIP3) and mixed lineage kinase domain-like (MLKL) interaction in necroptotic signaling. *Journal of Biological Chemistry*, 288(23), pp.16247–16261.

Chen, X. et al., 2014. Translocation of mixed lineage kinase domain-like protein to plasma membrane leads to necrotic cell death. *Cell research*, 24(1), pp.105–21. Available at: http://www.pubmedcentral.nih.gov/articlerender.fcgi?artid=3879712&tool=pmcentrez&ren

dertype=abstract.

Cho, Y. et al., 2010. NIH Public Access. , 137(6), pp.1112–1123.

Cho, Y.S. et al., 2009. Phosphorylation-Driven Assembly of the RIP1-RIP3 Complex Regulates Programmed Necrosis and Virus-Induced Inflammation. *Cell*, 137(6), pp.1112–1123. Available at: http://dx.doi.org/10.1016/j.cell.2009.05.037.

Christofferson, D.E. et al., 2012. A novel role for RIP1 kinase in mediating TNFα production. *Cell death & disease*, 3, p.e320. Available at: http://www.pubmedcentral.nih.gov/articlerender.fcgi?artid=3388236&tool=pmcentrez&rendertype=abstract [Accessed March 26, 2014].

Christofferson, D.E., Li, Y. & Yuan, J., 2014. Control of Life-or-Death Decisions by RIP1 Kinase. *Annual review of physiology*, 76(September), pp.129–50. Available at: http://www.ncbi.nlm.nih.gov/pubmed/24079414 [Accessed February 17, 2014].

Christofferson, D.E. & Yuan, J., 2010. Necroptosis as an alternative form of programmed cell death. *Current opinion in cell biology*, 22(2), pp.263–8. Available at: http://www.pubmedcentral.nih.gov/articlerender.fcgi?artid=2854308&tool=pmcentrez&rendertype=abstract [Accessed January 20, 2015].

Clark, K. et al., 2011. Novel cross-talk within the IKK family controls innate immunity. *The Biochemical journal*, 434(1), pp.93–104. Available at: http://www.ncbi.nlm.nih.gov/pubmed/21138416 [Accessed March 26, 2014].

Clark, K. et al., 2009. Use of the pharmacological inhibitor BX795 to study the regulation and physiological roles of TBK1 and IκB Kinase ∈:A distinct upstream kinase mediates ser-172 phosphorylation and activation. *Journal of Biological Chemistry*, 284(21), pp.14136–14146.

Clarke, P. et al., 2003. Two distinct phases of virus-induced nuclear factor kappa B regulation enhance tumor necrosis factor-related apoptosis-inducing ligand-mediated apoptosis in virus-infected cells. *The Journal of biological chemistry*, 278(20), pp.18092–100. Available at: http://www.ncbi.nlm.nih.gov/pubmed/12637521 [Accessed April 24, 2015].

Cook, W.D. et al., 2014. RIPK1- and RIPK3-induced cell death mode is determined by target availability. *Cell death and differentiation*, pp.1–13. Available at: http://www.ncbi.nlm.nih.gov/pubmed/24902899 [Accessed June 7, 2014].

Craven, R.R. et al., 2009. Staphylococcus aureus alpha-hemolysin activates the NLRP3-inflammasome in human and mouse monocytic cells. *PloS one*, 4(10), p.e7446. Available at: http://www.pubmedcentral.nih.gov/articlerender.fcgi?artid=2758589&tool=pmcentrez&rendertype=abstract [Accessed April 24, 2015].

Crook, N.E., Clem, R.J. & Miller, L.K., 1993. An Apoptosis-Inhibiting Baculovirus Gene with a Zinc Finger-Like Motif. , 67(4), pp.2168–2174.

Cuda, C.M. et al., 2014. Caspase-8 Acts as a Molecular Rheostat To Limit RIPK1- and MyD88-Mediated Dendritic Cell Activation. *Journal of immunology (Baltimore, Md. : 1950)*. Available at: http://www.ncbi.nlm.nih.gov/pubmed/24808358 [Accessed June 1, 2014].

Cusson-Hermance, N. et al., 2005. Rip1 mediates the Trif-dependent toll-like receptor 3- and 4-induced NF-{kappa}B activation but does not contribute to interferon regulatory factor 3 activation. *The Journal of biological chemistry*, 280(44), pp.36560–6. Available at: http://www.ncbi.nlm.nih.gov/pubmed/16115877 [Accessed February 24, 2014].

Dannappel, M. et al., 2014. RIPK1 maintains epithelial homeostasis by inhibiting apoptosis and necroptosis. *Nature*, 513(7516), pp.90–94. Available at: http://dx.doi.org/10.1038/nature13608.

Danthi, P. et al., 2013. CHAPTER 3 REOVIRUS RECEPTORS , CELL ENTRY , AND PROAPOPTOTIC SIGNALING. , pp.42–71.

Davis, A.J., Díaz, D. a D.J. & Mecsas, J., 2010. A dominant-negative needle mutant blocks type III secretion of early but not late substrates in Yersinia. *Molecular microbiology*, 76(1), pp.236–59. Available at: http://www.pubmedcentral.nih.gov/articlerender.fcgi?artid=2911021&tool=pmcentrez&rendertype=abstract [Accessed December 2, 2014].

Davis, A.J. & Mecsas, J., 2007. Mutations in the Yersinia pseudotuberculosis type III secretion system needle protein, YscF, that specifically abrogate effector translocation into host cells. *Journal of Bacteriology*, 189(1), pp.83–97.

Degterev, A. et al., 2005. Chemical inhibitor of nonapoptotic cell death with therapeutic potential for ischemic brain injury. *Nature chemical biology*, 1(2), pp.112–9. Available at: http://www.ncbi.nlm.nih.gov/pubmed/16408008 [Accessed March 23, 2014].

Degterev, A. et al., 2008. Identification of RIP1 kinase as a specific cellular target of necrostatins. *Nature chemical biology*, 4(5), pp.313–21. Available at: http://www.ncbi.nlm.nih.gov/pubmed/18408713 [Accessed March 26, 2014].

Degterev, A., Maki, J.L. & Yuan, J., 2013. Activity and specificity of necrostatin-1, small-molecule inhibitor of RIP1 kinase. *Cell death and differentiation*, 20(2), p.366. Available at: http://www.pubmedcentral.nih.gov/articlerender.fcgi?artid=3554332&tool=pmcentrez&rendertype=abstract [Accessed March 26, 2014].

Demmler-Harrison, G.J., 2015. Congenital cytomegalovirus infection: Clinical features and diagnosis. *Uptodate*. Available at: http://www.uptodate.com/contents/congenital-cytomegalovirus-infection-clinical-features-and-diagnosis?source=search_result&search=cmv&selectedTitle=2~150.

Deveraux, Q.L. & Reed, J.C., 1999. REVIEW IAP family proteins — suppressors of apoptosis. , pp.239–252.

Dickens, L.S. et al., 2012. The “complexities” of life and death: Death receptor signalling platforms. *Experimental Cell Research*, 318(11), pp.1269–1277. Available at: http://dx.doi.org/10.1016/j.yexcr.2012.04.005.

Dillon, C.P. et al., 2014. RIPK1 Blocks Early Postnatal Lethality Mediated by Caspase-8 and RIPK3. *Cell*, 157(5), pp.1189–1202. Available at: http://www.ncbi.nlm.nih.gov/pubmed/24813850 [Accessed May 23, 2014].

DJ, G. & Weller, S., 1988. Factor(s) present in herpes simplex virus type 1-infected cells can

compensate for the loss of the large subunit of the viral ribonucleotide reductase: characterization of an ICP6 deletion mutant. *Virology*.

Dobbelstein, M. et al., 1996. Protection against Apoptosis by the Vaccinia Virus SPI-2 (B13R) Gene Product. , 70(9), pp.6479–6485.

Dolin, R., 2015. Epidemiology of influenza. *Uptodate*. Available at: http://www.uptodate.com/contents/epidemiology-of-influenza?source=search_result&search=Dolin+INfluenza&selectedTitle=3~150 [Accessed November 5, 2015].

Dondelinger, Y. et al., 2014. MLKL Compromises Plasma Membrane Integrity by Binding to Phosphatidylinositol Phosphates. *Cell Reports*, 7(4), pp.971–981. Available at: http://dx.doi.org/10.1016/j.celrep.2014.04.026.

Dondelinger, Y. et al., 2013. RIPK3 contributes to TNFR1-mediated RIPK1 kinase-dependent apoptosis in conditions of cIAP1/2 depletion or TAK1 kinase inhibition. *Cell death and differentiation*, 20(10), pp.1381–92. Available at: http://www.pubmedcentral.nih.gov/articlerender.fcgi?artid=3770330&tool=pmcentrez&rendertype=abstract [Accessed April 25, 2015].

Doyle, S. et al., 2002. IRF3 mediates a TLR3/TLR4-specific antiviral gene program. *Immunity*, 17(3), pp.251–63. Available at: http://www.ncbi.nlm.nih.gov/pubmed/12354379.

Dufour, F. et al., 2011. The ribonucleotide reductase R1 subunits of herpes simplex virus types 1 and 2 protect cells against TNFα- and FasL-induced apoptosis by interacting with caspase-8. *Apoptosis : an international journal on programmed cell death*, 16(3), pp.256–71. Available at: http://www.ncbi.nlm.nih.gov/pubmed/21107701 [Accessed April 26, 2015].

Duprez, L. et al., 2011. RIP kinase-dependent necrosis drives lethal systemic inflammatory response syndrome. *Immunity*, 35(6), pp.908–18. Available at: http://www.ncbi.nlm.nih.gov/pubmed/22195746 [Accessed April 22, 2015].

Feoktistova, M. et al., 2011. cIAPs Block Ripotosome Formation, a RIP1 / Caspase-8 Containing Intracellular Cell Death Complex Differentially Regulated by cFLIP Isoforms. , pp.449–463.

Fitzgerald, K. a et al., 2003. IKKepsilon and TBK1 are essential components of the IRF3 signaling pathway. *Nature immunology*, 4(5), pp.491–6. Available at: http://www.ncbi.nlm.nih.gov/pubmed/12692549 [Accessed March 24, 2014].

Friel, T.J., 2014. Epidemiology, clinical manifestations, and treatment of cytomegalovirus infection in immunocompetent adults. *Uptodate*. Available at: http://www.uptodate.com/contents/epidemiology-clinical-manifestations-and-treatment-of-cytomegalovirus-infection-in-immunocompetent-adults?source=search_result&search=cmv&selectedTitle=1~150.

Galluzzi, L. et al., 2010. Viral strategies for the evasion of immunogenic cell death. *Journal of internal medicine*, 267(5), pp.526–42. Available at: http://www.ncbi.nlm.nih.gov/pubmed/20433579 [Accessed April 24, 2015].

Galluzzi, L. & Kroemer, G., 2008. Necroptosis: a specialized pathway of programmed necrosis.

Cell, 135(7), pp.1161–3. Available at: http://www.ncbi.nlm.nih.gov/pubmed/19109884 [Accessed May 23, 2014].

Gatot, J.-S. et al., 2007. Lipopolysaccharide-mediated interferon regulatory factor activation involves TBK1-IKKepsilon-dependent Lys(63)-linked polyubiquitination and phosphorylation of TANK/I-TRAF. *The Journal of biological chemistry*, 282(43), pp.31131–46. Available at: http://www.ncbi.nlm.nih.gov/pubmed/17823124 [Accessed December 2, 2014].

Günther, C. et al., 2011. Caspase-8 regulates TNF-α-induced epithelial necroptosis and terminal ileitis. *Nature*, 477(7364), pp.335–9. Available at: http://www.pubmedcentral.nih.gov/articlerender.fcgi?artid=3373730&tool=pmcentrez&rendertype=abstract [Accessed November 2, 2014].

Guo, H. et al., 2015. Herpes simplex virus suppresses necroptosis in human cells. *Cell host & microbe*, 17(2), pp.243–51. Available at: http://www.ncbi.nlm.nih.gov/pubmed/25674983 [Accessed February 17, 2015].

Guo, W. et al., 2011. Ablation of Fmrp in adult neural stem cells disrupts hippocampus-dependent learning. *Nature medicine*, 17(5), pp.559–65. Available at: http://www.pubmedcentral.nih.gov/articlerender.fcgi?artid=3140952&tool=pmcentrez&rendertype=abstract [Accessed February 24, 2014].

He, S. et al., 2009. Receptor interacting protein kinase-3 determines cellular necrotic response to TNF-alpha. *Cell*, 137(6), pp.1100–11. Available at: http://www.ncbi.nlm.nih.gov/pubmed/19524512 [Accessed November 2, 2014].

He, S. et al., 2011. Toll-like receptors activate programmed necrosis in macrophages through a receptor-interacting kinase-3-mediated pathway. *Proceedings of the National Academy of Sciences*, 108(50), pp.20054–20059.

Hildebrand, J.M. et al., 2014. Activation of the pseudokinase MLKL unleashes the four-helix bundle domain to induce membrane localization and necroptotic cell death. *Proceedings of the National Academy of Sciences of the United States of America*, 111(42). Available at: http://www.ncbi.nlm.nih.gov/pubmed/25288762 [Accessed October 8, 2014].

Hitomi, J. et al., 2008. Identification of a molecular signaling network that regulates a cellular necrotic cell death pathway. *Cell*, 135(7), pp.1311–23. Available at: http://www.pubmedcentral.nih.gov/articlerender.fcgi?artid=2621059&tool=pmcentrez&rendertype=abstract [Accessed May 24, 2014].

Hohmann, E.L., 2014. Microbiology and epidemiology of salmonellosis. *Uptodate*. Available at: http://www.uptodate.com/contents/microbiology-and-epidemiology-of-salmonellosis?source=search_result&search=Salmonella&selectedTitle=2~150.

Holler, N. et al., 2000. Fas triggers an alternative, caspase-8-independent cell death pathway using the kinase RIP as effector molecule. *Nature immunology*, 1(6), pp.489–495.

Hu, S. et al., 1997. A Novel Family of Viral Death Effector Domain-containing Molecules That Inhibit Both C-95 an Tumor Necrosis Factor Receptor-1-induced Apoptosis *. *The Journal of biological chemistry*, 272(15), pp.9621–9625.

Huang, Z. et al., 2015. RIP1/RIP3 Binding to HSV-1 ICP6 Initiates Necroptosis to Restrict Virus Propagation in Mice. *Cell host & microbe*, 17(2), pp.229–42. Available at: http://www.ncbi.nlm.nih.gov/pubmed/25674982 [Accessed February 17, 2015].

Ito, Y. et al., 2016. RIPK1 mediates axonal degeneration by promoting inflammation and necroptosis in ALS. *Science*, 353(6299), pp.603–608. Available at: http://www.sciencemag.org/cgi/doi/10.1126/science.aaf6803.

Ivashkiv, L.B. & Donlin, L.T., 2013. Regulation of type I interferon responses. *Nature reviews. Immunology*, 14(1), pp.36–49. Available at: http://www.ncbi.nlm.nih.gov/pubmed/24362405.

Kabsch, K. & Alonso, a., 2002. The Human Papillomavirus Type 16 E5 Protein Impairs TRAIL- and FasL-Mediated Apoptosis in HaCaT Cells by Different Mechanisms. *Journal of Virology*, 76(23), pp.12162–12172. Available at: http://jvi.asm.org/cgi/doi/10.1128/JVI.76.23.12162-12172.2002.

Kaczmarek, A., Vandenabeele, P. & Krysko, D. V, 2013. Necroptosis: the release of damage-associated molecular patterns and its physiological relevance. *Immunity*, 38(2), pp.209–23. Available at: http://www.ncbi.nlm.nih.gov/pubmed/23438821 [Accessed January 22, 2014].

Kagan, J.C. et al., 2008. TRAM couples endocytosis of Toll-like receptor 4 to the induction of interferon-beta. *Nature immunology*, 9(4), pp.361–8. Available at: http://www.pubmedcentral.nih.gov/articlerender.fcgi?artid=4112825&tool=pmcentrez&rendertype=abstract.

Kaiser, W.J. et al., 2014. RIP1 suppresses innate immune necrotic as well as apoptotic cell death during mammalian parturition. *Proceedings of the National Academy of Sciences of the United States of America*, 111(21), pp.7753–8. Available at: http://www.ncbi.nlm.nih.gov/pubmed/24821786 [Accessed July 27, 2014].

Kaiser, W.J. et al., 2013. Toll-like receptor 3-mediated necrosis via TRIF, RIP3, and MLKL. *The Journal of biological chemistry*, 288(43), pp.31268–79. Available at: http://www.ncbi.nlm.nih.gov/pubmed/24019532 [Accessed May 28, 2014].

Kaiser, W.J. & Offermann, M.K., 2005. Apoptosis Induced by the Toll-Like Receptor Adaptor TRIF Is Dependent on Its Receptor Interacting Protein Homotypic Interaction Motif. *The Journal of Immunology*, 174(8), pp.4942–4952. Available at: http://www.jimmunol.org/cgi/doi/10.4049/jimmunol.174.8.4942 [Accessed June 28, 2014].

Kang, T.-B. et al., 2014. *Activation of the NLRP3 inflammasome by proteins that signal for necroptosis.* 1st ed., Elsevier Inc. Available at: http://www.ncbi.nlm.nih.gov/pubmed/25065886 [Accessed April 24, 2015].

Kaser, A., Zeissig, S. & Blumberg, R.S., 2010. Inflammatory bowel disease. *Annual review of immunology*, 28, pp.573–621. Available at: http://www.ncbi.nlm.nih.gov/pubmed/20192811 [Accessed April 13, 2015].

Kawai, T. & Akira, S., 2010. The role of pattern-recognition receptors in innate immunity: update on Toll-like receptors. *Nature immunology*, 11(5), pp.373–84. Available at: http://www.ncbi.nlm.nih.gov/pubmed/20404851.

Kawai, T. & Akira, S., 2006. TLR signaling. *Seminars in Immunology*, 19, pp.24–32.

Kearney, C.J. et al., 2015. Necroptosis suppresses inflammation via termination of TNF- or LPS-induced cytokine and chemokine production. *Cell death and differentiation*, 22(8), pp.1313–27. Available at: http://www.ncbi.nlm.nih.gov/pubmed/25613374.

Kearney, C.J. et al., 2014. RIPK1 Can Function as an Inhibitor Rather Than an Initiator of RIPK3-dependent Necroptosis. *The FEBS journal*. Available at: http://www.ncbi.nlm.nih.gov/pubmed/25195660 [Accessed September 15, 2014].

Kelliher, M.A. et al., 1998. The Death Domain Kinase RIP Mediates the TNF-Induced NF- □ B Signal. , 8, pp.297–303.

Kennedy, C.L. et al., 2009. Programmed cellular necrosis mediated by the pore-forming alpha-toxin from Clostridium septicum. *PLoS pathogens*, 5(7), p.e1000516. Available at: http://www.pubmedcentral.nih.gov/articlerender.fcgi?artid=2705182&tool=pmcentrez&rendertype=abstract [Accessed April 24, 2015].

Kim, S.J. & Li, J., 2013. Caspase blockade induces RIP3-mediated programmed necrosis in Toll-like receptor-activated microglia. *Cell Death and Disease*, 4(7), pp.e716-12. Available at: http://dx.doi.org/10.1038/cddis.2013.238.

Kitur, K. et al., 2015. Toxin-Induced Necroptosis Is a Major Mechanism of Staphylococcus aureus Lung Damage. *PLoS pathogens*, 11(4), p.e1004820. Available at: http://www.ncbi.nlm.nih.gov/pubmed/25880560 [Accessed April 20, 2015].

Klein, R.S., 2015a. Clinical manifestations and diagnosis of herpes simplex virus type 1 infection. *Uptodate*. Available at: http://www.uptodate.com/contents/clinical-manifestations-and-diagnosis-of-herpes-simplex-virus-type-1-infection?source=search_result&search=HSV&selectedTitle=1~150.

Klein, R.S., 2015b. Herpes simplex virus type 1 encephalitis. *Uptodate*. Available at: http://www.uptodate.com/contents/herpes-simplex-virus-type-1-encephalitis?source=search_result&search=HSV+encephalitis&selectedTitle=1~46.

Knapp, O. et al., 2010. Clostridium septicum alpha-toxin forms pores and induces rapid cell necrosis. *Toxicon : official journal of the International Society on Toxinology*, 55(1), pp.61–72. Available at: http://www.ncbi.nlm.nih.gov/pubmed/19632260 [Accessed April 24, 2015].

Kotton, C.N. & Hohmann, E.L., 2013. Pathogenesis of Salmonella gastroenteritis. *Uptodate*. Available at: http://www.uptodate.com/contents/pathogenesis-of-salmonella-gastroenteritis?source=search_result&search=Salmonella&selectedTitle=3~150.

Kovalenko, A. et al., 2009. Caspase-8 deficiency in epidermal keratinocytes triggers an inflammatory skin disease. *The Journal of experimental medicine*, 206(10), pp.2161–77. Available at: http://www.pubmedcentral.nih.gov/articlerender.fcgi?artid=2757876&tool=pmcentrez&rendertype=abstract [Accessed March 26, 2014].

Krajewska, M. et al., 2011. Neuronal deletion of caspase 8 protects against brain injury in mouse models of controlled cortical impact and kainic acid-induced excitotoxicity. *PLoS ONE*,

6(9).

Kumar, V. et al., 2010. *Pathologic Basis of Disease* 8th ed., Saunders.

Kuriakose, T. et, 2016. HHS Public Access. , 1(2), pp.3–14.

Lamkanfi, M. & Dixit, V.M., 2010. Manipulation of host cell death pathways during microbial infections. *Cell host & microbe*, 8(1), pp.44–54. Available at: http://www.ncbi.nlm.nih.gov/pubmed/20638641 [Accessed April 23, 2015].

Langelier, Y. et al., 2002. The R1 subunit of herpes simplex virus ribonucleotide reductase protects cells against apoptosis at , or upstream of , caspase-8 activation. , pp.2779–2789.

LaRock, C.N. & Cookson, B.T., 2012. The Yersinia virulence effector YopM binds caspase-1 to arrest inflammasome assembly and processing. *Cell host & microbe*, 12(6), pp.799–805. Available at: http://www.pubmedcentral.nih.gov/articlerender.fcgi?artid=3703949&tool=pmcentrez&rendertype=abstract [Accessed July 24, 2014].

Laster, S.M., Wood, J.G. & Gooding, L.R., 1988. Tumor necrosis factor can induce both apoptic and necrotic forms of cell lysis. *Journal of immunology (Baltimore, Md. : 1950)*, 141(8), pp.2629–34. Available at: http://www.ncbi.nlm.nih.gov/pubmed/3171180.

Lawlor, K.E. et al., 2015. RIPK3 promotes cell death and NLRP3 inflammasome activation in the absence of MLKL. *Nature Communications*, 6, p.6282. Available at: http://www.nature.com/doifinder/10.1038/ncomms7282.

Lawlor, M.S. et al., 2005. Identification of Klebsiella pneumoniae virulence determinants using an intranasal infection model. *Molecular microbiology*, 58(4), pp.1054–73. Available at: http://www.ncbi.nlm.nih.gov/pubmed/16262790 [Accessed July 26, 2015].

Lawlor, M.S., Handley, S. a & Miller, V.L., 2006. Comparison of the host responses to wild-type and cpsB mutant Klebsiella pneumoniae infections. *Infection and immunity*, 74(9), pp.5402–7. Available at: http://www.pubmedcentral.nih.gov/articlerender.fcgi?artid=1594822&tool=pmcentrez&rendertype=abstract [Accessed July 26, 2015].

Li, J. et al., 2012. The RIP1/RIP3 necrosome forms a functional amyloid signaling complex required for programmed necrosis. *Cell*, 150(2), pp.339–50. Available at: http://www.pubmedcentral.nih.gov/articlerender.fcgi?artid=3664196&tool=pmcentrez&rendertype=abstract [Accessed October 16, 2014].

Li, L. et al., 2014. The Gβγ-Src signaling pathway regulates TNF-induced necroptosis via control of necrosome translocation. *Cell research*, 2, pp.1–16. Available at: http://www.ncbi.nlm.nih.gov/pubmed/24513853 [Accessed February 27, 2014].

Li, M. & Beg, A.A., 2000. Induction of Necrotic-Like Cell Death by Tumor Necrosis Factor Alpha and Caspase Inhibitors : Novel Mechanism for Killing Virus-Infected Cells. , 74(16), pp.7470–7477.

Li, S. et al., 2013. Pathogen blocks host death receptor signalling by arginine GlcNAcylation of death domains. *Nature*, 501(7466), pp.242–6. Available at:

http://www.ncbi.nlm.nih.gov/pubmed/23955153 [Accessed April 24, 2015].

Van Lieshout, M.H.P. et al., 2015. TIR-Domain-Containing Adaptor-Inducing Interferon-β (TRIF) Mediates Antibacterial Defense during Gram-Negative Pneumonia by Inducing Interferon-γ. *Journal of Innate Immunity*, 7(6), pp.637–646.

Lin, C.-F. et al., 2010. Different types of cell death induced by enterotoxins. *Toxins*, 2(8), pp.2158–76. Available at: http://www.pubmedcentral.nih.gov/articlerender.fcgi?artid=3153280&tool=pmcentrez&rendertype=abstract [Accessed April 24, 2015].

Linkermann, A. & Green, D.R., 2014. Necroptosis. *The New England journal of medicine*, 370(5), pp.455–65. Available at: http://www.pubmedcentral.nih.gov/articlerender.fcgi?artid=4035222&tool=pmcentrez&rendertype=abstract [Accessed April 24, 2015].

Lukens, J.R. et al., 2013. RIP1-driven autoinflammation targets IL-1α independently of inflammasomes and RIP3. *Nature*, 498(7453), pp.224–7. Available at: http://www.pubmedcentral.nih.gov/articlerender.fcgi?artid=3683390&tool=pmcentrez&rendertype=abstract [Accessed July 27, 2014].

Macdonald, T.T. & Monteleone, G., 2005. Immunity, Inflammation, and Allergy in the Gut. , (March), pp.1920–1925.

Macen, J.L. et al., 1996. orthopoxvirus cytokine. , 93(August), pp.9108–9113.

Madrigal, A.G. et al., 2012. Pathogen-mediated proteolysis of the cell death regulator RIPK1 and the host defense modulator RIPK2 in human aortic endothelial cells. *PLoS Pathogens*, 8(6).

Mandal, P. et al., 2014. RIP3 Induces Apoptosis Independent of Pronecrotic Kinase Activity. *Molecular Cell*, 56(4), pp.481–495. Available at: http://dx.doi.org/10.1016/j.molcel.2014.10.021.

Matsumura, H. et al., 2000. Necrotic death pathway in Fas receptor signaling. *Journal of Cell Biology*, 151(6), pp.1247–1255.

McComb, S. et al., 2012. cIAP1 and cIAP2 limit macrophage necroptosis by inhibiting Rip1 and Rip3 activation. *Cell death and differentiation*, 19(11), pp.1791–801. Available at: http://www.pubmedcentral.nih.gov/articlerender.fcgi?artid=3469059&tool=pmcentrez&rendertype=abstract [Accessed May 12, 2015].

McCoy, M.W., Moreland, S.M. & Detweiler, C.S., 2012. Hemophagocytic macrophages in murine typhoid fever have an anti-inflammatory phenotype. *Infection and immunity*, 80(10), pp.3642–9. Available at: http://www.pubmedcentral.nih.gov/articlerender.fcgi?artid=3457584&tool=pmcentrez&rendertype=abstract [Accessed April 26, 2015].

McNamara, C.R. et al., 2013. Akt Regulates TNFα synthesis downstream of RIP1 kinase activation during necroptosis. *PloS one*, 8(3), p.e56576. Available at: http://www.pubmedcentral.nih.gov/articlerender.fcgi?artid=3585731&tool=pmcentrez&rendertype=abstract.

Meylan, E. et al., 2004. RIP1 is an essential mediator of Toll-like receptor 3-induced NF-kappa B activation. *Nature immunology*, 5(5), pp.503–7. Available at: http://www.ncbi.nlm.nih.gov/pubmed/15064760 [Accessed November 2, 2014].

Micheau, O. & Tschopp, J., 2003. Induction of TNF receptor I-mediated apoptosis via two sequential signaling complexes. *Cell*, 114(2), pp.181–190.

Miller, E. a. & Ernst, J.D., 2009. Anti-TNF immunotherapy and tuberculosis reactivation: another mechanism revealed. *Journal of Clinical Investigation*, 119(5), pp.1079–1082. Available at: http://www.jci.org/articles/view/39143.

Mocarski, E.S., Upton, J.W. & Kaiser, W.J., 2012. Viral infection and the evolution of caspase 8-regulated apoptotic and necrotic death pathways. *Nature reviews. Immunology*, 12(2), pp.79–88. Available at: http://www.ncbi.nlm.nih.gov/pubmed/22193709 [Accessed January 29, 2014].

Moquin, D.M., McQuade, T. & Chan, F.K.-M., 2013. CYLD deubiquitinates RIP1 in the TNFα-induced necrosome to facilitate kinase activation and programmed necrosis. *PloS one*, 8(10), p.e76841. Available at: http://www.pubmedcentral.nih.gov/articlerender.fcgi?artid=3788787&tool=pmcentrez&rendertype=abstract [Accessed March 25, 2014].

Moriwaki, K. et al., 2015. A RIPK3-caspase 8 complex mediates atypical pro-IL-1β processing. *Journal of immunology (Baltimore, Md. : 1950)*, 194(4), pp.1938–44. Available at: http://www.ncbi.nlm.nih.gov/pubmed/25567679 [Accessed April 24, 2015].

Moriwaki, K. et al., 2016. The Mitochondrial Phosphatase PGAM5 Is Dispensable for Necroptosis but Promotes Inflammasome Activation in Macrophages. *Journal of immunology (Baltimore, Md. : 1950)*, 196(1), pp.407–415.

Moriwaki, K. et al., 2014. The Necroptosis Adaptor RIPK3 Promotes Injury-Induced Cytokine Expression and Tissue Repair. *Immunity*, 41(4), pp.567–578. Available at: http://linkinghub.elsevier.com/retrieve/pii/S1074761314003501 [Accessed October 16, 2014].

Morris, E.J. et al., 2013. Discovery of a novel ERK inhibitor with activity in models of acquired resistance to BRAF and MEK inhibitors. *Cancer Discovery*, 3(7), pp.742–750.

Murphy, J.M. et al., 2013. The pseudokinase MLKL mediates necroptosis via a molecular switch mechanism. *Immunity*, 39(3), pp.443–53. Available at: http://www.ncbi.nlm.nih.gov/pubmed/24012422 [Accessed October 24, 2014].

Najjar, M. et al., 2016. RIPK1 and RIPK3 Kinases Promote Cell-Death-Independent Inflammation by Toll-like Receptor 4. *Immunity*, 45(1), pp.46–59. Available at: http://linkinghub.elsevier.com/retrieve/pii/S1074761316302102.

Newton, K., Sun, X. & Dixit, V.M., 2004. Kinase RIP3 is dispensable for normal NF-kappa Bs, signaling by the B-cell and T-cell receptors, tumor necrosis factor receptor 1, and Toll-like receptors 2 and 4. *Molecular and cellular biology*, 24(4), pp.1464–9. Available at: http://www.pubmedcentral.nih.gov/articlerender.fcgi?artid=344190&tool=pmcentrez&rendertype=abstract.

Nix, R.N. et al., 2007. Hemophagocytic macrophages harbor Salmonella enterica during persistent infection. *PLoS pathogens*, 3(12), p.e193. Available at: http://www.pubmedcentral.nih.gov/articlerender.fcgi?artid=2134957&tool=pmcentrez&rendertype=abstract [Accessed April 24, 2015].

Nogusa, S., Thapa, R.J., et al., 2016. RIPK3 Activates Parallel Pathways of MLKL-Driven Necroptosis and FADD-Mediated Apoptosis to Protect against Influenza A Virus Article RIPK3 Activates Parallel Pathways of MLKL-Driven Necroptosis and FADD-Mediated Apoptosis. *Cell Host & Microbe*, pp.1–12.

Nogusa, S., Slifker, M.J., et al., 2016. RIPK3 Is Largely Dispensable for RIG-I-Like Receptor- and Type I Interferon-Driven Transcriptional Responses to Influenza A Virus in Murine Fibroblasts. *Plos One*, 11(7), p.e0158774. Available at: http://dx.plos.org/10.1371/journal.pone.0158774.

O'Donnell, M.A. et al., 2011. Caspase 8 inhibits programmed necrosis by processing CYLD. *Nature cell biology*, 13(12), pp.1437–42. Available at: http://www.pubmedcentral.nih.gov/articlerender.fcgi?artid=3229661&tool=pmcentrez&rendertype=abstract [Accessed August 5, 2014].

O'Ryan, M.G. & Matson, D.O., 2015. Clinical manifestations and diagnosis of rotavirus infection. *Uptodate*. Available at: http://www.uptodate.com/contents/clinical-manifestations-and-diagnosis-of-rotavirus-infection?source=search_result&search=rotavirus&selectedTitle=1~82.

Oberst, A. et al., 2011. Catalytic activity of the caspase-8-FLIP(L) complex inhibits RIPK3-dependent necrosis. *Nature*, 471(7338), pp.363–7. Available at: http://www.pubmedcentral.nih.gov/articlerender.fcgi?artid=3077893&tool=pmcentrez&rendertype=abstract [Accessed August 13, 2014].

Ofengeim, D. et al., 2015. Activation of Necroptosis in Multiple Sclerosis. *Cell reports*, 10(11), pp.1836–1849. Available at: http://www.ncbi.nlm.nih.gov/pubmed/25801023 [Accessed March 26, 2015].

Ofengeim, D. & Yuan, J., 2013. Regulation of RIP1 kinase signalling at the crossroads of inflammation and cell death. *Nature reviews. Molecular cell biology*, 14(11), pp.727–36. Available at: http://www.ncbi.nlm.nih.gov/pubmed/24129419 [Accessed March 22, 2014].

Okazaki, K. & Sagata, N., 1995. The Mos/MAP kinase pathway stabilizes c-Fos by phosphorylation and augments its transforming activity in NIH 3T3 cells. *The EMBO journal*, 14(20), pp.5048–59. Available at: http://www.pubmedcentral.nih.gov/articlerender.fcgi?artid=394608&tool=pmcentrez&rendertype=abstract%5Cnhttp://www.ncbi.nlm.nih.gov/pubmed/7588633%5Cnhttp://www.pubmedcentral.nih.gov/articlerender.fcgi?artid=PMC394608.

Omoto, S. et al., 2015. Suppression of RIP3-dependent Necroptosis by Human Cytomegalovirus. *The Journal of biological chemistry*, (404). Available at: http://www.ncbi.nlm.nih.gov/pubmed/25778401 [Accessed April 24, 2015].

Orozco, S. et al., 2014. RIPK1 both positively and negatively regulates RIPK3 oligomerization and necroptosis. *Cell death and differentiation*, 21(10), pp.1511–1521. Available at:

http://www.ncbi.nlm.nih.gov/pubmed/24902904 [Accessed July 23, 2014].

Osborn, S.L. et al., 2010. Fas-associated death domain (FADD) is a negative regulator of T-cell receptor-mediated necroptosis. *Proceedings of the National Academy of Sciences of the United States of America*, 107(29), pp.13034–9. Available at: http://www.pubmedcentral.nih.gov/articlerender.fcgi?artid=2919948&tool=pmcentrez&rendertype=abstract [Accessed May 12, 2015].

Pasparakis, M. & Vandenabeele, P., 2015. Necroptosis and its role in inflammation. *Nature*, 517(7534), pp.311–320. Available at: http://www.ncbi.nlm.nih.gov/pubmed/25592536.

Pearson, J.S. et al., 2013. A type III effector antagonizes death receptor signalling during bacterial gut infection. *Nature*, 501(7466), pp.247–251. Available at: http://www.nature.com/doifinder/10.1038/nature12524 [Accessed March 20, 2015].

Peleg, A.Y. & Hooper, D.C., 2010. Hospital-Acquired Infections Due to Gram-Negative Bacteria. *New England Journal of Medicine*.

Peterson, L.W. et al., 2016. Cell-Extrinsic TNF Collaborates with TRIF Signaling To Promote *Yersinia* -Induced Apoptosis. *The Journal of Immunology*, 197(10), pp.4110–4117. Available at: http://www.jimmunol.org/lookup/doi/10.4049/jimmunol.1601294.

Philip, N.H. et al., 2014. Caspase-8 mediates caspase-1 processing and innate immune defense in response to bacterial blockade of NF-κB and MAPK signaling. *Proceedings of the National Academy of Sciences of the United States of America*, 111(20), pp.7385–90. Available at: http://www.ncbi.nlm.nih.gov/pubmed/24799700 [Accessed September 30, 2014].

Polykratis, A. et al., 2014. Cutting Edge: RIPK1 Kinase Inactive Mice Are Viable and Protected from TNF-Induced Necroptosis In Vivo. *Journal of immunology (Baltimore, Md. : 1950)*. Available at: http://www.ncbi.nlm.nih.gov/pubmed/25015821 [Accessed July 23, 2014].

Power, M.R. et al., 2007. A role of Toll-IL-1 receptor domain-containing adaptor-inducing IFN-beta in the host response to Pseudomonas aeruginosa lung infection in mice. *Journal of immunology (Baltimore, Md. : 1950)*, 178(5), pp.3170–3176.

Pozniak, A., 2015. Clinical manifestations and evaluation of pulmonary tuberculosis. *Uptodate*. Available at: http://www.uptodate.com/contents/clinical-manifestations-and-evaluation-of-pulmonary-tuberculosis?source=search_result&search=Clinical+manifestations+and+evaluation+of+pulmonary+tb&selectedTitle=1~107.

Pujol, C. et al., 2009. Yersinia pestis can reside in autophagosomes and avoid xenophagy in murine macrophages by preventing vacuole acidification. *Infection and immunity*, 77(6), pp.2251–61. Available at: http://www.pubmedcentral.nih.gov/articlerender.fcgi?artid=2687347&tool=pmcentrez&rendertype=abstract [Accessed April 26, 2015].

Pujol, C. & Bliska, J.B., 2005. Turning Yersinia pathogenesis outside in: subversion of macrophage function by intracellular yersiniae. *Clinical immunology (Orlando, Fla.)*, 114(3), pp.216–26. Available at: http://www.ncbi.nlm.nih.gov/pubmed/15721832 [Accessed April 24, 2015].

Quarato, G. et al., 2016. Sequential Engagement of Distinct MLKL Phosphatidylinositol-Binding Sites Executes Necroptosis. *Molecular Cell*, 61(4), pp.589–601. Available at: http://dx.doi.org/10.1016/j.molcel.2016.01.011.

Rajput, A. et al., 2011. RIG-I RNA helicase activation of IRF3 transcription factor is negatively regulated by caspase-8-mediated cleavage of the RIP1 protein. *Immunity*, 34(3), pp.340–51. Available at: http://www.ncbi.nlm.nih.gov/pubmed/21419663 [Accessed April 24, 2015].

Richardson-burns, S.M., Kominsky, D.J. & Tyler, K.L., 2002. Reovirus-induced neuronal apoptosis is mediated by caspase 3 and is associated with the activation of death receptors. , pp.365–380.

Rickard, J. a et al., 2014. RIPK1 Regulates RIPK3-MLKL-Driven Systemic Inflammation and Emergency Hematopoiesis. *Cell*, 8, pp.1–14. Available at: http://www.ncbi.nlm.nih.gov/pubmed/24813849 [Accessed May 23, 2014].

Robinson, N. et al., 2012. Type I interferon induces necroptosis in macrophages during infection with Salmonella enterica serovar Typhimurium. *Nature immunology*, 13(10), pp.954–62. Available at: http://www.pubmedcentral.nih.gov/articlerender.fcgi?artid=4005791&tool=pmcentrez&rendertype=abstract [Accessed April 24, 2015].

Roca, F.J. & Ramakrishnan, L., 2013. TNF dually mediates resistance and susceptibility to mycobacteria via mitochondrial reactive oxygen species. *Cell*, 153(3), pp.521–34. Available at: http://www.pubmedcentral.nih.gov/articlerender.fcgi?artid=3790588&tool=pmcentrez&rendertype=abstract [Accessed January 10, 2015].

Rodrigue-Gervais, I.G. et al., 2014. Cellular inhibitor of apoptosis protein cIAP2 protects against pulmonary tissue necrosis during influenza virus infection to promote host survival. *Cell host & microbe*, 15(1), pp.23–35. Available at: http://www.ncbi.nlm.nih.gov/pubmed/24439895 [Accessed May 12, 2015].

Roy, C.R. & Mocarski, E.S., 2007. Pathogen subversion of cell-intrinsic innate immunity. *Nature immunology*, 8(11), pp.1179–87. Available at: http://www.ncbi.nlm.nih.gov/pubmed/17952043 [Accessed April 24, 2015].

Ruiz, J. et al., 2016. Systemic Activation of TLR3-Dependent TRIF Signaling Confers Host Defense against Gram-Negative Bacteria in the Intestine. *Frontiers in Cellular and Infection Microbiology*, 5(January), pp.1–11. Available at: http://journal.frontiersin.org/article/10.3389/fcimb.2015.00105.

Sakaguchi, S. et al., 2003. Essential role of IRF-3 in lipopolysaccharide-induced interferon-β gene expression and endotoxin shock. *Biochemical and Biophysical Research Communications*, 306(4), pp.860–866. Available at: http://linkinghub.elsevier.com/retrieve/pii/S0006291X03010490 [Accessed March 26, 2014].

Saleh, D. et al., 2017. Kinase Activities of RIPK1 and RIPK3 Can Kinase Activities of RIPK1 and RIPK3 Can Direct IFN-b Synthesis Induced by Lipopolysaccharide. *The Journal of Immunology*, 198(10). Available at:

http://www.jimmunol.org/content/early/2017/04/29/jimmun%0Ahttp://www.jimmunol.org/.

Saleh, D. & Degterev, A., 2015. Emerging Roles for RIPK1 and RIPK3 in Pathogen-Induced Cell Death and Host Immunity. In *Current topics in microbiology and immunology*.

Schluger, N. & Rom, W., 1998. The host immune response to tuberculosis. *American Journal of Respiratory and Critical Care Medicine*, 157(19). Available at: http://www.atsjournals.org/doi/abs/10.1164/ajrccm.157.3.9708002 [Accessed June 18, 2015].

Schotte, P. et al., 1999. Non-specific effects of methyl ketone peptide inhibitors of caspases. *FEBS letters*, 442(1), pp.117–121. Available at: http://doi.wiley.com/10.1016/S0014-5793%2898%2901640-8%5Cnpapers3://publication/doi/10.1016/S0014-5793(98)01640-8.

Schworer, S.A. et al., 2014. Toll-like Receptor-Mediated Downregulation of the Deubiquitinase CYLD Protects Macrophages from Necroptosis in Wild-Derived Mice. *The Journal of biological chemistry*. Available at: http://www.ncbi.nlm.nih.gov/pubmed/24706750 [Accessed August 5, 2014].

Seifert, L. et al., 2016. The necrosome promotes pancreatic oncogenesis via CXCL1 and Mincle-induced immune suppression. *Nature*, pp.1–17. Available at: http://www.nature.com/doifinder/10.1038/nature17403.

Sexton, D.J., 2014. Epidemiology, microbiology and pathogenesis of plague (Yersinia pestis infection). *Uptodate*. Available at: http://www.uptodate.com/contents/epidemiology-microbiology-and-pathogenesis-of-plague-yersinia-pestis-infection?source=search_result&search=Pestis&selectedTitle=1~25.

Shisler, J.L. & Moss, B., 2001. Molluscum contagiosum virus inhibitors of apoptosis: The MC159 v-FLIP protein blocks Fas-induced activation of procaspases and degradation of the related MC160 protein. *Virology*, 282(1), pp.14–25. Available at: http://www.ncbi.nlm.nih.gov/pubmed/11259186 [Accessed April 26, 2015].

Silke, J., Rickard, J.A. & Gerlic, M., 2015. The diverse role of RIP kinases in necroptosis and inflammation. *Nature Immunology*, 16(7), pp.689–697. Available at: http://www.nature.com/doifinder/10.1038/ni.3206.

Skaletskaya, a et al., 2001. A cytomegalovirus-encoded inhibitor of apoptosis that suppresses caspase-8 activation. *Proceedings of the National Academy of Sciences of the United States of America*, 98(14), pp.7829–34. Available at: http://www.pubmedcentral.nih.gov/articlerender.fcgi?artid=35427&tool=pmcentrez&rendertype=abstract.

Solis, M. et al., 2007. Involvement of TBK1 and IKKepsilon in lipopolysaccharide-induced activation of the interferon response in primary human macrophages. *European journal of immunology*, 37(2), pp.528–39. Available at: http://www.ncbi.nlm.nih.gov/pubmed/17236232 [Accessed March 26, 2014].

Sotolongo, J. et al., 2011. Host innate recognition of an intestinal bacterial pathogen induces TRIF-dependent protective immunity. *The Journal of experimental medicine*, 208(13), pp.2705–16. Available at:

http://www.pubmedcentral.nih.gov/articlerender.fcgi?artid=3244044&tool=pmcentrez&rendertype=abstract [Accessed December 1, 2014].

Sridharan, H. & Upton, J.W., 2014. Programmed necrosis in microbial pathogenesis. *Trends in microbiology*, 22(4), pp.199–207. Available at: http://www.ncbi.nlm.nih.gov/pubmed/24565922 [Accessed March 26, 2015].

Sun, L. et al., 2012. Mixed lineage kinase domain-like protein mediates necrosis signaling downstream of RIP3 kinase. *Cell*, 148(1–2), pp.213–27. Available at: http://www.ncbi.nlm.nih.gov/pubmed/22265413 [Accessed September 12, 2014].

Takahashi, N. et al., 2014. RIPK1 ensures intestinal homeostasis by protecting the epithelium against apoptosis. *Nature*, 513(7516), pp.95–99. Available at: http://www.nature.com/doifinder/10.1038/nature13706 [Accessed September 3, 2014].

Tan, Y. & Kagan, J.C., 2014. A cross-disciplinary perspective on the innate immune responses to bacterial lipopolysaccharide. *Molecular cell*, 54(2), pp.212–23. Available at: http://www.ncbi.nlm.nih.gov/pubmed/24766885 [Accessed October 26, 2014].

Tauxe, R. V., 2013. Clinical manifestations and diagnosis of Yersinia infections. *Uptodate*. Available at: http://www.uptodate.com/contents/clinical-manifestations-and-diagnosis-of-yersinia-infections?source=search_result&search=Yersinia&selectedTitle=1~92.

Tenev, T. et al., 2011. The Ripoptosome, a Signaling Platform that Assembles in Response to Genotoxic Stress and Loss of IAPs. *Molecular Cell*, 43(3), pp.432–448. Available at: http://dx.doi.org/10.1016/j.molcel.2011.06.006.

Teng, X. et al., 2005. Structure–activity relationship study of novel necroptosis inhibitors. *Bioorganic & Medicinal Chemistry Letters*, 15(22), pp.5039–5044.

Thapa, R.J. et al., 2016. DAI Senses Influenza A Virus Genomic RNA and Activates RIPK3-Dependent Cell Death. *Cell Host and Microbe*, 20(5), pp.674–681. Available at: http://dx.doi.org/10.1016/j.chom.2016.09.014.

Thapa, R.J. et al., 2013. Interferon-induced RIP1/RIP3-mediated necrosis requires PKR and is licensed by FADD and caspases. *Proceedings of the National Academy of Sciences of the United States of America*, 110(33), pp.E3109-18. Available at: http://www.pubmedcentral.nih.gov/articlerender.fcgi?artid=3746924&tool=pmcentrez&rendertype=abstract [Accessed October 26, 2014].

Thome, M. et al., 1997. Viral FLICE-inhibitory proteins (FLIPs) prevent apoptosis induced by death receptors.pdf. *Nature*, 386, pp.517–521.

Thompson, C.B., 1995. Apoptosis in the Pathogenesis and Treatment of Disease. *Science, New Series*, 26712519(5203), pp.1456–1462. Available at: http://www.jstor.org/stable/2886538%5Cnhttp://www.jstor.org/page/.

Thurau, M. et al., 2006. The TRAF3-binding site of human molluscipox virus FLIP molecule MC159 is critical for its capacity to inhibit Fas-induced apoptosis. *Cell death and differentiation*, 13(9), pp.1577–85. Available at: http://www.ncbi.nlm.nih.gov/pubmed/16410799 [Accessed April 26, 2015].

Ting, A.T. & Pimentel-muiffios, F.X., 1996. RIP activation apoptosis. , 15(22), pp.6189–6196.

Tobin, D.M. et al., 2012. Host genotype-specific therapies can optimize the inflammatory response to mycobacterial infections. *Cell*, 148(3), pp.434–46. Available at: http://www.pubmedcentral.nih.gov/articlerender.fcgi?artid=3433720&tool=pmcentrez&rendertype=abstract [Accessed April 27, 2015].

Tobin, D.M. et al., 2010. The lta4h locus modulates susceptibility to mycobacterial infection in zebrafish and humans. *Cell*, 140(5), pp.717–30. Available at: http://www.pubmedcentral.nih.gov/articlerender.fcgi?artid=2907082&tool=pmcentrez&rendertype=abstract [Accessed April 25, 2015].

Turner, S.J. et al., 2000. Characterization of the ectromelia virus serpin , SPI-2. , 64, pp.2425–2430.

Ulrichs, T. & Kaufmann, S.H.E., 2006. New insights into the function of granulomas in human tuberculosis. *The Journal of pathology*, 208(2), pp.261–9. Available at: http://www.ncbi.nlm.nih.gov/pubmed/16362982 [Accessed April 27, 2015].

Upton, J.W., Kaiser, W.J. & Mocarski, E.S., 2012. DAI/ZBP1/DLM-1 complexes with RIP3 to mediate virus-induced programmed necrosis that is targeted by murine cytomegalovirus vIRA. *Cell host & microbe*, 11(3), pp.290–7. Available at: http://www.pubmedcentral.nih.gov/articlerender.fcgi?artid=3531981&tool=pmcentrez&rendertype=abstract [Accessed June 28, 2014].

Upton, J.W., Kaiser, W.J. & Mocarski, E.S., 2010. Virus inhibition of RIP3-dependent necrosis. *Cell host & microbe*, 7(4), pp.302–13. Available at: http://www.ncbi.nlm.nih.gov/pubmed/20413098 [Accessed May 24, 2014].

Vandenabeele, P., Galluzzi, L., et al., 2010. Molecular mechanisms of necroptosis: an ordered cellular explosion. *Nature reviews. Molecular cell biology*, 11(10), pp.700–14. Available at: http://www.ncbi.nlm.nih.gov/pubmed/20823910 [Accessed August 5, 2014].

Vandenabeele, P., Declercq, W., et al., 2010. The role of the kinases RIP1 and RIP3 in TNF-induced necrosis. *Science signaling*, 3(115), p.re4. Available at: http://www.ncbi.nlm.nih.gov/pubmed/20354226 [Accessed June 1, 2014].

Vercammen, D. et al., 1998. Inhibition of caspases increases the sensitivity of L929 cells to necrosis mediated by tumor necrosis factor. *The Journal of experimental medicine*, 187(9), pp.1477–85. Available at: http://www.pubmedcentral.nih.gov/articlerender.fcgi?artid=2212268&tool=pmcentrez&rendertype=abstract.

Viboud, G.I. & Bliska, J.B., 2005. Yersinia outer proteins: role in modulation of host cell signaling responses and pathogenesis. *Annual review of microbiology*, 59, pp.69–89. Available at: http://www.ncbi.nlm.nih.gov/pubmed/15847602 [Accessed March 15, 2015].

Vivarelli, M.S., 2004. RIP Links TLR4 to Akt and Is Essential for Cell Survival in Response to LPS Stimulation. *Journal of Experimental Medicine*, 200(3), pp.399–404. Available at: http://www.jem.org/cgi/doi/10.1084/jem.20040446.

Wang, H. et al., 2014. Mixed Lineage Kinase Domain-like Protein MLKL Causes Necrotic

Membrane Disruption upon Phosphorylation by RIP3. *Molecular Cell*, 54(1), pp.133–146. Available at: http://dx.doi.org/10.1016/j.molcel.2014.03.003.

Wang, L., Du, F. & Wang, X., 2008. TNF-?? Induces Two Distinct Caspase-8 Activation Pathways. *Cell*, 133(4), pp.693–703.

Wang, X. et al., 2014. Direct activation of RIP3/MLKL-dependent necrosis by herpes simplex virus 1 (HSV-1) protein ICP6 triggers host antiviral defense. *Proceedings of the National Academy of Sciences of the United States of America*, 111(43), pp.15438–43. Available at: http://www.ncbi.nlm.nih.gov/pubmed/25316792 [Accessed April 24, 2015].

Wang, X. et al., 2014. RNA viruses promote activation of the NLRP3 inflammasome through a RIP1-RIP3-DRP1 signaling pathway. *Nature Immunology*, 15(12). Available at: http://www.nature.com/doifinder/10.1038/ni.3015 [Accessed October 20, 2014].

Wang, X. et al., 2016. STING Requires the Adaptor TRIF to Trigger Innate Immune Responses to Microbial Infection. *Cell Host and Microbe*, 20(3), pp.329–341. Available at: http://dx.doi.org/10.1016/j.chom.2016.08.002.

Wanke, C.A., 2013. Pathogenic Escherichia coli. *Uptodate*. Available at: http://www.uptodate.com/contents/pathogenic-escherichia-coli?source=search_result&search=E.coli&selectedTitle=1~150.

Wegner, K.W., Saleh, D. & Degterev, A., 2016. Complex Pathologic Roles of RIPK1 and RIPK3: Moving Beyond Necroptosis. *Trends in Pharmacological Sciences*, 38(3), pp.202–225. Available at: http://dx.doi.org/10.1016/j.tips.2016.12.005.

Weinlich, R. et al., 2013. Protective roles for caspase-8 and cFLIP in adult homeostasis. *Cell reports*, 5(2), pp.340–8. Available at: http://www.pubmedcentral.nih.gov/articlerender.fcgi?artid=3843376&tool=pmcentrez&rendertype=abstract [Accessed May 12, 2015].

Welz, P.-S. et al., 2011. FADD prevents RIP3-mediated epithelial cell necrosis and chronic intestinal inflammation. *Nature*, 477(7364), pp.330–4. Available at: http://www.ncbi.nlm.nih.gov/pubmed/21804564 [Accessed March 10, 2015].

Weng, D. et al., 2014. Caspase-8 and RIP kinases regulate bacteria-induced innate immune responses and cell death. *Proceedings of the National Academy of Sciences of the United States of America*, 111(20), pp.7391–6. Available at: http://www.ncbi.nlm.nih.gov/pubmed/24799678 [Accessed July 10, 2014].

Wong, W.W.L. et al., 2014. cIAPs and XIAP regulate myelopoiesis through cytokine production in an RIPK1- And RIPK3-dependent manner. *Blood*, 123(16), pp.2562–2572.

Wu, J. et al., 2013. Mlkl knockout mice demonstrate the indispensable role of Mlkl in necroptosis. *Cell research*, 23(8), pp.994–1006. Available at: http://www.pubmedcentral.nih.gov/articlerender.fcgi?artid=3731568&tool=pmcentrez&rendertype=abstract [Accessed November 7, 2014].

Wu, X.-N. et al., 2014. Distinct roles of RIP1-RIP3 hetero- and RIP3-RIP3 homo-interaction in mediating necroptosis. *Cell death and differentiation*, pp.1–12. Available at: http://www.ncbi.nlm.nih.gov/pubmed/24902902 [Accessed June 7, 2014].

Xie, T., Peng, W., Liu, Y., et al., 2013. Structural basis of RIP1 inhibition by necrostatins. *Structure (London, England : 1993)*, 21(3), pp.493–9. Available at: http://www.ncbi.nlm.nih.gov/pubmed/23473668 [Accessed March 26, 2014].

Xie, T., Peng, W., Yan, C., et al., 2013. Structural insights into RIP3-mediated necroptotic signaling. *Cell reports*, 5(1), pp.70–8. Available at: http://www.ncbi.nlm.nih.gov/pubmed/24095729 [Accessed November 1, 2014].

Yamamoto, M. et al., 2002. Essential rolee for TIRAP i activation of the signaling cascade shared by TLR2 and TLR4. *Nature*, 420(November).

Yamamoto, M. et al., 2003. Role of adaptor TRIF in the MyD88-independent toll-like receptor signaling pathway. *Science (New York, N.Y.)*, 301(5633), pp.640–3. Available at: http://www.ncbi.nlm.nih.gov/pubmed/12855817 [Accessed July 14, 2014].

Yatim, N. et al., 2015. RIPK1 and NF- B signaling in dying cells determines cross-priming of CD8+ T cells. *Science*, 350(6258), pp.328–34. Available at: http://www.ncbi.nlm.nih.gov/pubmed/26405229.

Yatim, N. & Albert, M.L., 2011. Dying to replicate: the orchestration of the viral life cycle, cell death pathways, and immunity. *Immunity*, 35(4), pp.478–90. Available at: http://www.ncbi.nlm.nih.gov/pubmed/22035840 [Accessed May 12, 2015].

You, Z. et al., 2008. Necrostatin-1 reduces histopathology and improves functional outcome after controlled cortical impact in mice. *Journal of cerebral blood flow and metabolism : official journal of the International Society of Cerebral Blood Flow and Metabolism*, 28(9), pp.1564–73. Available at: http://www.pubmedcentral.nih.gov/articlerender.fcgi?artid=2831087&tool=pmcentrez&rendertype=abstract [Accessed March 26, 2014].

Zhang, D.-W. et al., 2009. RIP3, an energy metabolism regulator that switches TNF-induced cell death from apoptosis to necrosis. *Science (New York, N.Y.)*, 325(5938), pp.332–6. Available at: http://www.ncbi.nlm.nih.gov/pubmed/19498109 [Accessed October 31, 2014].

Zhang, S.Q. et al., 2000. Recruitment of the IKK Signalosome to the p55 TNF Receptor : RIP and A20 Bind to NEMO (IKK) upon Receptor Stimulation. , 12, pp.301–311.

Zhang, Y., Romanov, G. & Bliska, J.B., 2011. Type III secretion system-dependent translocation of ectopically expressed Yop effectors into macrophages by intracellular Yersinia pseudotuberculosis. *Infection and immunity*, 79(11), pp.4322–31. Available at: http://www.pubmedcentral.nih.gov/articlerender.fcgi?artid=3257923&tool=pmcentrez&rendertype=abstract [Accessed April 26, 2015].

Zhao, J. et al., 2012. Mixed lineage kinase domain-like is a key receptor interacting protein 3 downstream component of TNF-induced necrosis. *Proceedings of the National Academy of Sciences of the United States of America*, 109(14), pp.5322–7. Available at: http://www.pubmedcentral.nih.gov/articlerender.fcgi?artid=3325682&tool=pmcentrez&rendertype=abstract [Accessed April 25, 2015].